Supplementary Information (SI) for RSC Advances.
This journal is © The Royal Society of Chemistry 2024

Supporting information

Knoevenagel-IMHDA and -IMSDA sequences for the synthesis of chiral condensed *O,N*-, *S,N*- and *N*-heterocycles

Mihály Kajtár,[a,b] Sándor Balázs Király,[a*] Attila Bényei,[c] Attila Kiss-Szikszai,[a] Anita Kónya-Ábrahám,[a] Lilla Borbála Horváth,[d] Szilvia Bősze,[d] Andras Kotschy,[e] Attila Paczal,[e] Tibor Kurtán[a*]

[a]*Department of Organic Chemistry, University of Debrecen, Debrecen 4032, Egyetem square 1, Hungary.*
[b]*Doctoral School of Chemistry, University of Debrecen, 4032 Debrecen, Egyetem square 1, Hungary*
[c]*Department of Physical Chemistry, University of Debrecen, 4032 Debrecen, Egyetem square 1, Hungary*
[d]*Hungarian Research Network (HUN-REN), Research Group of Peptide Chemistry, Eötvös Loránd University, H1117 Budapest, Hungary.*
[e]*Servier Research Institute of Medicinal Chemistry, Budapest 1031, Hungary.*

Table of contents

Table of contents 2

Table of schemes 2

Table of figures 2

1.1 Preparation of the starting materials of the domino Knoevenagel-cyclization sequences 9

1.2 NMR spectra for the starting materials of domino-Knoevenagel-cyclization reactions 11

2. Mechanisms of the multi-step domino Knoevenagel-IMHDA reactions with Meldrum's acid. 13

3. Spectral data used for the determintion of relative configuration 1 15

4. NMR spectra of the products 17

5. X-Ray diffraction data 125

6. In vitro antiproliferative activity of the products of the domino reactions against U87, A2780 and HT-29 human cancer cell lines 134

7. References: 136

Table of schemes

Scheme S1. Preparation of compound **S4** with reductive amination of cynnamaldehyde (**S1**). 9

Scheme S2. Acetylation of the secondary amine **S4**. 9

Scheme S3. Acetal cleavage of **S5** resulting in **1d**. 10

Scheme S4. Mechanism for the multistep domino Knoevenagel-IMHDA reaction of substrate **1a** with Meldrum's acid in presence of different amines. 13

Scheme S5. Reaction mechanism of the multistep domino Knoevenagel-cyclization sequence of **1a** and Meldrum's acid in presence of Et_3N. 14

Table of figures

Figure S1. ^{1}H-NMR spectrum of the (*E*)-*N*-cinnamyl-*N*-(3-oxopropyl)acetamide (**1d)** in $CDCl_3$ at 400 MHz. 11
Figure S2. ^{13}C-NMR spectrum of the (*E*)-*N*-cinnamyl-*N*-(3-oxopropyl)acetamide (**1d**) in $CDCl_3$ at 100 MHz. 12
Table S1. Coupling constant data of the methine protons attached to the chirality centers and characteristic NOE effects observed for compounds **2**. 15
Table S2. Coupling constant data of the methine protons attached to the chirality centers and characteristic NOE effects observed for compounds **5**. 16
Figure S3. ^{1}H-NMR spectrum of the *rac*-(6a*R**,12*S**,12a*S**)-**3aa** in DMSO-d_6 at 500 MHz. 17
Figure S4. ^{13}C-NMR spectrum of the *rac*-(6a*R**,12*S**,12a*S**)-**3aa** in $CDCl_3$ at 100 MHz.....18
Figure S5. ROESY spectrum of the *rac*-(6a*R**,12*S**,12a*S**)-**3aa** in $CDCl_3$ at 500 MHz. 19
Figure S6. ^{1}H-NMR spectrum of the *rac*-(6a*R**,12*S**,12a*S**)-**3ab** in $CDCl_3$ at 500 MHz.....20
Figure S7. ^{13}C-NMR spectrum of the *rac*-(6a*R**,12*S**,12a*S**)-**3ab** in $CDCl_3$ at 100 MHz. 21
Figure S8. ROESY spectrum of the *rac*-(6a*R**,12*S**,12a*S**)-**3ab** in $CDCl_3$ at 500 MHz. 22
Figure S9. ^{1}H-NMR spectrum of the *rac*-(6a*R**,12*S**,12a*S**)-**3ac** in DMSO-d_6 at 500 MHz. 23
Figure S10. ^{13}C-NMR spectrum of the *rac*-(6a*R**,12*S**,12a*S**)-**3ac** in DMSO-d_6 at 125 MHz. 24
Figure S11. ROESY spectrum of the *rac*-(6a*R**,12*S**,12a*S**)-**3ac** in DMSO-d_6 at 500 MHz. 25
Figure S12. ^{1}H-NMR spectrum of the *rac*-(6a*R**,12*S**,12a*S**)-**3ad** and *rac*-(6a*R**,12*R**,12a*S**)-*epi*-**3ad** in DMSO-d_6 at 500 MHz.....26
Figure S13. ^{13}C-NMR spectrum of *rac*-(6a*R**,12*S**,12a*S**)-**3ag** and *rac*-(6a*R**,12*R**,12a*S**)-*epi*-**3ag** in $CDCl_3$ at 100 MHz. 27
Figure S14. ROESY spectrum of the *rac*-(6a*R**,12*S**,12a*S**)-**3ad** and *rac*-(6a*R**,12*R**,12a*S**)-*epi*-**3ad** in DMSO-d_6 at 500 MHz.....28
Figure S15. ^{1}H-NMR spectrum of the *rac*-(6a*R**,12*S*,*12a*S**)-**3ae** in acetone-d_6 at 500 MHz. 29
Figure S16. ^{13}C-NMR spectrum of the *rac*-(6a*R**,12S*,12a*S**)-**3ae** in acetone-d_6 at 125 MHz. 30
Figure S17. ROESY spectrum of the *rac*-(6a*R**,12*S**,12a*S**)-**3ae** in acetone-d_6 at 500 MHz.31
Figure S18. ^{1}H-NMR spectrum of the *rac*-(4*R**,4a*S**,10b*S**)-**2af** and *rac*-(4*R**,4a*S**,10b*R**)-*epi*-**2af** in DMSO-d_6 at 400 MHz.....32
Figure S19. ^{13}C-NMR spectrum of the *rac*-(4*R**,4a*S**,10b*S**)-**2af** and *rac*-(4*R**,4a*S**,10b*R**)-*epi*-**2af** in DMSO-d_6 at 100 MHz.....33

Figure S20. NOESY spectrum of the *rac*-(4*R**,4a*S**,10b*S**)-2af and *rac*-(4*R**,4a*S**,10b*R**)-*epi*-2af in DMSO-d_6 at 400 MHz 34
Figure S21. ^{1}H-NMR spectrum of the *rac*-(4*R**,4a*S**,10b*S**)-**2ag** and *rac*-(4*R**,4a*S**,10b*R**)-*epi*-**2ag** in DMSO-d_6 at 500 MHz. 35
Figure S22. ^{13}C-NMR spectrum of the *rac*-(4*R**,4a*S**,10b*S**)-**2ag** and *rac*-(4*R**,4a*S**,10b*R**)-*epi*-**2ag** in DMSO-d_6 at 125 MHz. 36
Figure S23. ROESY spectrum of the *rac*-(4*R**,4a*S**,10b*S**)-**2ag** and *rac*-(4*R**,4a*S**,10b*R**)-*epi*-**2ag** in DMSO-d_6 at 500 MHz. 37
Figure S24. ^{1}H-NMR spectrum of the *rac*-(6a*R**,12*S**,12a*S**)-**3ag** in DMSO-d_6 at 500 MHz. 38
Figure S25. ^{13}C-NMR spectrum of the *rac*-(6a*R**,12*S**,12a*S**)-**3ag** in DMSO-d_6 at 90 MHz. 39
Figure S26. HSQC spectrum of the *rac*-(6a*R**,12*S**,12a*S**)-**3ag** in DMSO-d_6 at 500 MHz. ..40
Figure S27. ROESY spectrum of the *rac*-(6a*R**,12*S**,12a*S**)-**3ag** in DMSO-d_6 at 500 MHz. 41
Figure S28. ^{1}H-NMR spectrum of the *rac*-(4*R**,4a*S**,10b*S**)-**2ah** and *rac*-(4*R**,4a*S**,10b*R**)-*epi*-**2ah** in $CDCl_3$ at 400 MHz. 42
Figure S29. ^{1}H-NMR spectrum of the *rac*-(4*R**,4a*S**,10b*S**)-**2ah** and *rac*-(4*R**,4a*S**,10b*R**)-*epi*-**2ah** in $CDCl_3$ at 100 MHz. 43
Figure S30. ^{1}H-NMR spectrum of the *rac*-(6a*R**,12*S**,12a*S**)-**3ah** in DMSO-d_6 at 500 MHz. 44
Figure S31. ^{13}C-NMR spectrum of the *rac*-(6a*R**,12*S**,12a*S**)-**3ah** in DMSO-d_6 at 125 MHz. 45
Figure S32. ROESY spectrum of the *rac*-(6a*R**,12*S**,12a*S**)-**3ah** in DMSO-d_6 at 500 MHz. 46
Figure S33. ^{1}H-NMR spectrum of *rac*-(4*R**,4a*S**,10b*S**)-**2ai** and *rac*-(4*R**,4a*S**,10b*R**)-*epi*-**2ai** in DMSO-d_6 at 500 MHz. 47
Figure S34. ^{13}C-NMR spectrum of *rac*-(4*R**,4a*S**,10b*S**)-**2ai** and *rac*-(4*R**,4a*S**,10b*R**)-*epi*-**2ai** in DMSO-d_6 at 125 MHz. 48
Figure S35. HSQC spectrum of *rac*-(4*R**,4a*S**,10b*S**)-**2ai** and *rac*-(4*R**,4a*S**,10b*R**)-*epi*-**2ai** in DMSO-d_6 at 500 MHz. 49
Figure S36. ROESY spectrum of *rac*-(4*R**,4a*S**,10b*S**)-**2ai** and *rac*-(4*R**,4a*S**,10b*R**)-*epi*-**2ai** in DMSO-d_6 at 500 MHz. 50
Figure S37. ^{1}H-NMR spectrum of *rac*-(4*R**,4a*S**,10b*S**)-**2bi** and *rac*-(4*R**,4a*S**,10b*R**)-*epi*-**2bi** in DMSO-d_6 at 500 MHz. 51
Figure S38. ^{13}C-NMR spectrum of *rac*-(4*R**,4a*S**,10b*S**)-**2bi** and *rac*-(4*R**,4a*S**,10b*R**)-*epi*-**2bi** in DMSO-d_6 at 125 MHz. 52

Figure S39. HSQC spectrum of *rac*-(4*R**,4a*S**,10b*S**)-**2bi** and *rac*-(4*R**,4a*S**,10b*R**)-*epi*-**2bi** in DMSO-d_6 at 500 MHz. 53
Figure S40. ^{1}H-NMR spectrum of *rac*-(4*R**,4a*S**,10b*S**)-**2ci** and *rac*-(4*R**,4a*S**,10b*R**)-*epi*-**2ci** in DMSO-d_6 at 500 MHz. 54
Figure S41. ^{13}C-NMR spectrum of *rac*-(4*R**,4a*S**,10b*S**)-**2ci** and *rac*-(4*R**,4a*S**,10b*R**)-*epi*-**2ci** in DMSO-d_6 at 125 MHz. 55
Figure S42. HSQC spectrum of *rac*-(4*R**,4a*S**,10b*S**)-**2ci** and *rac*-(4*R**,4a*S**,10b*R**)-*epi*-**2ci** in DMSO-d_6 at 500 MHz. 56
Figure S43. ^{1}H-NMR spectrum of the *rac*-(4*R**,4a*S**,10b*S**)-**4aj** in DMSO-d_6 at 400 MHz..57
Figure S44. ^{13}C-NMR spectrum of the *rac*-(4*R**,4a*S**,10b*S**)-**4aj** in DMSO-d_6 at 100 MHz.58
Figure S45. NOESY spectrum of the *rac*-(4*R**,4a*S**,10b*S**)-**4aj** in DMSO-d_6 at 400 MHz. ..59
Figure S46. ^{1}H-NMR spectrum of *rac*-(4*R**,4a*S**,10b*S**)-**2ak** in DMSO-d_6 at 500 MHz.....60
Figure S47. ^{13}C-NMR spectrum of *rac*-(4*R**,4a*S**,10b*S**)-**2ak** in $CDCl_3$ at 100 MHz. 61
Figure S48. HSQC spectrum of *rac*-(4*R**,4a*S**,10b*S**)-**2ak** in $CDCl_3$ at 400 MHz. 62
Figure S49. ^{1}H-NMR spectrum of *rac*-(4*R**,4a*S**,10b*S**)-**2bk** in $CDCl_3$ at 500 MHz. 63
Figure S50. ^{13}C-NMR spectrum of *rac*-(4*R**,4a*S**,10b*S**)-**2bk** in $CDCl_3$ at 125 MHz. 64
Figure S51. NOESY spectrum of *rac*-(4*R**,4a*S**,10b*S**)-**2bk** in $CDCl_3$ at 500 MHz. 65
Figure S52. ^{1}H-NMR spectrum of *rac*-(4*R**,4a*S**,10b*S**)-**2bl** in $CDCl_3$ at 400 MHz. 66
Figure S53. ^{13}C-NMR spectrum of *rac*-(4*R**,4a*S**,10b*S**)-**2bl** in $CDCl_3$ at 100 MHz. 67
Figure S54. NOESY spectrum of *rac*-(4*R**,4a*S**,10b*S**)-**2bl** in $CDCl_3$ at 400 MHz. 68
Figure S55. ^{1}H-NMR spectrum of *rac*-(4*R**,4a*S**,10b*R**)-*epi*-**2am** in DMSO-d_6 at 500 MHz. 69
Figure S56. ^{13}C-NMR spectrum of *rac*-(4*R**,4a*S**,10b*R**)-*epi*-**2am** in DMSO-d_6 at 90 MHz. 70
Figure S57. HSQC spectrum of *rac*-(4*R**,4a*S**,10b*R**)-*epi*-**2am** in DMSO-d_6 at 400 MHz...71
Figure S58. ROESY spectrum of *rac*-(4*R**,4a*S**,10b*R**)-*epi*-**2am** in DMSO-d_6 at 500 MHz.72
Figure S59. ^{1}H-NMR spectrum of *rac*-(4*R**,4a*S**,10b*R**)-*epi*-**2bm** in DMSO-d_6 at 500 MHz. 73
Figure S60. ^{13}C-NMR spectrum of *rac*-(4*R**,4a*S**,10b*R**)-*epi*-**2bm** in DMSO-d^6 at 100 MHz. 74
Figure S61. HSQC spectrum of *rac*-(4*R**,4a*S**,10b*R**)-*epi*-**2bm** in DMSO-d_6 at 500 MHz...75
Figure S62. ^{1}H-NMR spectrum of *rac*-(4*R**,4a*S**,10b*S**)-**2an** and *rac*-(4*R**,4a*S**,10b*R**)-*reg*-**2an** in DMSO-d_6 at 500 MHz. 76

Figure S63. ^{13}C-NMR spectrum of *rac*-(4*R**,4a*S**,10b*S**)-**2an** and *rac*-(4*R**,4a*S**,10b*R**)-*reg*-**2an** in DMSO-d_6 at 125 MHz. 77
Figure S64. HSQC spectrum of *rac*-(4*R**,4a*S**,10b*S**)-**2an** and *rac*-(4*R**,4a*S**,10b*R**)-*reg*-**2an** in DMSO-d_6 at 500 MHz 78
Figure S65. ROESY spectrum of *rac*-(4*R**,4a*S**,10b*S**)-**2an** and *rac*-(4*R**,4a*S**,10b*R**)-*reg*-**2an** in DMSO-d_6 at 500 MHz 79
Figure S66. ^{1}H-NMR spectrum of *rac*-(4*R**,4a*S**,10b*S**)-**2bn** and *rac*-(4*R**,4a*S**,10b*R**)-*reg*-**2bn** in DMSO-d_6 at 500 MHz. 80
Figure S67. ^{13}C-NMR spectrum of *rac*-(4*R**,4a*S**,10b*S**)-**2bn** and *rac*-(4*R**,4a*S**,10b*R**)-*reg*-**2bn** in DMSO-d_6 at 125 MHz. 81
Figure S68. ^{1}H-NMR spectrum of the ~5:4 mixture of *rac*-(1*R**,4*R**,4a*S**,10b*R**)-*dia1*-**5a** and *rac*-(1*S**,4*R**,4a*S**,10b*S**)- *dia2*-**5a** in $CDCl_3$ at 500 MHz. 82
Figure S69. ^{13}C-NMR spectrum of the ~5:4 mixture of *rac*-(1*R**,4*R**,4a*S**,10b*R**)-*dia1*-**5a** and *rac*-(1*S**,4*R**,4a*S**,10b*S**)- *dia2*-**5a** in $CDCl_3$ at 125 MHz. 83
Figure S70. ROESY spectrum of the ~5:4 mixture of *rac*-(1*R**,4*R**,4a*S**,10b*R**)-*dia1*-**5a** and *rac*-(1*S**,4*R**,4a*S**,10b*S**)-*dia2*-**5a** in $CDCl_3$ at 500 MHz. 84
Figure S71. ^{1}H-NMR spectrum of the *rac*-(1*R**,4*R**,4a*S**,10b*R**)-*dia1*-**5b** in $CDCl_3$ at 400 MHz. 85
Figure S72. ^{13}C-NMR spectrum of the *rac*-(1*R**,4*R**,4a*S**,10b*R**)-*dia1*-**5b** in $CDCl_3$ at 100 MHz. 86
Figure S73. NOESY spectrum of the *rac*-(1*R**,4*R**,4a*S**,10b*R**)-*dia1*-**5b** in $CDCl_3$ at 400 MHz. 87
Figure S74. ^{1}H-NMR spectrum of the *rac*-(1*S**,4*R**,4a*S**,10b*S**)-*dia2*-**5b** in $CDCl_3$ at 400 MHz. 88
Figure S75. ^{13}C-NMR spectrum of the *rac*-(1*S**,4*R**,4a*S**,10b*S**)-*dia2*-**5b** in $CDCl_3$ at 100 MHz. 89
Figure S76. NOESY spectrum of the *rac*-(1*S**,4*R**,4a*S**,10b*S**)-*dia2*-**5b** in $CDCl_3$ at 400 MHz. 90
Figure S77. ^{1}H-NMR spectrum of the *rac*-(1*R**,4*R**,4a*S**,10b*R**)-*dia1*-**5c** in $CDCl_3$ at 500 MHz. 91
Figure S78. ^{13}C-NMR spectrum of the *rac*-(1*R**,4*R**,4a*S**,10b*R**)-*dia1*-**5c** in $CDCl_3$ at 125 MHz. 92
Figure S79. ROESY spectrum of the *rac*-(1*R**,4*R**,4a*S**,10b*R**)-*dia1*-**5c** in $CDCl_3$ at 500 MHz. 93

Figure S80. ^{1}H-NMR spectrum of the *rac*-(1*S**,4*R**,4a*S**,10b*S**)-*dia2*-**5c** in $CDCl_3$ at 500 MHz. 94
Figure S81. ^{13}C-NMR spectrum of the *rac*-(1*S**,4*R**,4a*S**,10b*S**)-*dia2*-**5c** in $CDCl_3$ at 125 MHz. 95
Figure S82. ROESY spectrum of the *rac*-(1*S**,4*R**,4a*S**,10b*S**)-*dia2*-**5c** in $CDCl_3$ at 500 MHz. 96
Figure S83. ^{1}H-NMR spectrum of the *rac*-(1*S**,4*R**,4a*S**,10b*S**)- *dia2*-**5d** in $CDCl_3$ at 500 MHz. 97
Figure S84. ^{13}C-NMR spectrum of the *rac*-(1*S**,4*R**,4a*S**,10b*S**)-*dia2*-**5d** in $CDCl_3$ at 125 MHz. 98
Figure S85. ROESY spectrum of the *rac*-(1*S**,4*R**,4a*S**,10b*S**)-*dia2*-**5d** in $CDCl_3$ at 500 MHz. 99
Figure S86. ^{1}H-NMR spectrum of the *rac*-(1*S**,4*R**,4a*S**,10b*S**)-*dia2*-**5e** in $CDCl_3$ at 500 MHz. 100
Figure S87. ^{13}C-NMR spectrum of the *rac*-(1*S**,4*R**,4a*S**,10b*S**)-*dia2*-**5e** in $CDCl_3$ at 125 MHz. 101
Figure S88. HMBC spectrum of the *rac*-(1*S**,4*R**,4a*S**,10b*S**)-*dia2*-**5e** in $CDCl_3$ at 500 MHz. 102
Figure S89. ROESY spectrum of the *rac*-(1*S**,4*R**,4a*S**,10b*S**)-*dia2*-**5e** in $CDCl_3$ at 500 MHz. 103
Figure S90. ^{1}H-NMR spectrum of the *rac*-(1*R**,4*R**,4a*S**,10b*R**)-*dia1*-**5e** in $CDCl_3$ at 500 MHz. 104
Figure S91. ^{13}C-NMR spectrum of the *rac*-(1*R**,4*R**,4a*S**,10b*R**)-*dia1*-**5e** in DMSO-d_6 at 125 MHz. 105
Figure S92. ROESY spectrum of the *rac*-(1*R**,4*R**,4a*S**,10b*R**)-*dia1*-**5e** in $CDCl_3$ at 500 MHz. 106
Figure S93. ^{1}H-NMR spectrum of the *rac*-(1*S**,4*R**,4a*S**,10b*S**)-*dia2*-**5f** in $CDCl_3$ at 400 MHz. 107
Figure S94. ^{13}C-NMR spectrum of the *rac*-(1*S**,4*R**,4a*S**,10b*S**)-*dia2*-**5f** in DMSO-d_6 at 100 MHz. 108
Figure S95. ^{1}H-NMR spectrum of the *rac*-(1*S**,4*R**,4a*S**,10b*S**)-*dia2*-**5g** in $CDCl_3$ at 400 MHz. 109
Figure S96. ^{13}C-NMR spectrum of the *rac*-(1*S**,4*R**,4a*S**,10b*S**)-*dia2*-**5g** in $CDCl_3$ at 100 MHz. 110

Figure S97. ^{1}H-NMR spectrum of the *rac*-(4a*S**,5*R**,10b*R**)-**6p** in $CDCl_3$ at 400 MHz. 111
Figure S98. ^{13}C-NMR spectrum of the *rac*-(4a*S**,5*R**,10b*R**)-**6p** in $CDCl_3$ at 100 MHz. 112
Figure S99. ^{1}H-NMR spectrum of the *rac*-(4a*S**,5*R**,9b*R**)-**6q** in $CDCl_3$ at 400 MHz. 113
Figure S100. ^{13}C-NMR spectrum of the *rac*-(4a*S**,5*R**,9b*R**)-**6q** in $CDCl_3$ at 100 MHz. 114
Figure S101. NOESY spectrum of the *rac*-(4a*S**,5*R**,9b*R**)-**6q** in $CDCl_3$ at 400 MHz. 115
Figure S102. ^{1}H-NMR spectrum of the *rac*-(6*R**,6a*S**,10a*R**)-**6r** in $CDCl_3$ at 400 MHz. 116
Figure S103. ^{13}C-NMR spectrum of the *rac*-(6*R**,6a*S**,10a*R**)-**6r** in $CDCl_3$ at 100 MHz. ..117
Figure S104. ^{1}H-NMR spectrum of the *rac*-(6*R**,6a*S**,10a*R**)-**6s** in $CDCl_3$ at 400 MHz. 118
Figure S105. ^{13}C-NMR spectrum of the *rac*-(6*R**,6a*S**,10a*R**)-**6s** in $CDCl_3$ at 100 MHz. 119
Figure S106. ^{1}H-NMR spectrum of the *rac*-(1*R**,4a*R**,8a*S**)-**6k** in acetone-d_6 at 500 MHz. 120
Figure S107. ^{13}C-NMR spectrum of the *rac*-(1*R**,4a*R**,8a*S**)-**6k** in acetone-d_6 at 125 MHz. 121
Figure S108. ROESY spectrum of the *rac*-(1*R**,4a*R**,8a*S**)-**6k** in acetone-d_6 at 500 MHz. 122
Figure S109. ^{1}H-NMR spectrum of the *rac*-(1*R**,4a*R**,8a*S**)-**6i** in $CDCl_3$ at 400 MHz. 123
Figure S110. ^{13}C-NMR spectrum of the *rac*-(1*R**,4a*R**,8a*S**)-**6i** in $CDCl_3$ at 100 MHz. 124

1.1 Preparation of the starting materials of the domino Knoevenagel-cyclization sequences

Substrates **1a-c** of the domino Knoevenagel-cyclization sequences were prepared on the basis of our publication.[1]

(*E*)-*N*-(3,3-diethoxypropyl)-3-phenylprop-2-en-1-amine (**1d**):

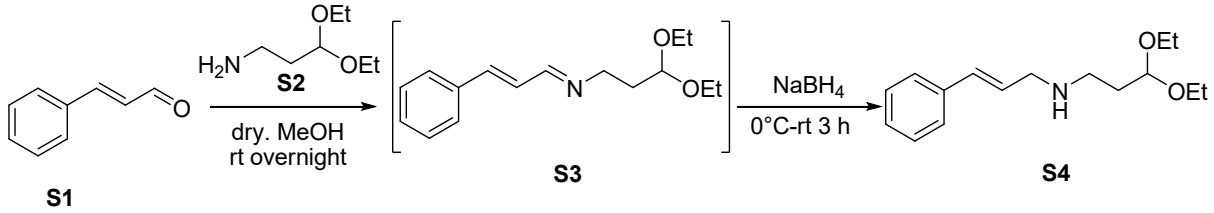

Scheme S1. Preparation of compound **S4** with reductive amination of cynnamaldehyde (**S1**).

In a flame-dried three-necked round-bottom flask equipped with a reflux condenser and a $CaCl_2$ drying tube, cinnamaldehyde (**S1**, 20 mmol) was dissolved in 20 ml MeOH and 3,3-diethoxy-propane-1-amine (**S2**, 20 mmol, 1.0 equivalent) was added to the mixture, and it was stirred overnight at room temperature. The mixture was then cooled to 0 °C in an ice bath, and sodium tetrahydroborate (25 mmol, 1.25 equivalent) was added in two portions. The mixture was allowed to warm up to room temperature and stirred for two hours. The reaction mixture was then filtered through a celite plug and it was washed with methanol. The methanol was removed *in vacuo* and the resulting crude oil was dissolved in dichloromethane and extracted three times with water (30 ml). The organic phase was dried over $MgSO_4$, filtered, washed and concentrated *in vacuo*, affording the secondary amine **S4**, which was used for further transformations without purification and characterization.

(*E*)-*N*-cinnamyl-*N*-(3,3-diethoxypropyl)acetamide (**S5**):

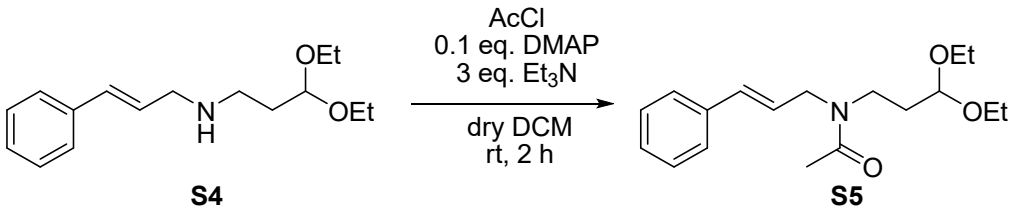

Scheme S2. Acetylation of the secondary amine **S4**.

500 mg **S4** amine derivative (2.17 mmol), DMAP (0.1 eq. 0.217 mmol) and triethyl amine (3 eq. 6.51 mmol) were dissolved in 10 ml dry dichloromethane and a solution of acetyl chloride (1.05 eq. 1 M in dichloromethane) was added to the mixture. The reaction was stirred at room

temperature for 2 hours, then the mixture was poured on 30 ml of water. It was extracted three times with 30 ml of dichloromethane. The combined organic phase was dried over $MgSO_4$, filtered, washed and concentrated *in vacuo*, affording the amide derivative **S5**, which was used without further purification or characterisation.

(*E*)-*N*-cinnamyl-*N*-(3-oxopropyl)acetamide (**1d**):

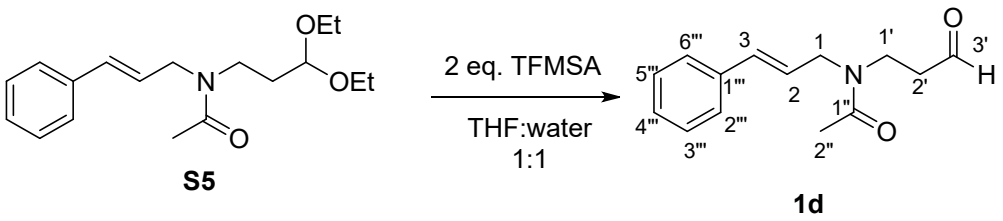

Scheme S3. Acetal cleavage of **S5** resulting in **1d**.

150 mg amide derivative **S5** (0.49 mmol) was dissolved in 4 ml water/THF 1:1 and 87 µl of trifluoromethanesulfonic acid (TFMSA) was added to the mixture. The reaction was stirred for 2 hours and then it was poured on 50 ml of cc. $NaHCO_3$ solution, and it was extracted three times with 30 ml of dichloromethane. The organic phase was dried over $MgSO_4$, filtered, washed and concentrated *in vacuo*. The crude product was purified with column chromatography (hexane/acetone 3:1) affording **1d** as yellow oil (91 % for three steps) R_f = 0.19 (hexane/acetone 3:1).

^{1}H NMR (400 MHz, $CDCl_3$) δ 2.10 (s, 3 H, 2”-H), 2.70 - 2.84 (m, 2 H, 2’-H), 3.59 - 3.72 (m, 2 H, 1’-H), 3.95 - 4.21 (m, 2 H, 1-H), 5.99 - 6.23 (m, 1 H, 2-H), 6.37 - 6.55 (m, 1 H, 3-H), 7.14 - 7.45 (m, 5 H, Ph-H), 9.76 (s, 1 H, C*H*O).

^{13}C NMR (100 MHz, $CDCl_3$) δ 21.6 (C-2”), 40.3 (C-2’), 42.9 (C-1’), 51.5 (C-1), 124.0 and 126.4 (C-3”’ and C-5”’), 128.0 (C-4”’), 128.6 and 128.7 (C-2”’ and C-6”’), 132.0 (C-4”’), 136.0 (C-1”’), 171.1 (C-1”), 200.9 (**C**HO).

IR: (KBr) ν: 2932, 2348, 2309, 1716, 1622, 1475, 1418, 1361, 1231, 1170, 1131, 1063, 1030.
HRMS: calcd. for $C_{14}H_{18}NO_2$ $[M+H]^+$ 232.1337, found 232.1338.

1.2 NMR spectra for the starting materials of domino-Knoevenagel-cyclization reactions

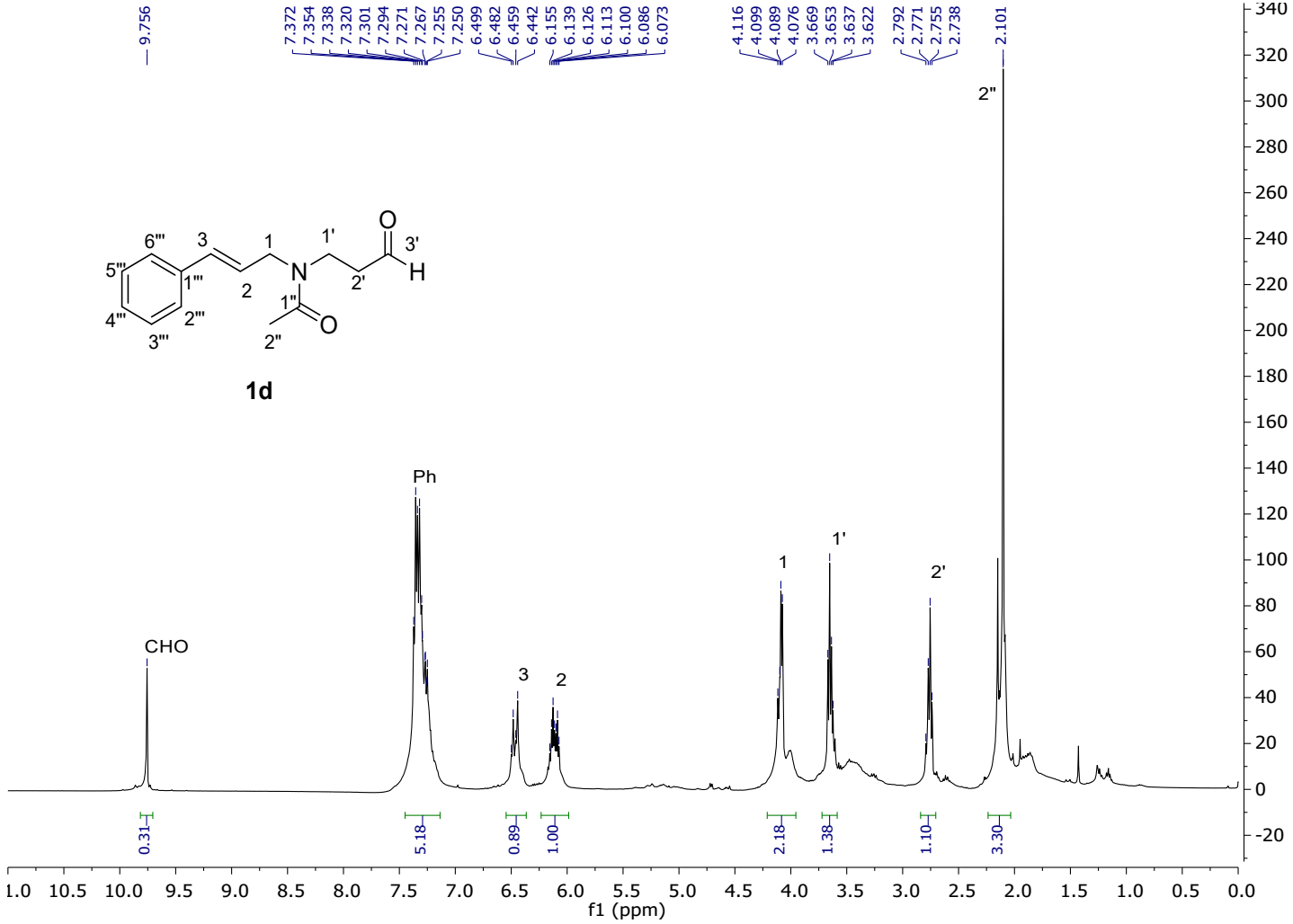

Figure S1. ^{1}H-NMR spectrum of the (*E*)-*N*-cinnamyl-*N*-(3-oxopropyl)acetamide (**1d**) in $CDCl_3$ at 400 MHz.

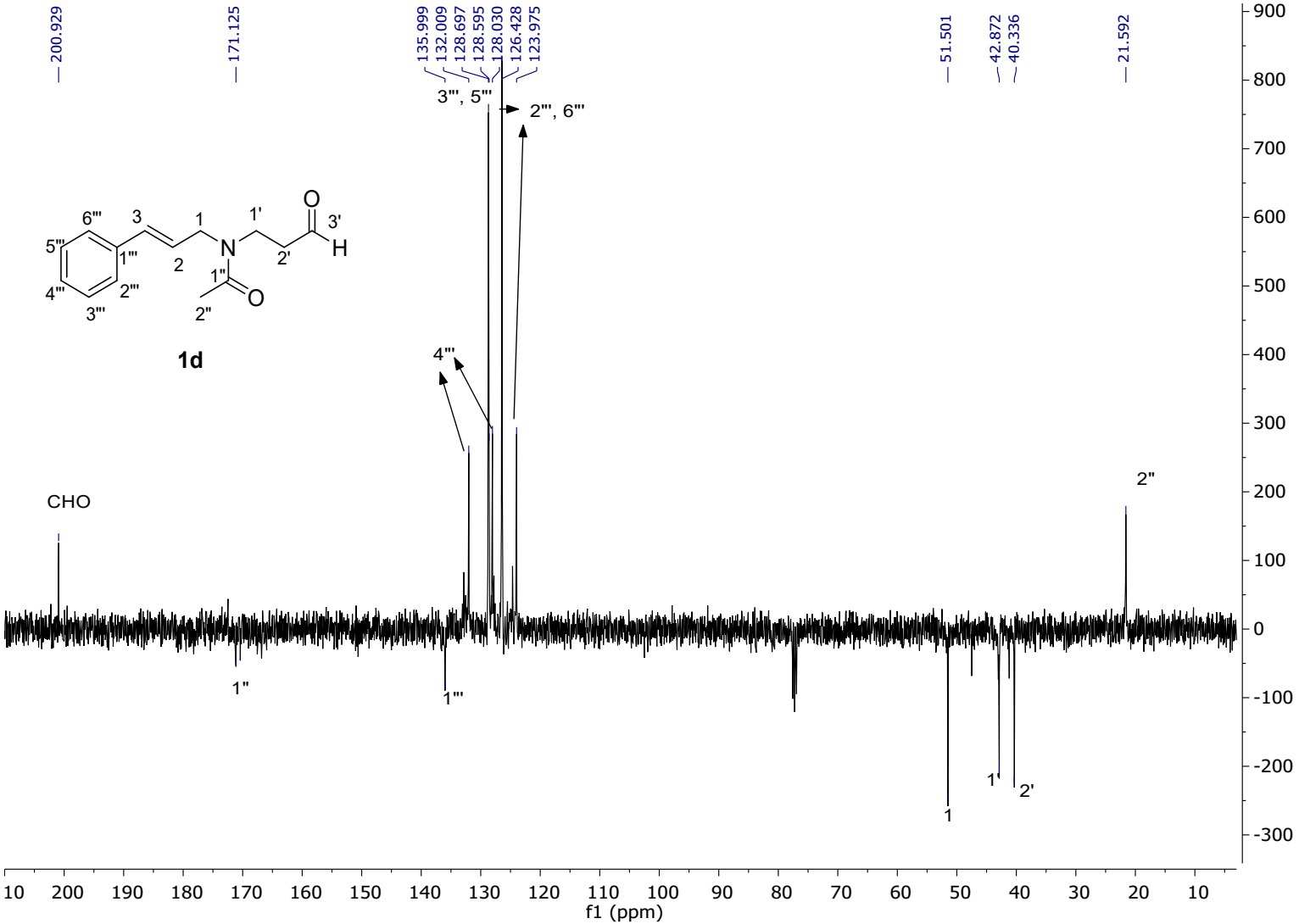

Figure S2. ^{13}C-NMR spectrum of the (*E*)-*N*-cinnamyl-*N*-(3-oxopropyl)acetamide (**1d**) in $CDCl_3$ at 100 MHz.

2. Mechanisms of the multi-step domino Knoevenagel-IMHDA reactions with Meldrum's acid.

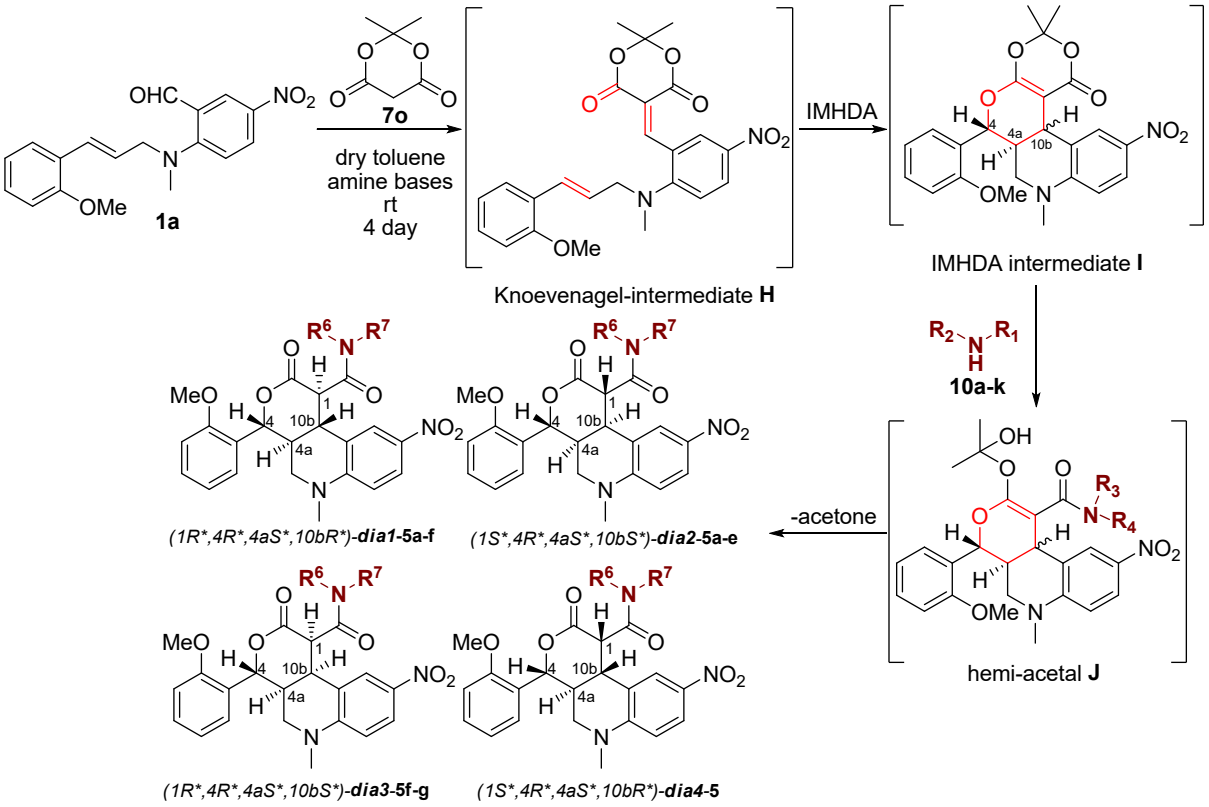

Scheme S4. Mechanism for the multistep domino Knoevenagel-IMHDA reaction of substrate **1a** with Meldrum's acid in presence of different amines.

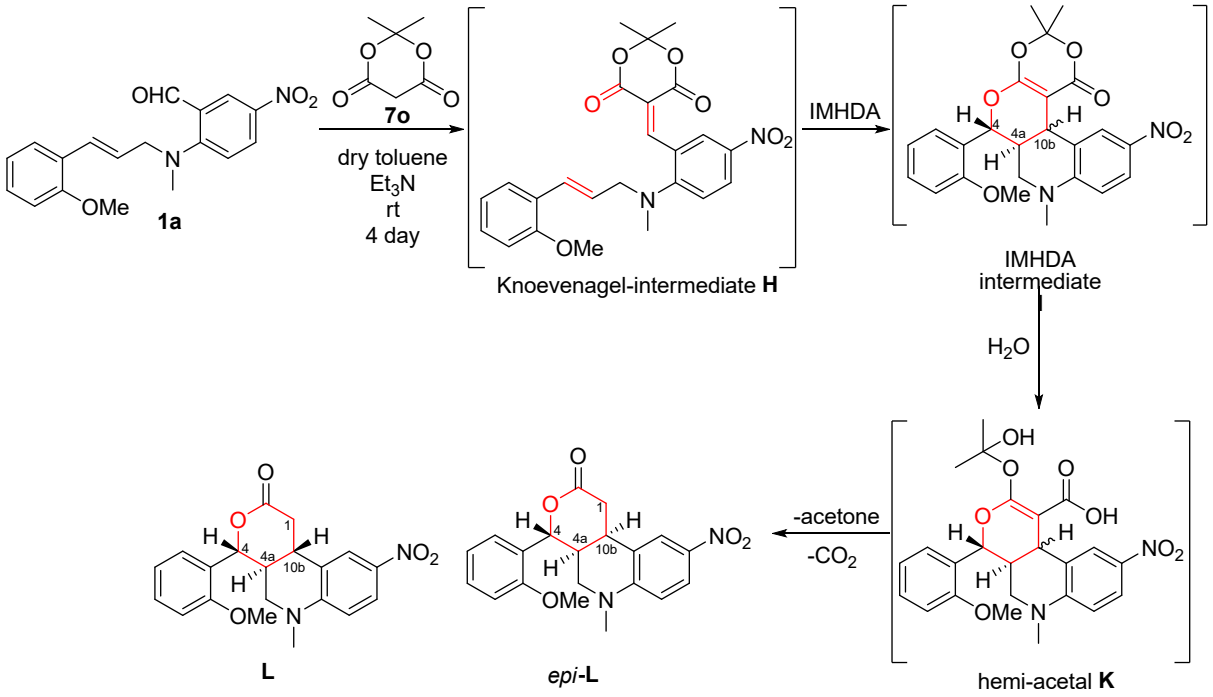

Scheme S5. Reaction mechanism of the multistep domino Knoevenagel-cyclization sequence of **1a** and Meldrum's acid in presence of Et_3N.

3. Spectral data used for the determination of the relative configuration

TABLE S1. Coupling constant data of the methine protons attached to the chirality centers and characteristic NOE effects observed for compounds **2.**

Compound	J(4-H)	J(4a-H)	J(10b-H)	Characteristic NOE
2af	broad singlet	broad multiplet	overlap	10b-H/4-H
epi-**2af**	d, 6.6 Hz	multiplet	d, 4.7 Hz	10b-H/4a-H
2ag	broad singlet	broad multiplet	overlap	10b-H/4-H
epi-**2ag**	d, 6.7 Hz	multiplet	overlap	10b-H/4a-H
2ah[a]	overlap	multiplet	d, 6.6 Hz	N/A
epi-**2ah**[a]	d, 4.6 Hz	multiplet	d, 4.6 Hz	N/A
2ai	broad singlet	overlap	d, 9.0 Hz	10b-H/4-H
epi-**2ai**	d, 6.2 Hz	multiplet	d, 5.2 Hz	10b-H/4a-H
2bi	d, 10.0 Hz	multiplet	d, 11.0 Hz	N/A
epi-**2bi**	d, 5.3 Hz	multiplet	d, 4.2 Hz	N/A
2ci	d, 10.0 Hz	multiplet	d, 10.9 Hz	N/A
epi-**2ci**	broad dublet, 3.2 Hz	broad multiplet	d, 4.1 Hz	N/A
4aj	d, 10.6 Hz	multiplet	d, 11.0 Hz	10b-H/4-H
2ak	broad singlet	broad multiplet	d, 12.0 Hz	N/A
2bk	d, 10.2 Hz	overlap	d, 11.2 Hz	10b-H/4-H
2bl	d, 10.1 Hz	multiplet	d, 11.2 Hz	10b-H/4-H
epi-**2am**	broad singlet	broad multiplet	d, 3.4 Hz	10b-H/4a-H
epi-**2bm**	d, 11 Hz	overlap	d, 3.5 Hz	N/A
2an	broad singlet, overlap	broad multiplet	d, 9.5 Hz	none visible
reg-**2an**	d, 10.9 Hz	multiplet	d, 3.1 Hz	10b-H/4a-H
2bn	d, 10.1 Hz	overlap	d, 11.0 Hz	N/A
reg-**2bn**	d, 11.4 Hz	overlap	d, 3.4 Hz	N/A

a) relative configuration was assigned based on analogy, using the chemical shift and splitting of the 4-H signals.

TABLE S2. Coupling constant data of the protons attached to the chirality centers and characteristic NOE effects observed for compounds **5.**

Compound	J(4-H)	J(4a-H)	J(10b-H)	J(1-H)	Characteristic NOE
dia1-**5a**	d, 10.4 Hz	multiplet	dd, 11.5, 10.5 Hz	d, 10.5 Hz	4-H/10b-H; 4a-H/1-H
dia2-**5a**	d, 2.9 Hz	multiplet	dd, 9.8, 5.2 Hz	d, 9.8 Hz	4a-H/10b-H
dia1-**5b**	d, 10.5 Hz	multiplet	dd, 11.8, 10.2 Hz	d, 10.2 Hz	4-H/10b-H; 4a-H/1-H
dia2-**5b**	d, 3.0 Hz	overlap	dd, 10.0, 4.5 Hz	d, 10.0 Hz	4a-H/10b-H
dia1-**5c**	d, 10.3 Hz	multiplet	11.5, 10.0 Hz	d, 10.0 Hz	4-H/10b-H; 4a-H/1-H
dia2-**5c**	d, 3.0 Hz	multiplet	dd, 9.8, 4.7 Hz	d, 9.8 Hz	4-H/1-H; 4a-H/10b-H
dia2-**5d**[a]	d, 2.5 Hz	multiplet	overlap	overlap	overlapping signals
dia1-**5e**	d, 4.0 Hz	multiplet	overlap	d, 9.3 Hz[b]	4a-H/1-H
dia2-**5e**	d, 5.9 Hz	overlap	broad multiplet	d, 6.7 Hz[b]	4-H/1-H; 4a-H/10b-H
dia2-**5f**	d, 4.9 Hz	multiplet	dd, 8.4, 4.6 Hz	overlap	N/A
dia2-**5g**[c]	d, 3.9 Hz	multiplet	overlap	overlap	N/A

a) 10b-H and 1-H signals overlap, configuration was assigned based on analogy using the coupling constant of 4-H. b) coupling constants are inconclusive, configuration was assigned using NOE correlations. c) due to the overlap of the 10b-H signal, configuration was assigned based on analogy using the chemical shift of 4-H.

4. NMR spectra of the products

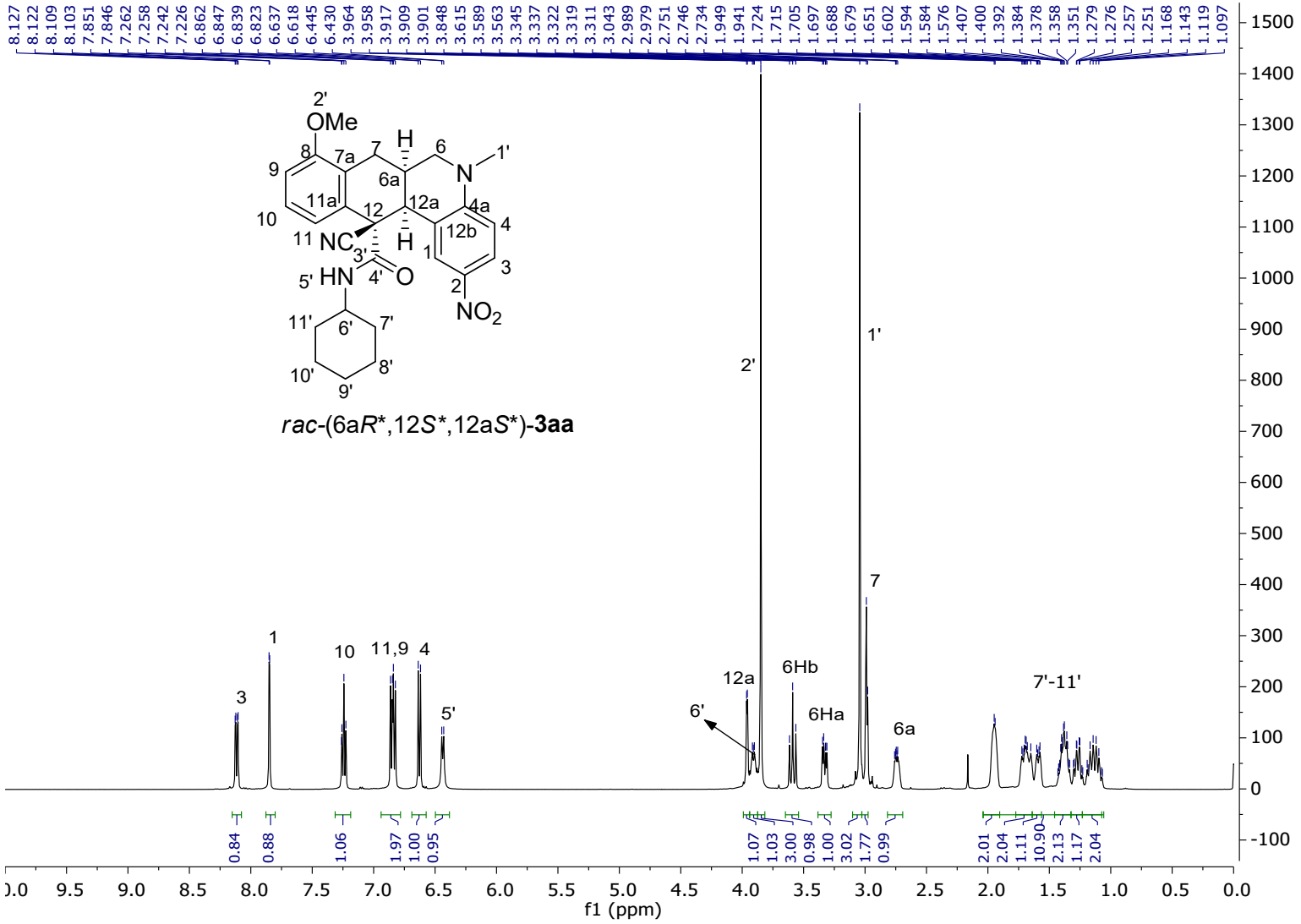

Figure S3. [1]H-NMR spectrum of the *rac*-(6a*R**,12*S**,12a*S**)-**3aa** in DMSO-d_6 at 500 MHz.

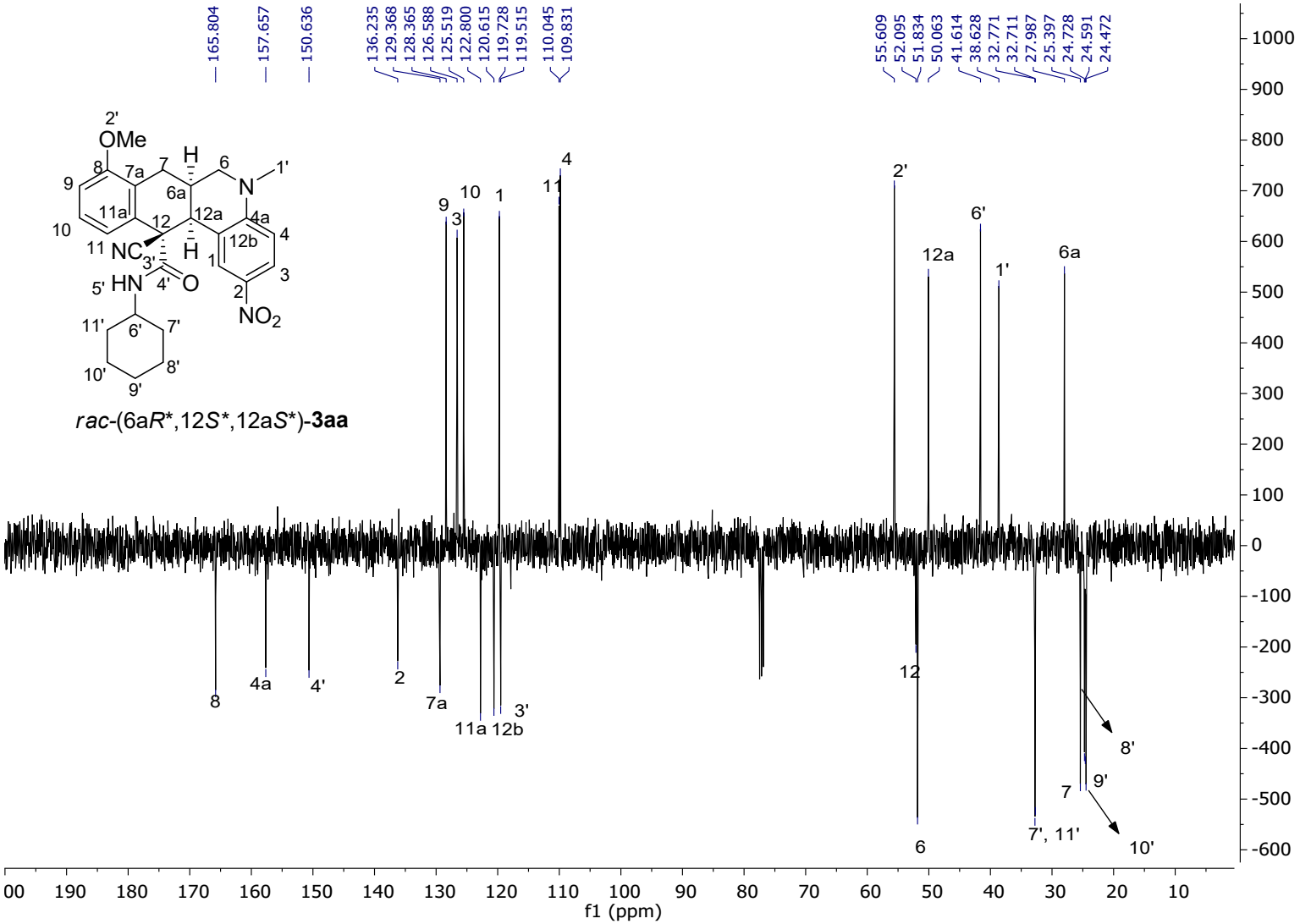

Figure S4. ^{13}C-NMR spectrum of the *rac*-(6a*R**,12*S**,12a*S**)-**3aa** in $CDCl_3$ at 100 MHz.

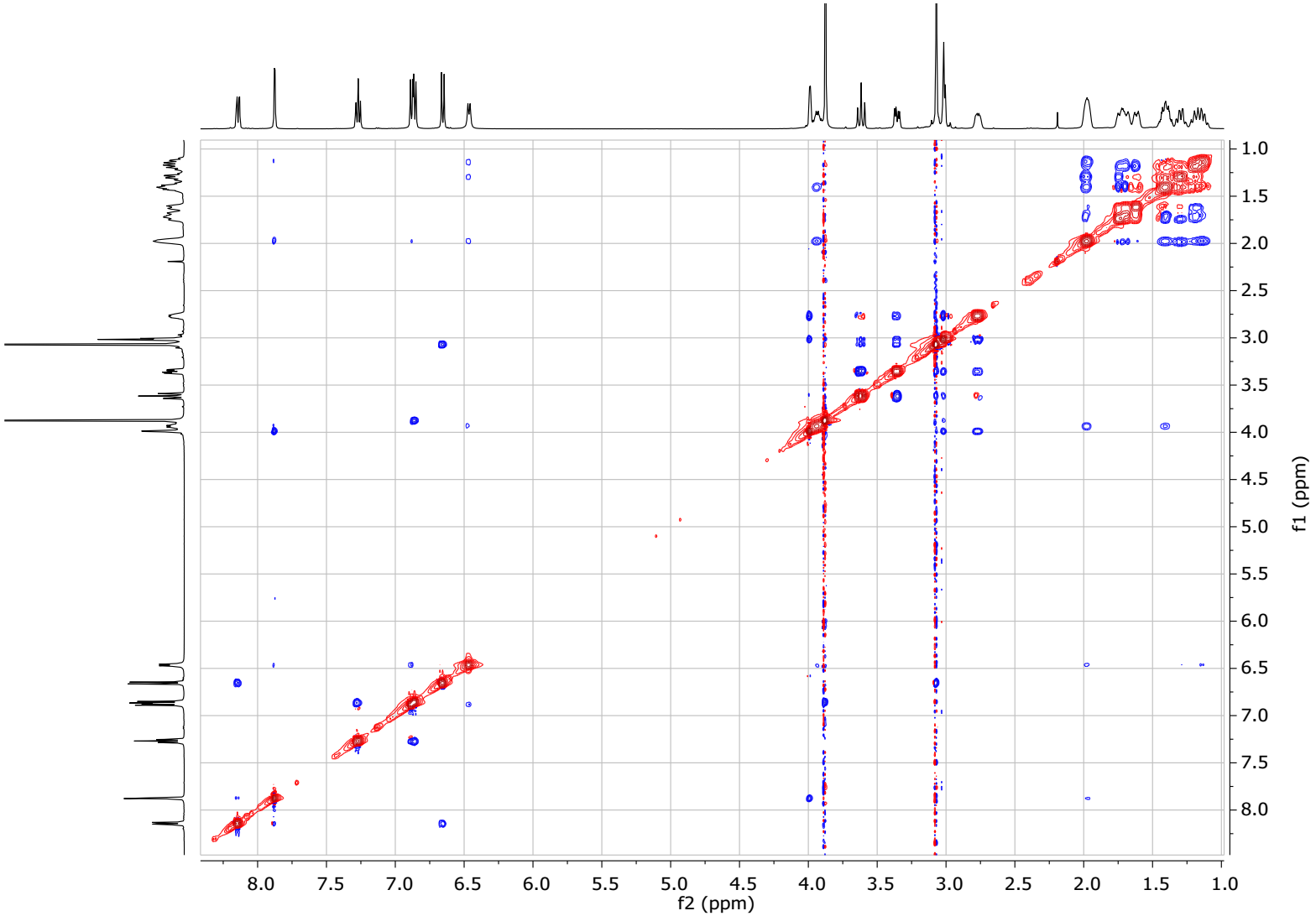

Figure S5. ROESY spectrum of the *rac*-(6a*R**,12*S**,12a*S**)-**3aa** in $CDCl_3$ at 500 MHz.

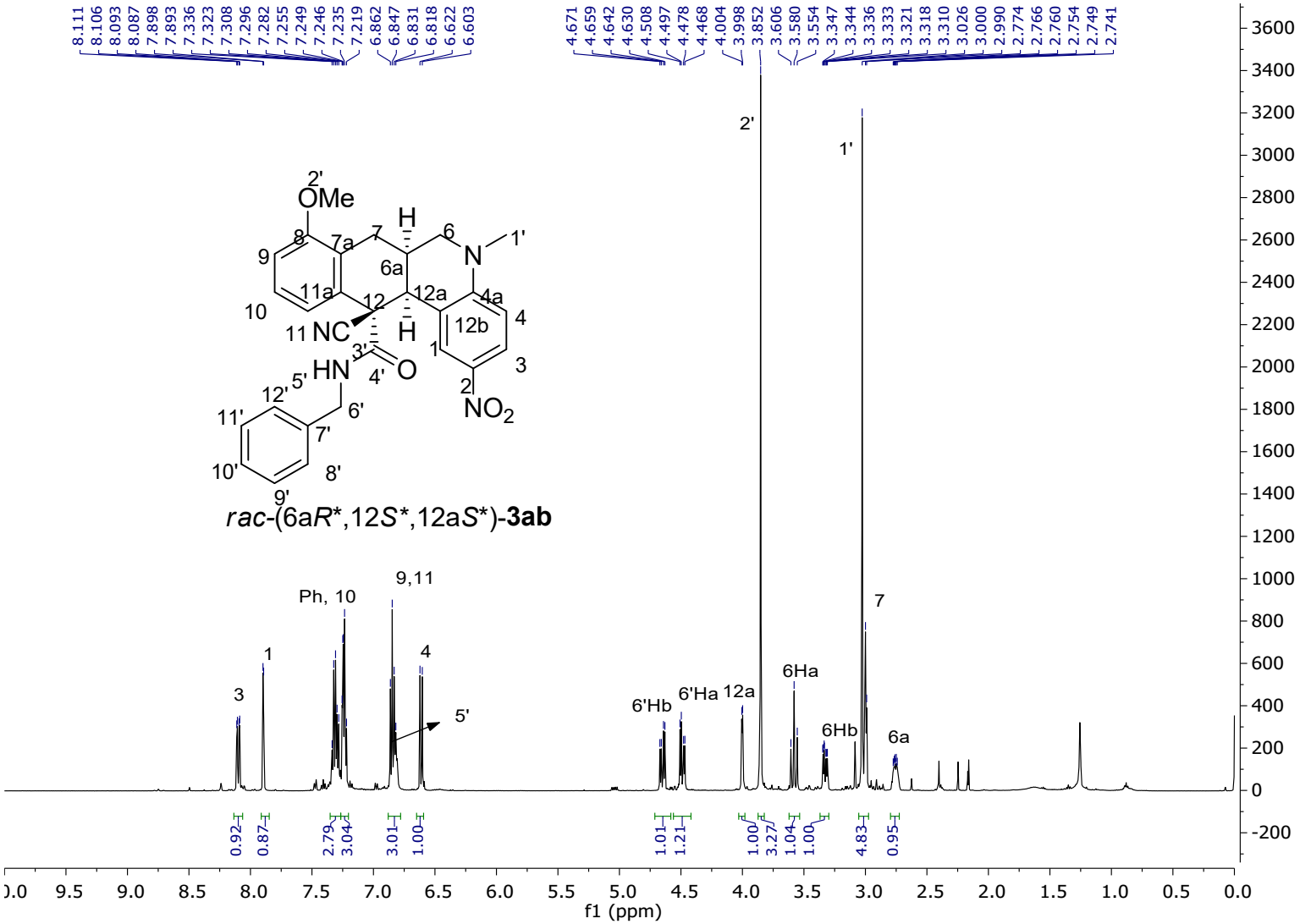

Figure S6. ^{1}H-NMR spectrum of the *rac*-(6a*R**,12*S**,12a*S**)-**3ab** in $CDCl_3$ at 500 MHz.

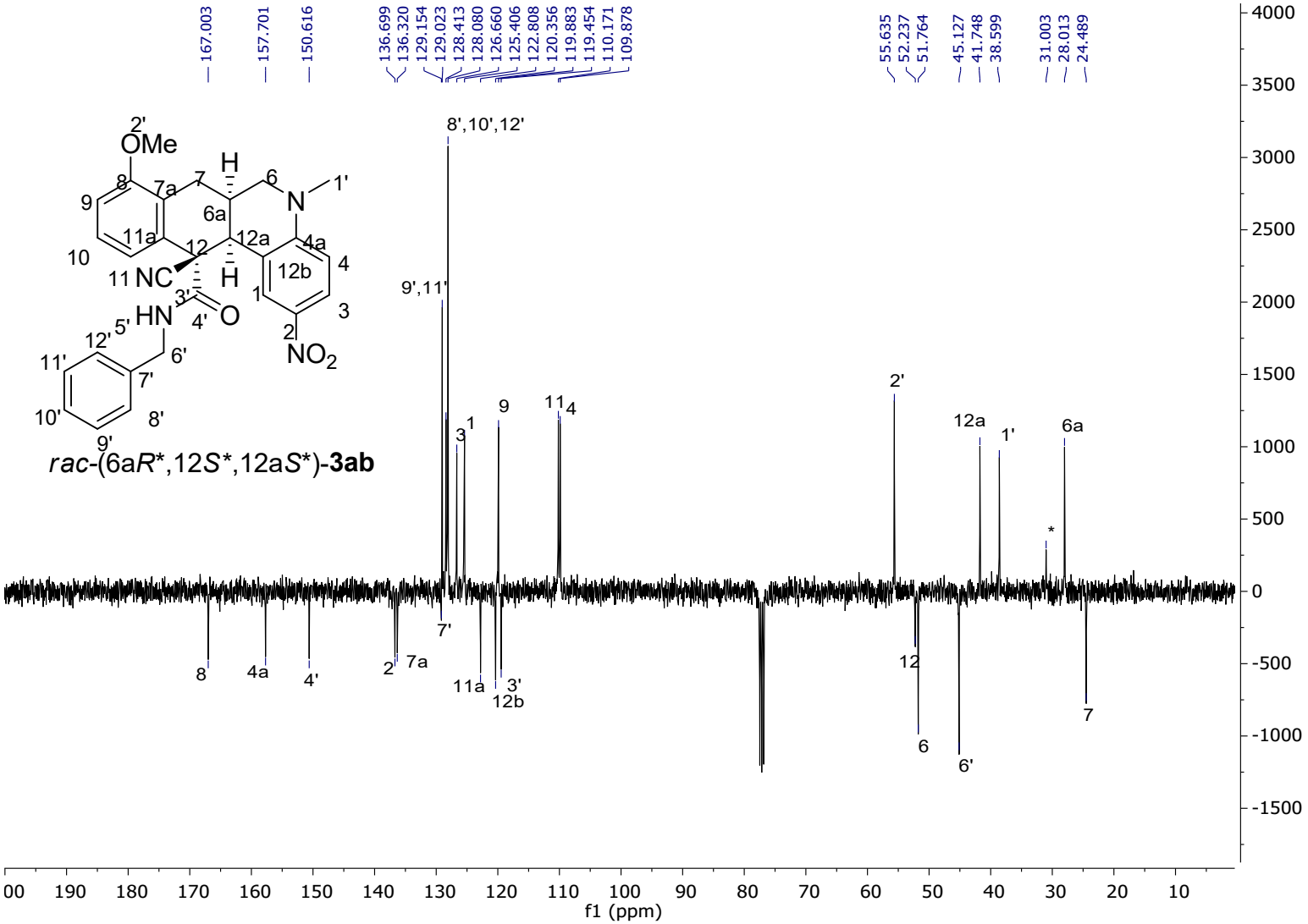

Figure S7. ^{13}C-NMR spectrum of the *rac*-(6a*R**,12*S**,12a*S**)-**3ab** in $CDCl_3$ at 100 MHz.

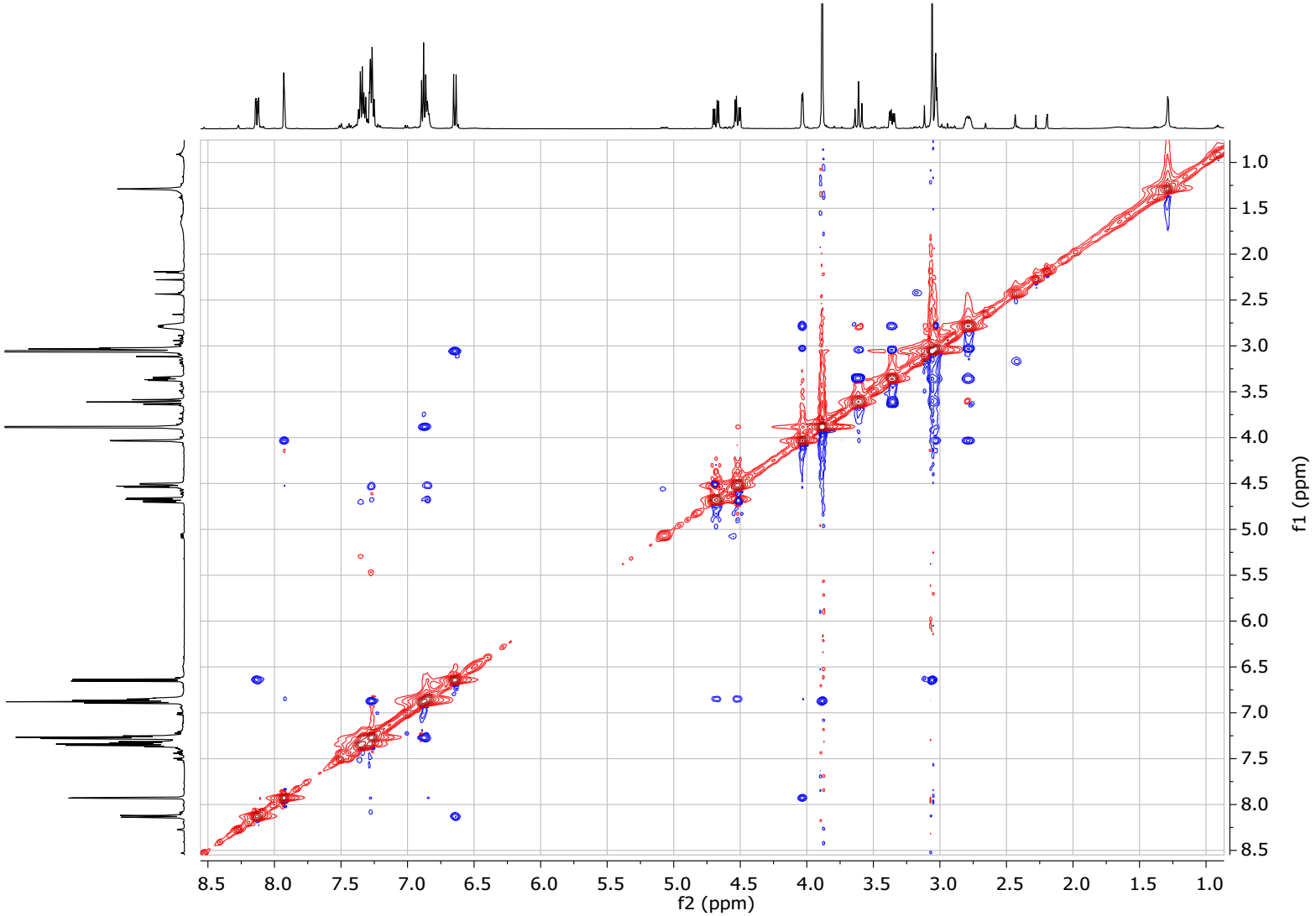

Figure S8. ROESY spectrum of the *rac*-(6a*R**,12*S**,12a*S**)-**3ab** in $CDCl_3$ at 500 MHz.

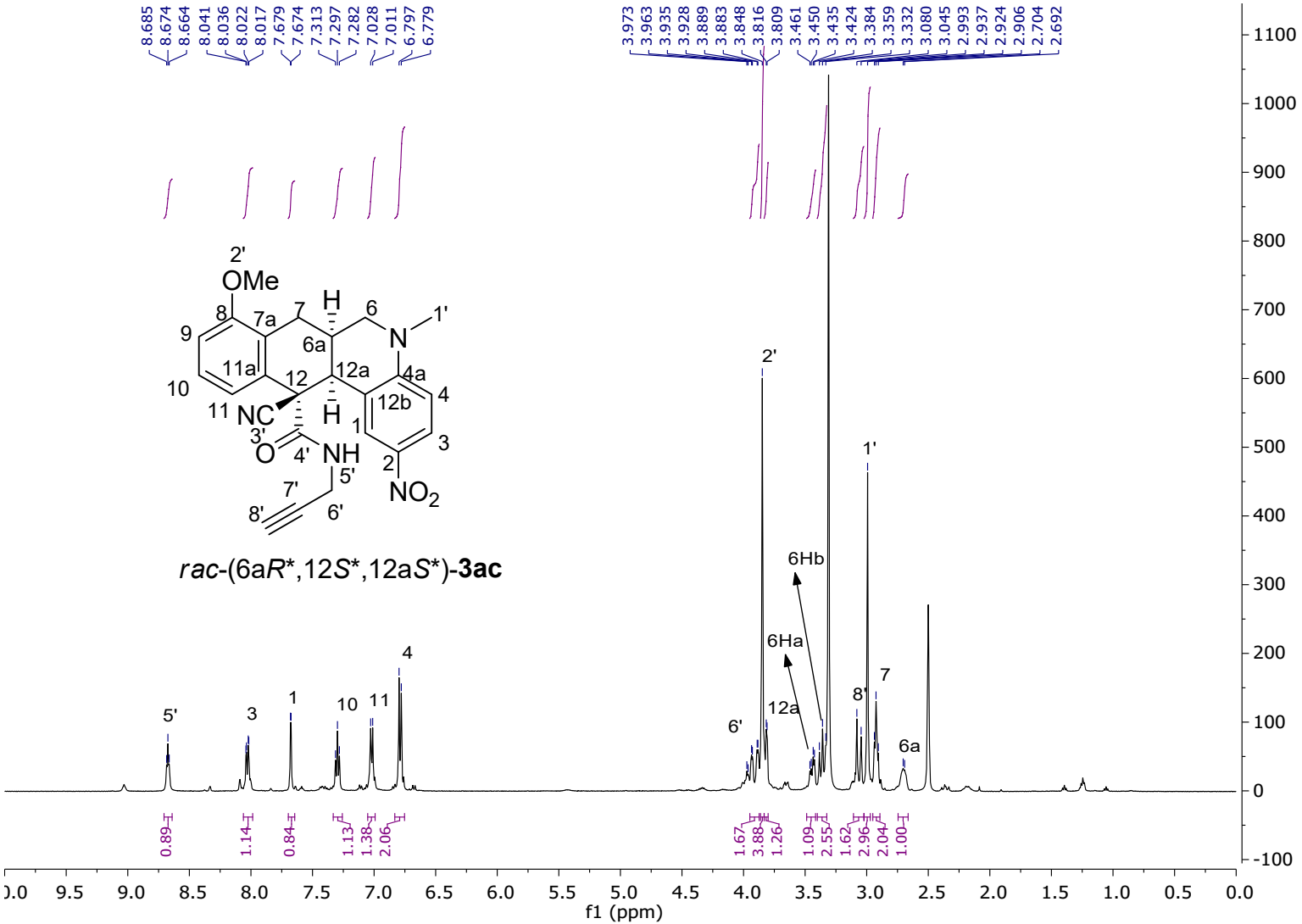

Figure S9. ^{1}H-NMR spectrum of the *rac*-(6a*R**,12*S**,12a*S**)-**3ac** in DMSO-d_6 at 500 MHz.

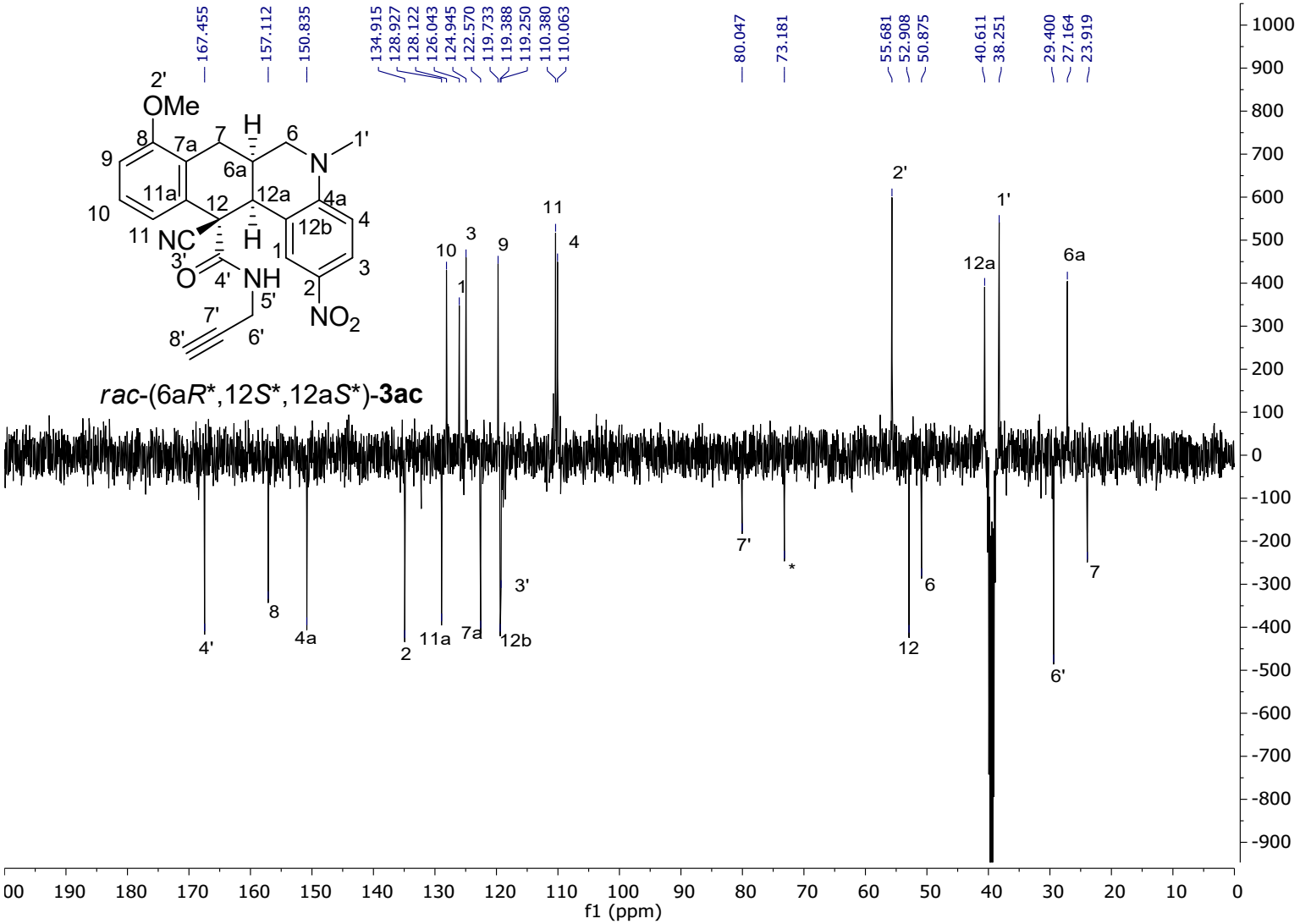

Figure S10. ^{13}C-NMR spectrum of the *rac*-(6a*R**,12*S**,12a*S**)-**3ac** in DMSO-d_6 at 125 MHz.

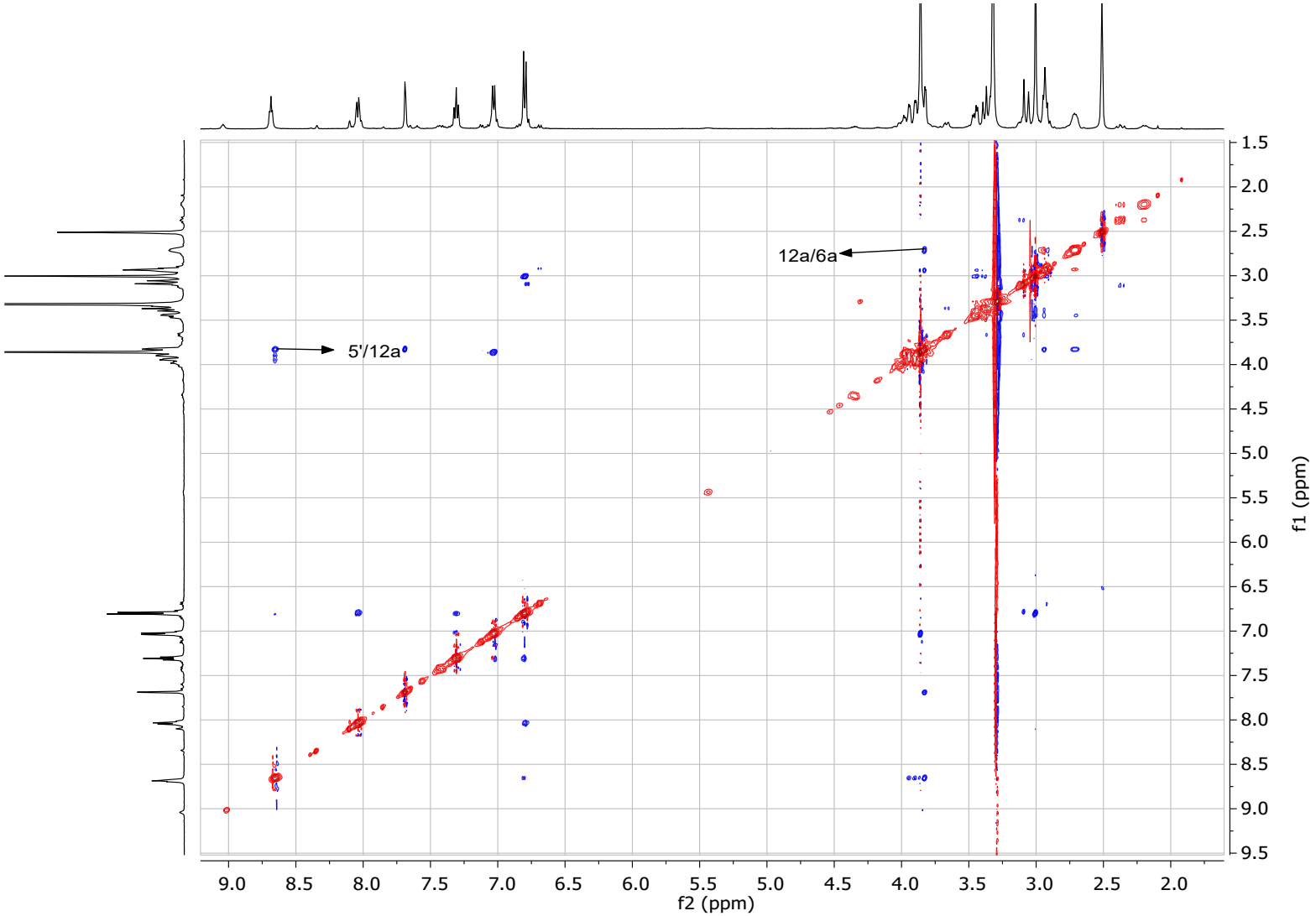

Figure S11. ROESY spectrum of the *rac*-(6a*R**,12*S**,12a*S**)-**3ac** in DMSO-d_6 at 500 MHz.

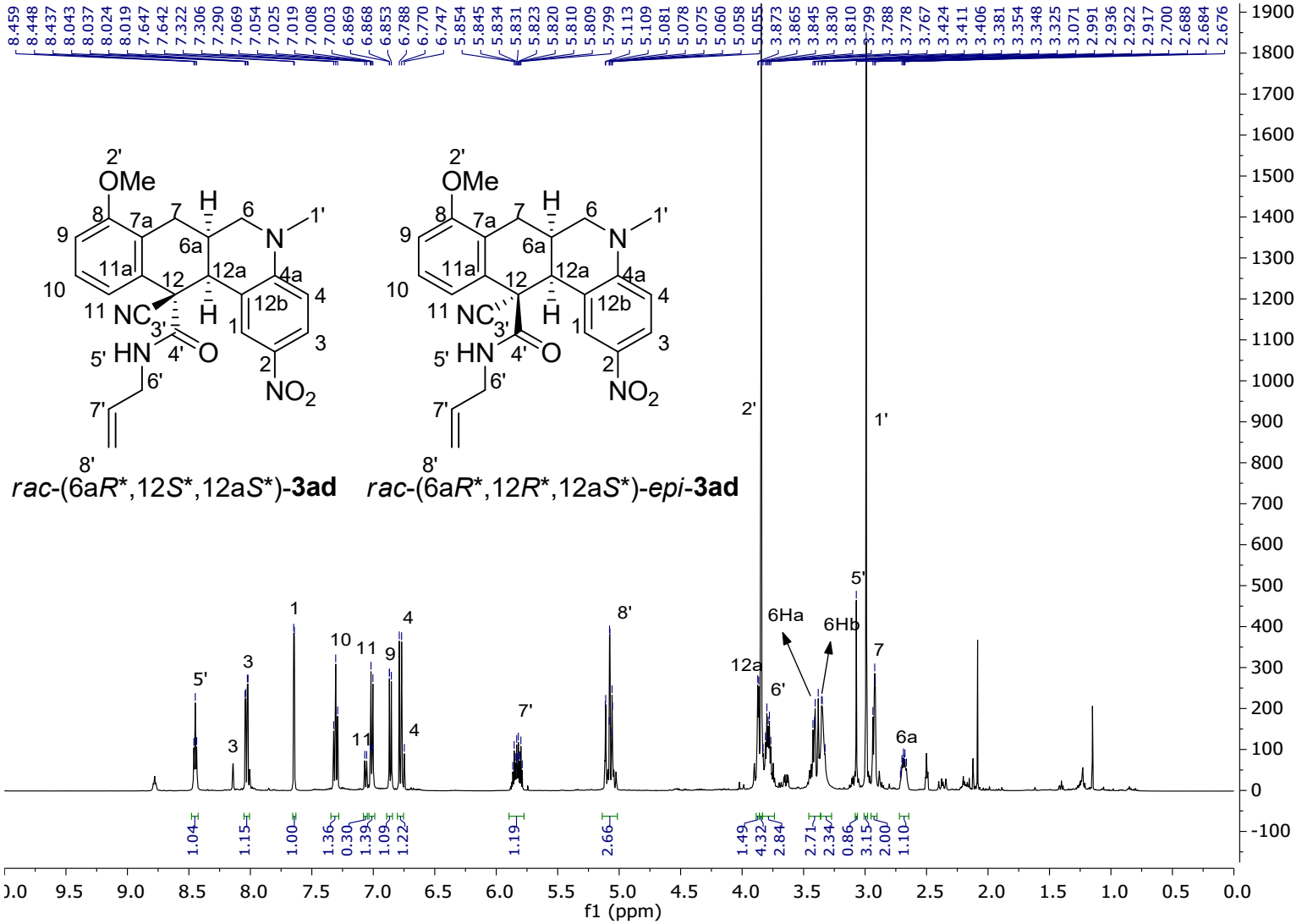

Figure S12. ^{1}H-NMR spectrum of the *rac*-(6a*R**,12*S**,12a*S**)-**3ad** and *rac*-(6a*R**,12*R**,12a*S**)-*epi*-**3ad** in DMSO-d_6 at 500 MHz.

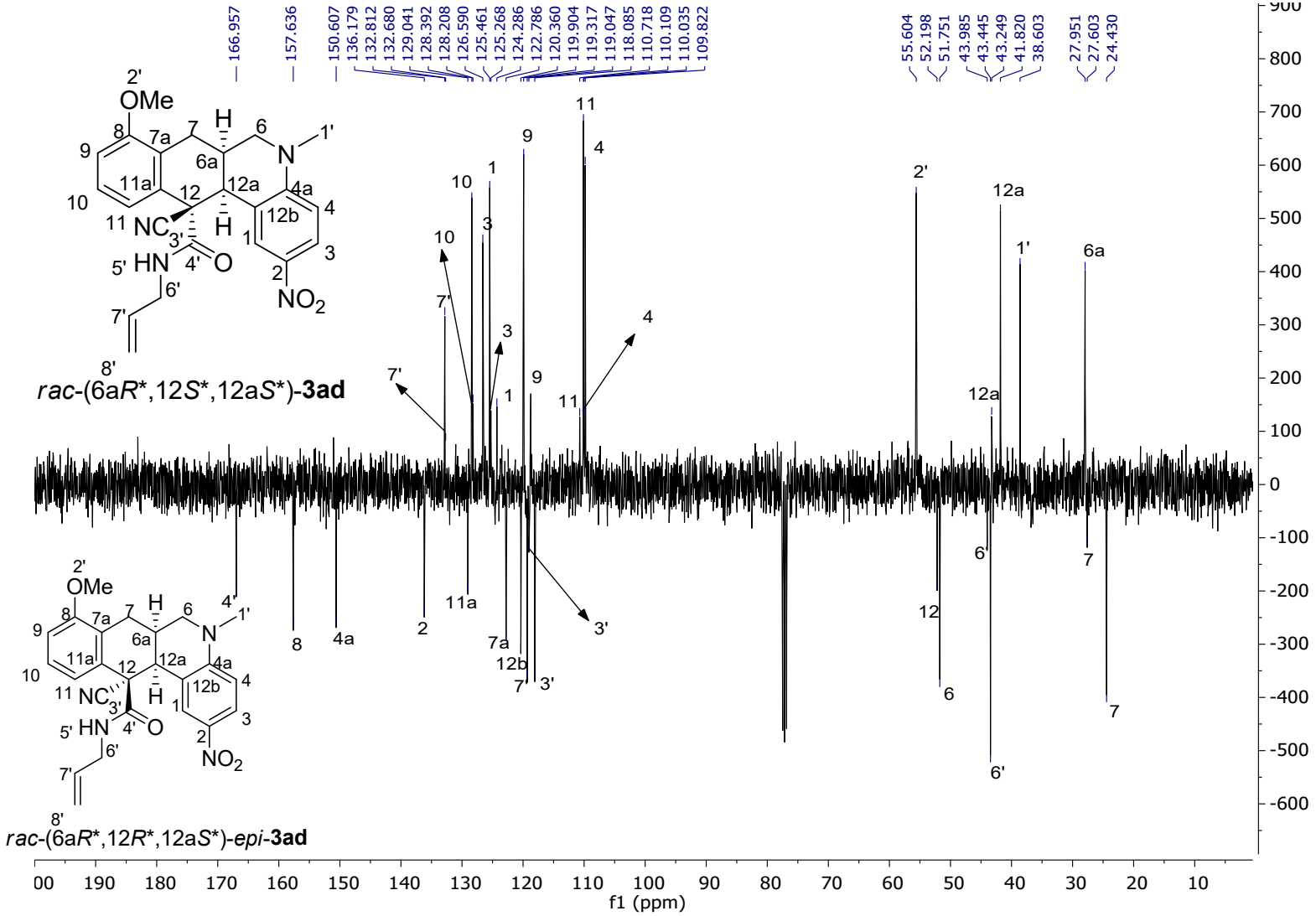

Figure S13. ^{13}C-NMR spectrum of *rac*-(6a*R**,12*S**,12a*S**)-**3ag** and *rac*-(6a*R**,12*R**,12a*S**)-*epi*-**3ag** in $CDCl_3$ at 100 MHz.

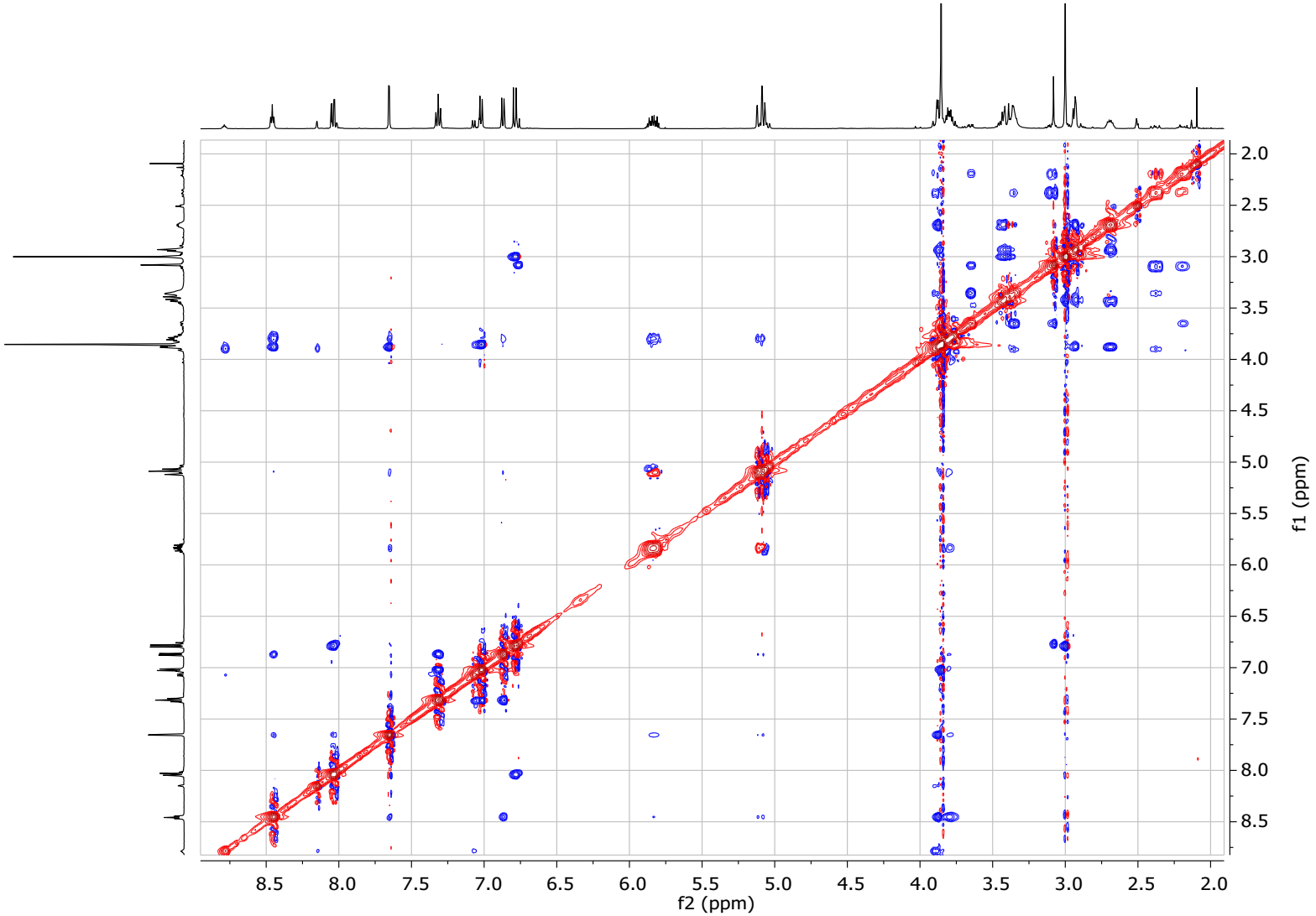

Figure S14. ROESY spectrum of the *rac*-(6a*R**,12*S**,12a*S**)-**3ad** and *rac*-(6a*R**,12*R**,12a*S**)-*epi*-**3ad** in DMSO-d_6 at 500 MHz.

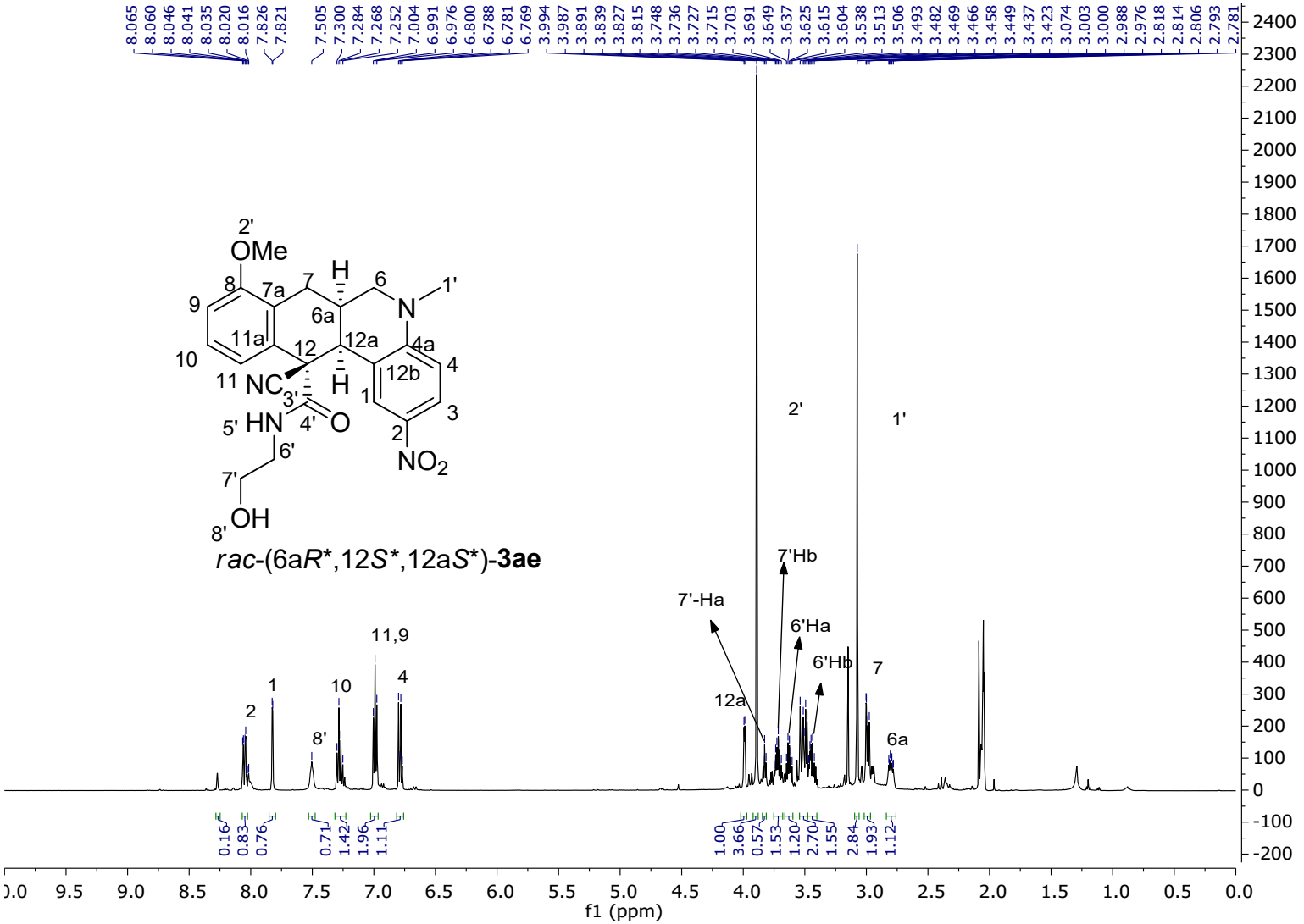

Figure S15. ^{1}H-NMR spectrum of the *rac*-(6a*R**,12*S*,*12a*S**)-**3ae** in acetone-d_6 at 500 MHz.

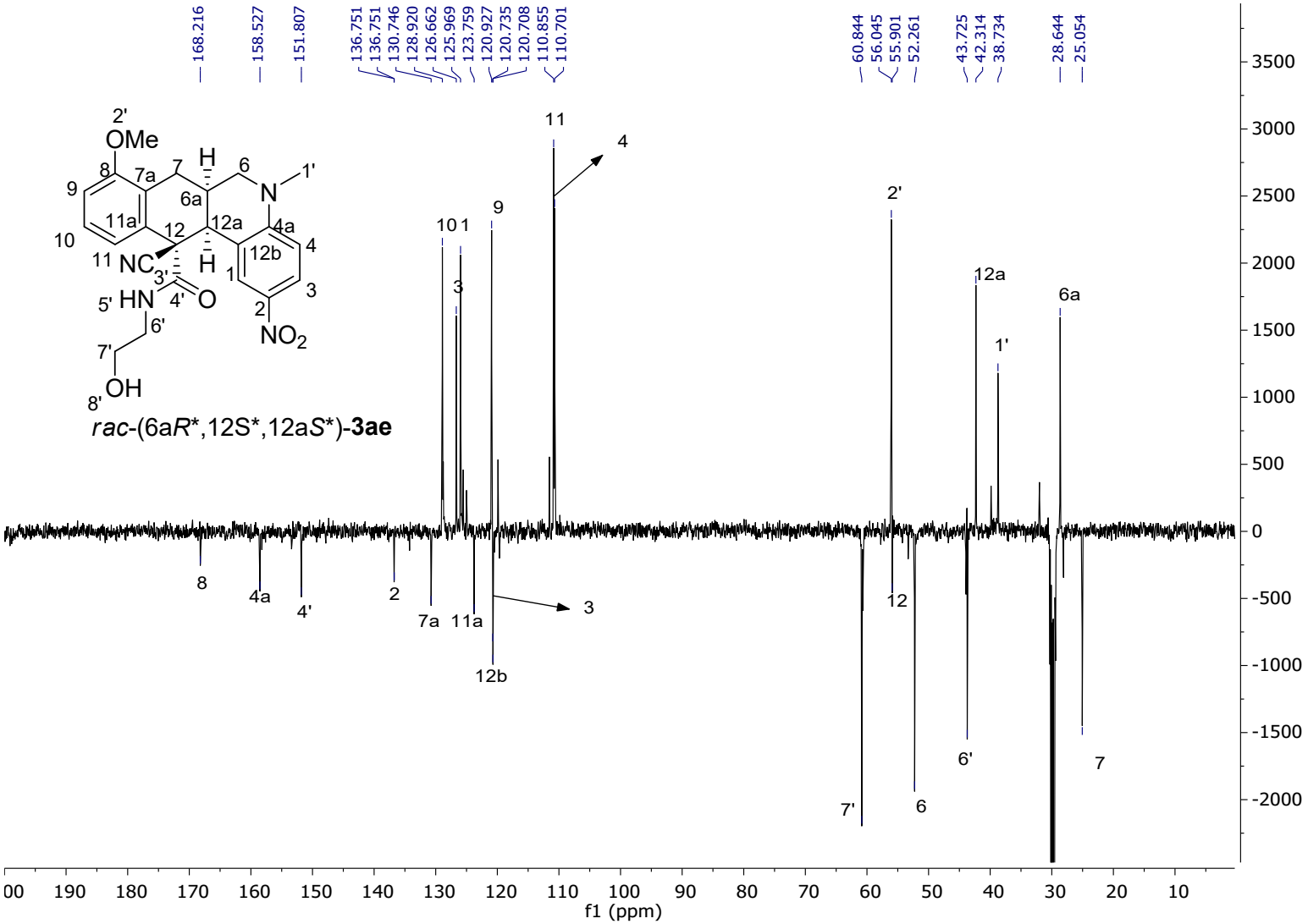

Figure S16. ^{13}C-NMR spectrum of the *rac*-(6a*R**,12S*,12a*S**)-**3ae** in acetone-d_6 at 125 MHz.

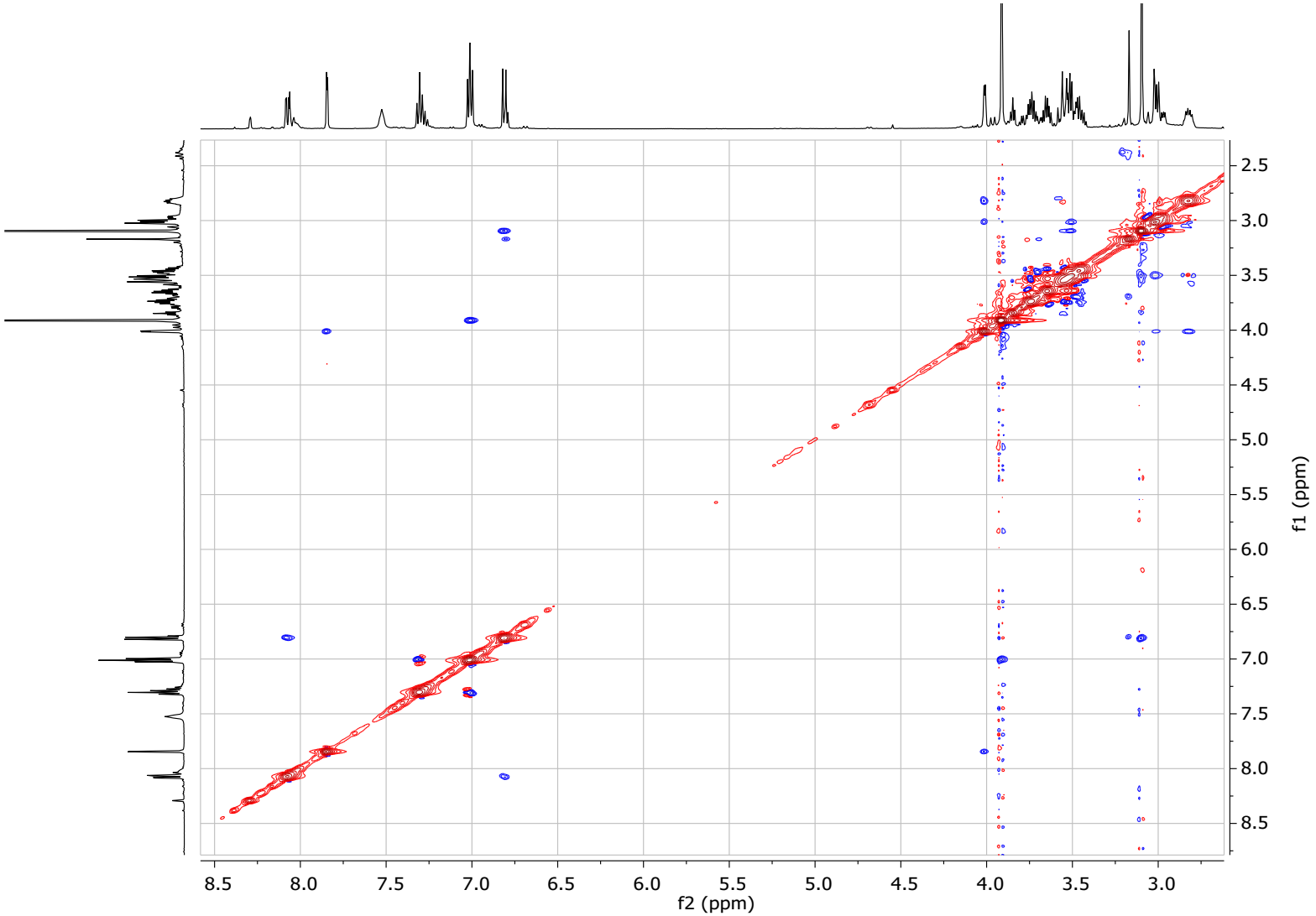

Figure S17. ROESY spectrum of the *rac*-(6a*R**,12*S**,12a*S**)-**3ae** in acetone-d_6 at 500 MHz.

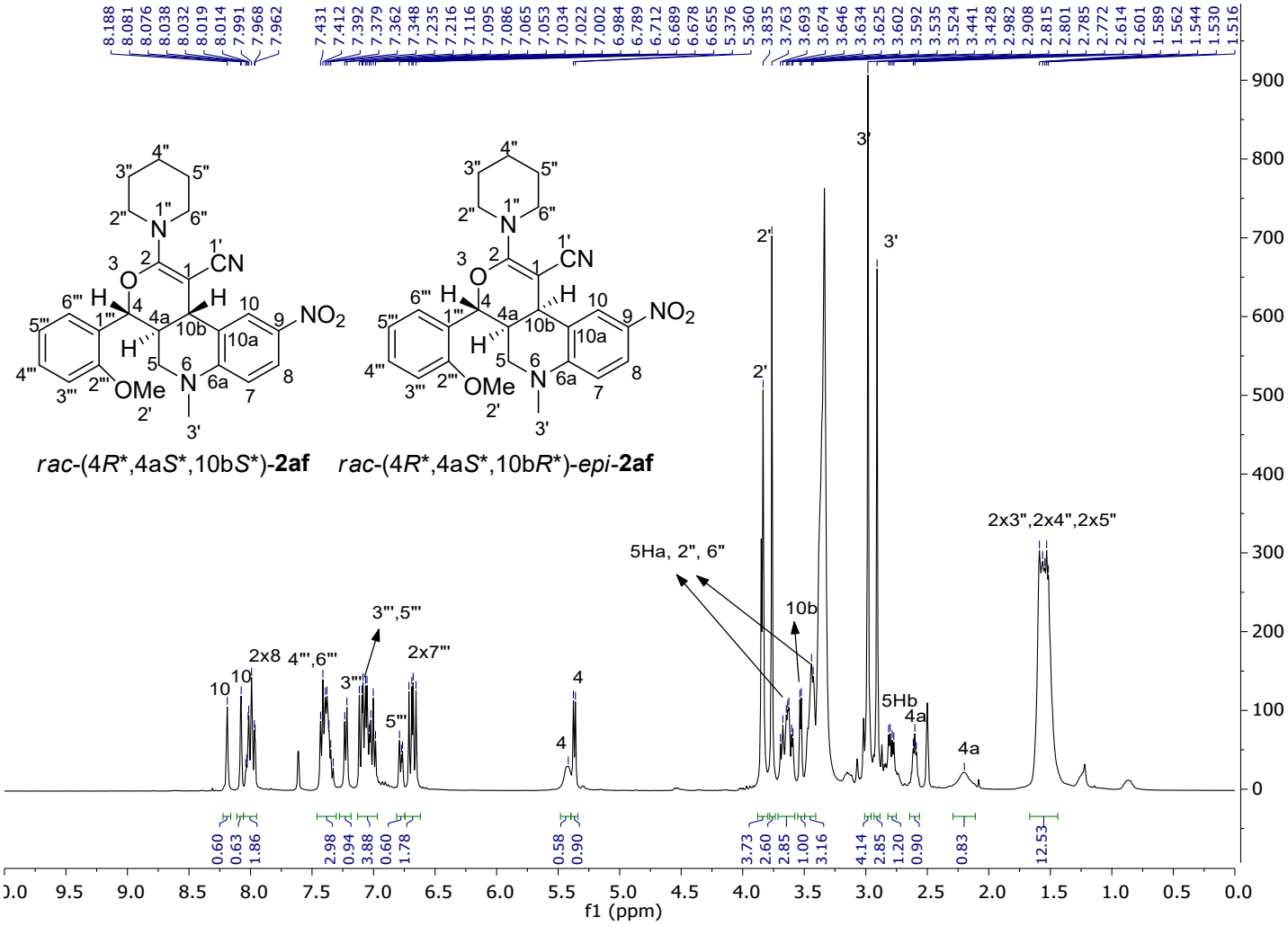

Figure S18. ^{1}H-NMR spectrum of the *rac*-(4*R**,4a*S**,10b*S**)-**2af** and *rac*-(4*R**,4a*S**,10b*R**)-*epi*-**2af** in DMSO-d_6 at 400 MHz.

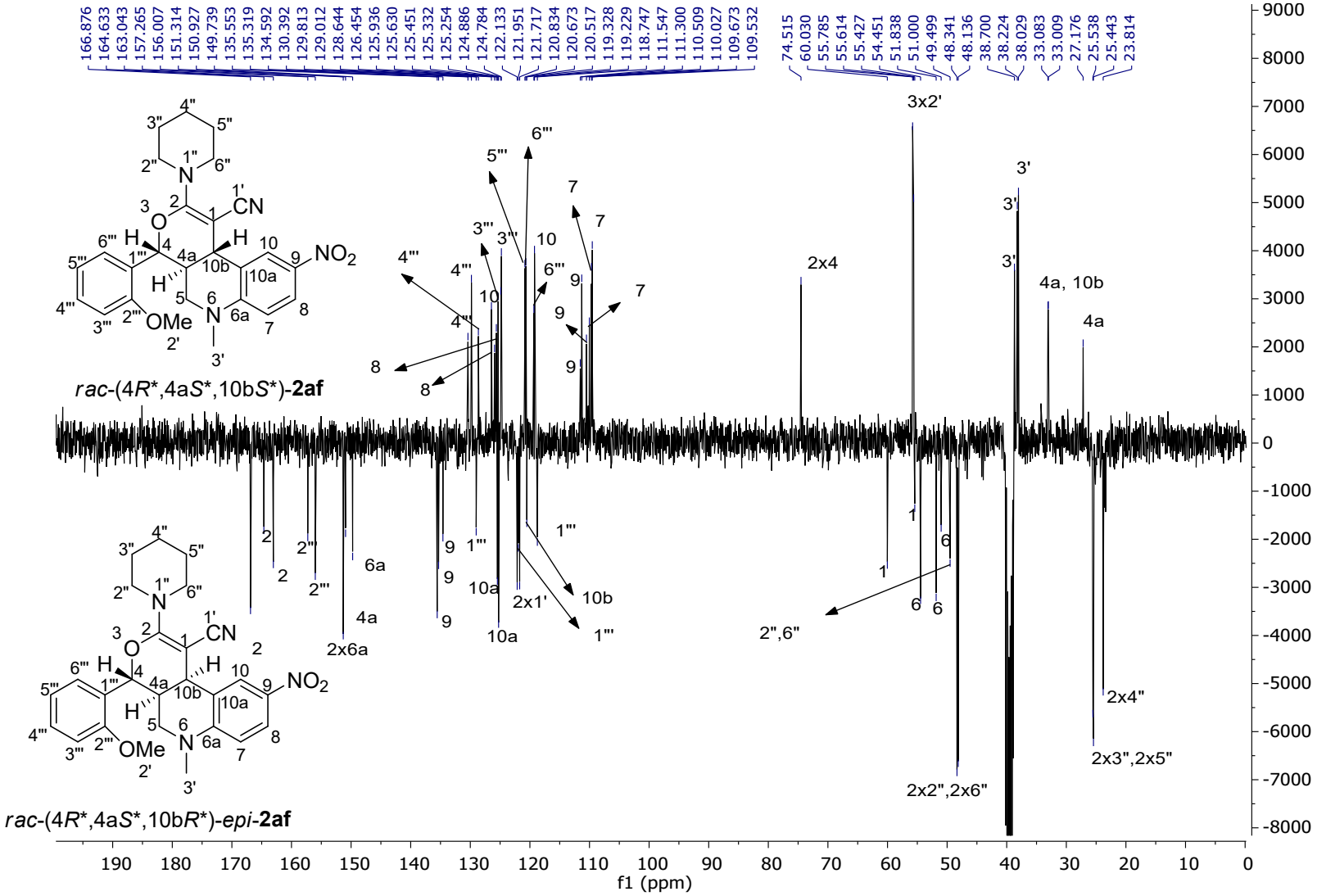

Figure S19. ^{13}C-NMR spectrum of the *rac*-(4*R**,4a*S**,10b*S**)-**2af** and *rac*-(4*R**,4a*S**,10b*R**)-*epi*-**2af** in DMSO-d_6 at 100 MHz.

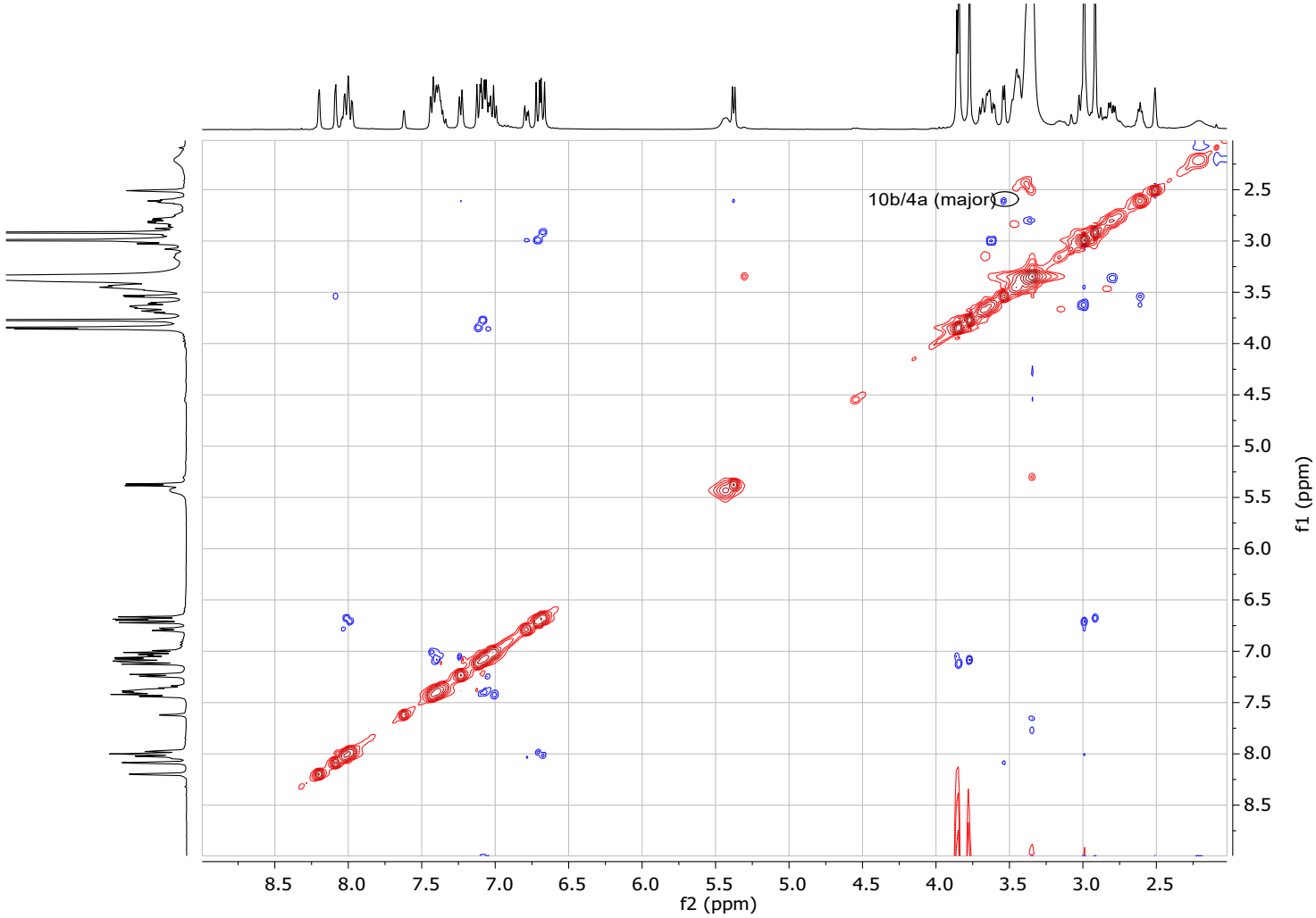

Figure S20. NOESY spectrum of the *rac*-(4*R**,4a*S**,10b*S**)-**2af** and *rac*-(4*R**,4a*S**,10b*R**)-*epi*-**2af** in DMSO-d_6 at 400 MHz

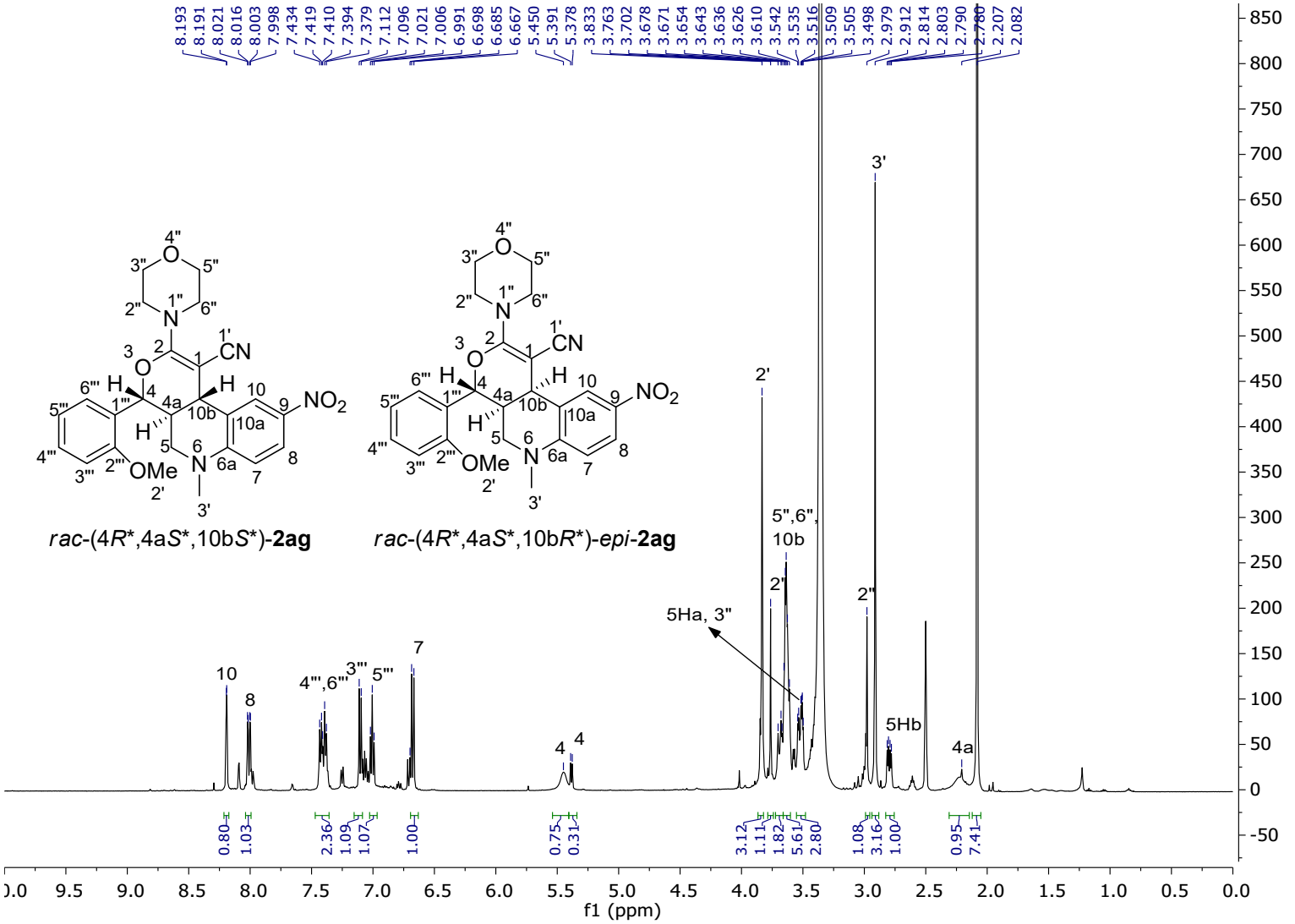

Figure S21. ^{1}H-NMR spectrum of the *rac*-(4*R**,4a*S**,10b*S**)-**2ag** and *rac*-(4*R**,4a*S**,10b*R**)-*epi*-**2ag** in DMSO-d_6 at 500 MHz.

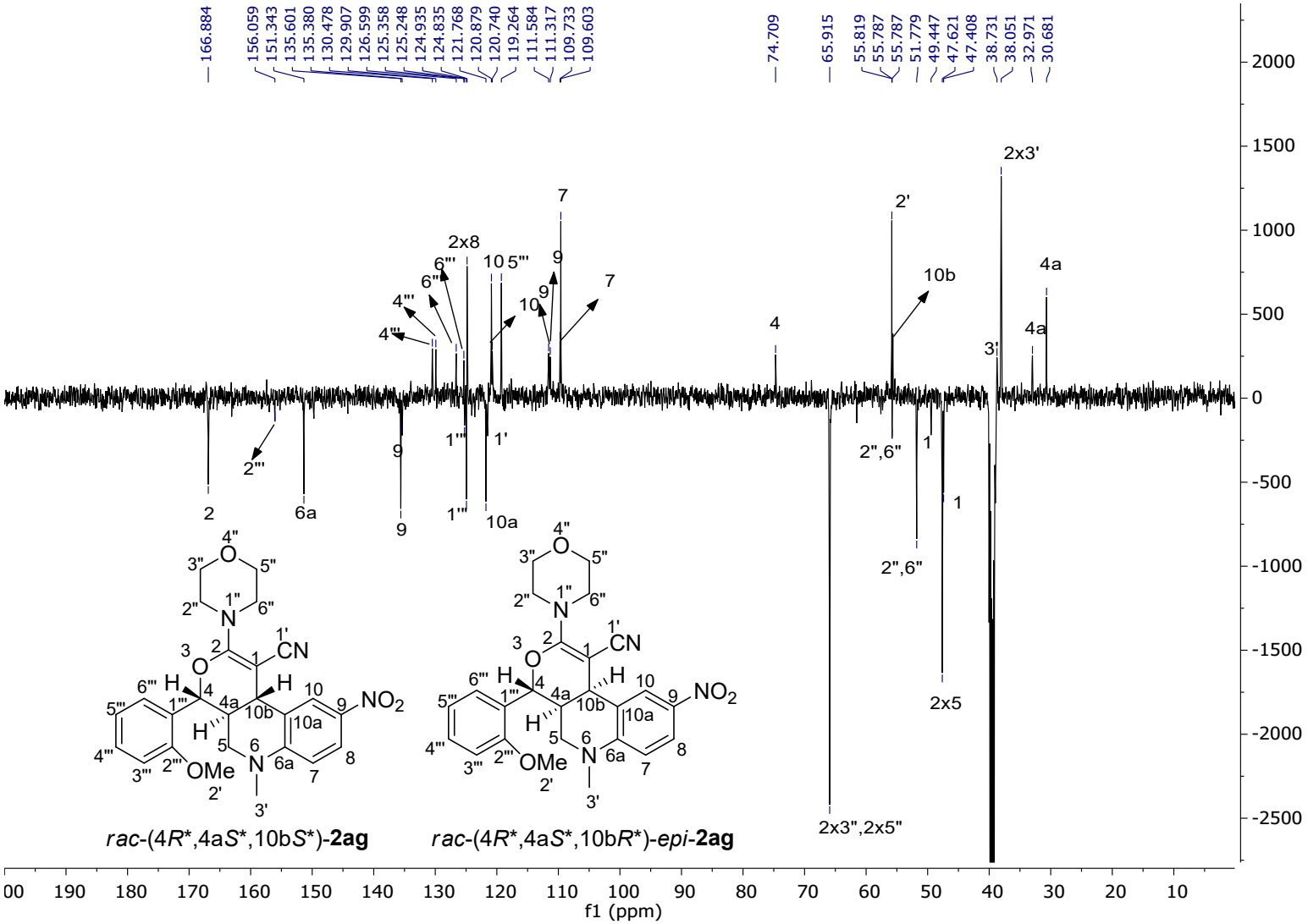

Figure S22. ^{13}C-NMR spectrum of the *rac*-(4*R**,4a*S**,10b*S**)-**2ag** and *rac*-(4*R**,4a*S**,10b*R**)-*epi*-**2ag** in DMSO-d$_6$ at 125 MHz.

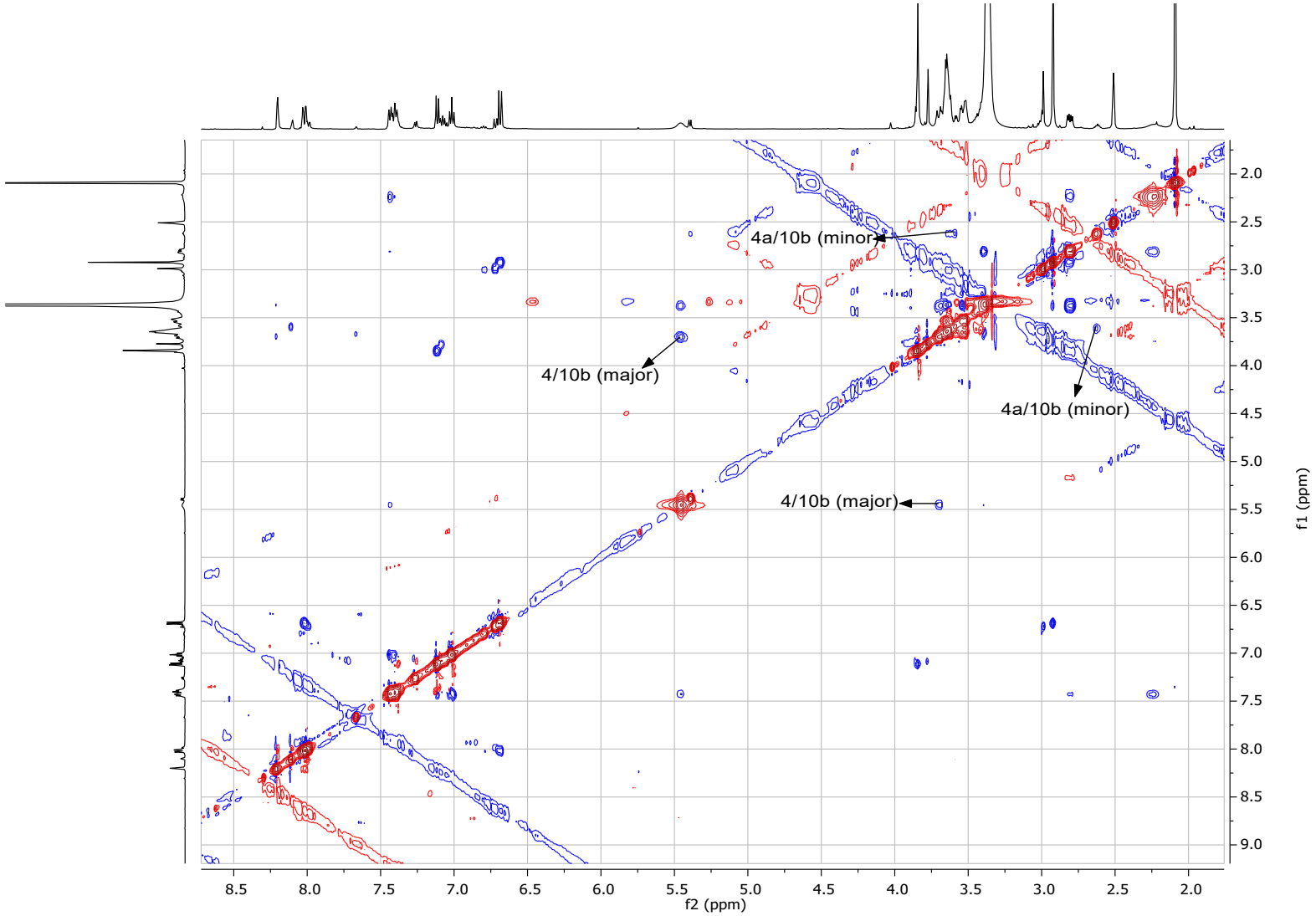

Figure S23. ROESY spectrum of the *rac*-(4*R**,4a*S**,10b*S**)-**2ag** and *rac*-(4*R**,4a*S**,10b*R**)-*epi*-**2ag** in DMSO-d_6 at 500 MHz.

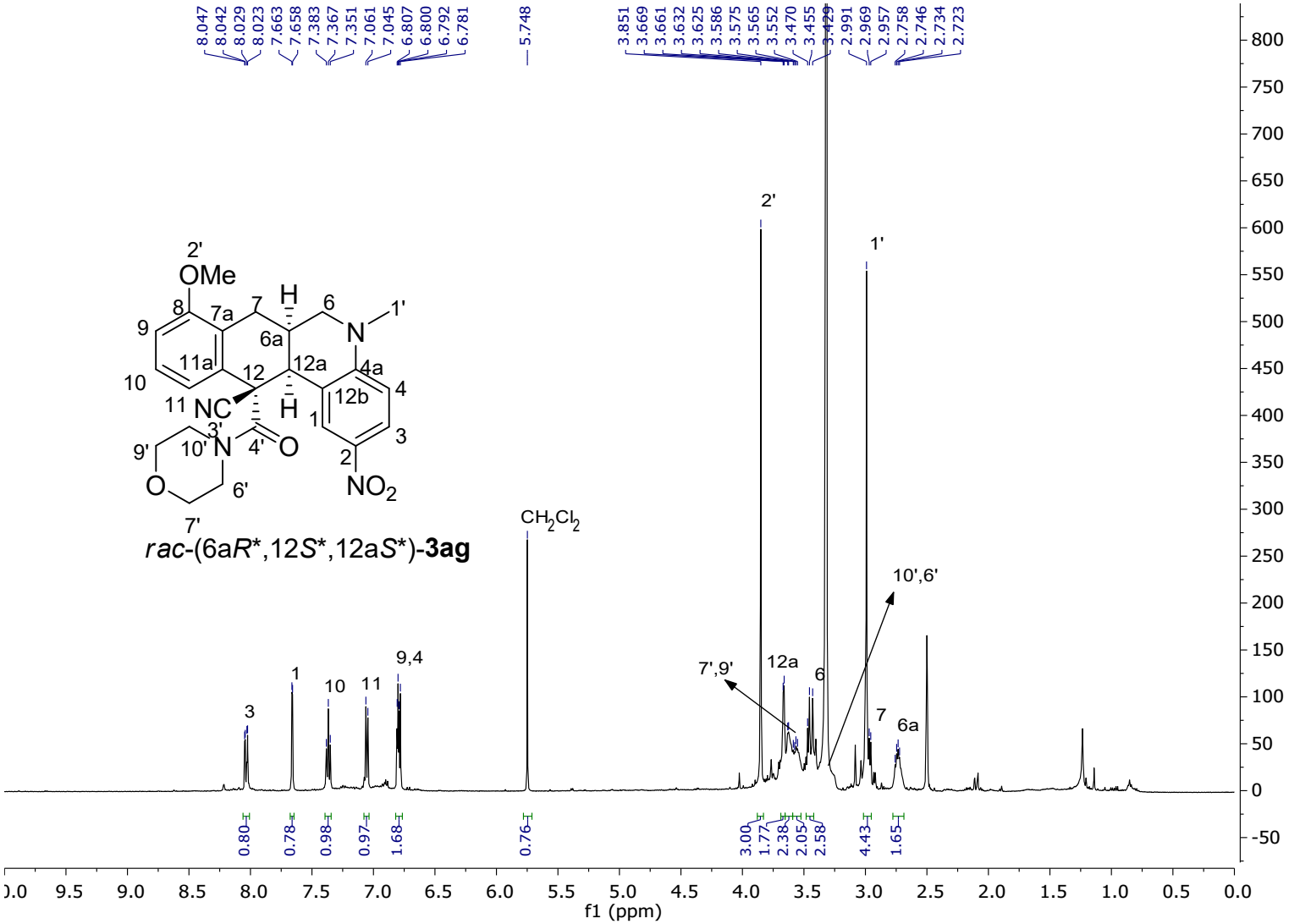

Figure S24. ^{1}H-NMR spectrum of the *rac*-(6a*R**,12*S**,12a*S**)-**3ag** in DMSO-d_6 at 500 MHz.

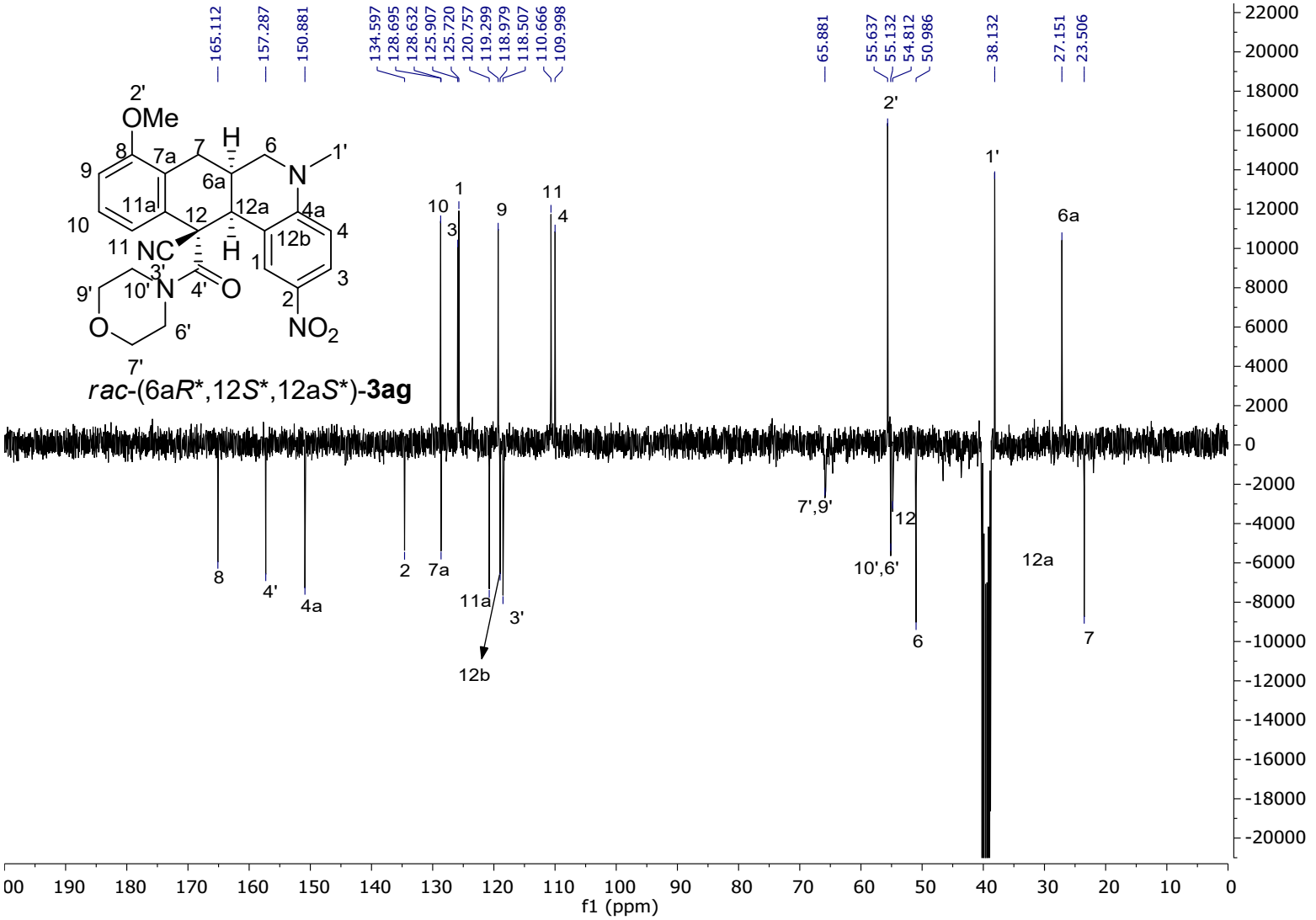

Figure S25. ^{13}C-NMR spectrum of the *rac*-(6a*R**,12*S**,12a*S**)-**3ag** in DMSO-d_6 at 90 MHz.

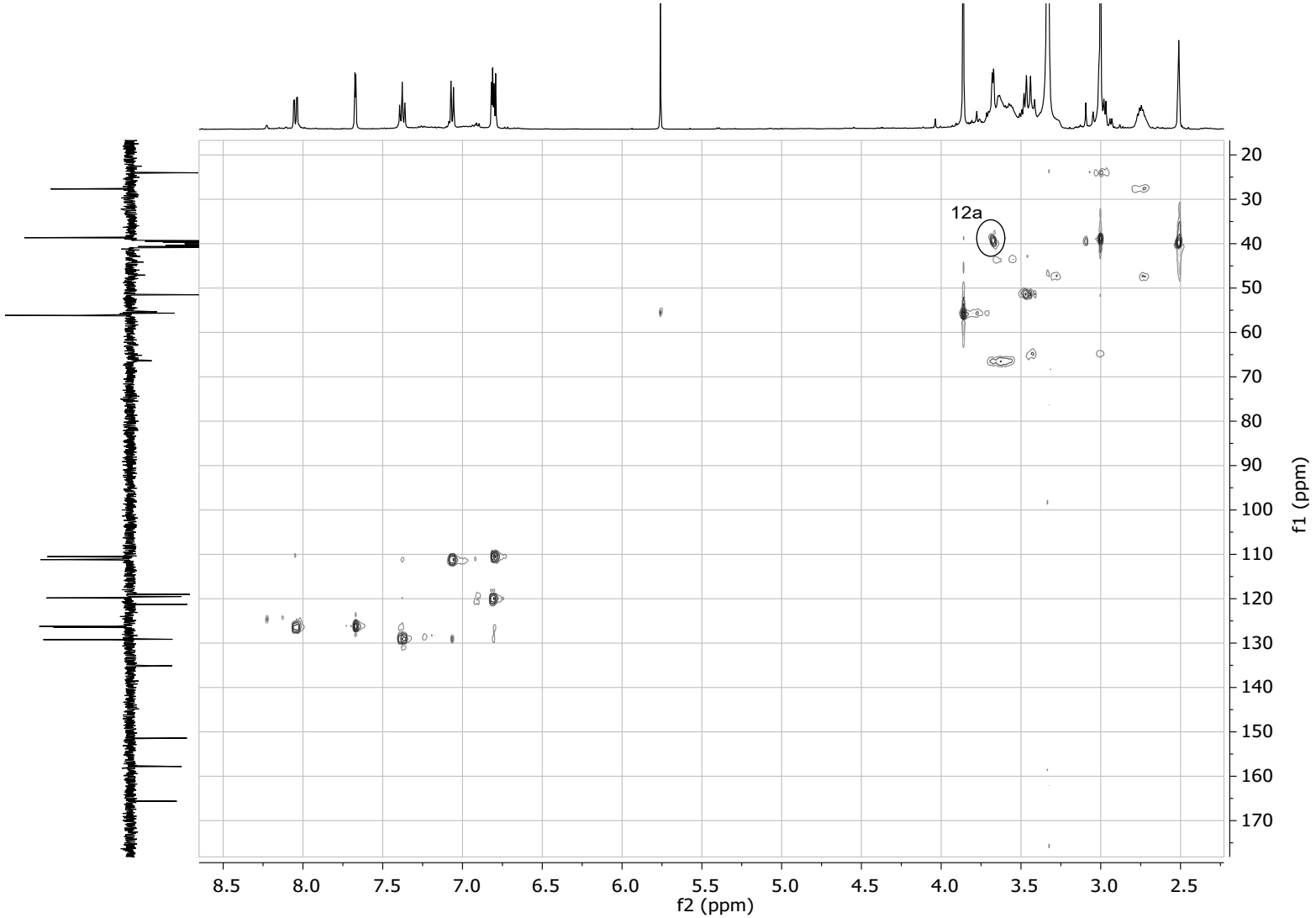

Figure S26. HSQC spectrum of the *rac*-(6a*R**,12*S**,12a*S**)-**3ag** in DMSO-d_6 at 500 MHz.

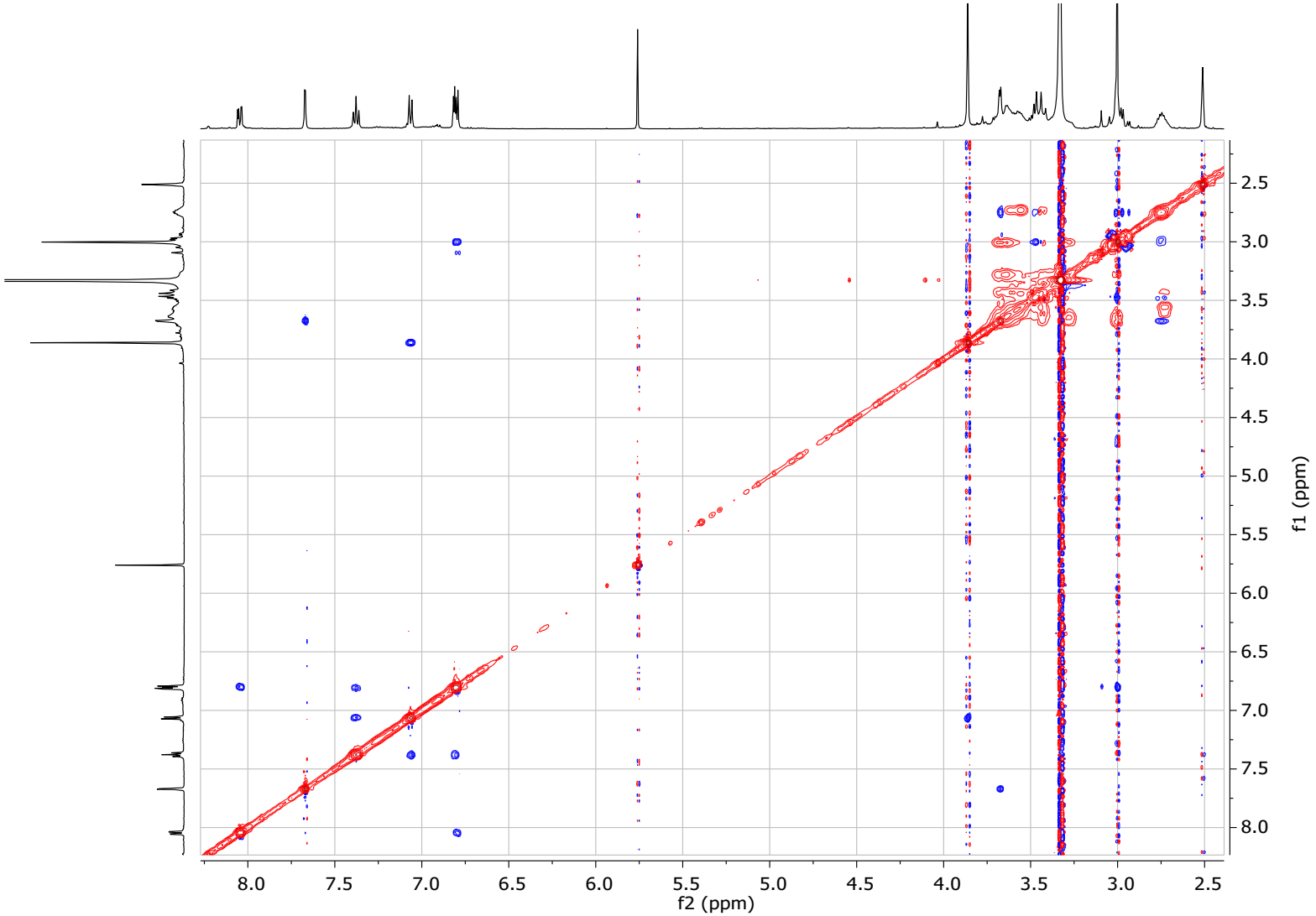

Figure S27. ROESY spectrum of the *rac*-(6a*R**,12*S**,12a*S**)-**3ag** in DMSO-d_6 at 500 MHz.

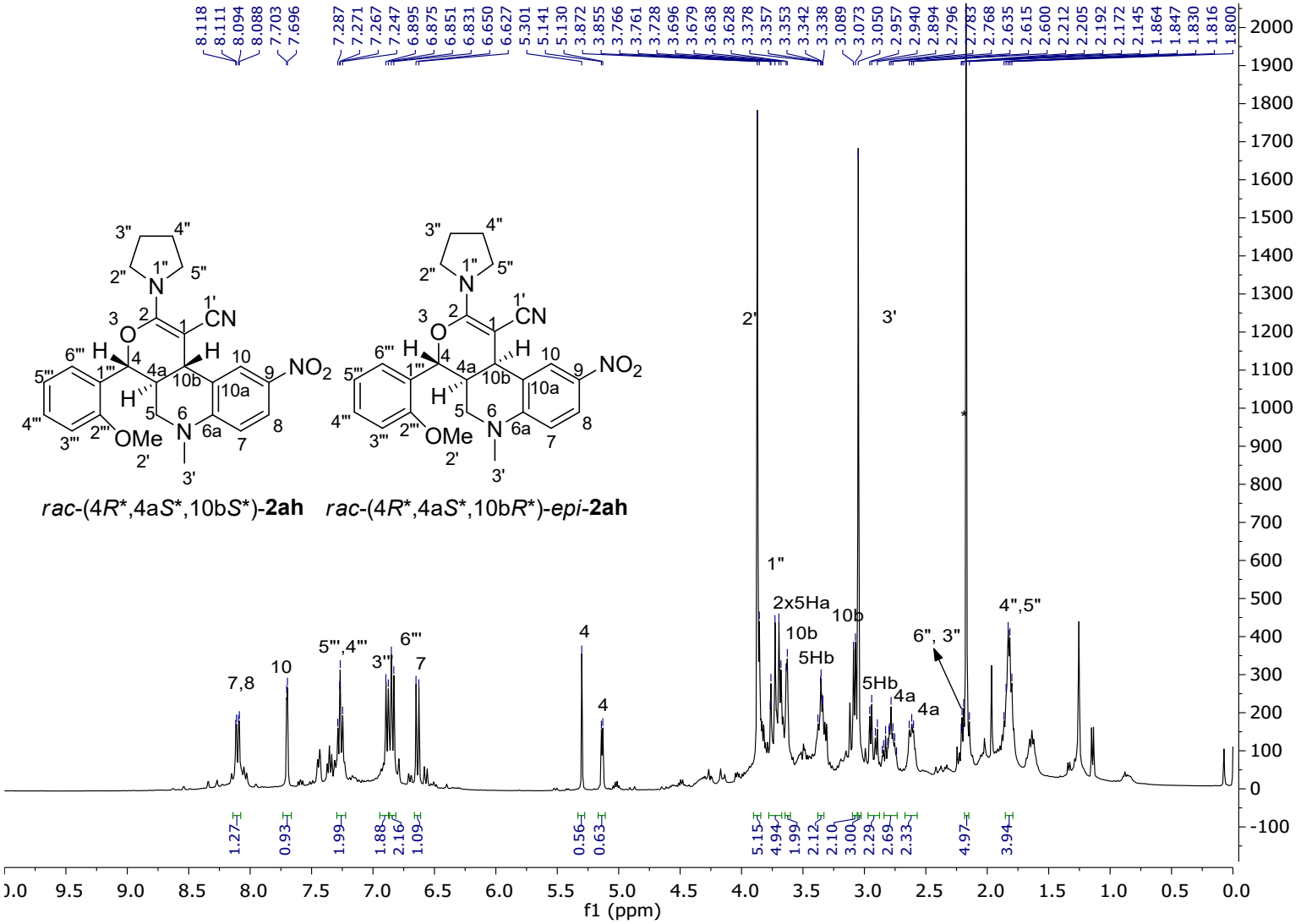

Figure S28. ^{1}H-NMR spectrum of the *rac*-(4*R**,4a*S**,10b*S**)-**2ah** and *rac*-(4*R**,4a*S**,10b*R**)-*epi*-**2ah** in $CDCl_3$ at 400 MHz.

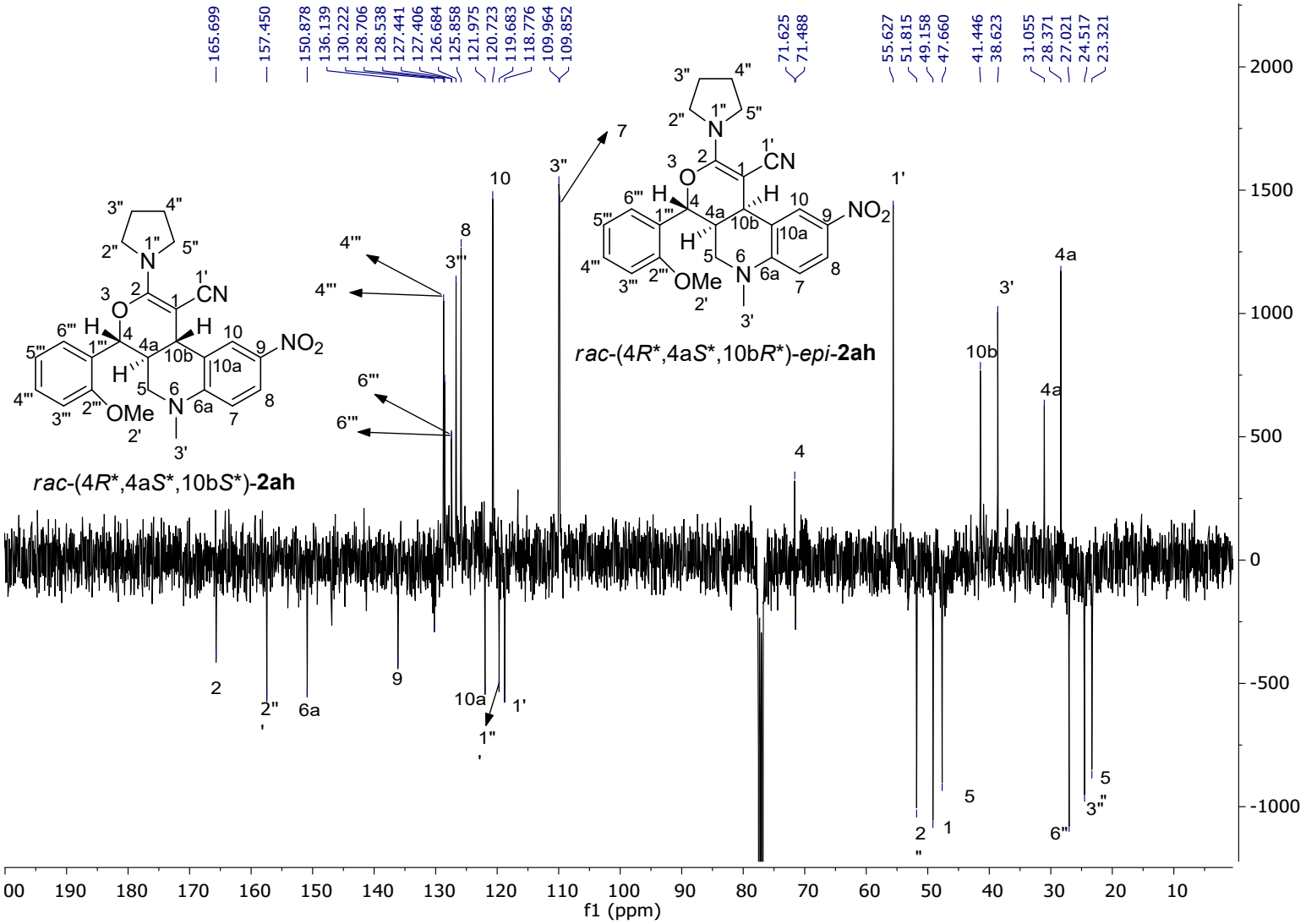

Figure S29. [1]H-NMR spectrum of the *rac*-(4*R**,4a*S**,10b*S**)-**2ah** and *rac*-(4*R**,4a*S**,10b*R**)-*epi*-**2ah** in $CDCl_3$ at 100 MHz.

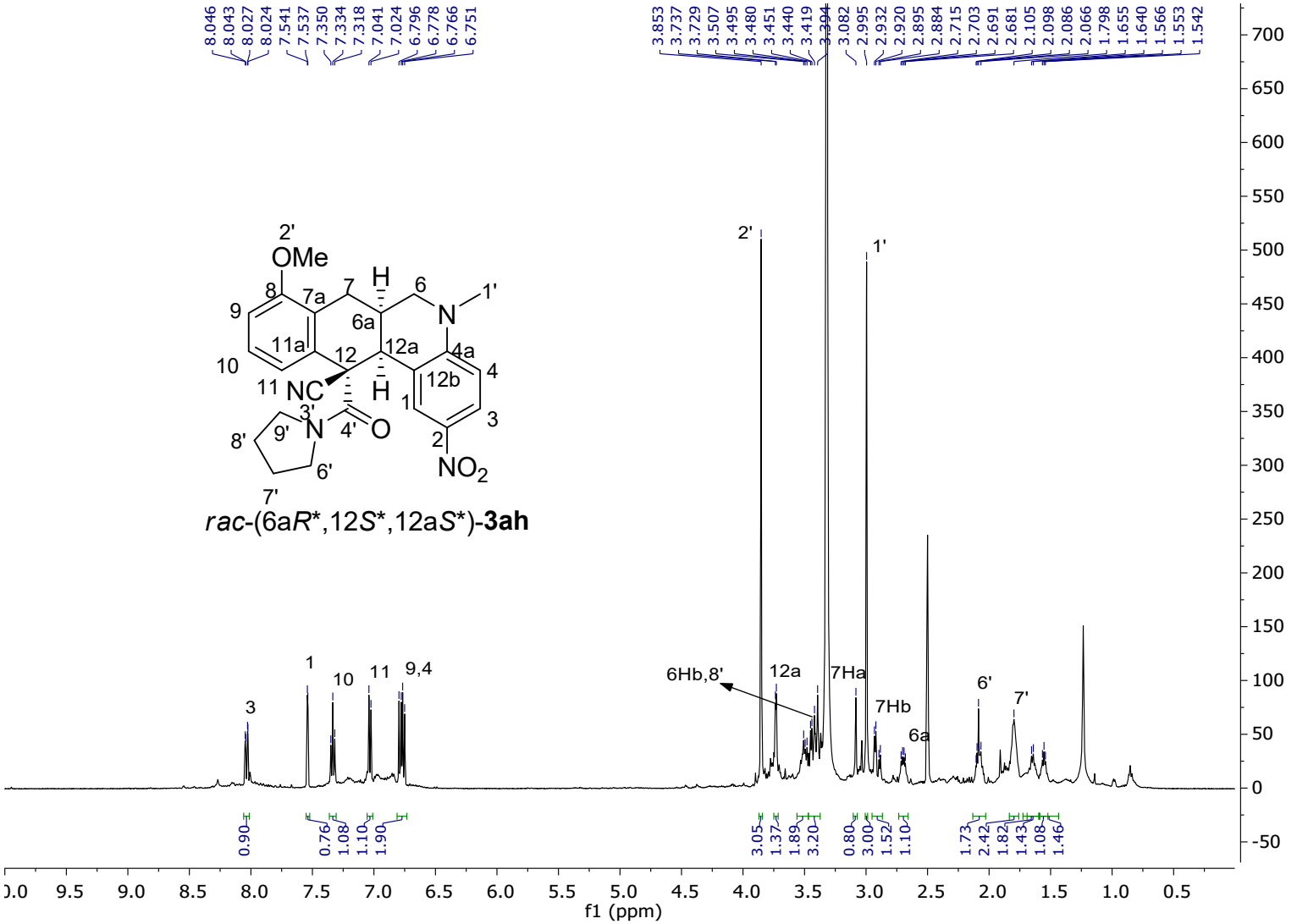

Figure S30. ^{1}H-NMR spectrum of the *rac*-(6a*R**,12*S**,12a*S**)-**3ah** in DMSO-d_6 at 500 MHz.

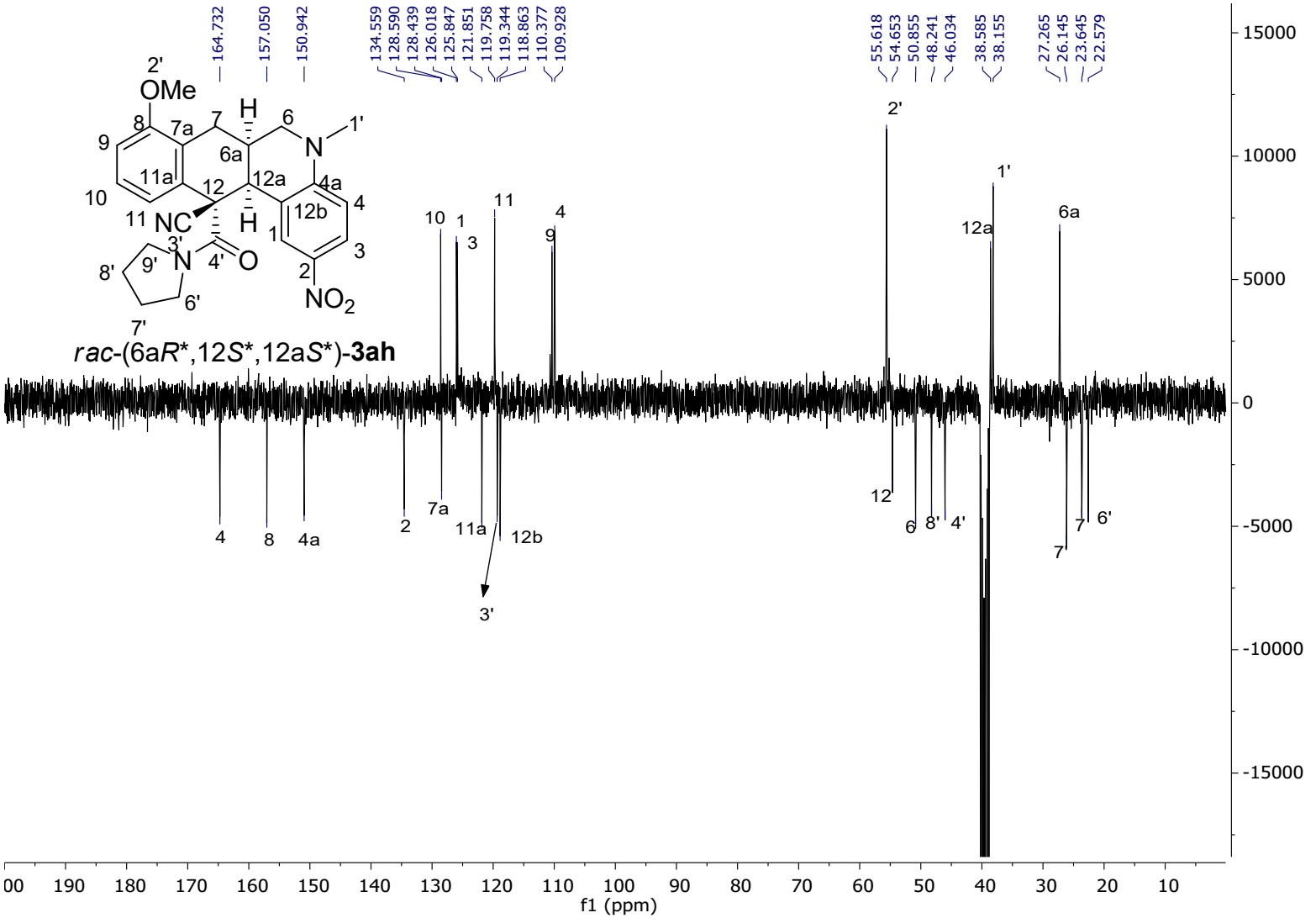

Figure S31. ^{13}C-NMR spectrum of the *rac*-(6a*R**,12*S**,12a*S**)-**3ah** in DMSO-d_6 at 125 MHz.

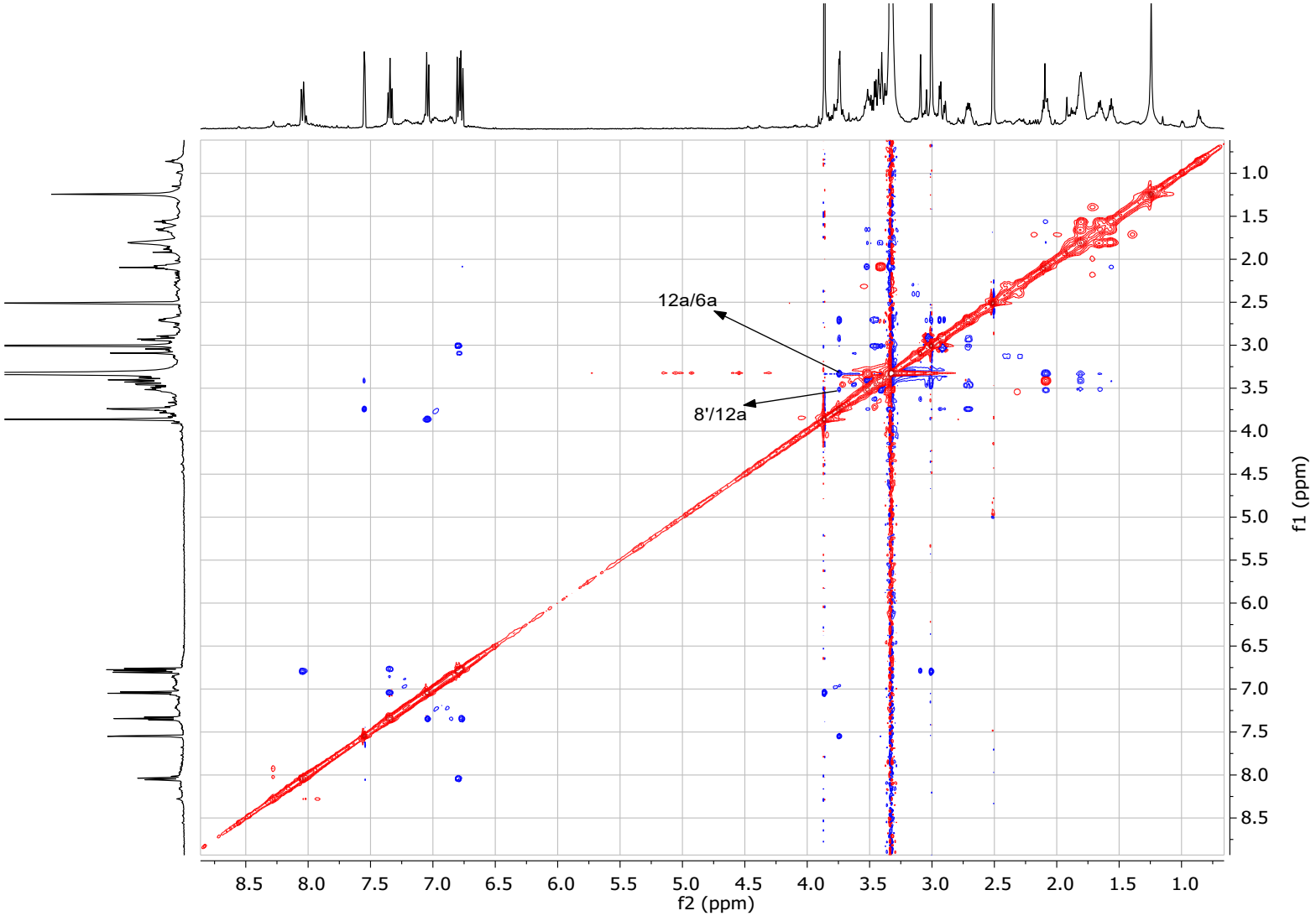

Figure S32. ROESY spectrum of the *rac*-(6a*R**,12*S**,12a*S**)-**3ah** in DMSO-d_6 at 500 MHz.

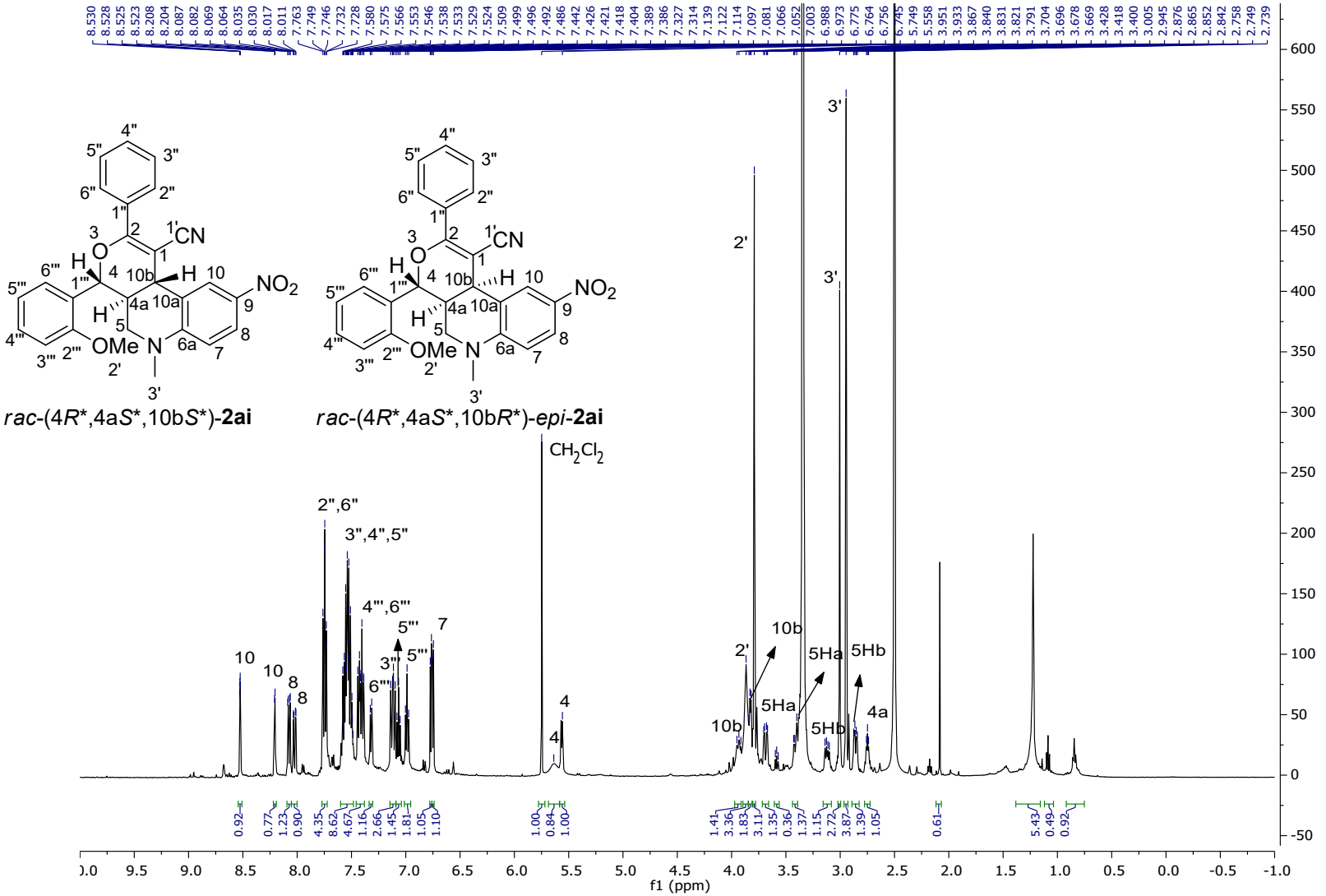

Figure S33. ^{1}H-NMR spectrum of *rac*-(4*R**,4a*S**,10b*S**)-**2ai** and *rac*-(4*R**,4a*S**,10b*R**)-*epi*-**2ai** in DMSO-d_6 at 500 MHz.

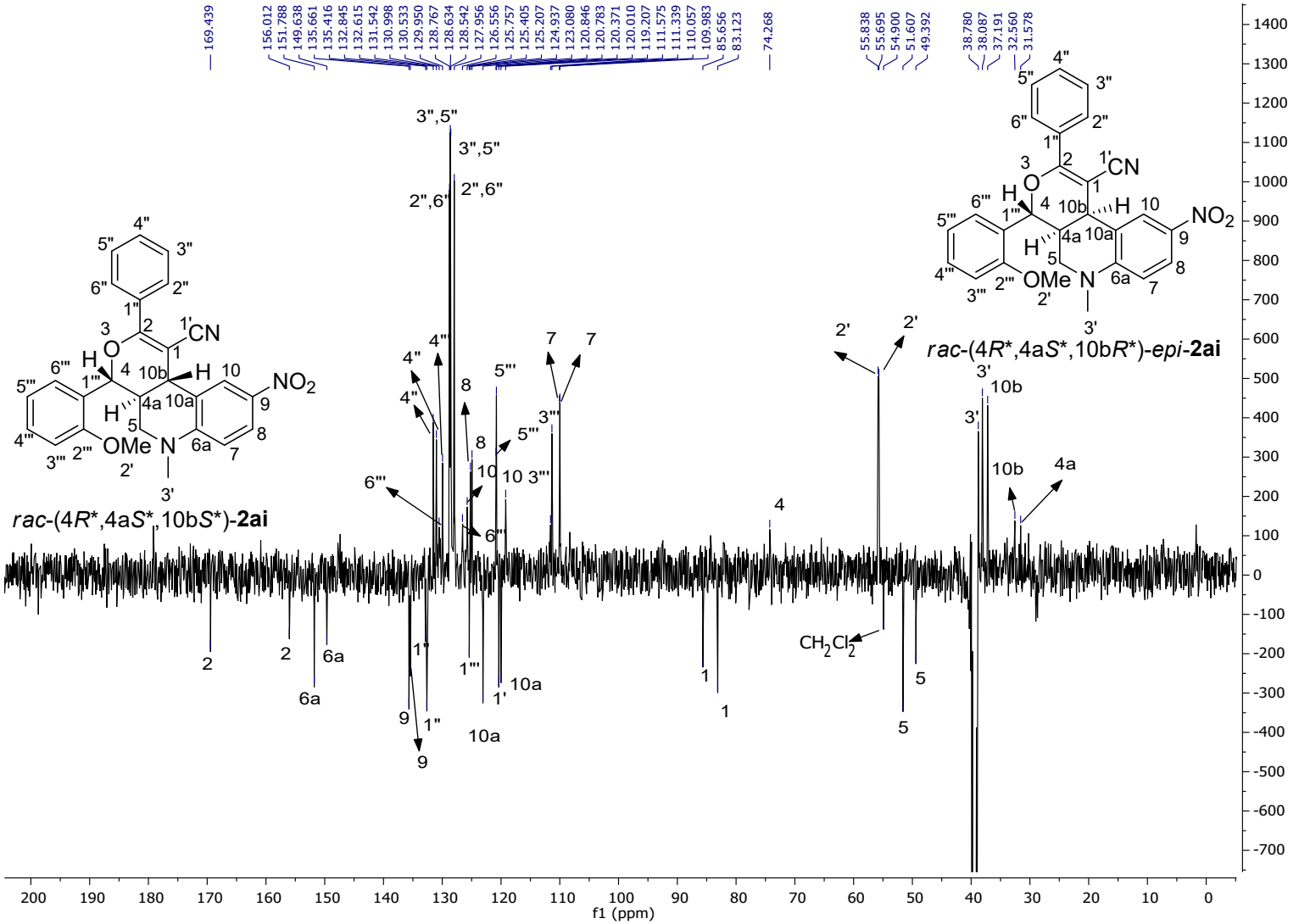

Figure S34. ^{13}C-NMR spectrum of *rac*-(4*R**,4a*S**,10b*S**)-**2ai** and *rac*-(4*R**,4a*S**,10b*R**)-*epi*-**2ai** in DMSO-d_6 at 125 MHz.

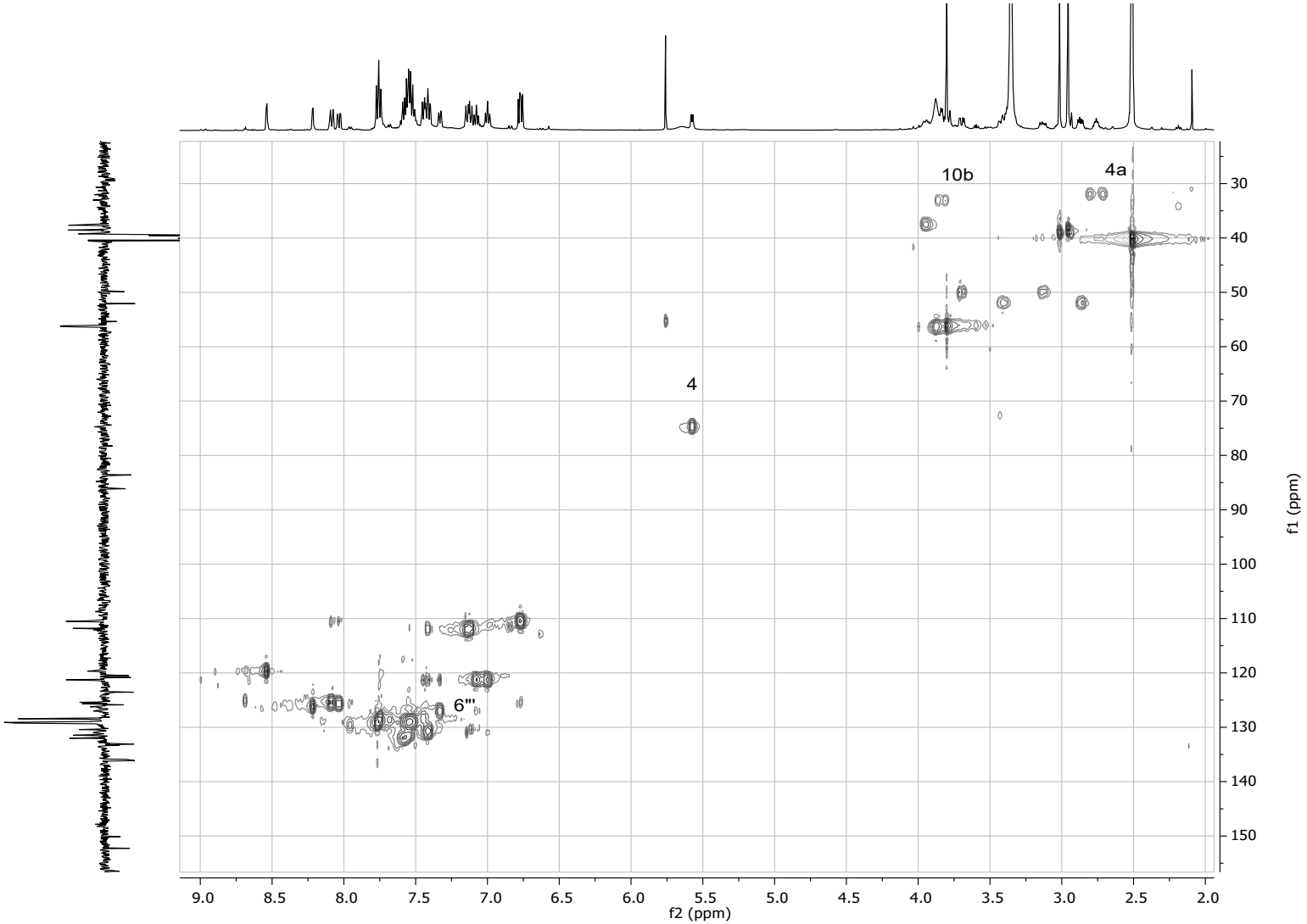

Figure S35. HSQC spectrum of *rac*-(4*R**,4a*S**,10b*S**)-**2ai** and *rac*-(4*R**,4a*S**,10b*R**)-*epi*-**2ai** in DMSO-d_6 at 500 MHz.

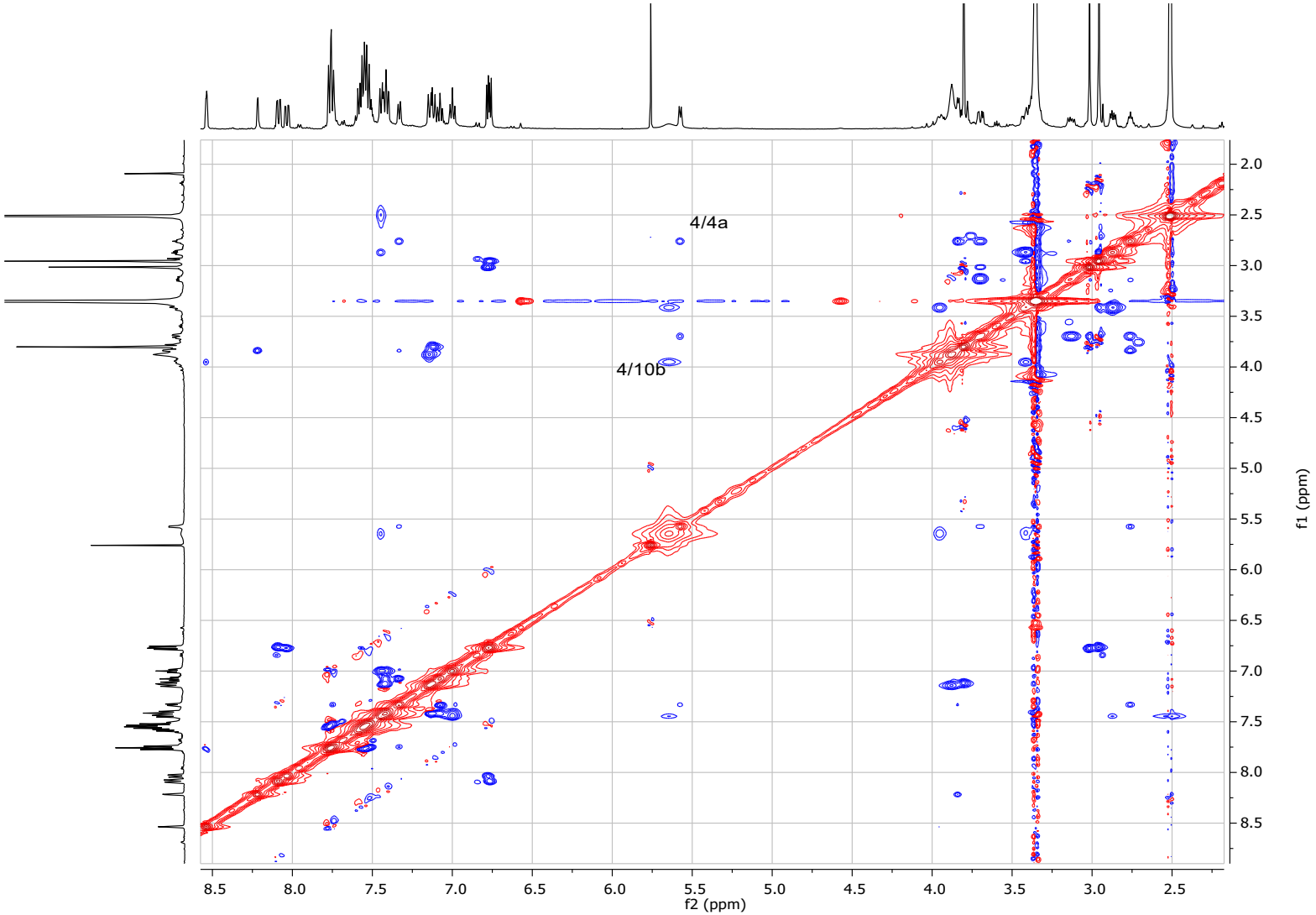

Figure S36. ROESY spectrum of *rac*-(4*R**,4a*S**,10b*S**)-**2ai** and *rac*-(4*R**,4a*S**,10b*R**)-*epi*-**2ai** in DMSO-d_6 at 500 MHz.

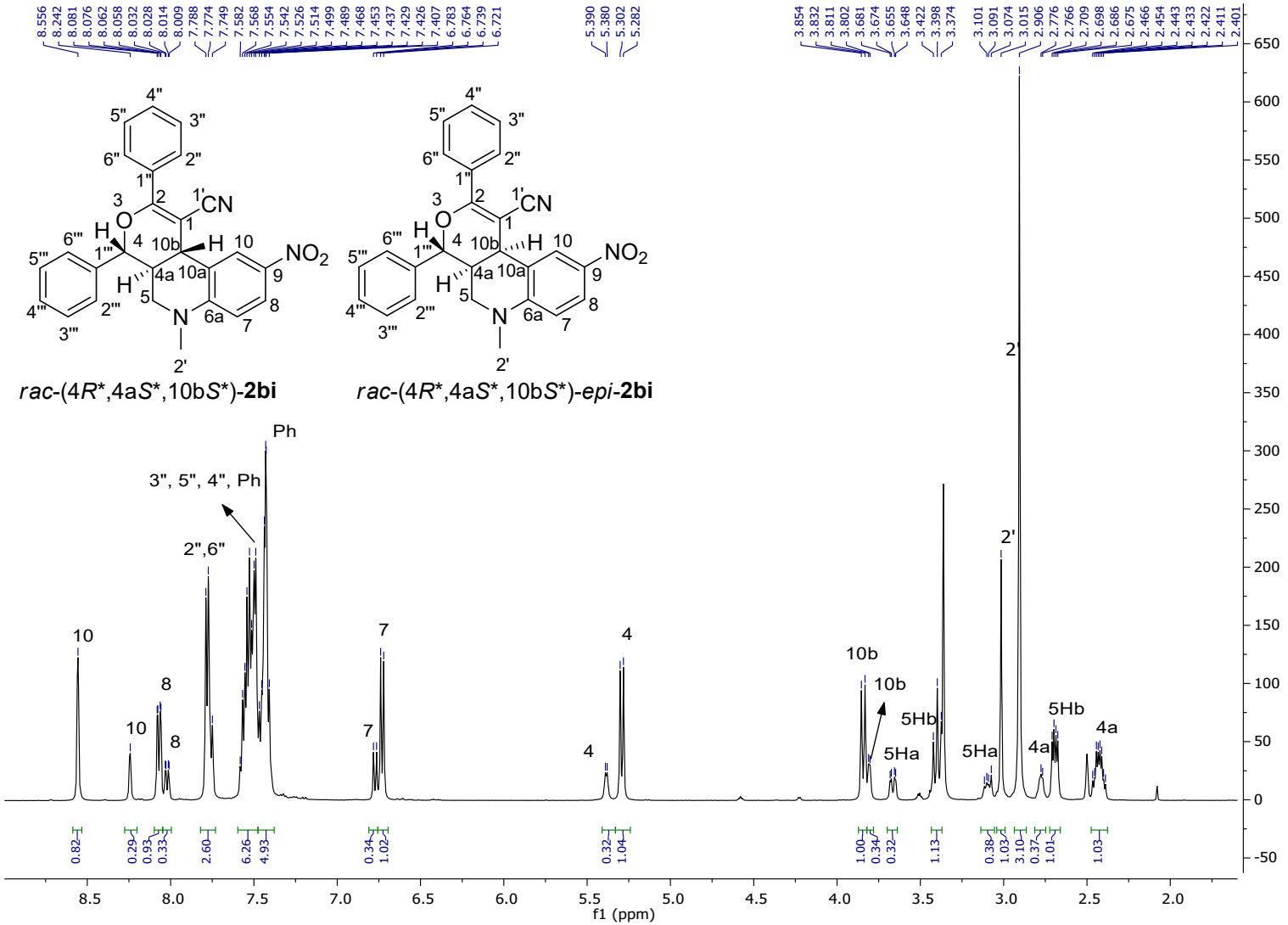

Figure S37. ^{1}H-NMR spectrum of *rac*-(4*R**,4a*S**,10b*S**)-**2bi** and *rac*-(4*R**,4a*S**,10b*R**)-*epi*-**2bi** in DMSO-d_6 at 500 MHz.

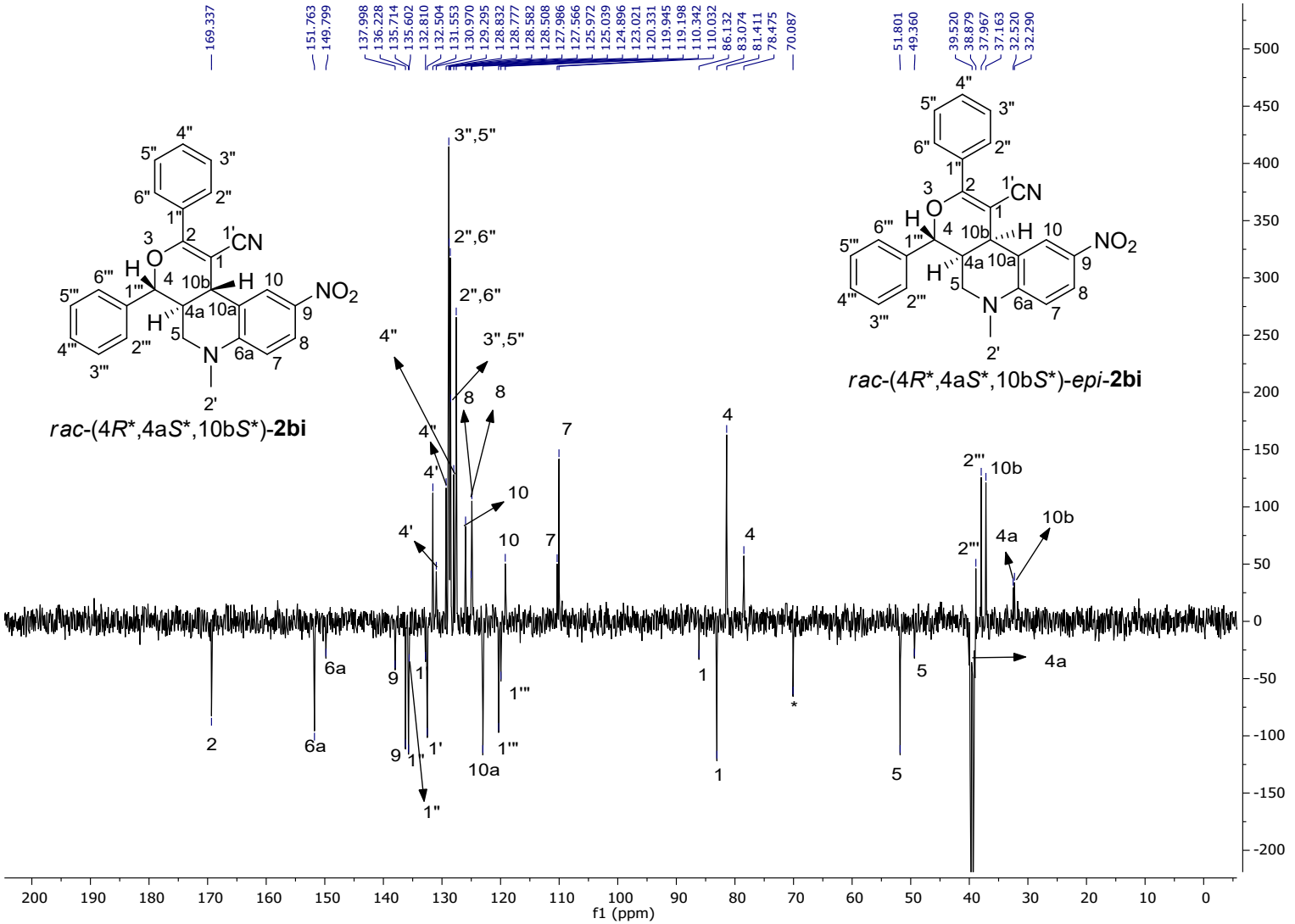

Figure S38. ^{13}C-NMR spectrum of *rac*-(4*R**,4a*S**,10b*S**)-**2bi** and *rac*-(4*R**,4a*S**,10b*R**)-*epi*-**2bi** in DMSO-d$_6$ at 125 MHz.

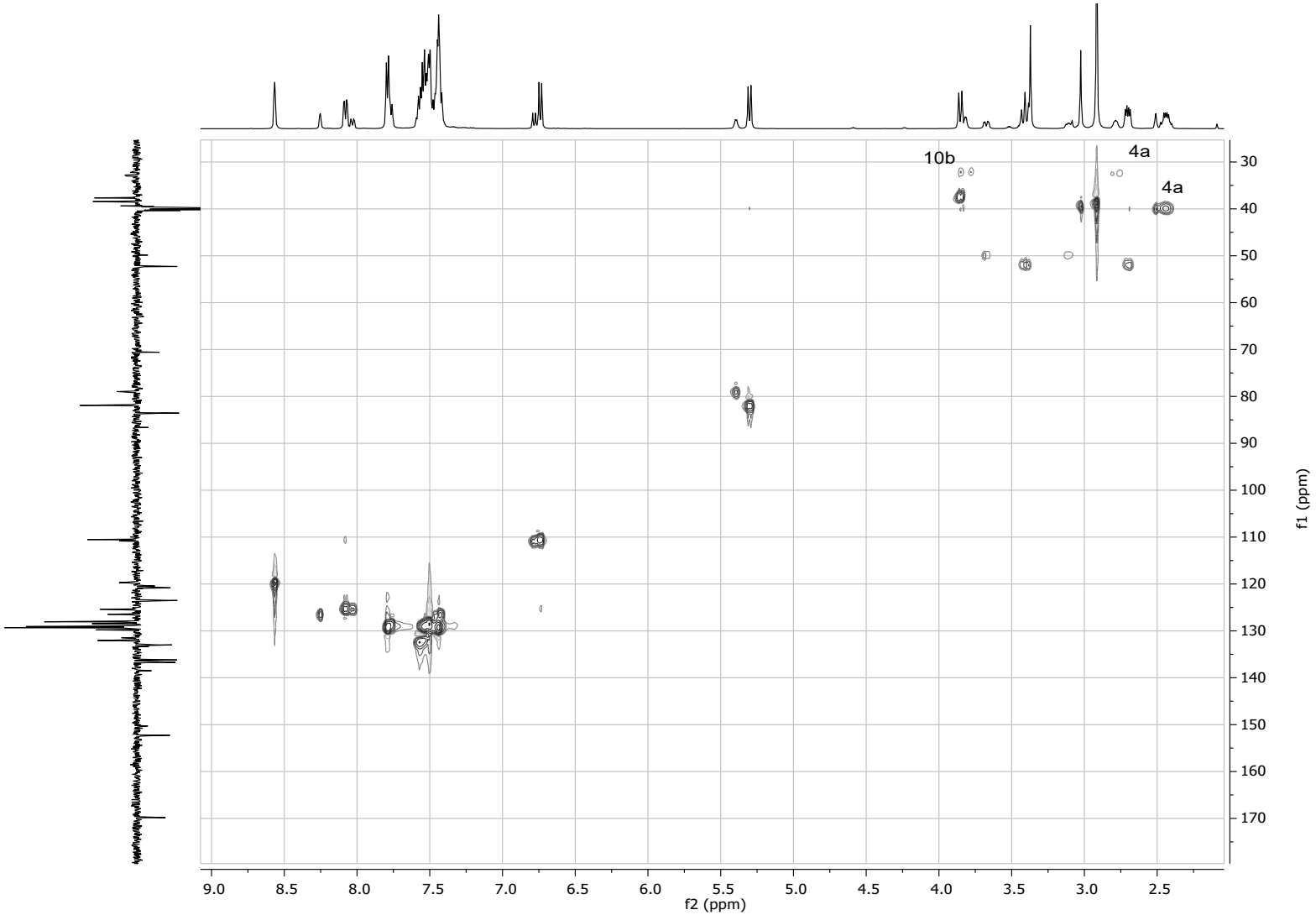

Figure S39. HSQC spectrum of *rac*-(4*R**,4a*S**,10b*S**)-**2bi** and *rac*-(4*R**,4a*S**,10b*R**)-*epi*-**2bi** in DMSO-d_6 at 500 MHz.

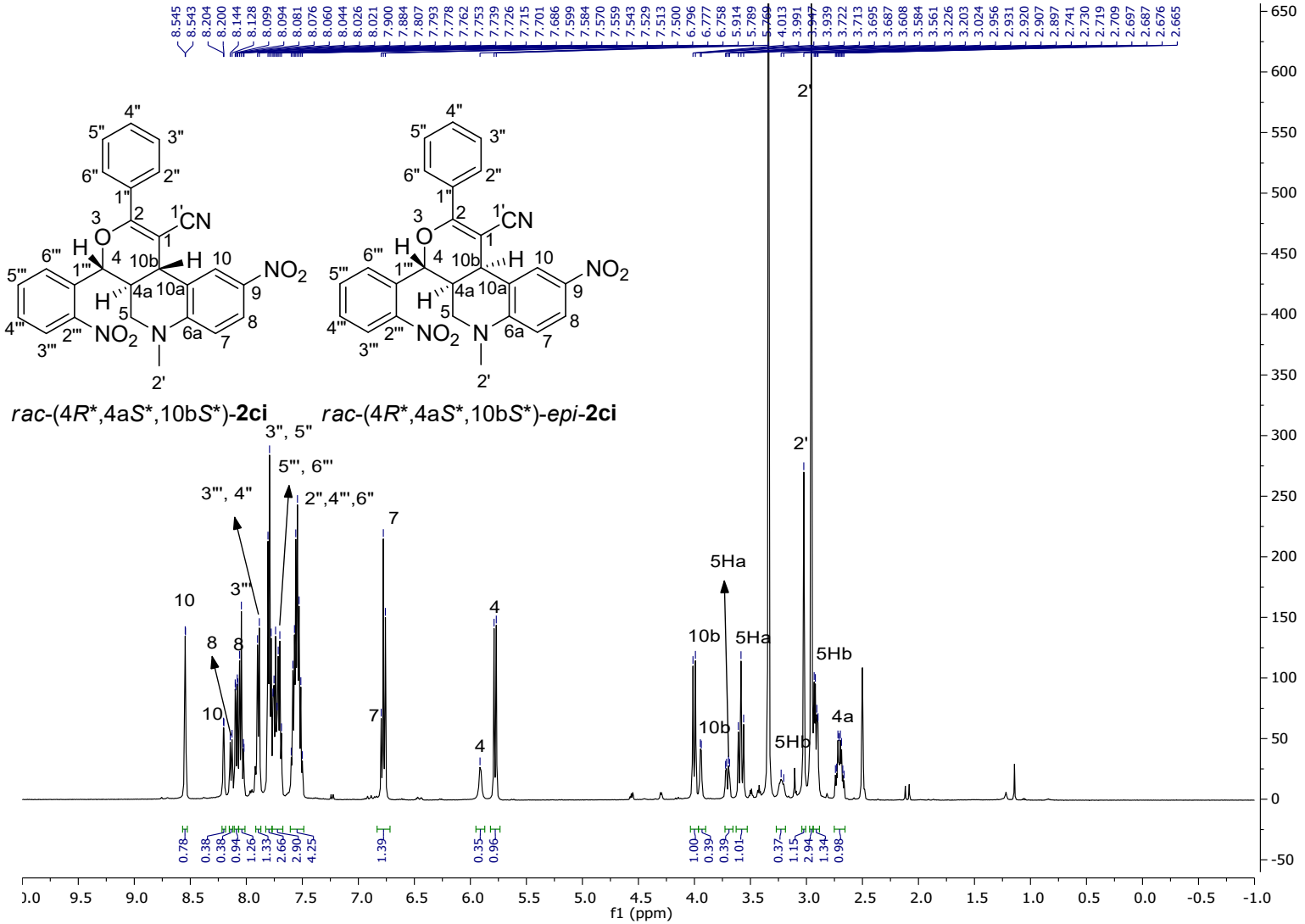

Figure S40. ^{1}H-NMR spectrum of *rac*-(4*R**,4a*S**,10b*S**)-**2ci** and *rac*-(4*R**,4a*S**,10b*R**)-*epi*-**2ci** in DMSO-d_6 at 500 MHz.

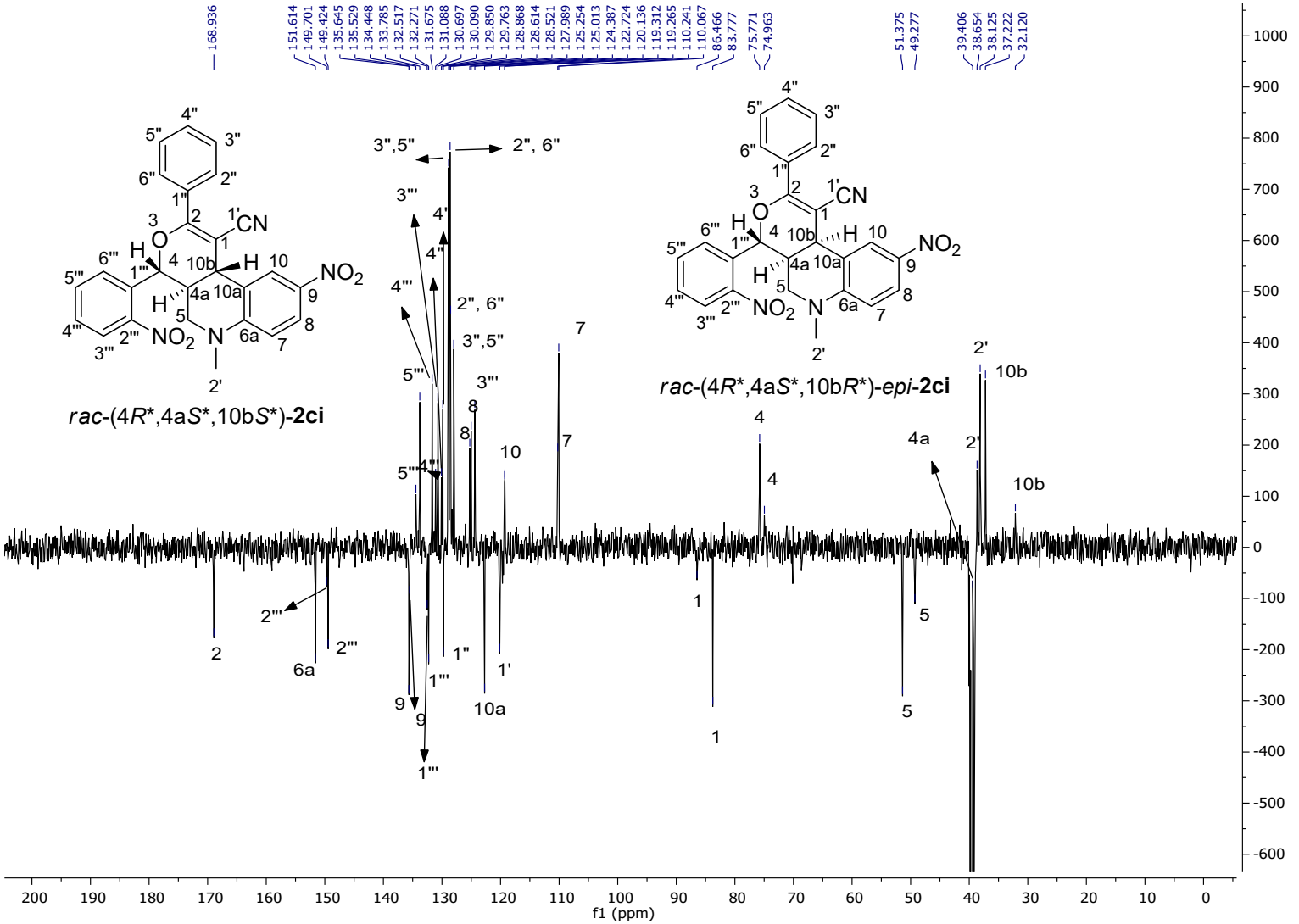

Figure S41. ^{13}C-NMR spectrum of *rac*-(4*R**,4a*S**,10b*S**)-**2ci** and *rac*-(4*R**,4a*S**,10b*R**)-*epi*-**2ci** in DMSO-d_6 at 125 MHz.

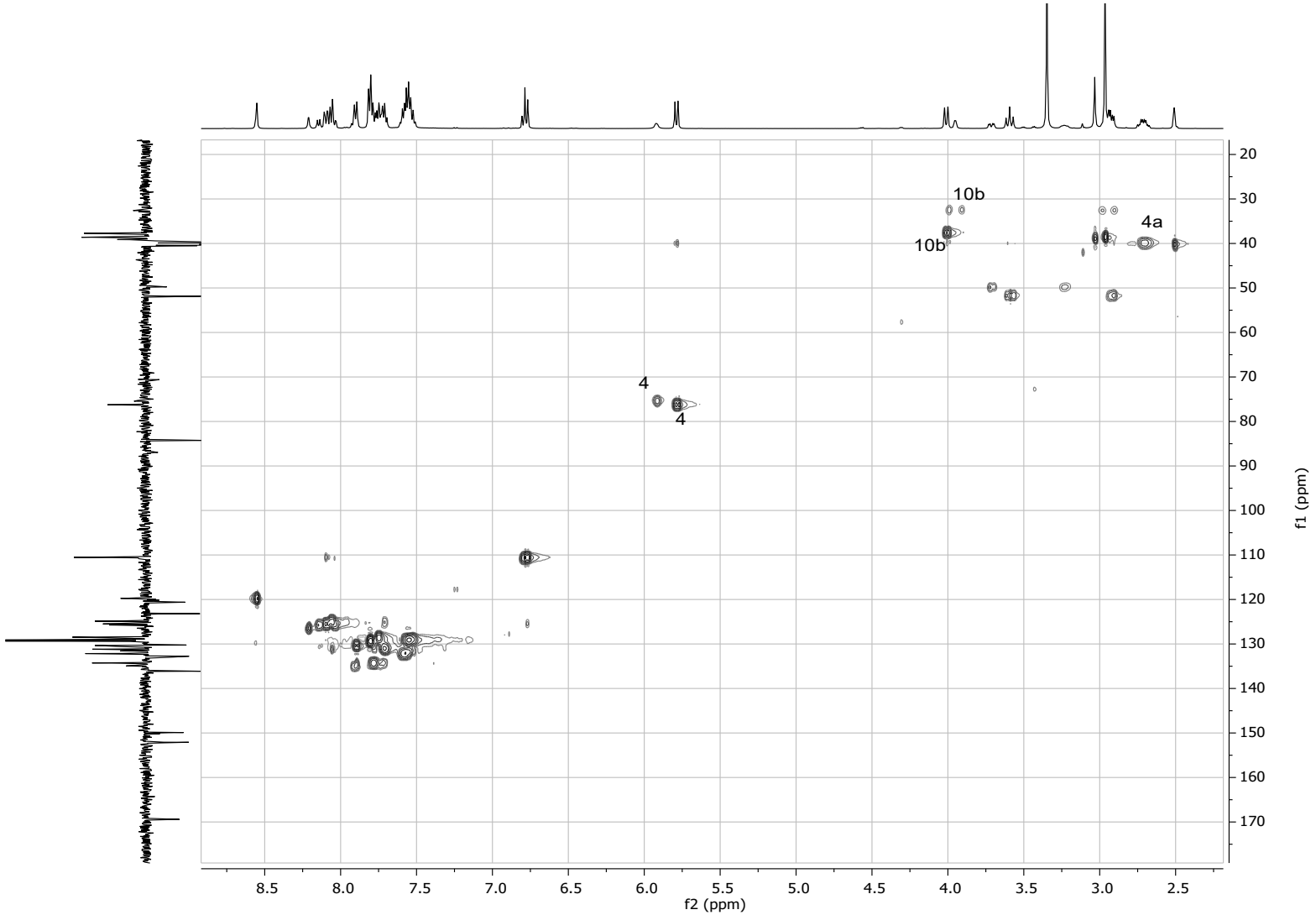

Figure S42. HSQC spectrum of *rac*-(4*R**,4a*S**,10b*S**)-**2ci** and *rac*-(4*R**,4a*S**,10b*R**)-*epi*-**2ci** in DMSO-d_6 at 500 MHz.

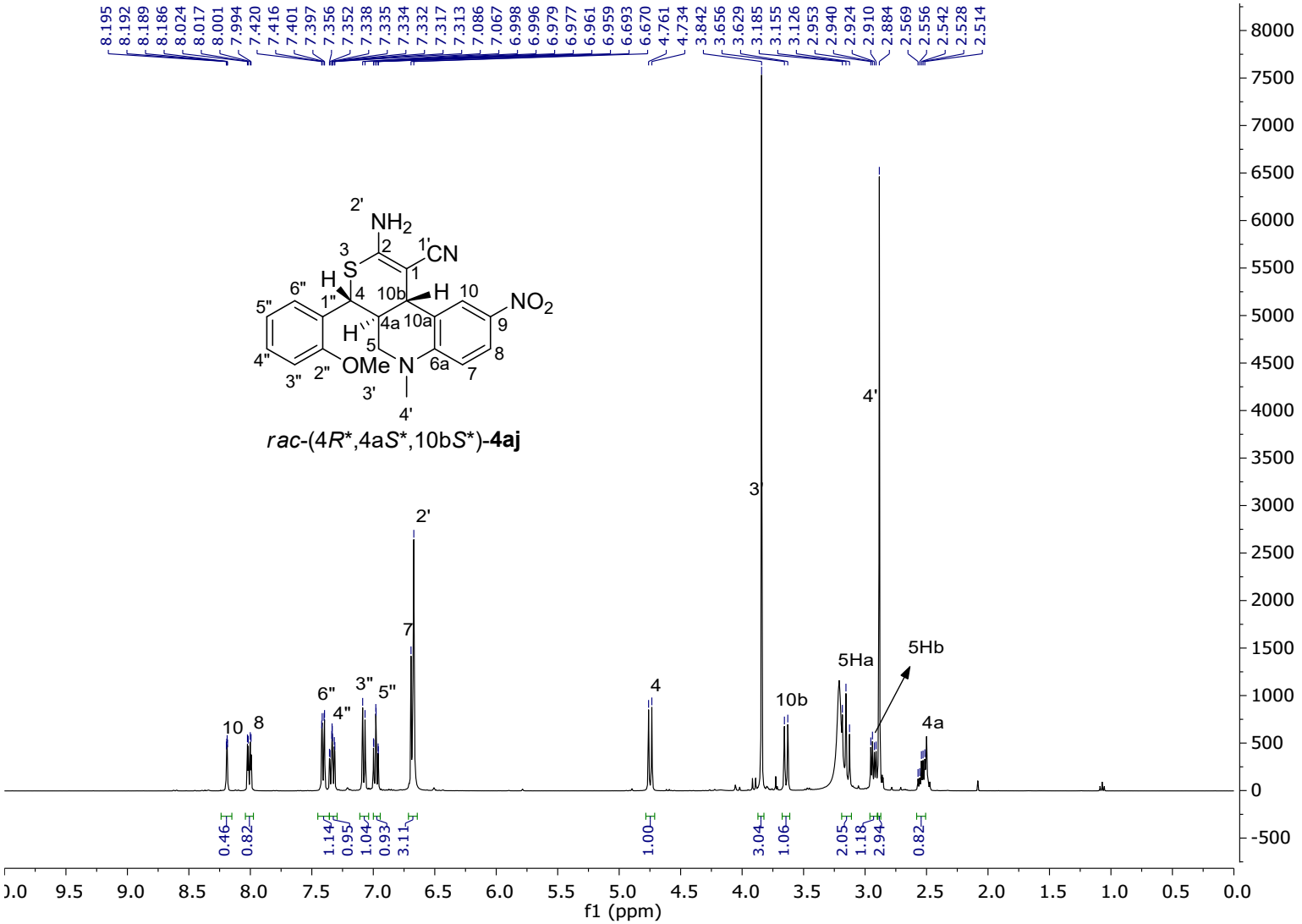

Figure S43. ^{1}H-NMR spectrum of the *rac*-(4*R**,4a*S**,10b*S**)-**4aj** in DMSO-d_6 at 400 MHz.

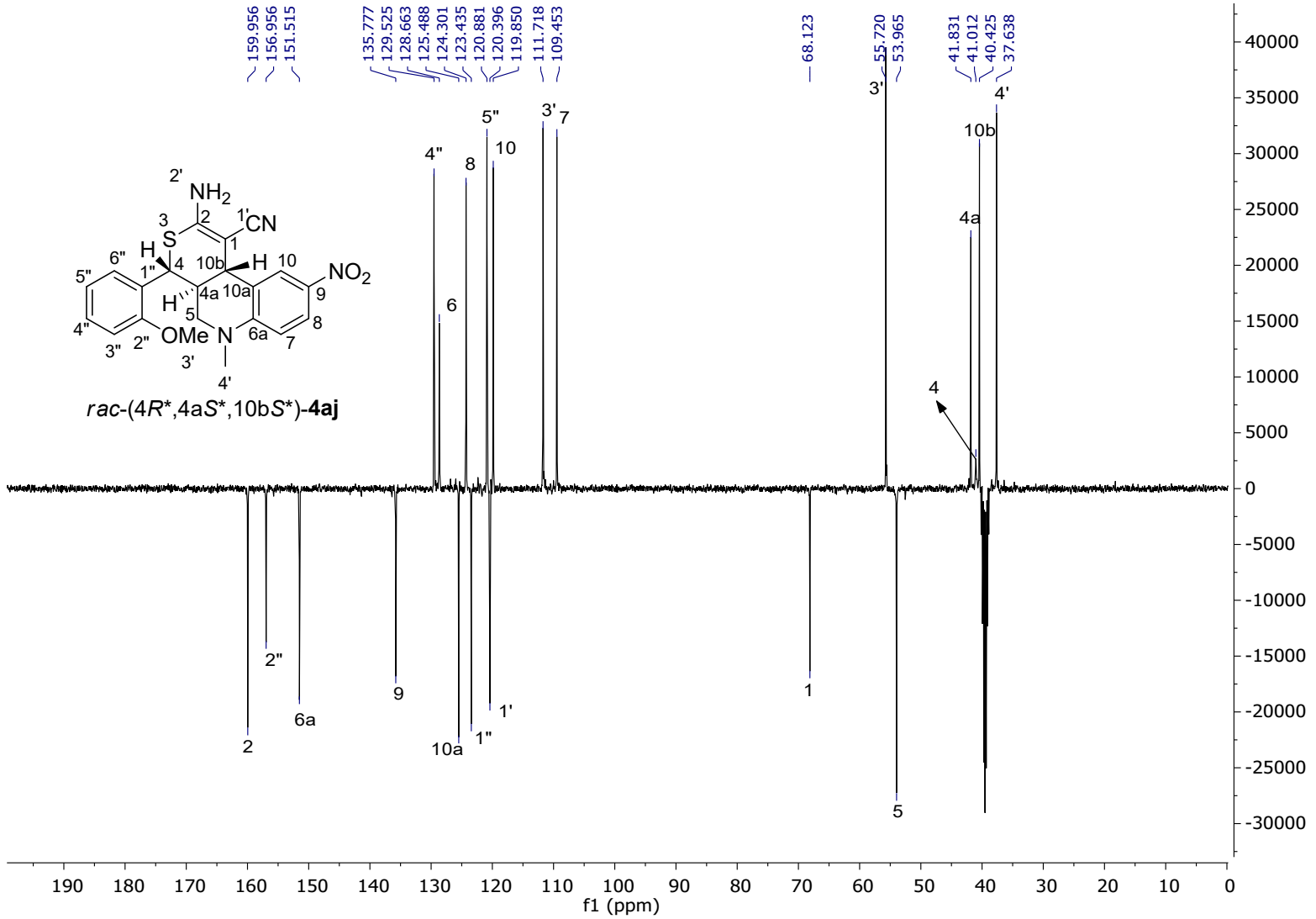

Figure S44. ^{13}C-NMR spectrum of the *rac*-(4*R**,4a*S**,10b*S**)-**4aj** in DMSO-d_6 at 100 MHz.

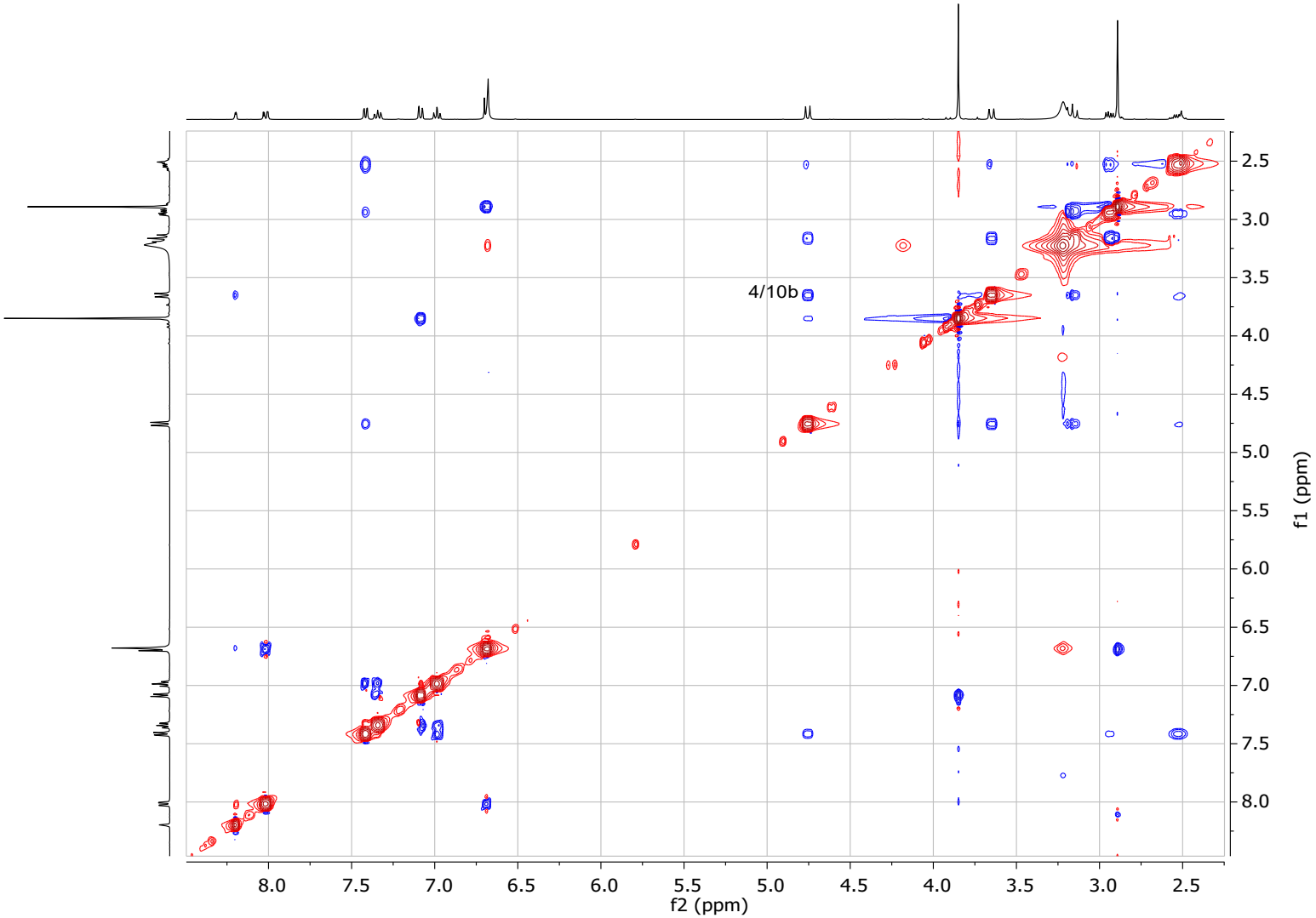

Figure S45. NOESY spectrum of the *rac*-(4*R**,4a*S**,10b*S**)-**4aj** in DMSO-d_6 at 400 MHz.

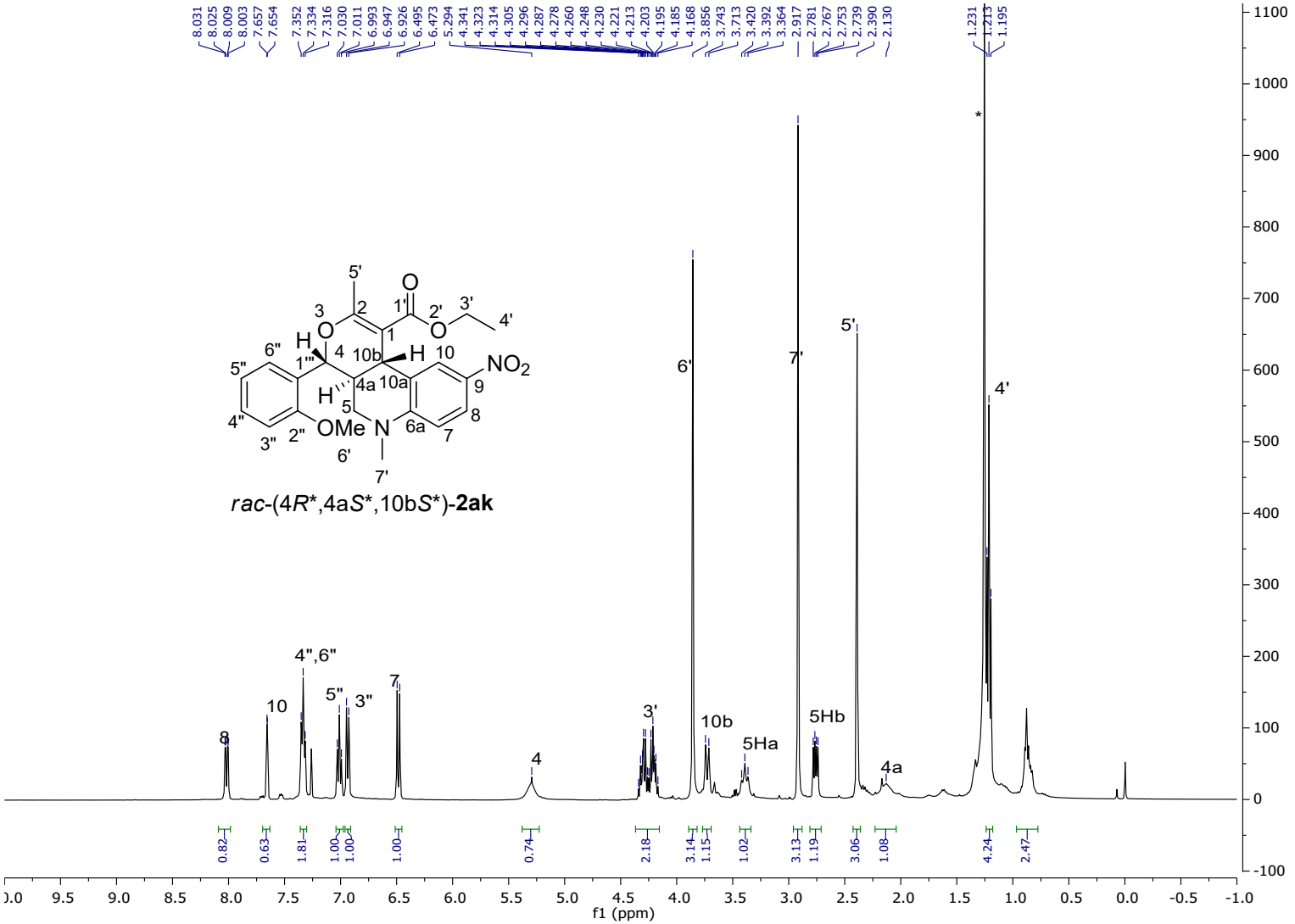

Figure S46. ^{1}H-NMR spectrum of *rac*-(4*R**,4a*S**,10b*S**)-**2ak** in DMSO-d_6 at 500 MHz.

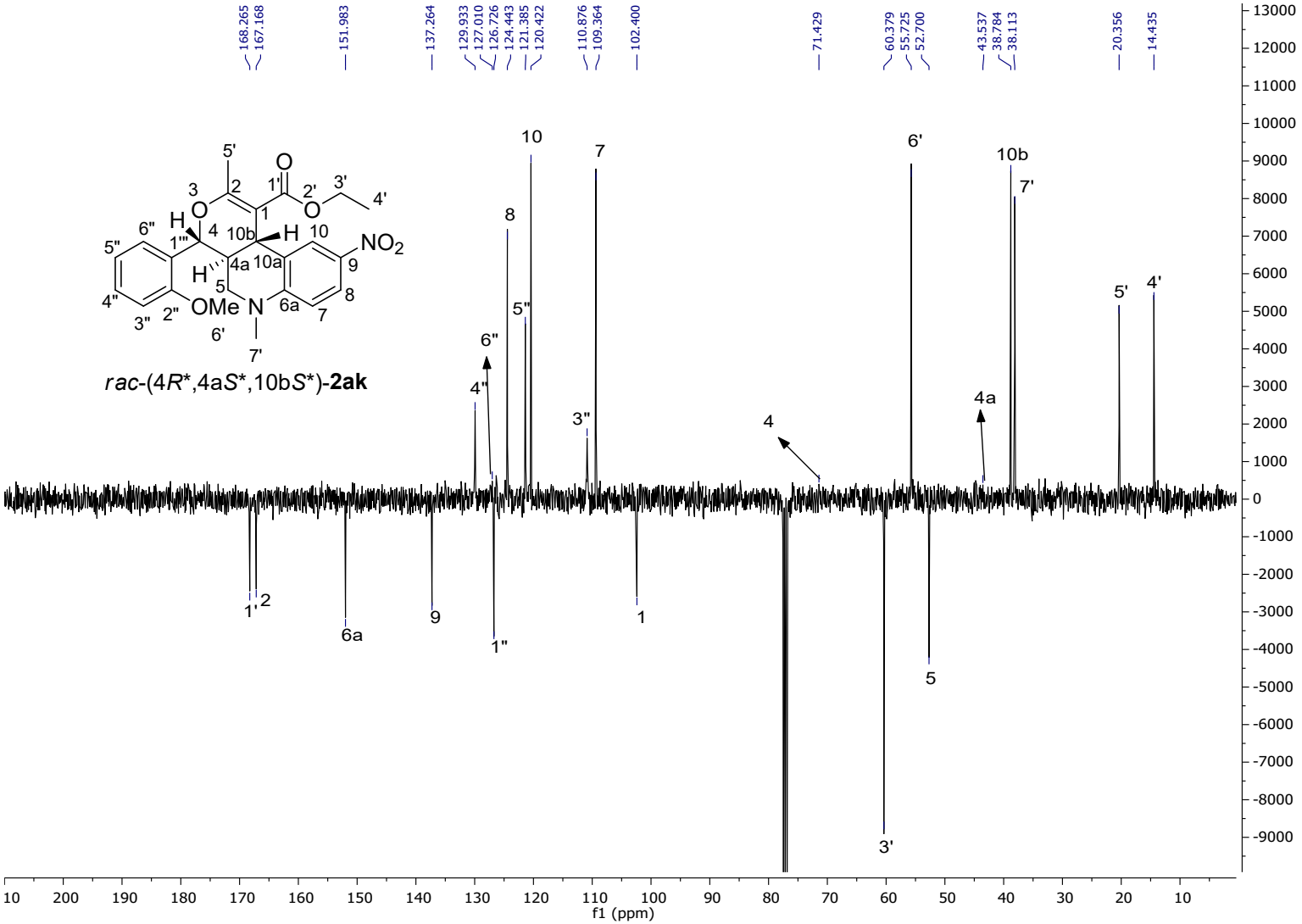

Figure S47. ^{13}C-NMR spectrum of *rac*-(4*R**,4a*S**,10b*S**)-**2ak** in $CDCl_3$ at 100 MHz.

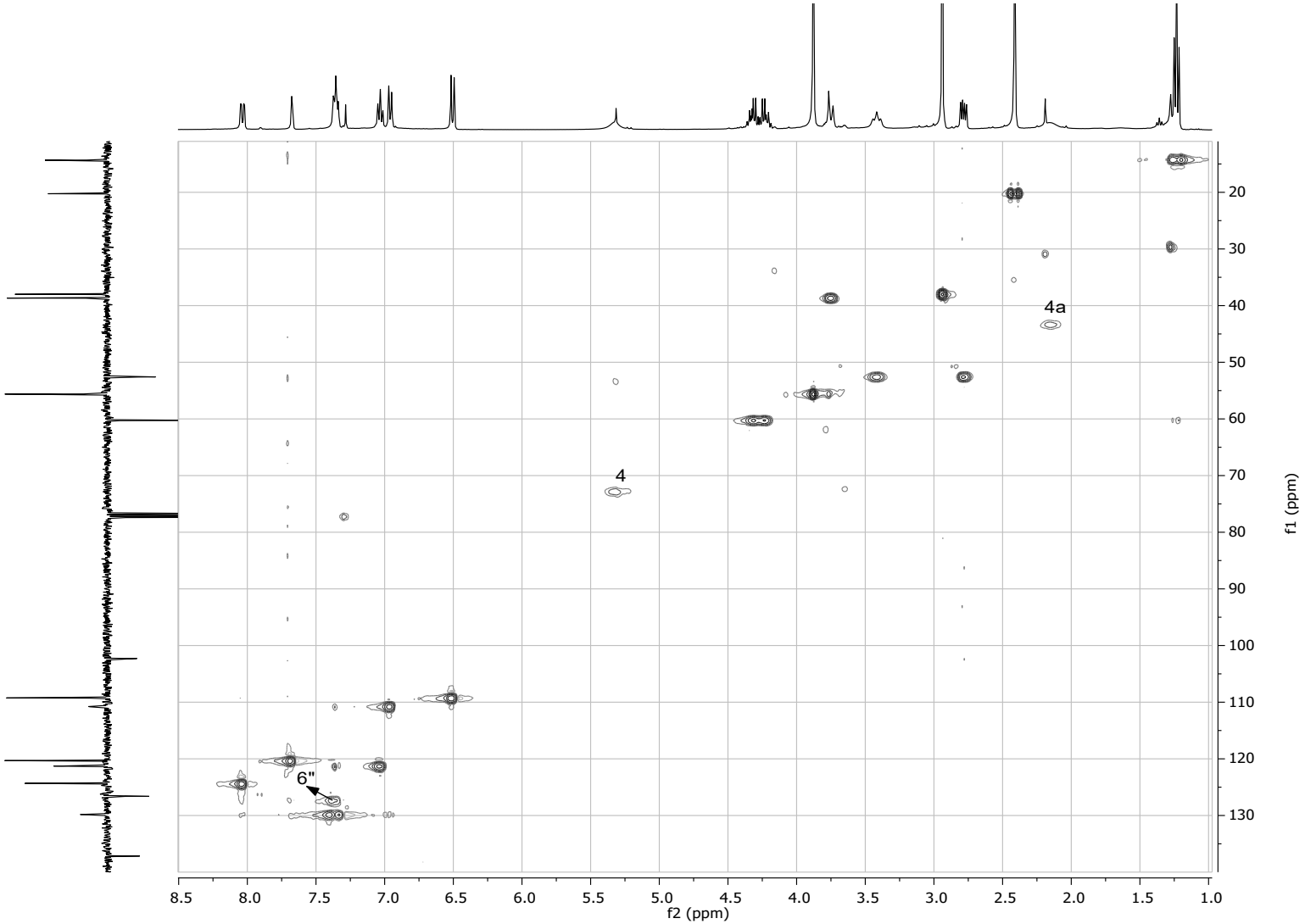

Figure S48. HSQC spectrum of *rac*-(4*R**,4a*S**,10b*S**)-**2ak** in $CDCl_3$ at 400 MHz.

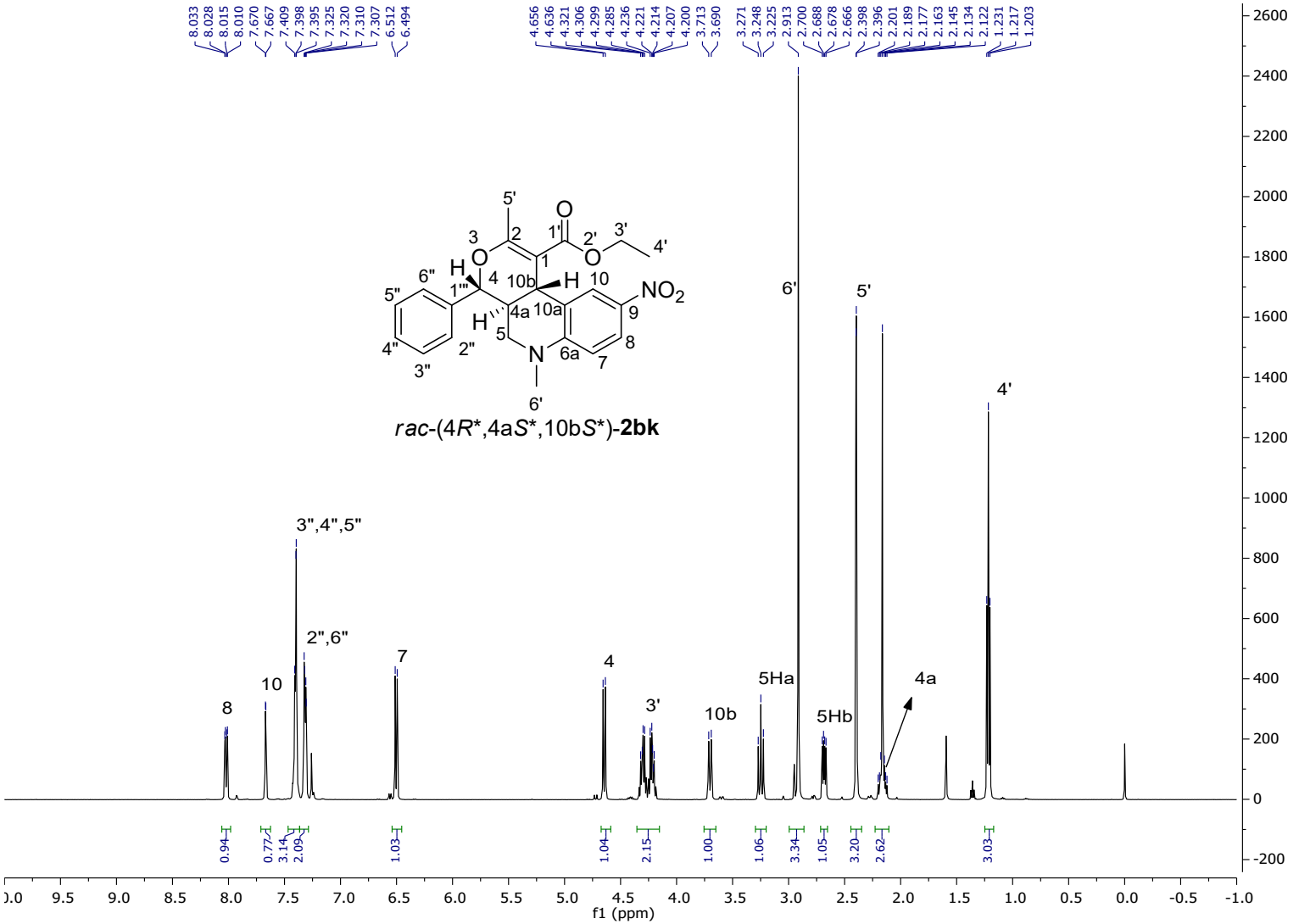

Figure S49. ^{1}H-NMR spectrum of *rac*-(4*R**,4a*S**,10b*S**)-**2bk** in $CDCl_3$ at 500 MHz.

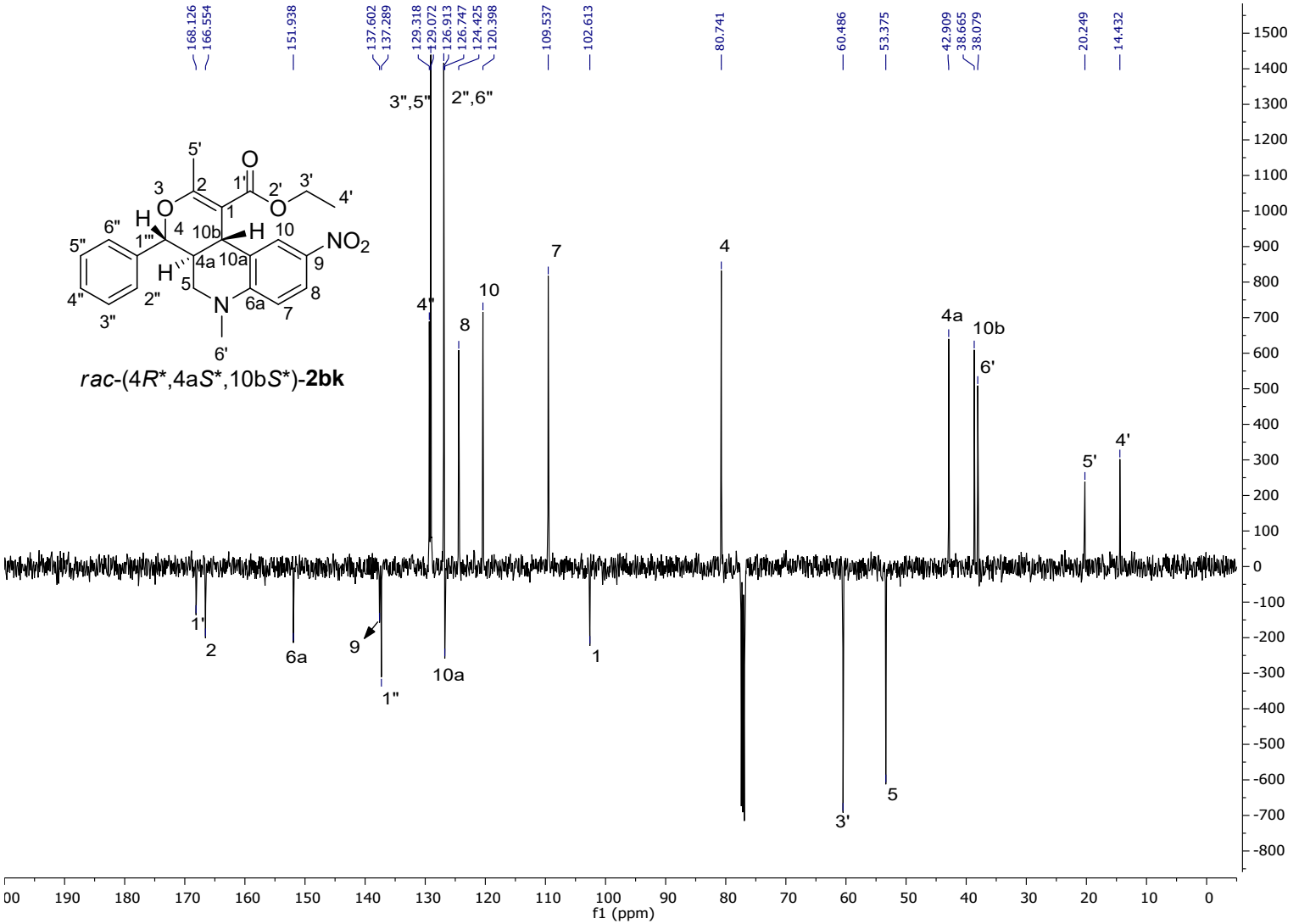

Figure S50. ^{13}C-NMR spectrum of *rac*-(4*R**,4a*S**,10b*S**)-**2bk** in $CDCl_3$ at 125 MHz.

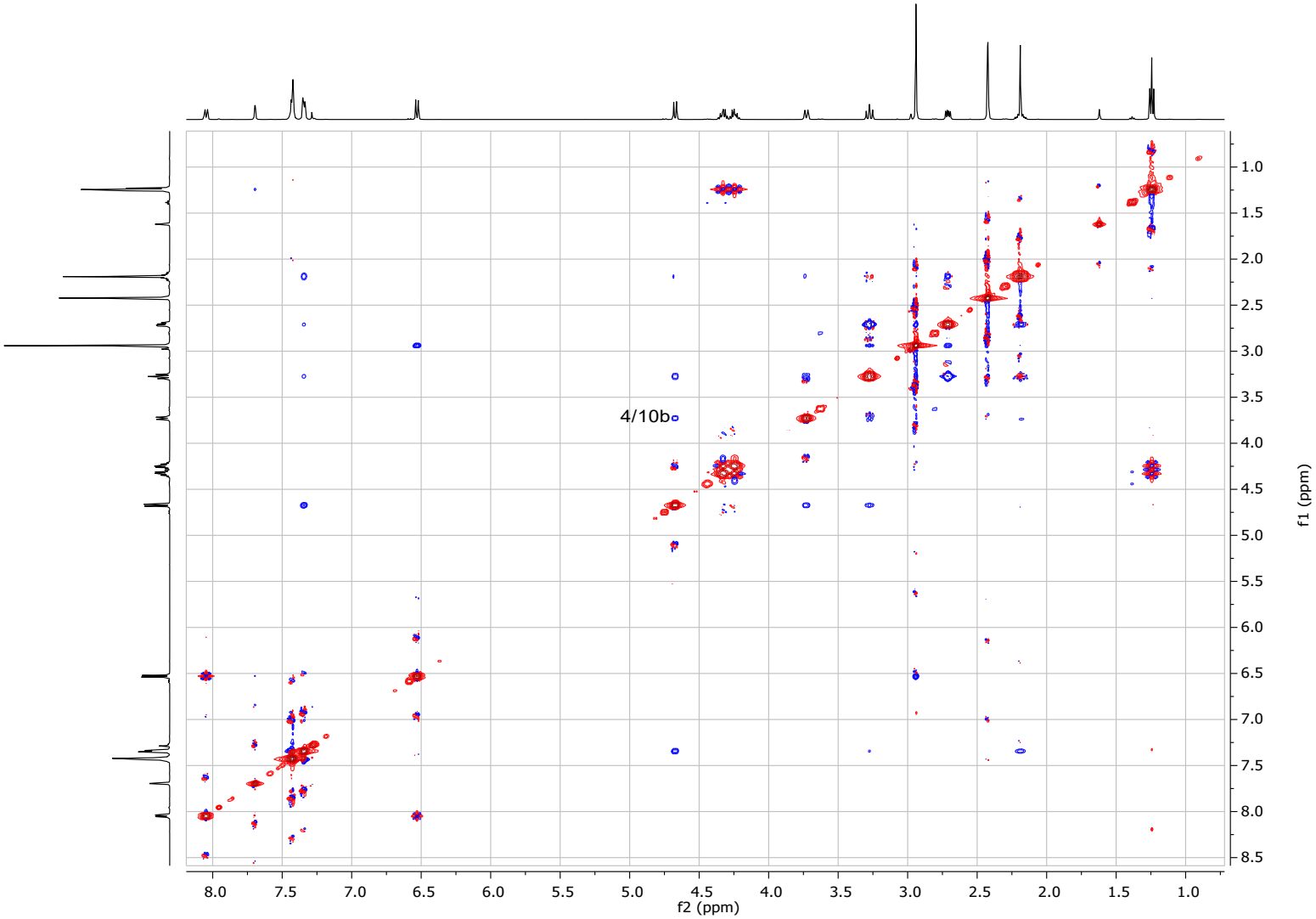

Figure S51. NOESY spectrum of *rac*-(4*R**,4a*S**,10b*S**)-**2bk** in $CDCl_3$ at 500 MHz.

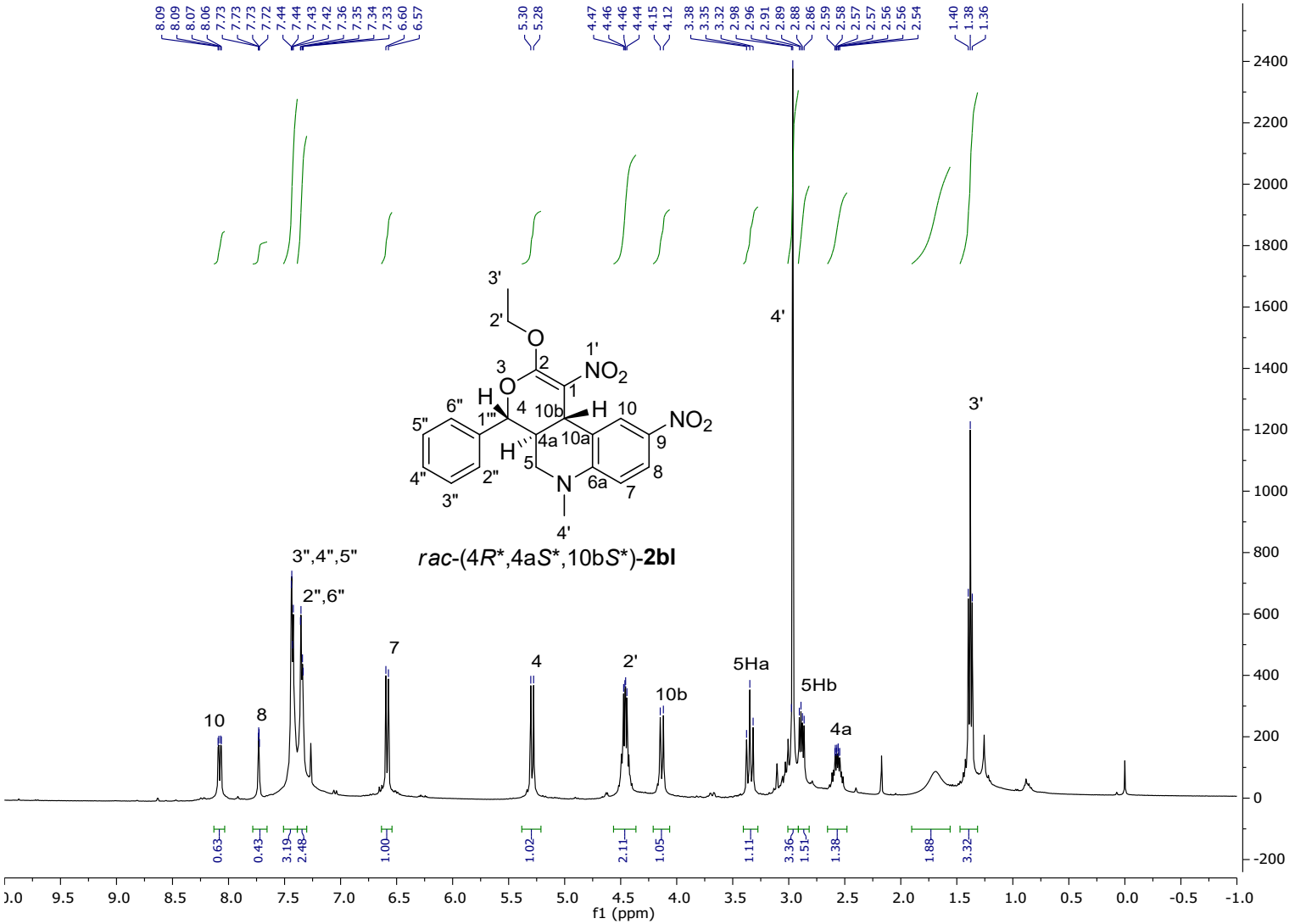

Figure S52. ^{1}H-NMR spectrum of *rac*-(4*R**,4a*S**,10b*S**)-**2bl** in $CDCl_3$ at 400 MHz.

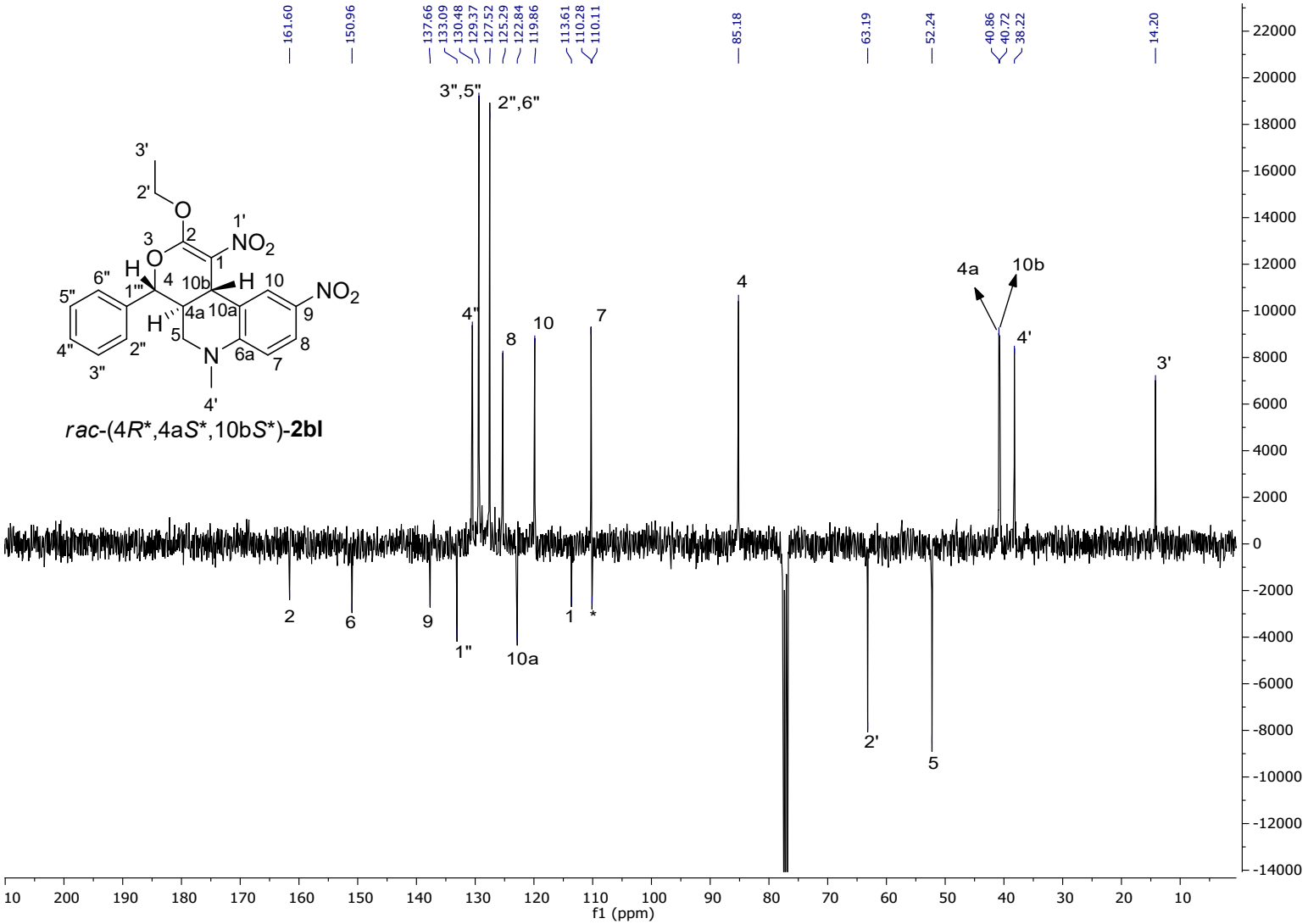

Figure S53. ^{13}C-NMR spectrum of *rac*-(4*R**,4a*S**,10b*S**)-**2bl** in $CDCl_3$ at 100 MHz.

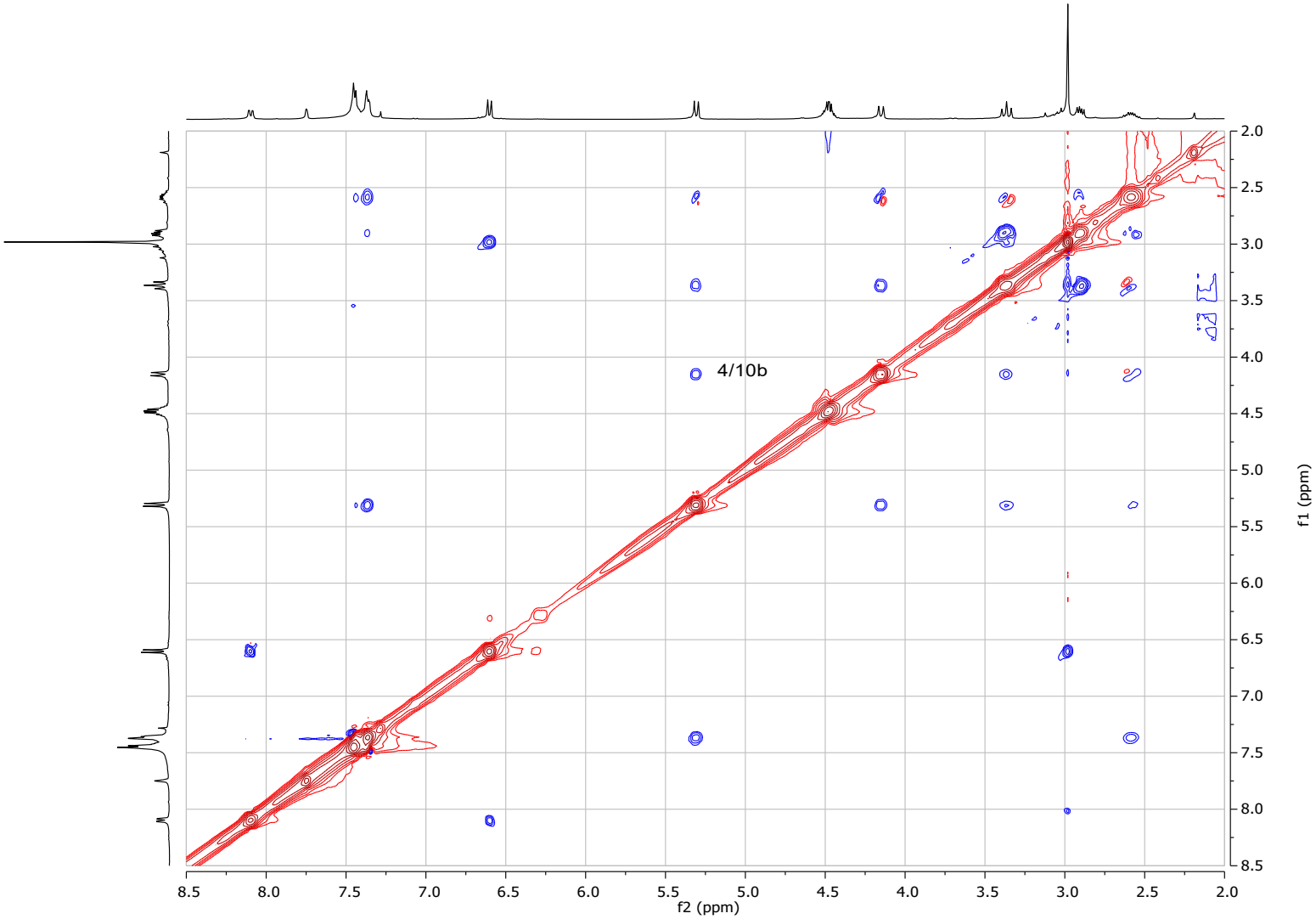

Figure S54. NOESY spectrum of *rac*-(4*R**,4a*S**,10b*S**)-**2bl** in $CDCl_3$ at 400 MHz.

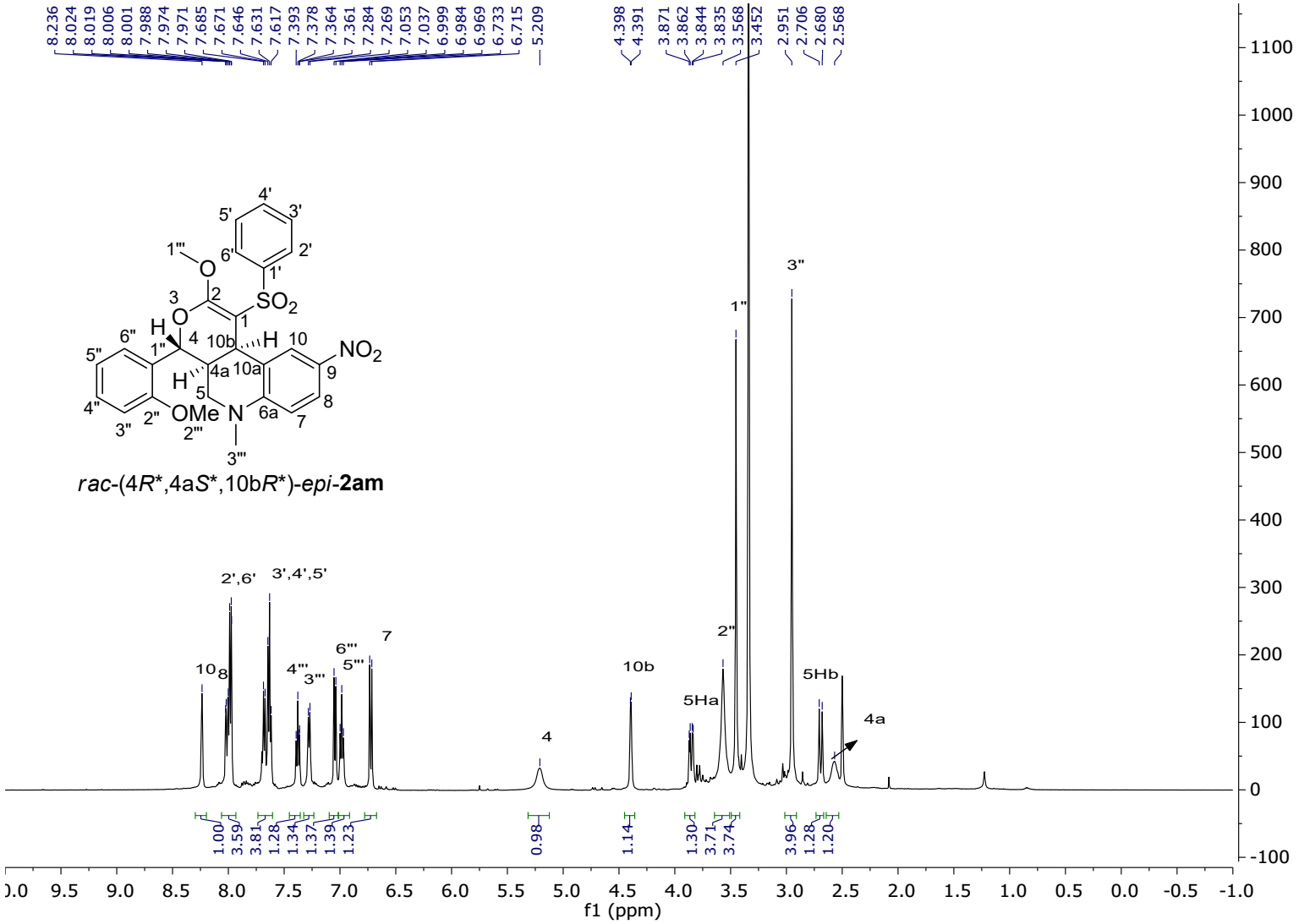

Figure S55. ^{1}H-NMR spectrum of *rac*-(4*R**,4a*S**,10b*R**)-*epi*-**2am** in DMSO-d_6 at 500 MHz.

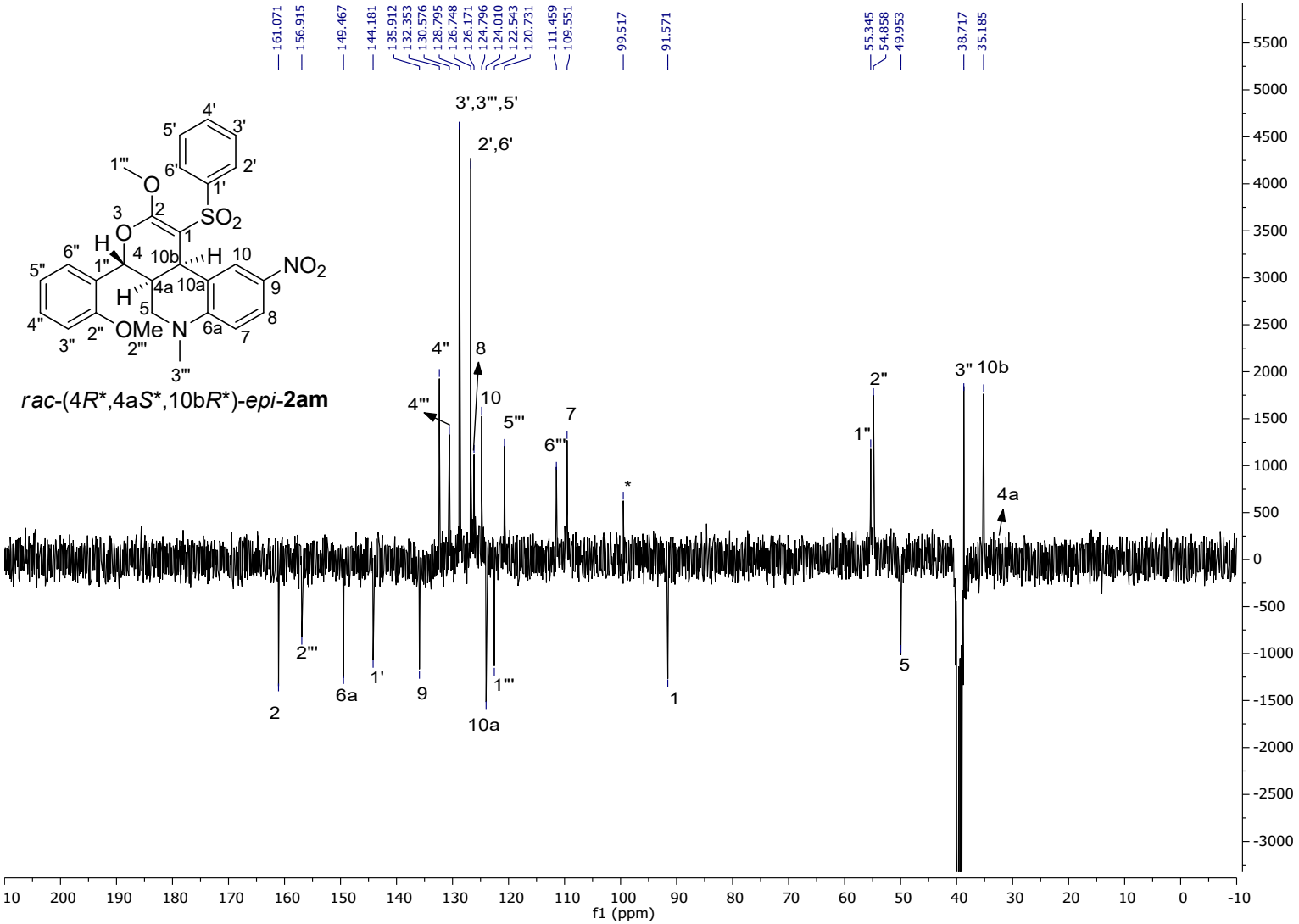

Figure S56. ^{13}C-NMR spectrum of *rac*-(4*R**,4a*S**,10b*R**)-*epi*-**2am** in DMSO-d_6 at 90 MHz.

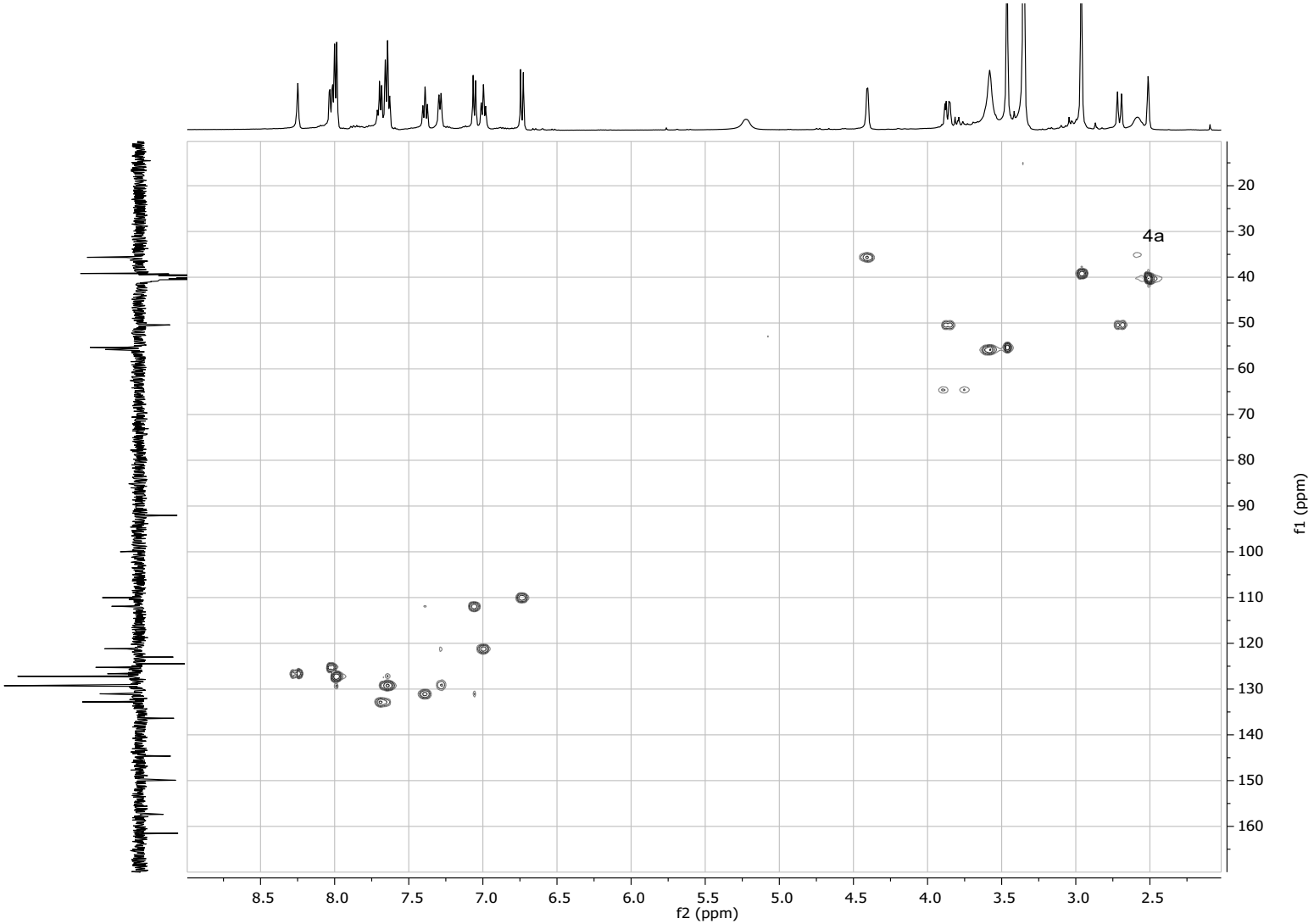

Figure S57. HSQC spectrum of *rac*-(4*R**,4a*S**,10b*R**)-*epi*-**2am** in DMSO-d_6 at 400 MHz.

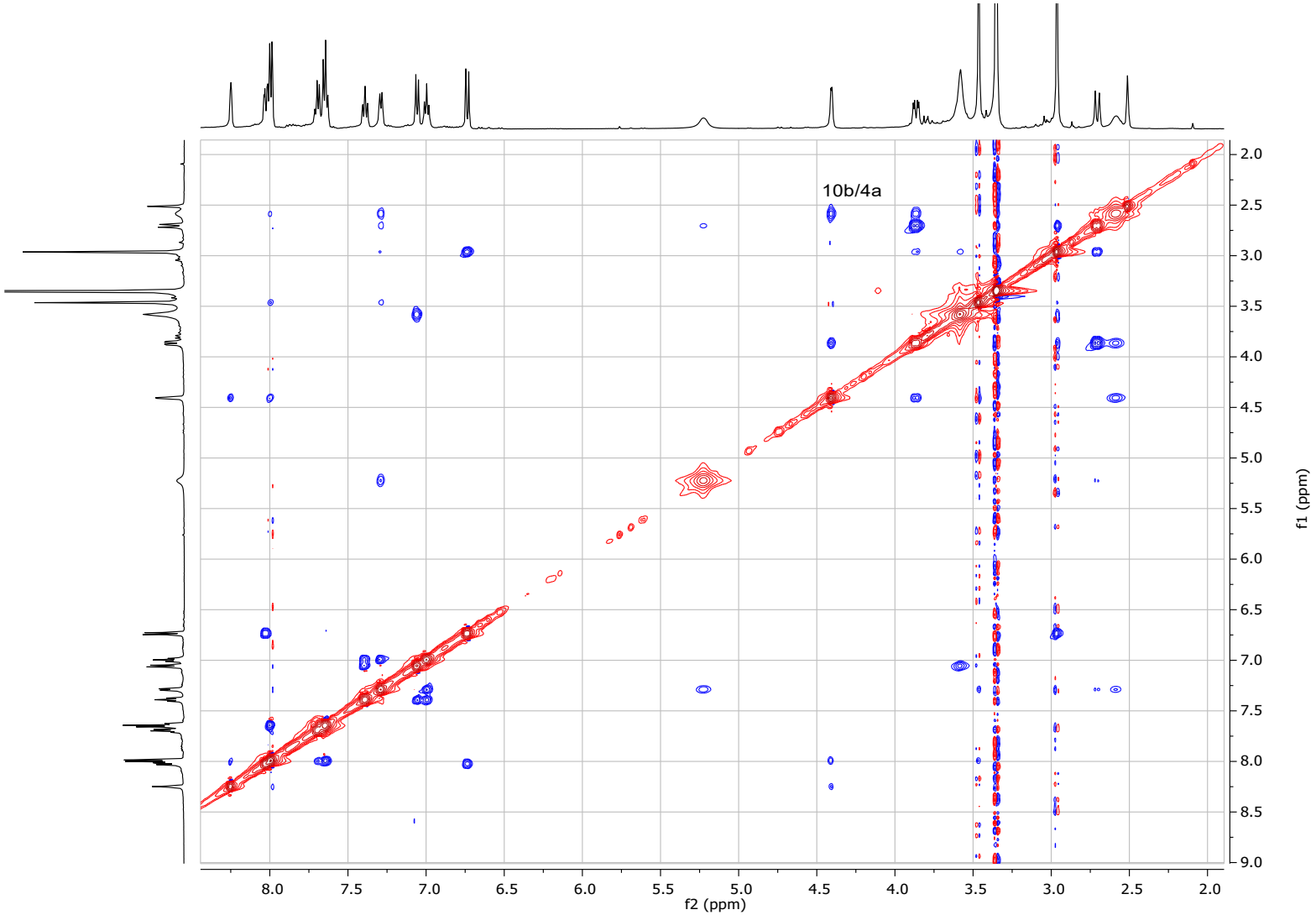

Figure S58. ROESY spectrum of *rac*-(4*R**,4a*S**,10b*R**)-*epi*-**2am** in DMSO-d_6 at 500 MHz.

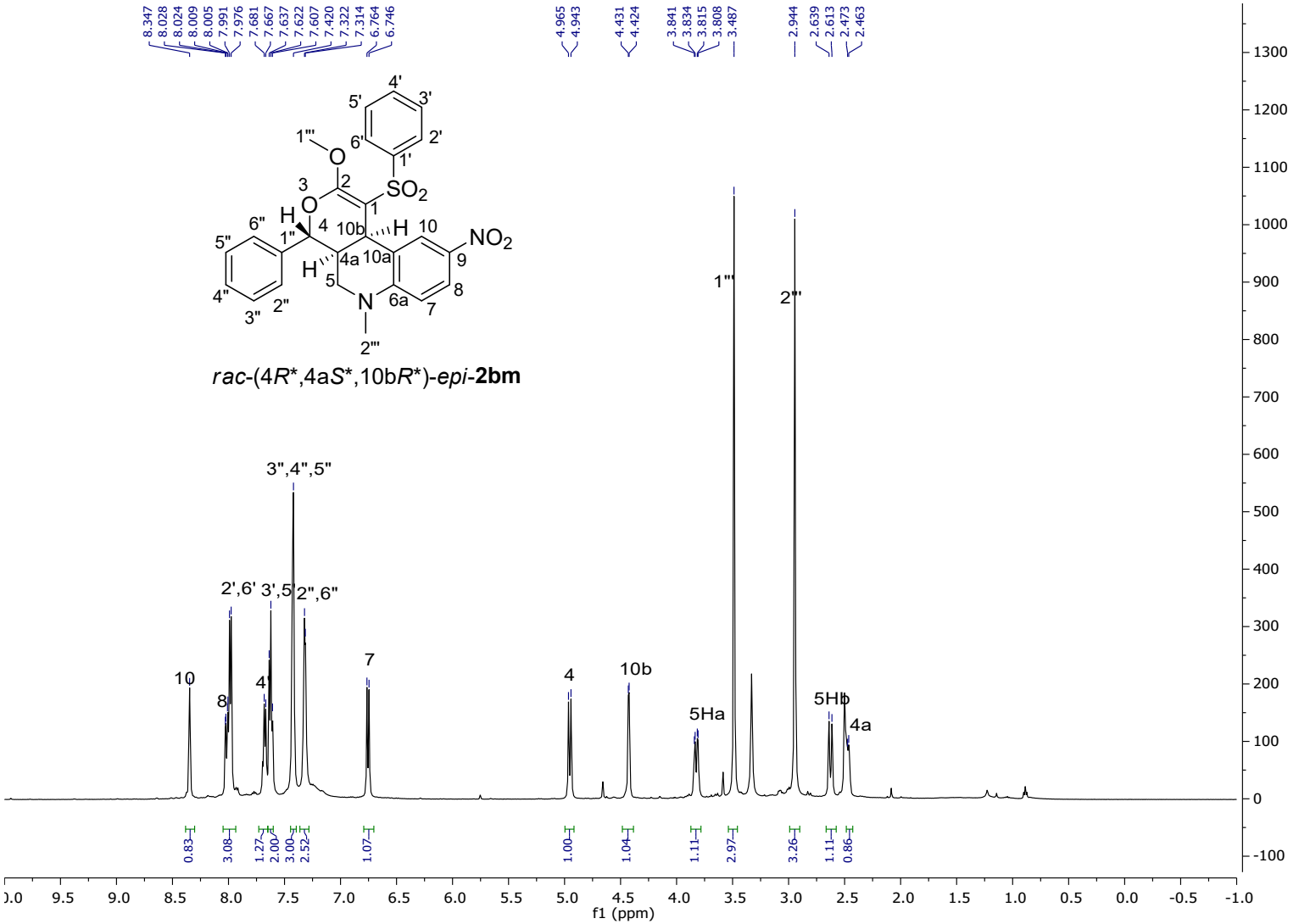

Figure S59. ^{1}H-NMR spectrum of *rac*-(4*R**,4a*S**,10b*R**)-*epi*-**2bm** in DMSO-d_6 at 500 MHz.

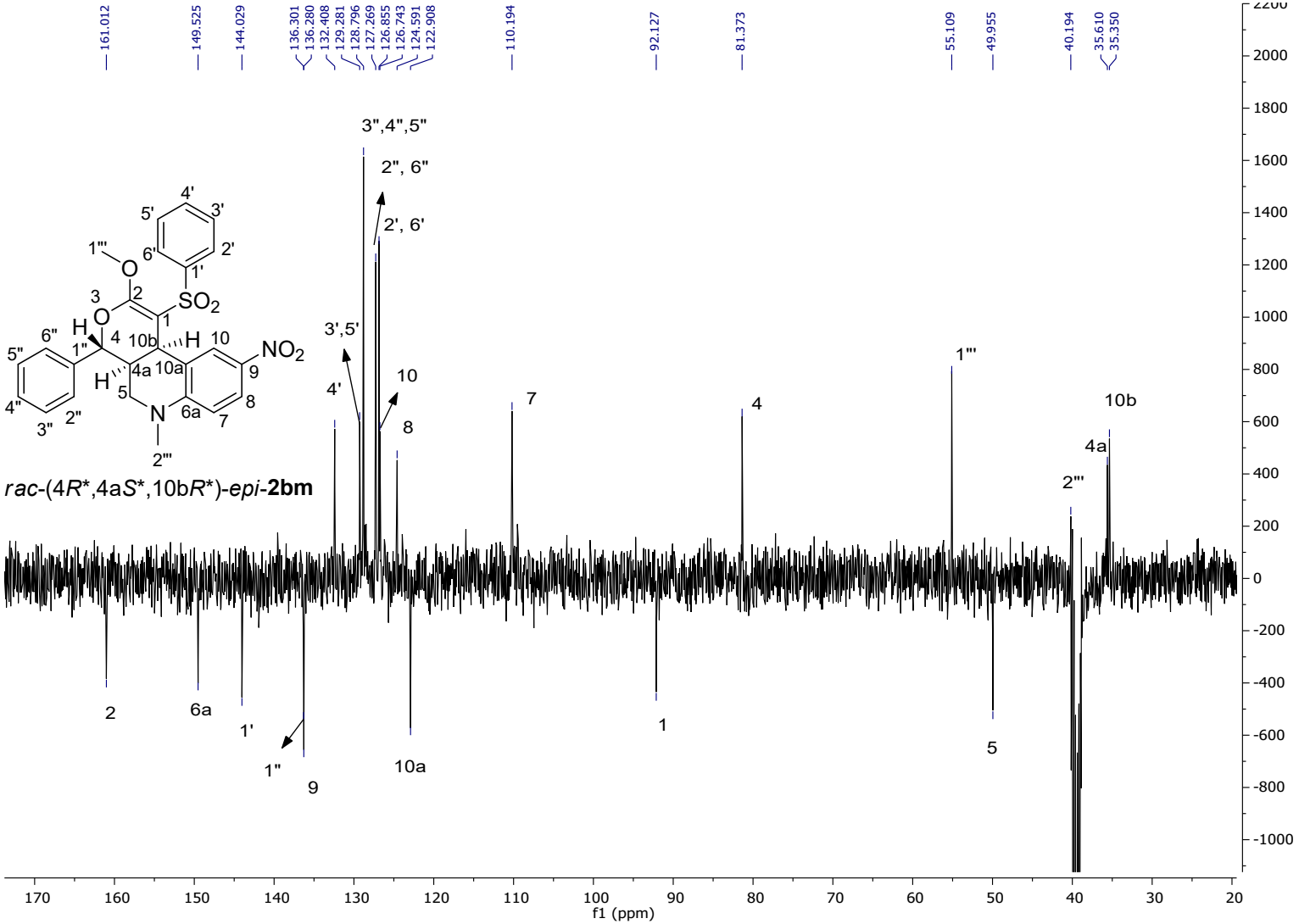

Figure S60. ^{13}C-NMR spectrum of *rac*-(4*R**,4a*S**,10b*R**)-*epi*-**2bm** in DMSO-d^6 at 100 MHz.

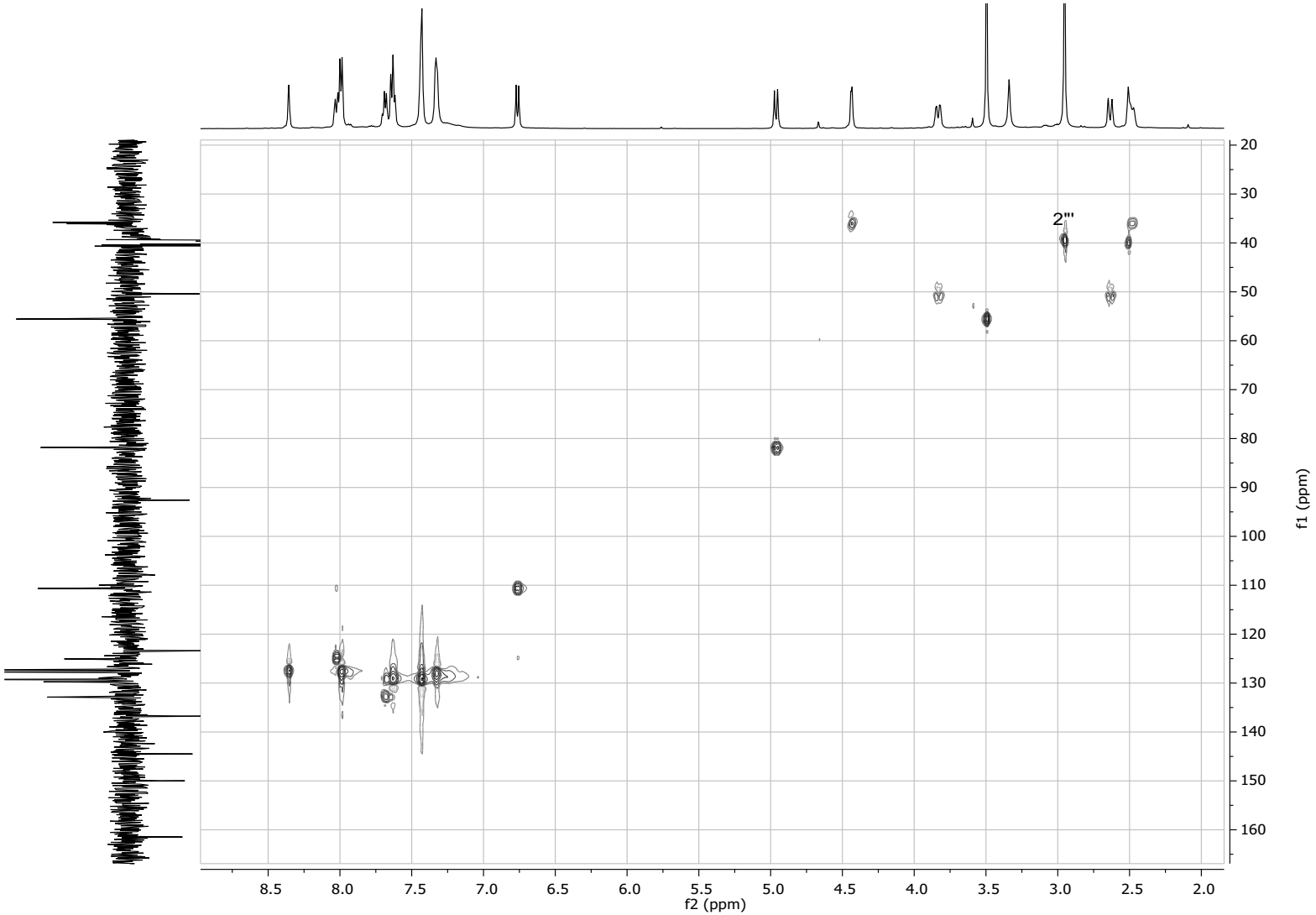

Figure S61. HSQC spectrum of *rac*-(4*R**,4a*S**,10b*R**)-*epi*-**2bm** in DMSO-d_6 at 500 MHz.

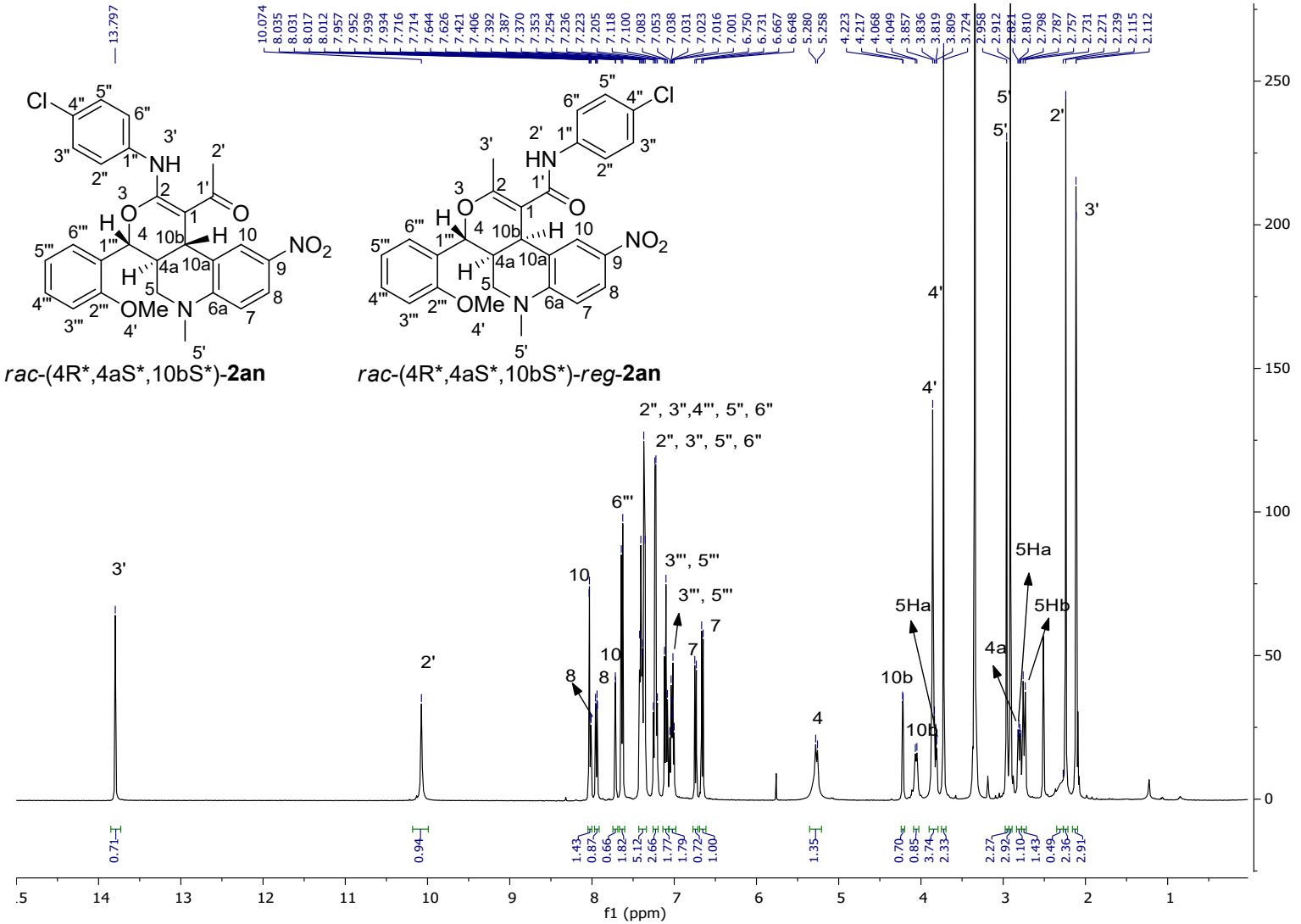

Figure S62. ^{1}H-NMR spectrum of *rac*-(4*R**,4a*S**,10b*S**)-**2an** and *rac*-(4*R**,4a*S**,10b*R**)-*reg*-**2an** in DMSO-d_6 at 500 MHz.

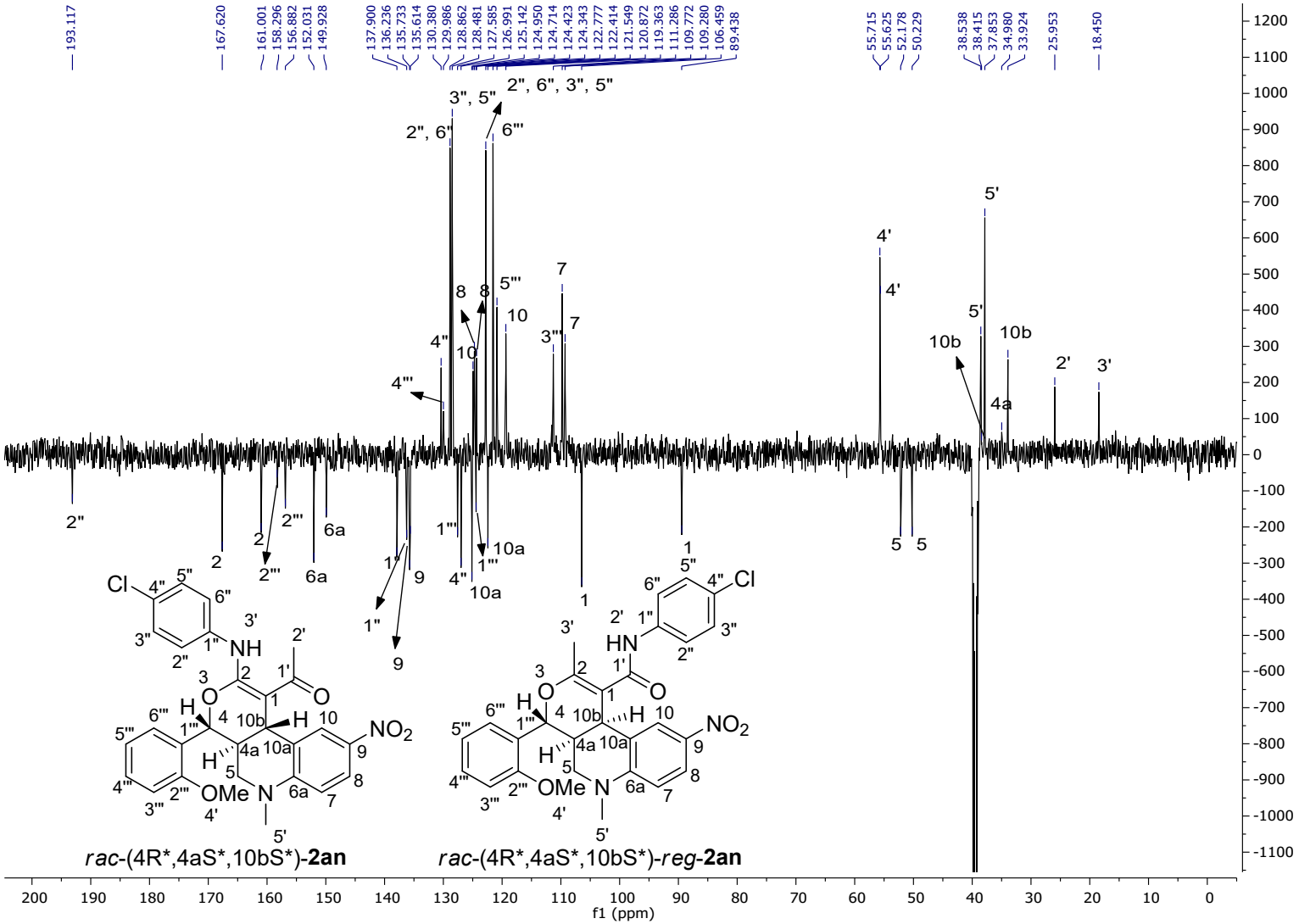

Figure S63. ^{13}C-NMR spectrum of *rac*-(4*R**,4a*S**,10b*S**)-**2an** and *rac*-(4*R**,4a*S**,10b*R**)-*reg*-**2an** in DMSO-d$_6$ at 125 MHz.

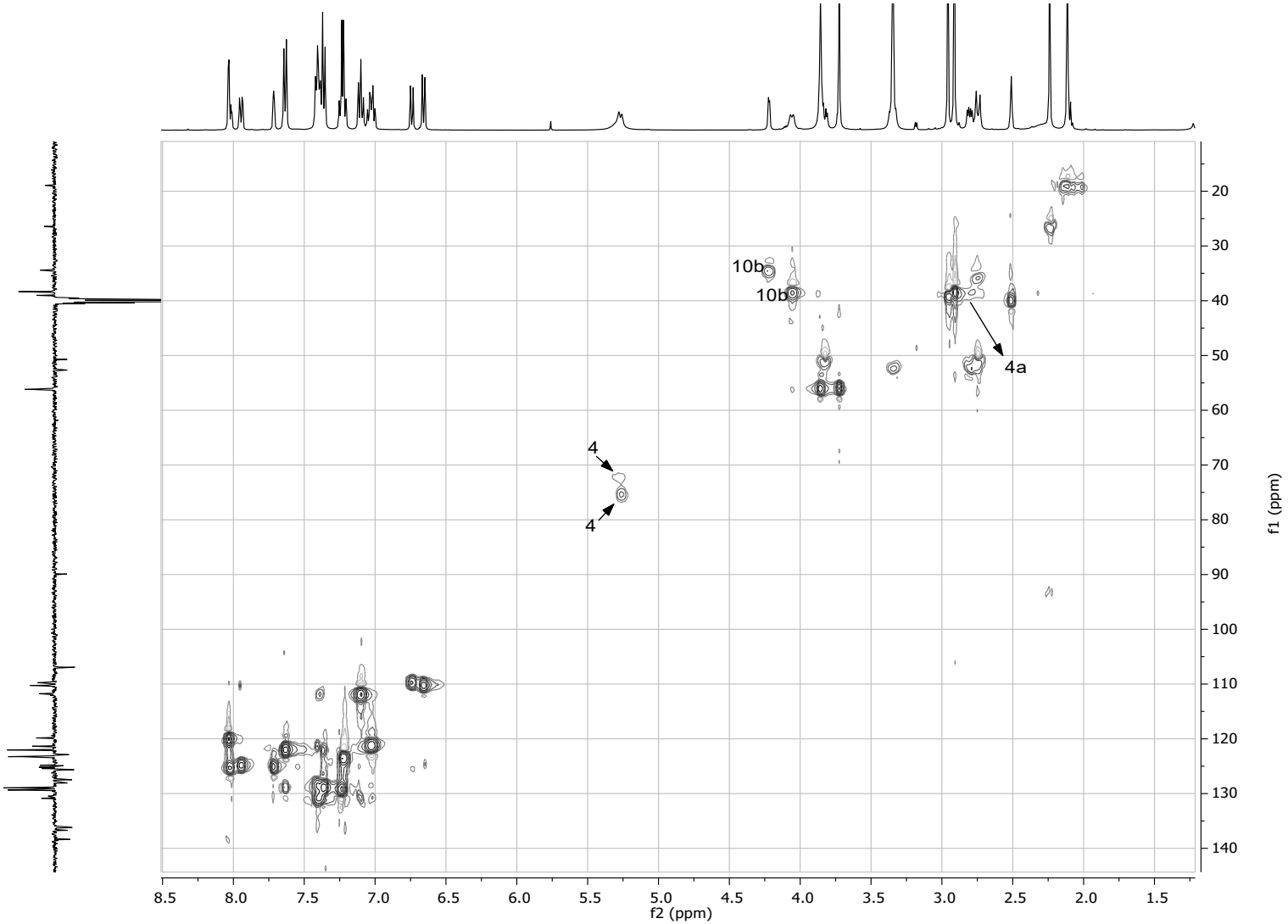

Figure S64. HSQC spectrum of *rac*-(4*R**,4a*S**,10b*S**)-**2an** and *rac*-(4*R**,4a*S**,10b*R**)-*reg*-**2an** in DMSO-d_6 at 500 MHz

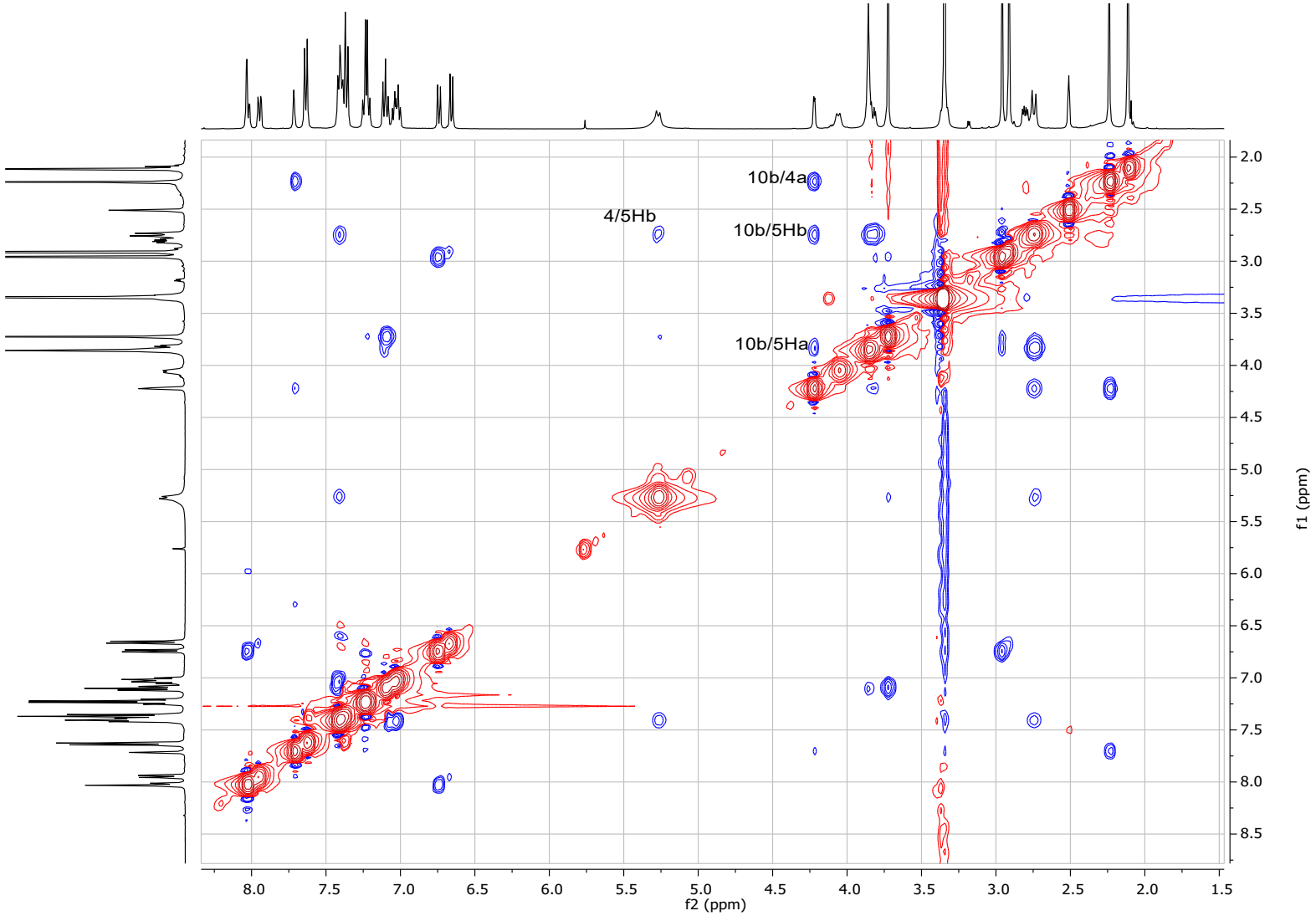

Figure S65. ROESY spectrum of *rac*-(4*R**,4a*S**,10b*S**)-**2an** and *rac*-(4*R**,4a*S**,10b*R**)-*reg*-**2an** in DMSO-d_6 at 500 MHz

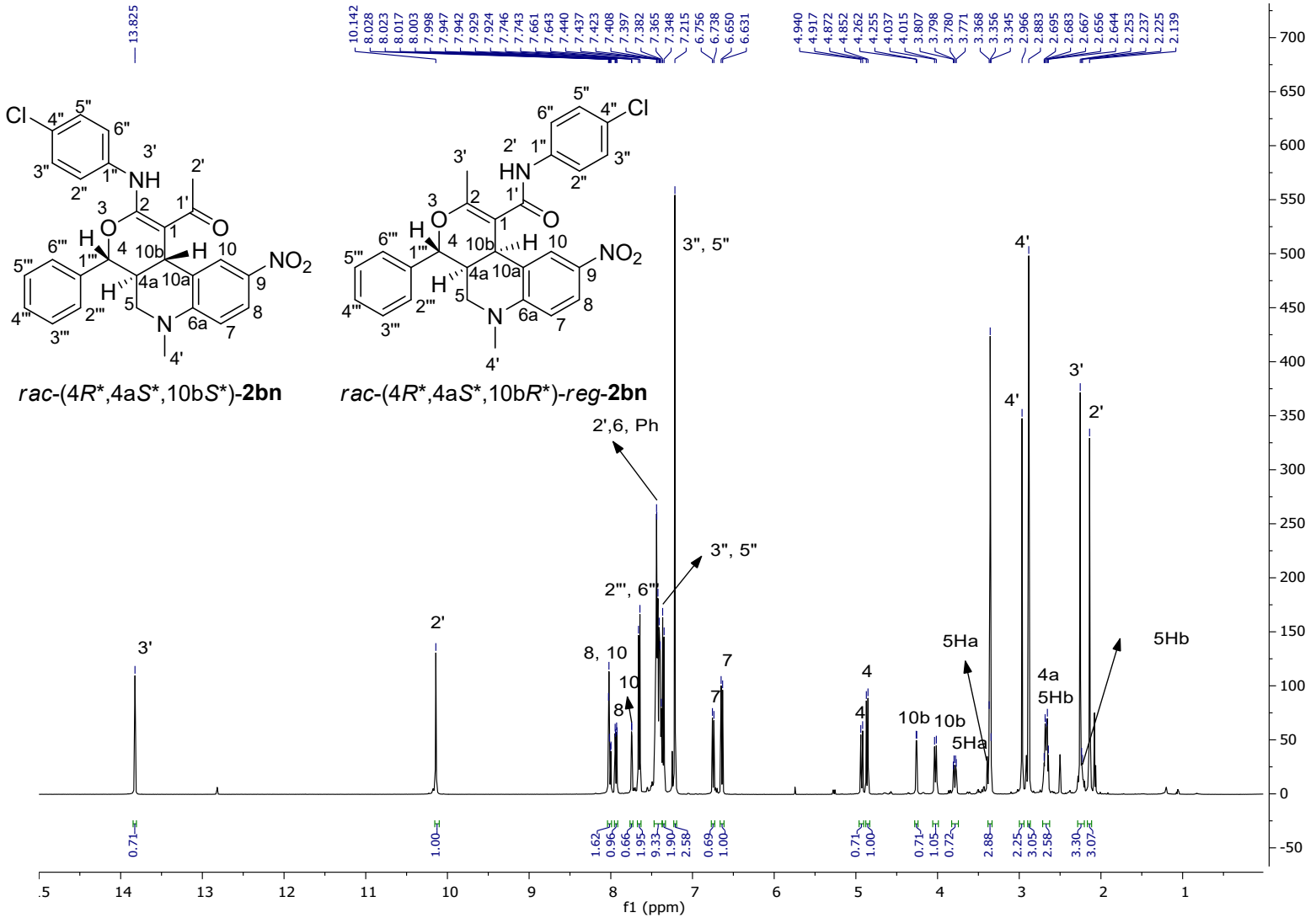

Figure S66. ^{1}H-NMR spectrum of *rac*-(4*R**,4a*S**,10b*S**)-**2bn** and *rac*-(4*R**,4a*S**,10b*R**)-*reg*-**2bn** in DMSO-d_6 at 500 MHz.

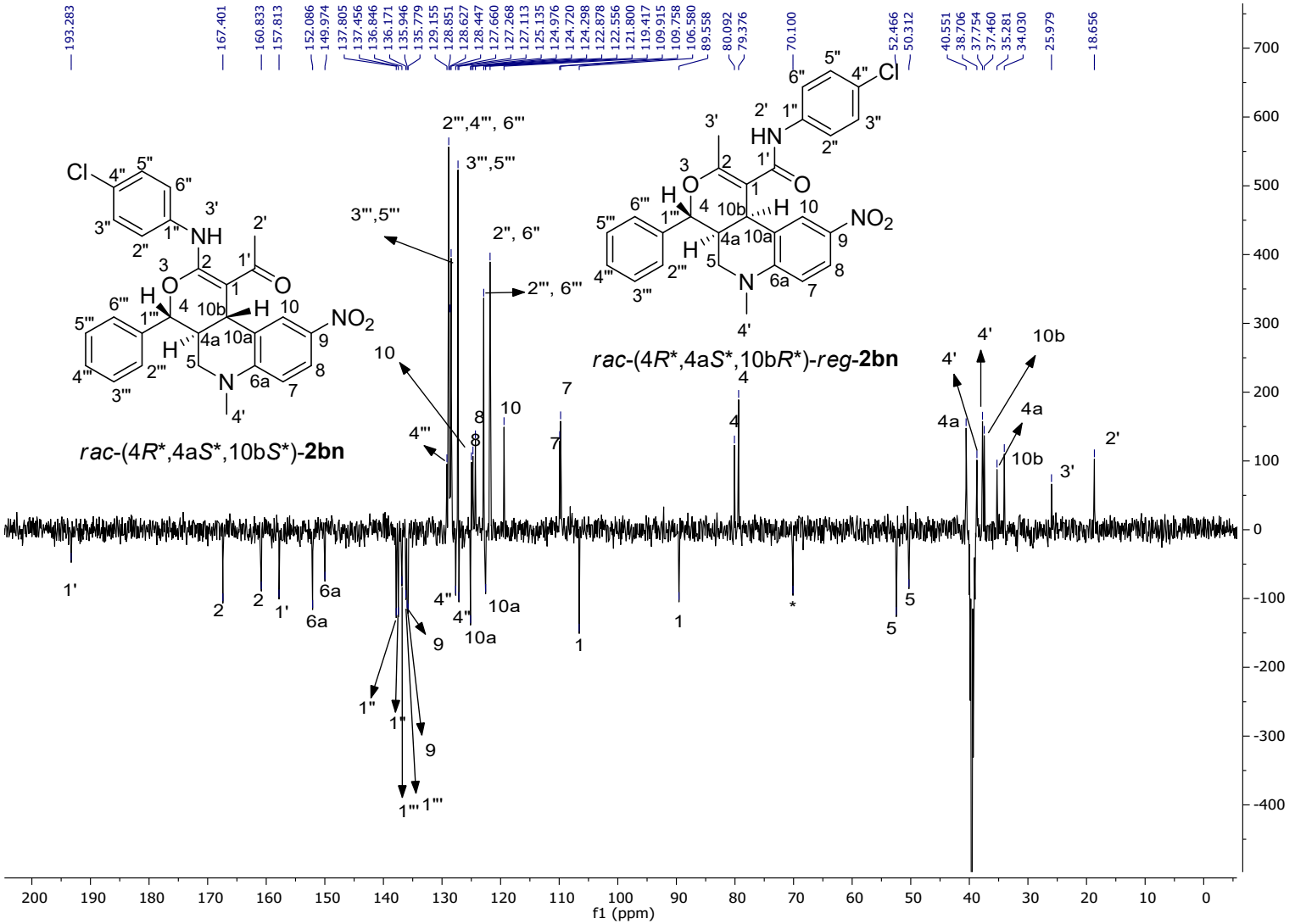

Figure S67. ^{13}C-NMR spectrum of *rac*-(4*R**,4a*S**,10b*S**)-**2bn** and *rac*-(4*R**,4a*S**,10b*R**)-*reg*-**2bn** in DMSO-d_6 at 125 MHz.

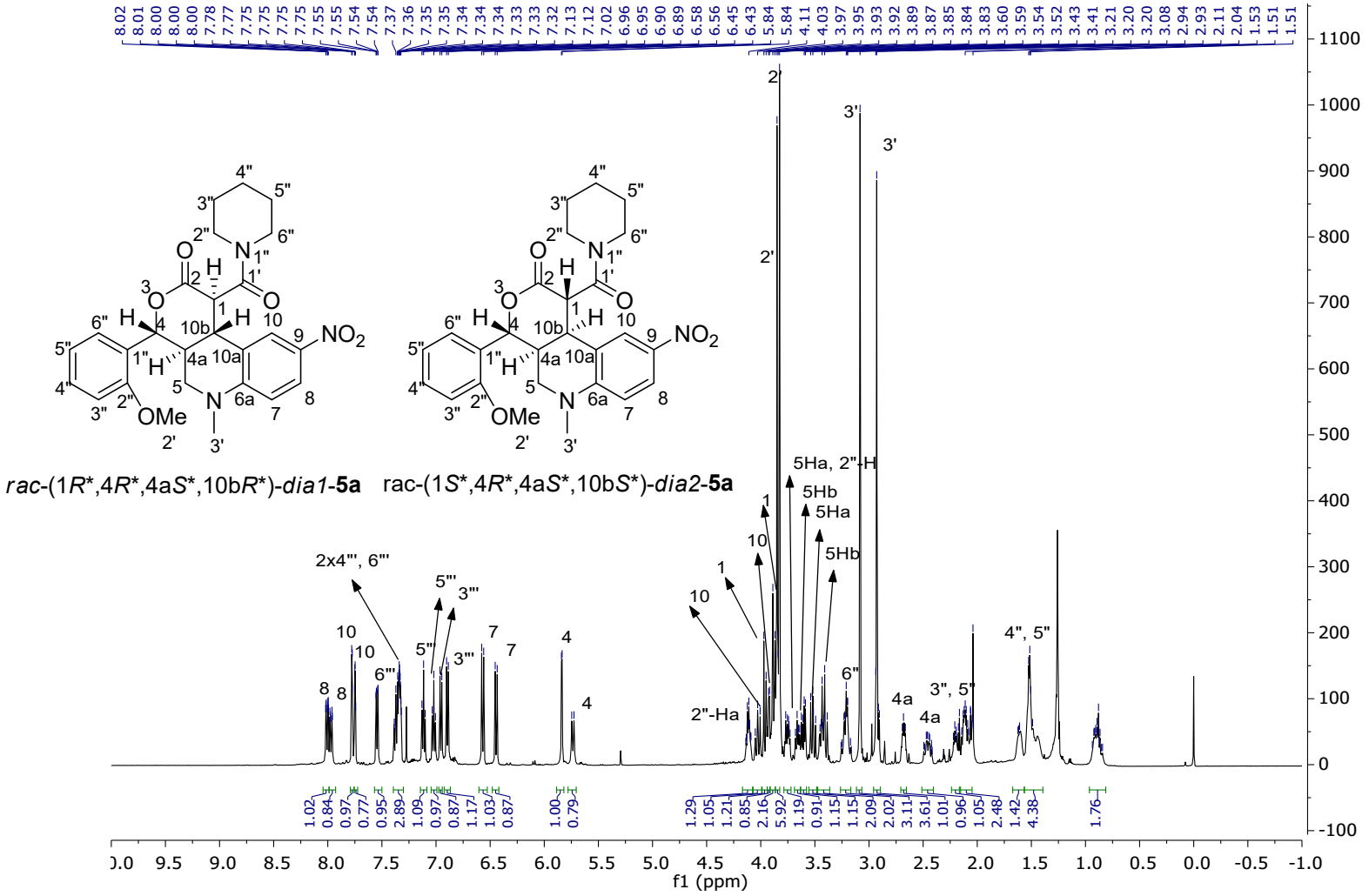

Figure S68. ^{1}H-NMR spectrum of the ~5:4 mixture of *rac*-(1*R**,4*R**,4a*S**,10b*R**)-*dia1*-**5a** and *rac*-(1*S**,4*R**,4a*S**,10b*S**)- *dia2*-**5a** in $CDCl_3$ at 500 MHz.

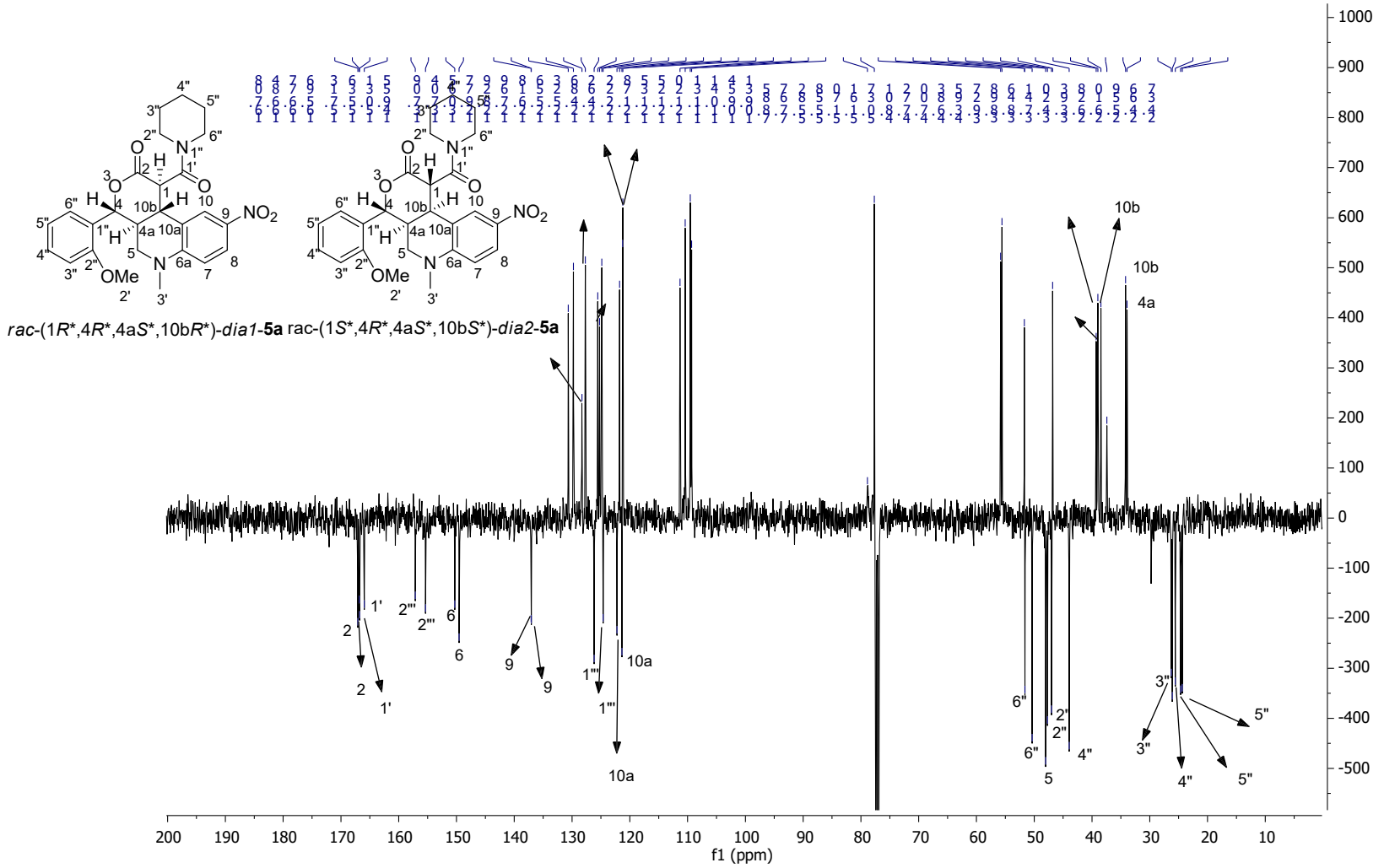

Figure S69. ^{13}C-NMR spectrum of the ~5:4 mixture of *rac*-(1*R**,4*R**,4a*S**,10b*R**)-*dia1*-**5a** and *rac*-(1*S**,4*R**,4a*S**,10b*S**)- *dia2*-**5a** in $CDCl_3$ at 125 MHz.

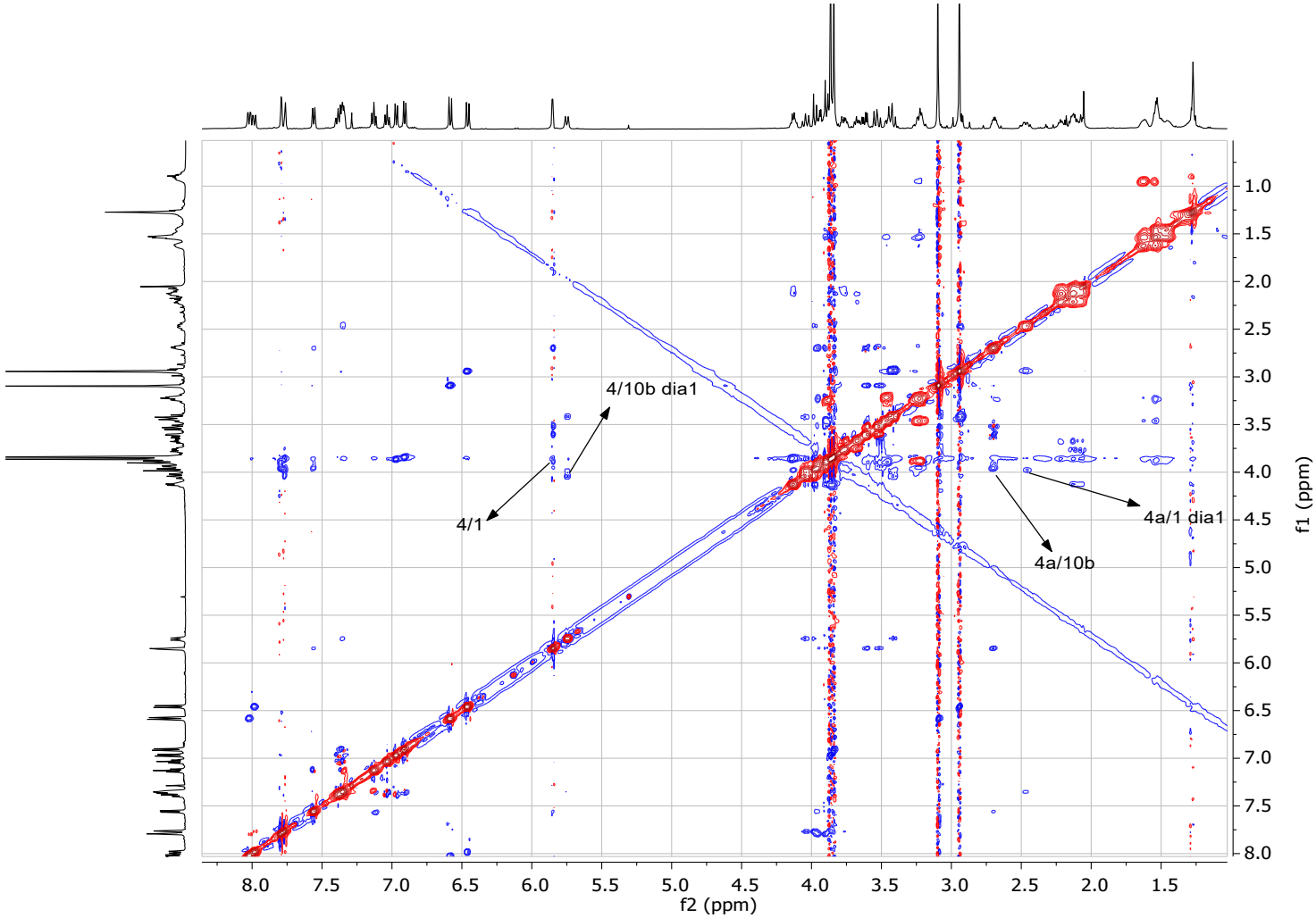

Figure S70. ROESY spectrum of the ~5:4 mixture of *rac*-(1*R**,4*R**,4a*S**,10b*R**)-*dia1*-**5a** and *rac*-(1*S**,4*R**,4a*S**,10b*S**)-*dia2*-**5a** in $CDCl_3$ at 500 MHz.

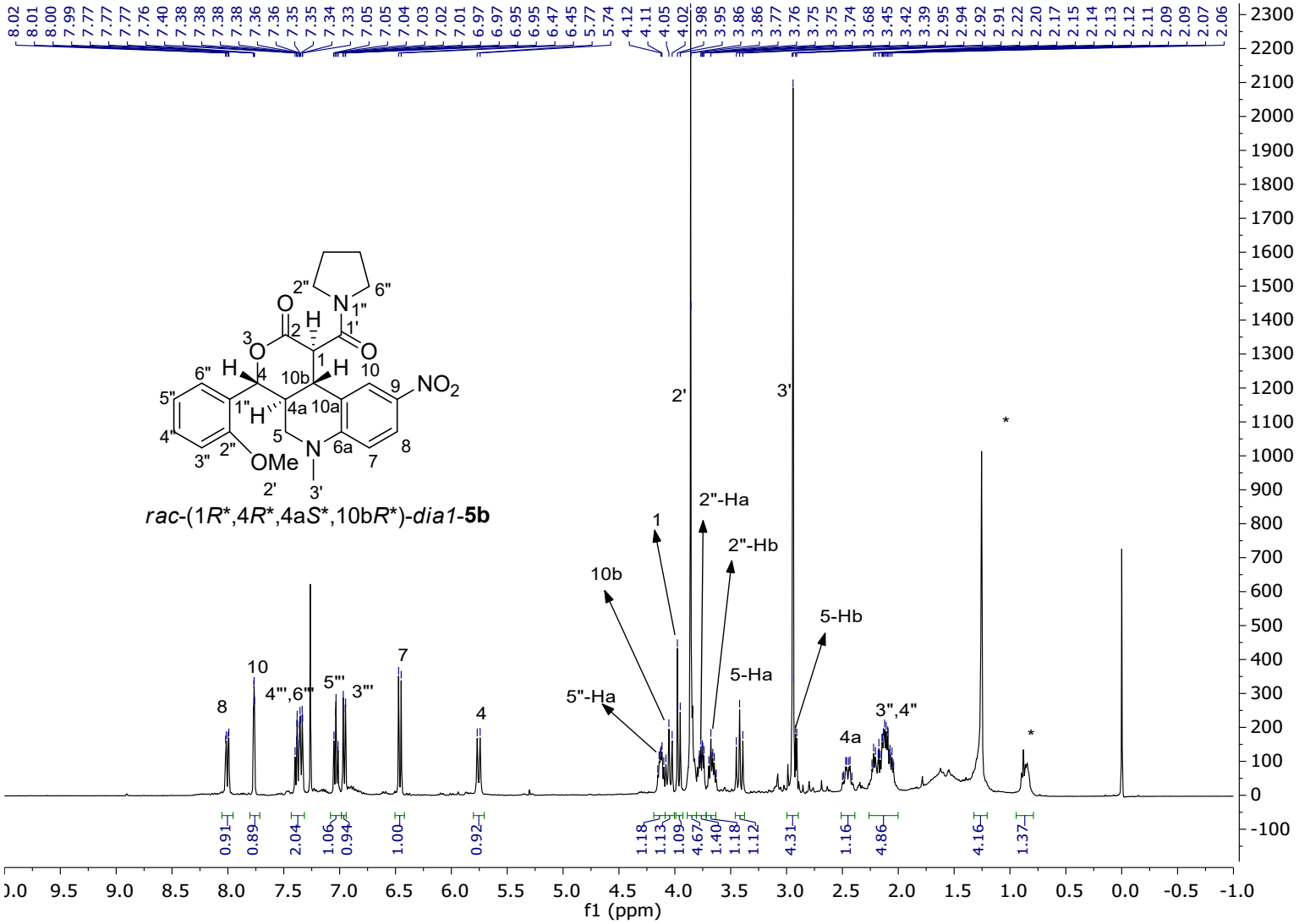

Figure S71. ^{1}H-NMR spectrum of the *rac*-(1*R**,4*R**,4a*S**,10b*R**)-*dia1*-**5b** in $CDCl_3$ at 400 MHz.

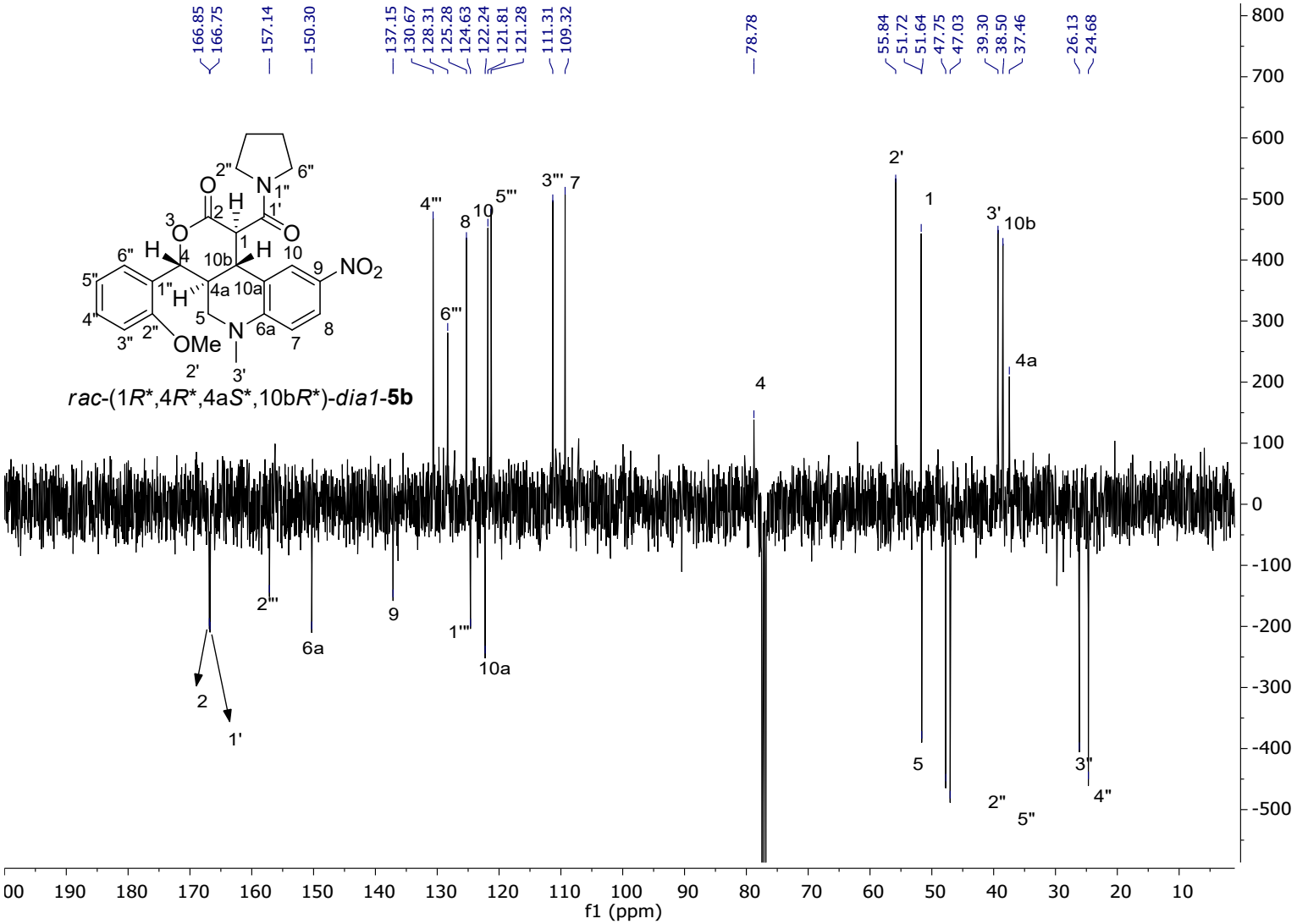

Figure S72. ^{13}C-NMR spectrum of the *rac*-(1*R**,4*R**,4a*S**,10b*R**)-*dia1*-**5b** in $CDCl_3$ at 100 MHz.

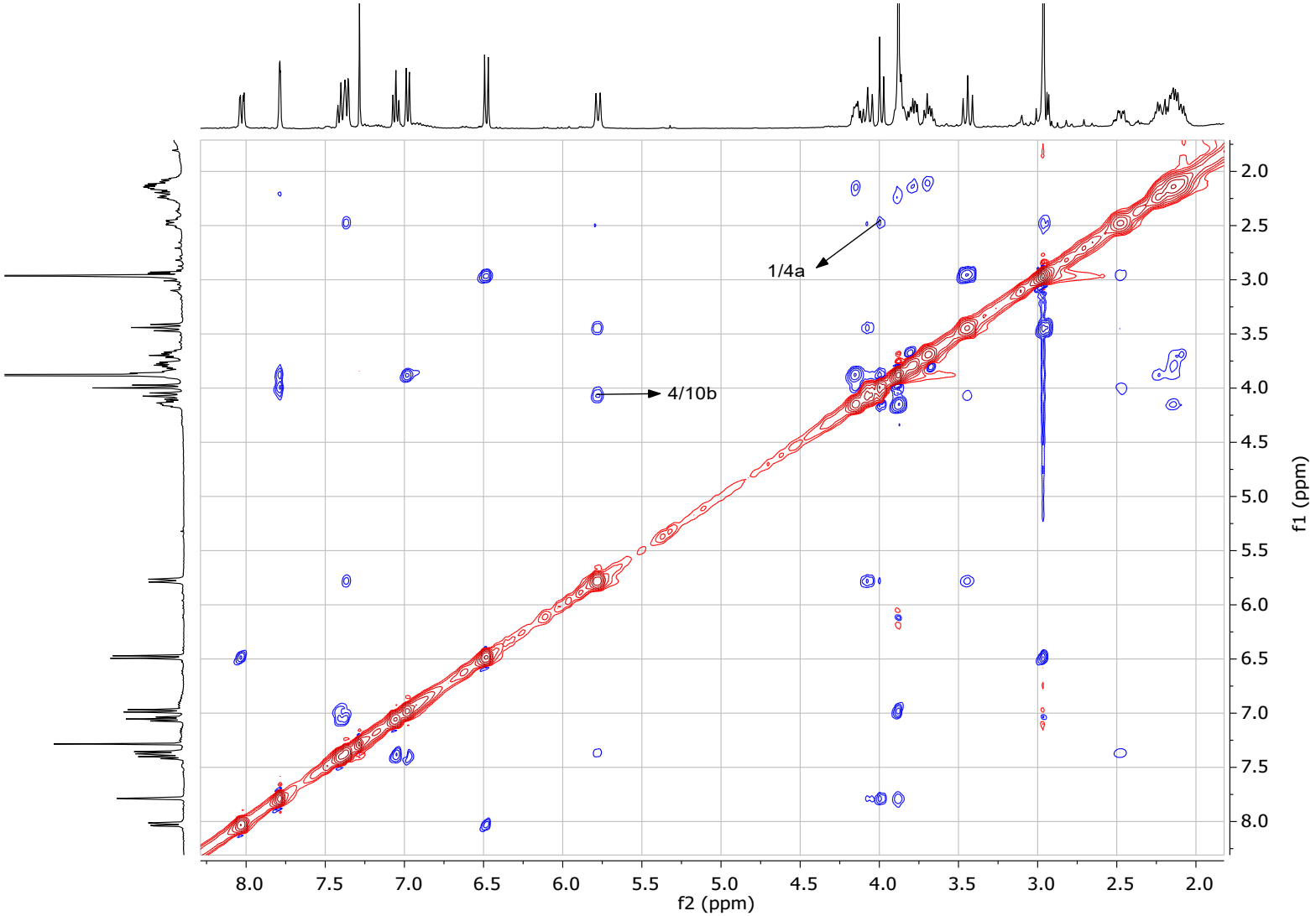

Figure S73. NOESY spectrum of the *rac*-(1*R**,4*R**,4a*S**,10b*R**)-*dia1*-**5b** in $CDCl_3$ at 400 MHz.

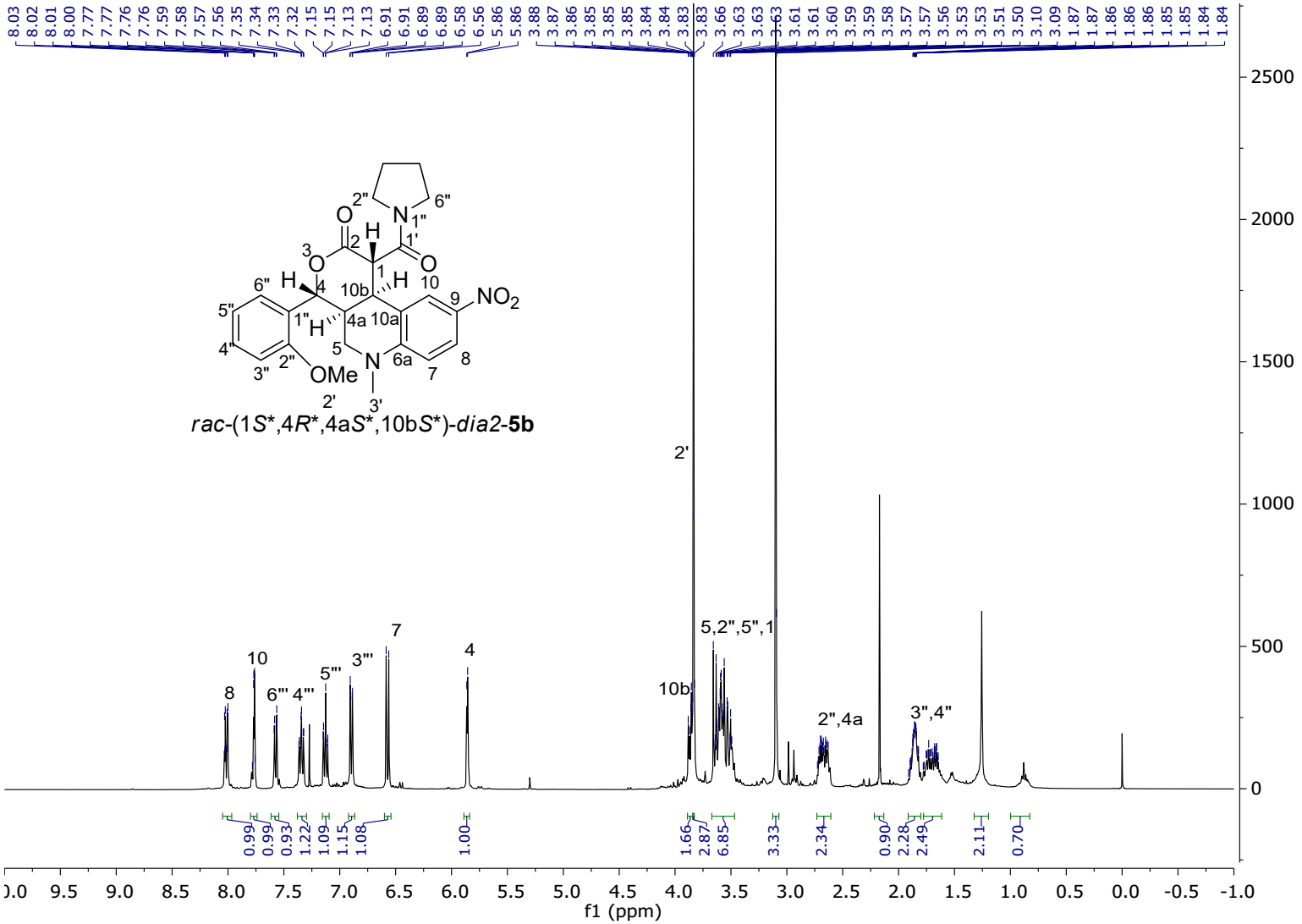

Figure S74. ^{1}H-NMR spectrum of the *rac*-(1*S**,4*R**,4a*S**,10b*S**)-*dia2*-**5b** in $CDCl_3$ at 400 MHz.

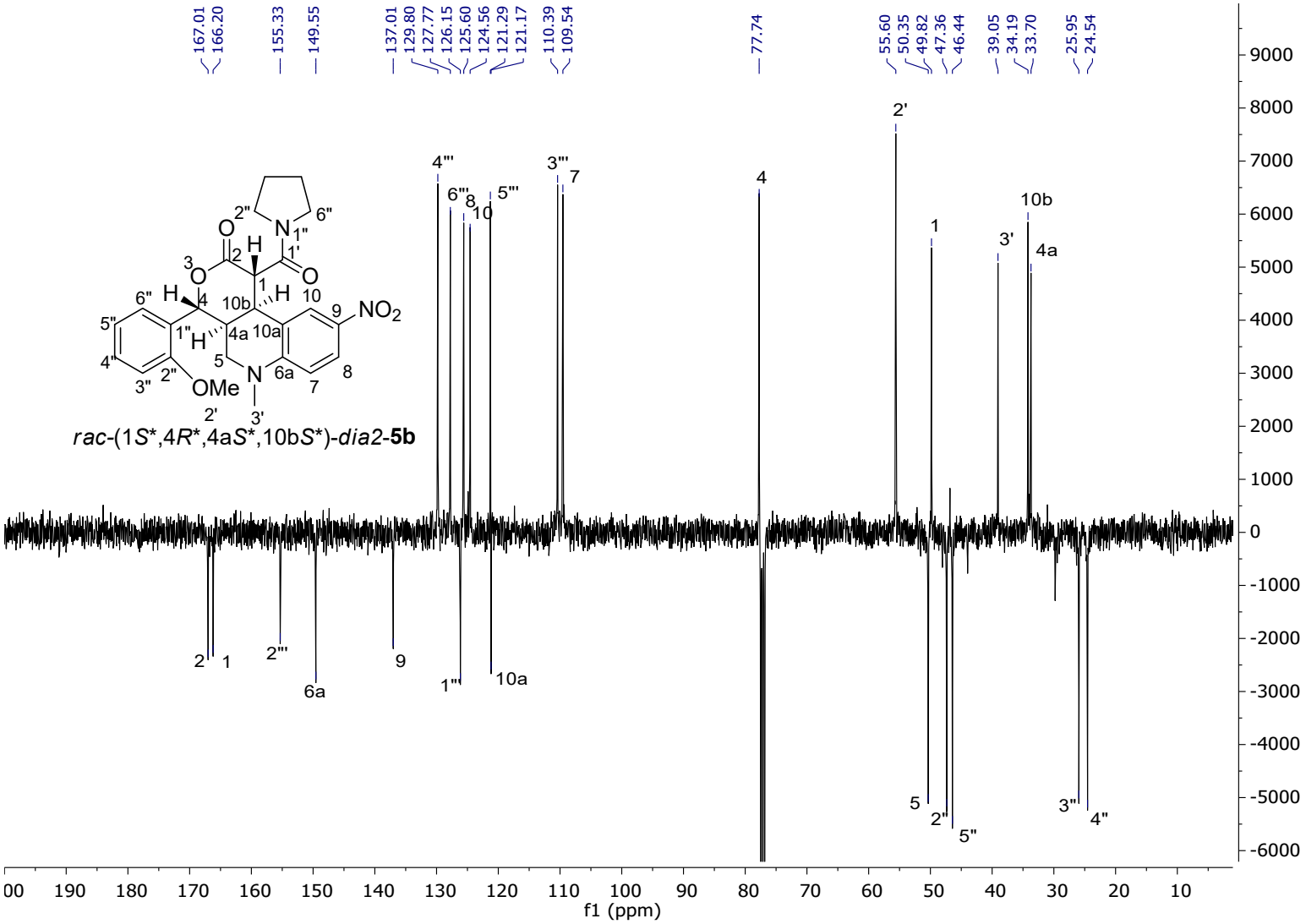

Figure S75. ^{13}C-NMR spectrum of the *rac*-(1*S**,4*R**,4a*S**,10b*S**)-*dia2*-**5b** in $CDCl_3$ at 100 MHz.

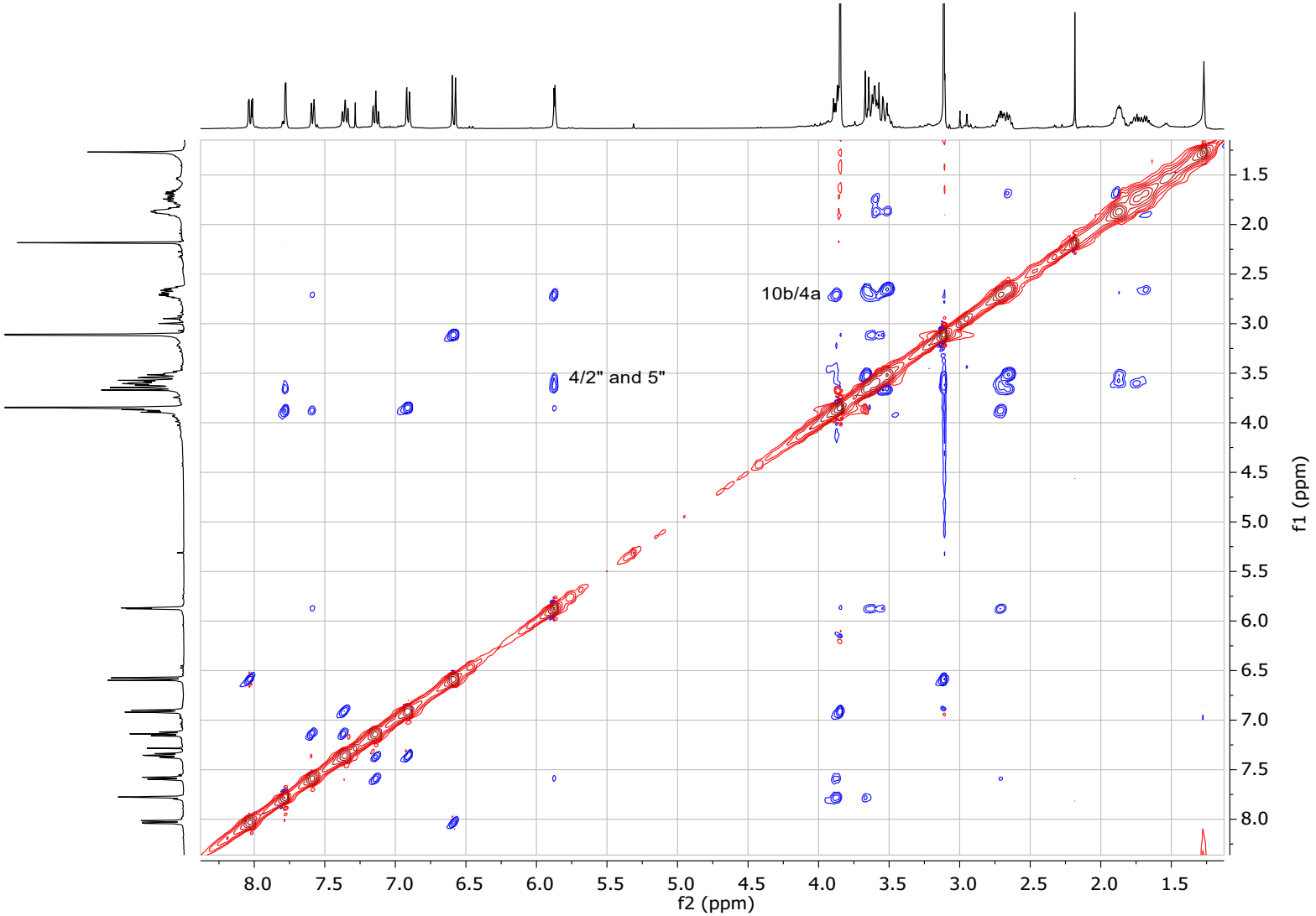

Figure S76. NOESY spectrum of the *rac*-(1*S**,4*R**,4a*S**,10b*S**)-*dia2*-**5b** in $CDCl_3$ at 400 MHz.

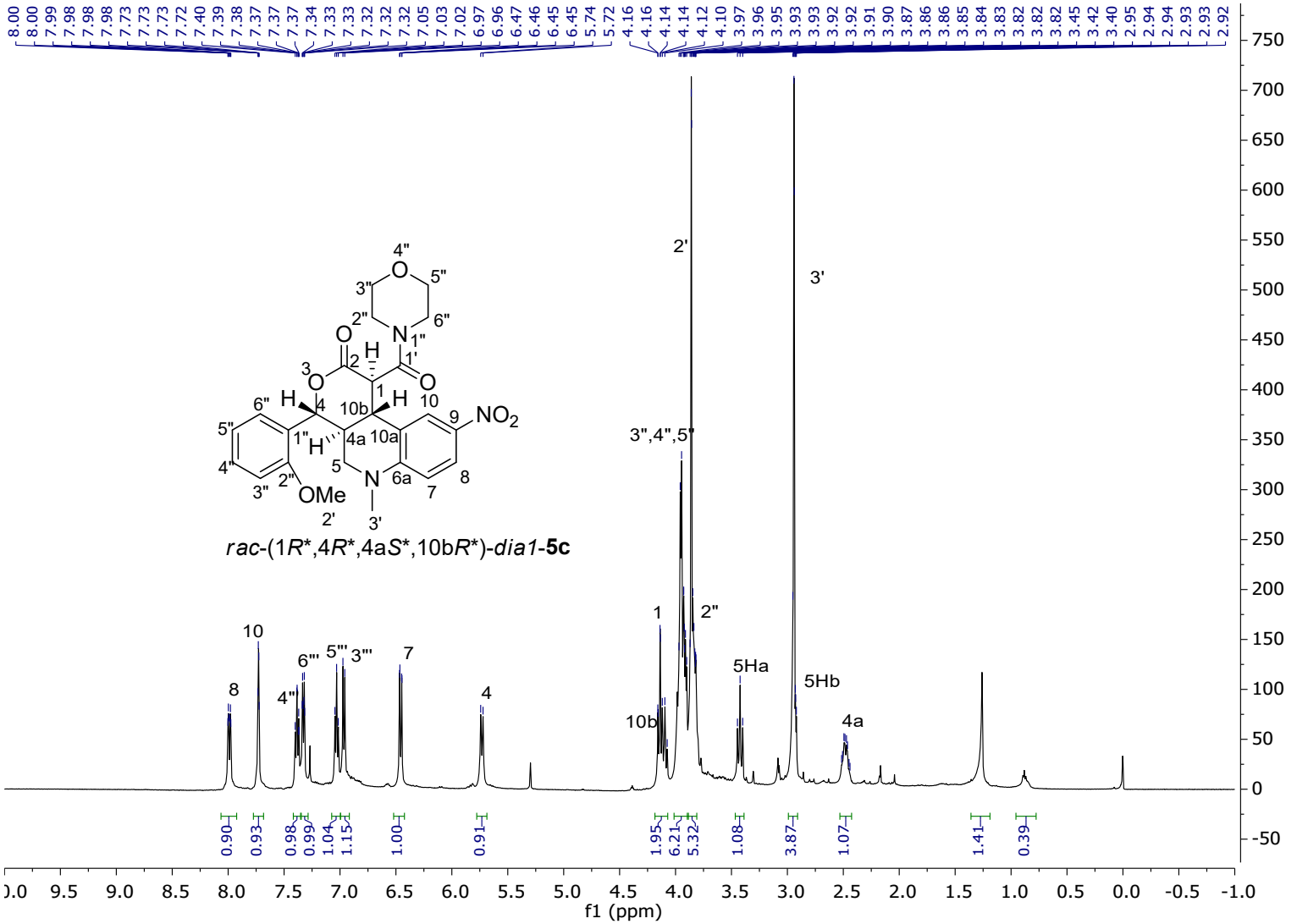

Figure S77. ^{1}H-NMR spectrum of the *rac*-(1*R**,4*R**,4a*S**,10b*R**)-*dia1*-**5c** in $CDCl_3$ at 500 MHz.

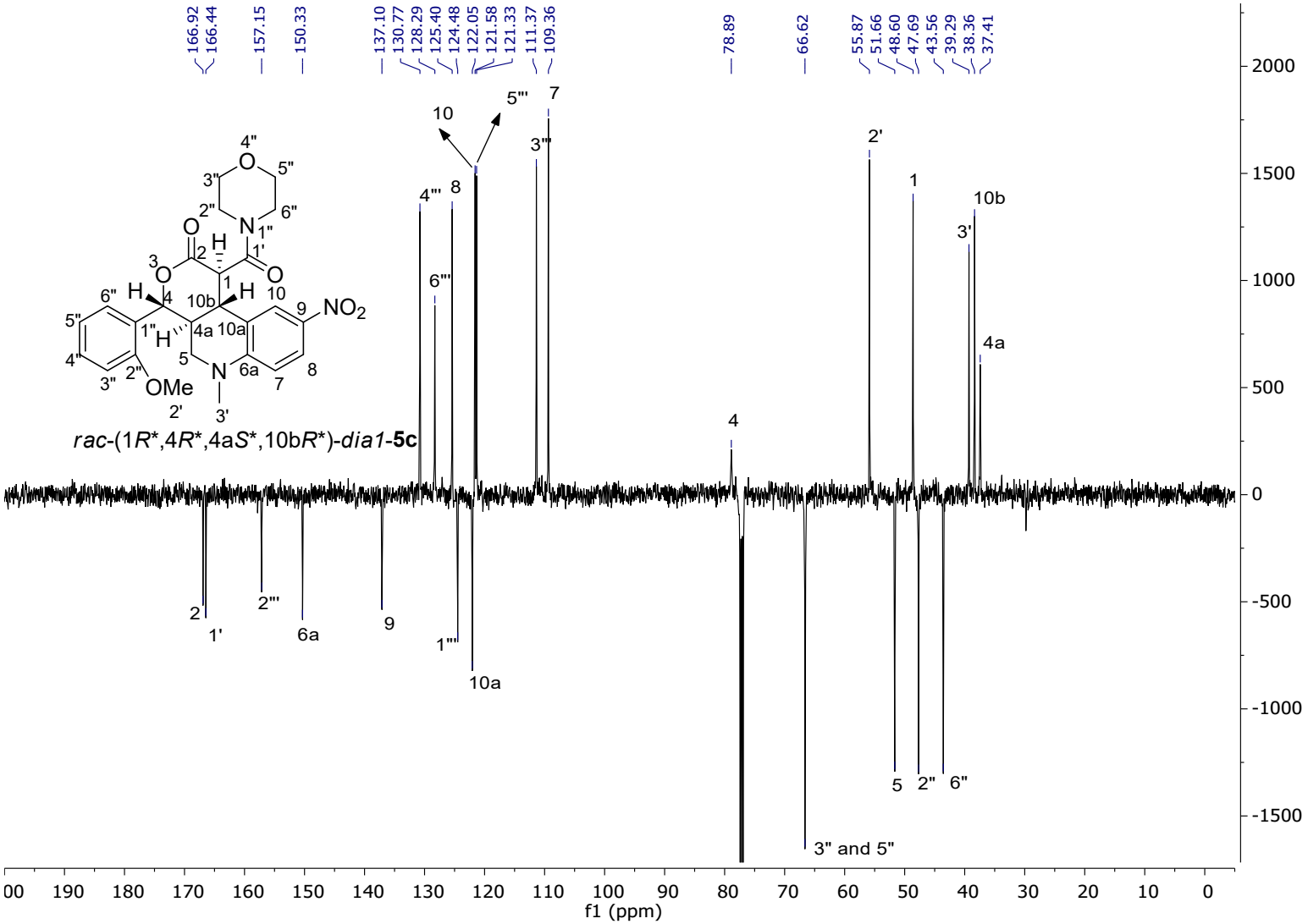

Figure S78. ^{13}C-NMR spectrum of the *rac*-(1*R**,4*R**,4a*S**,10b*R**)-*dia1*-**5c** in $CDCl_3$ at 125 MHz.

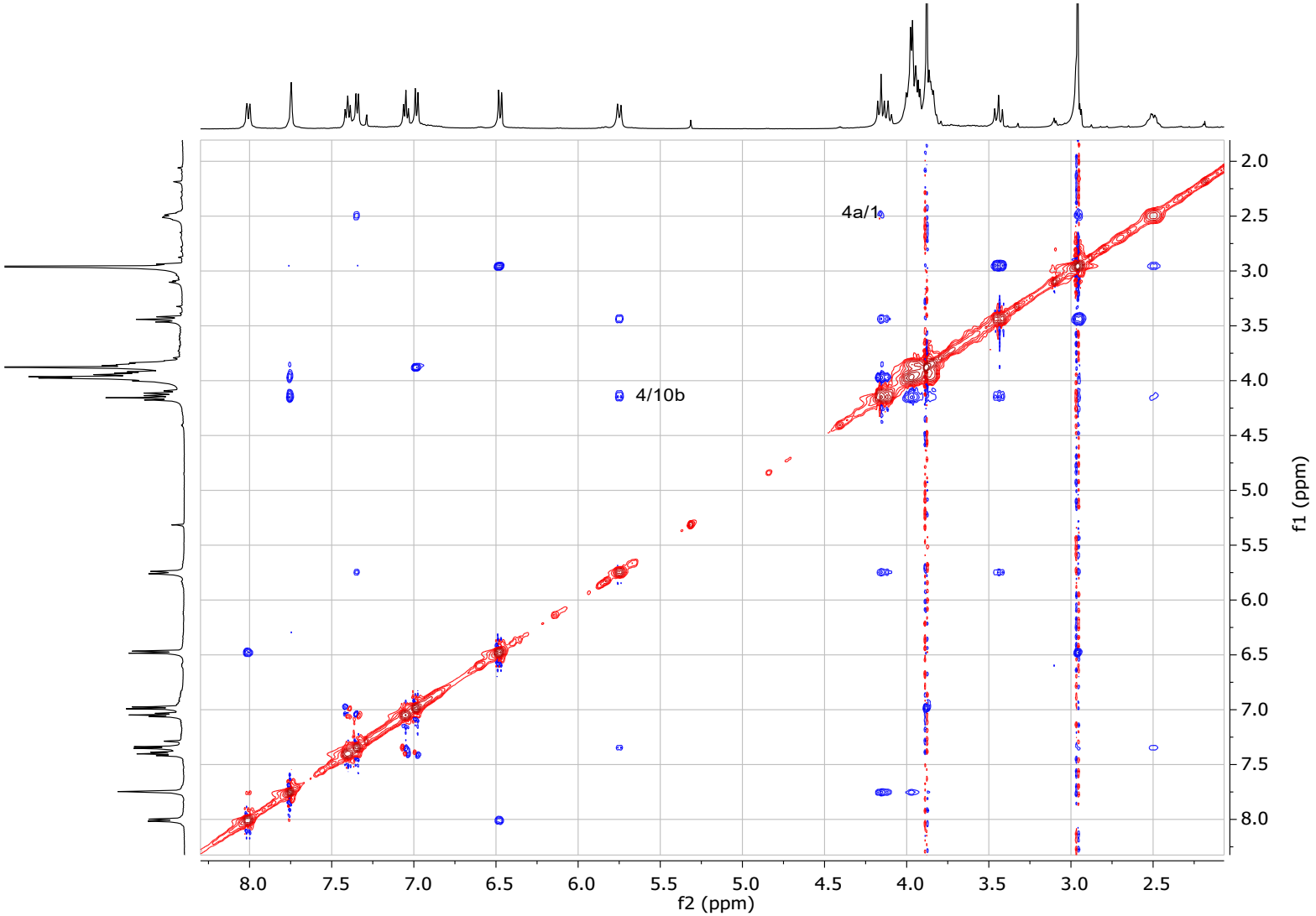

Figure S79. ROESY spectrum of the *rac*-(1*R**,4*R**,4a*S**,10b*R**)-*dia1*-**5c** in $CDCl_3$ at 500 MHz.

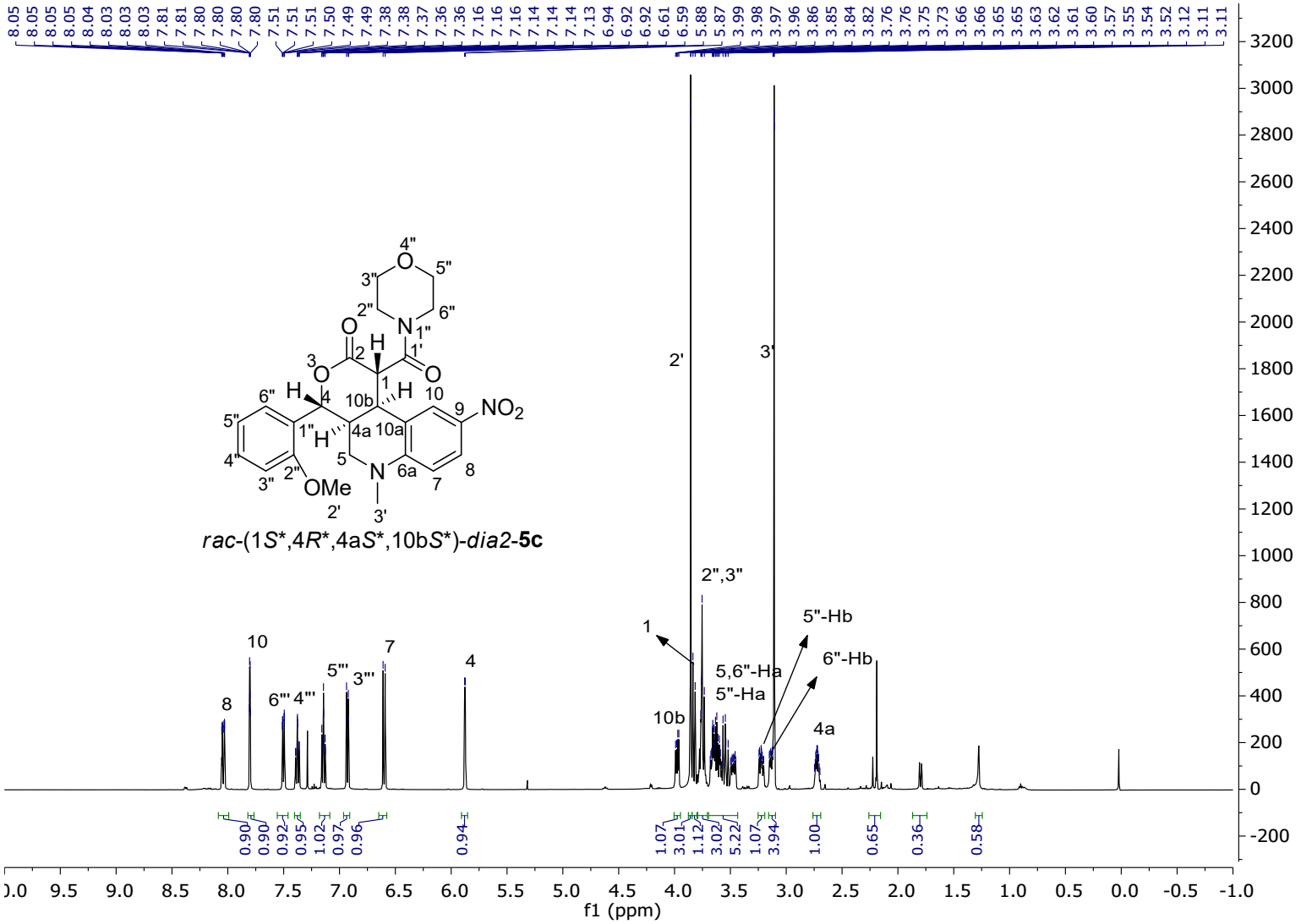

Figure S80. ^{1}H-NMR spectrum of the *rac*-(1*S**,4*R**,4a*S**,10b*S**)-*dia2*-**5c** in $CDCl_3$ at 500 MHz.

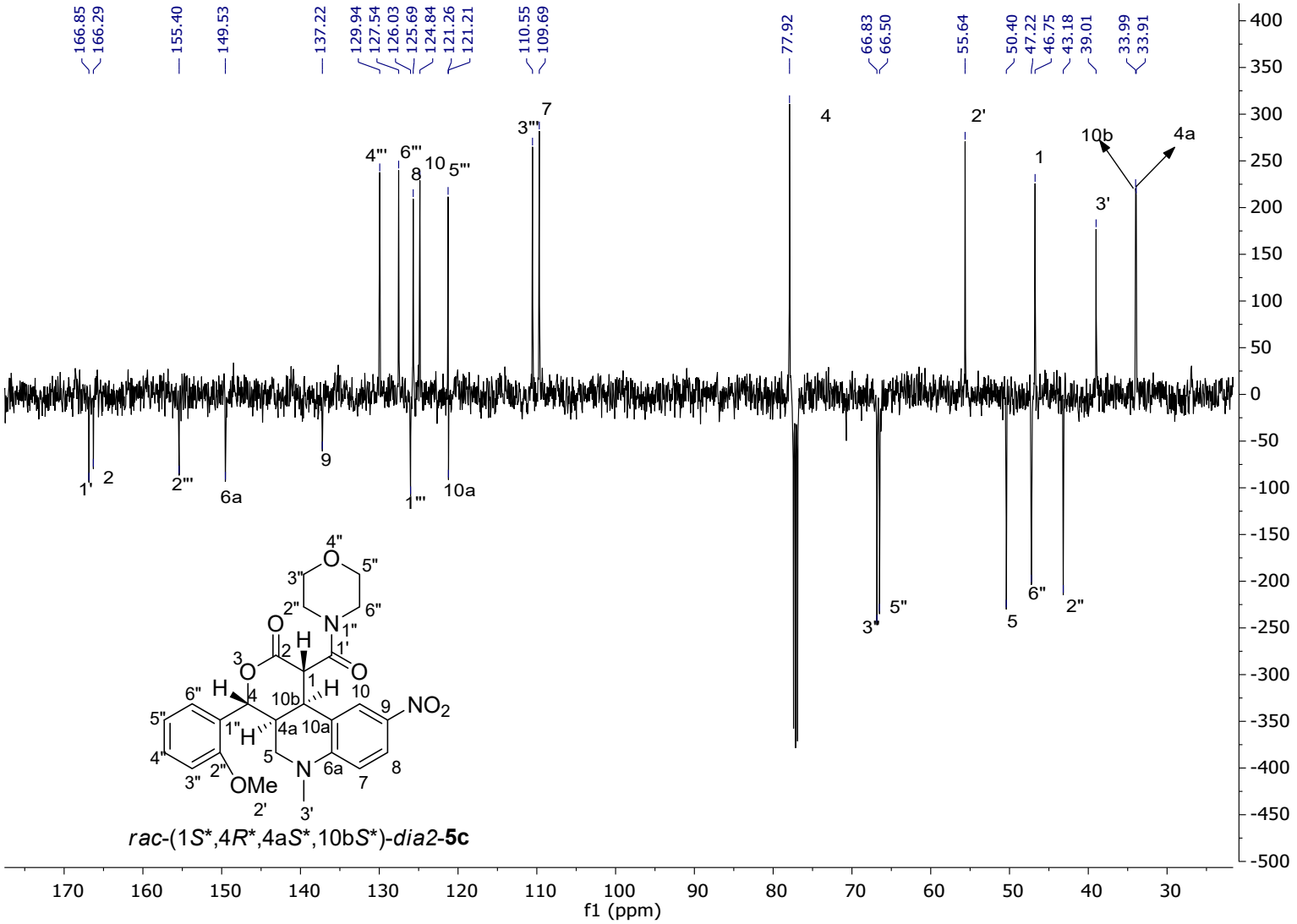

Figure S81. ^{13}C-NMR spectrum of the *rac*-(1*S**,4*R**,4a*S**,10b*S**)-*dia2*-**5c** in $CDCl_3$ at 125 MHz.

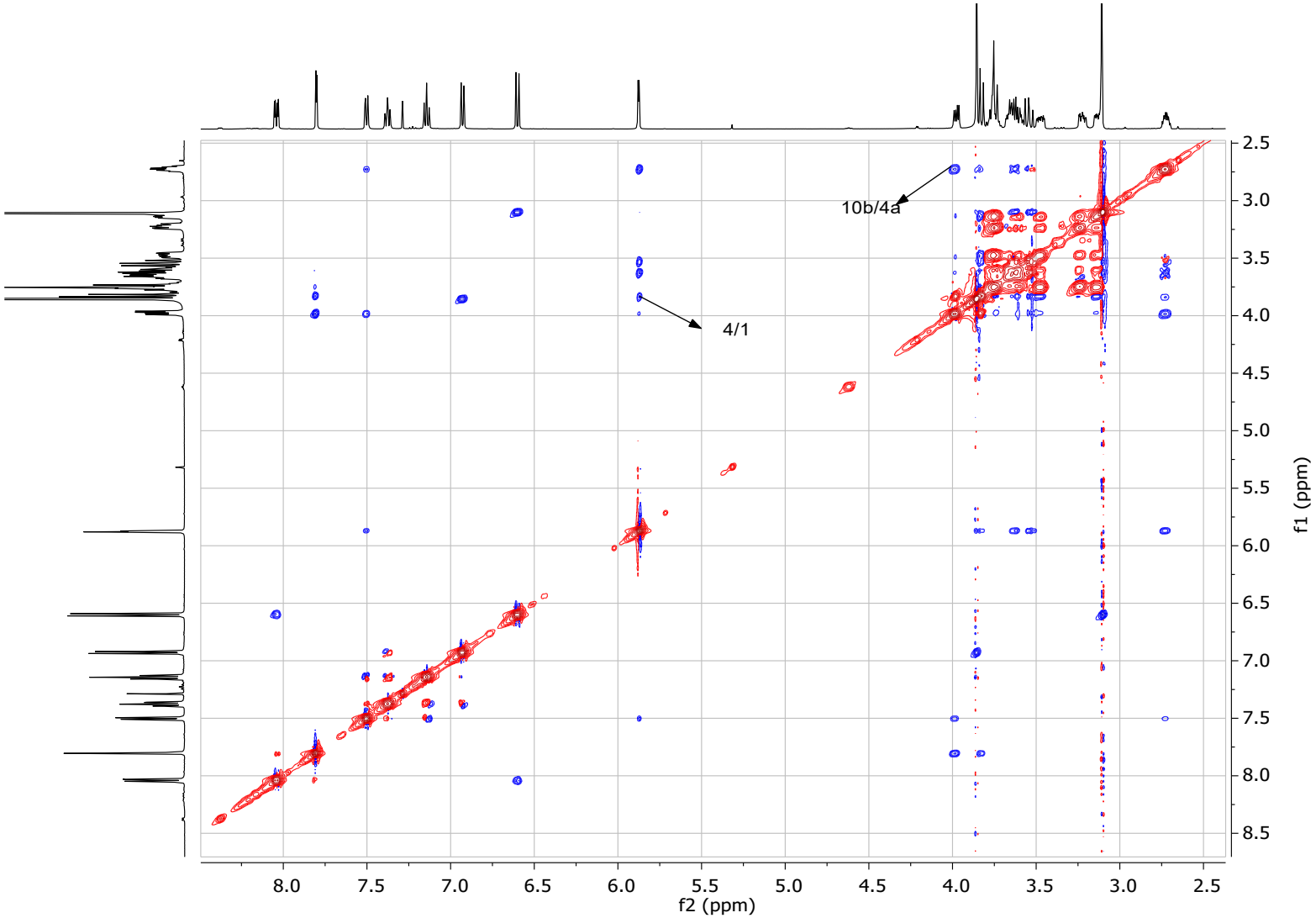

Figure S82. ROESY spectrum of the *rac*-(1*S**,4*R**,4a*S**,10b*S**)-*dia2*-**5c** in $CDCl_3$ at 500 MHz.

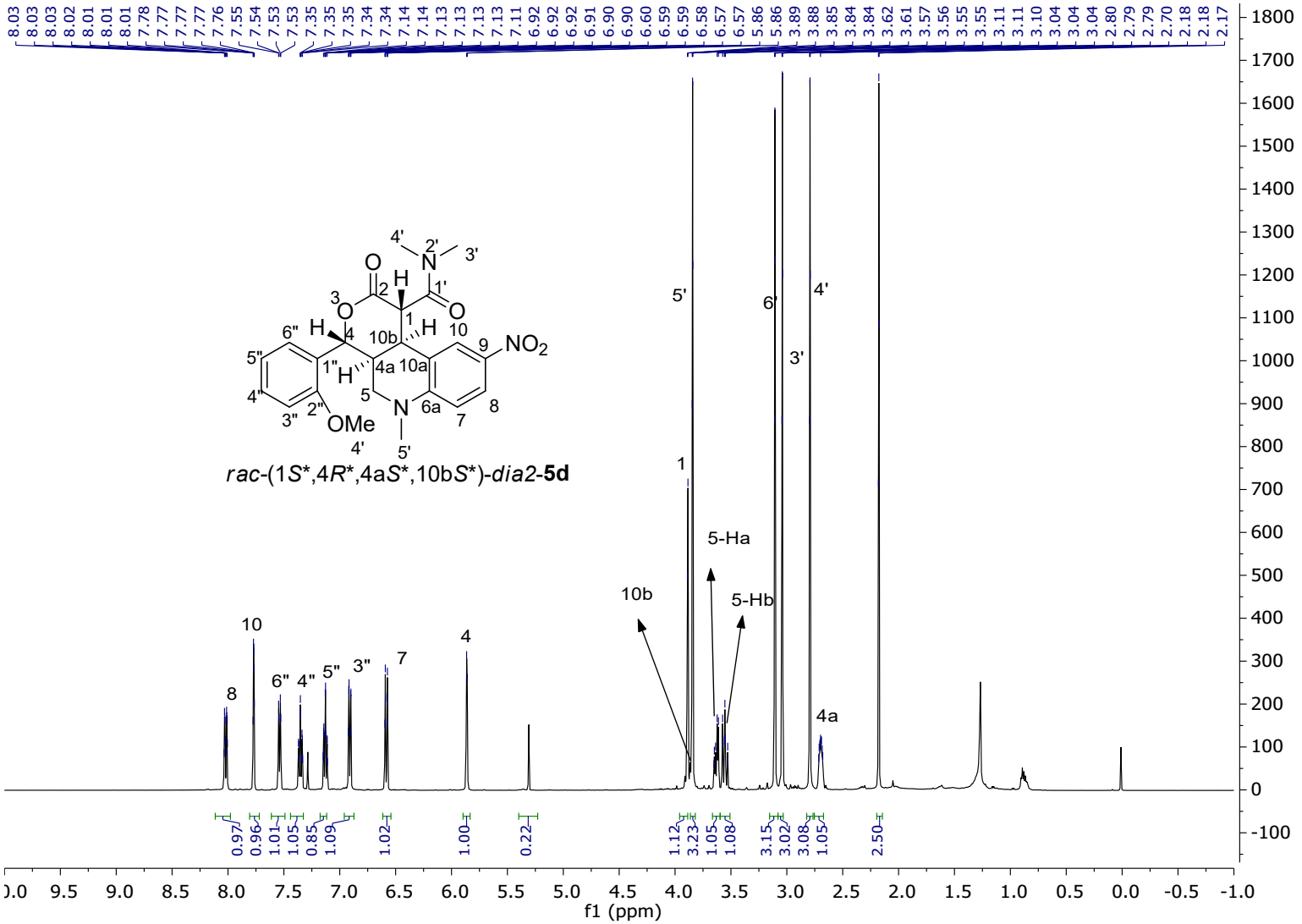

Figure S83. ^{1}H-NMR spectrum of the *rac*-(1*S**,4*R**,4a*S**,10b*S**)- *dia2*-**5d** in $CDCl_3$ at 500 MHz.

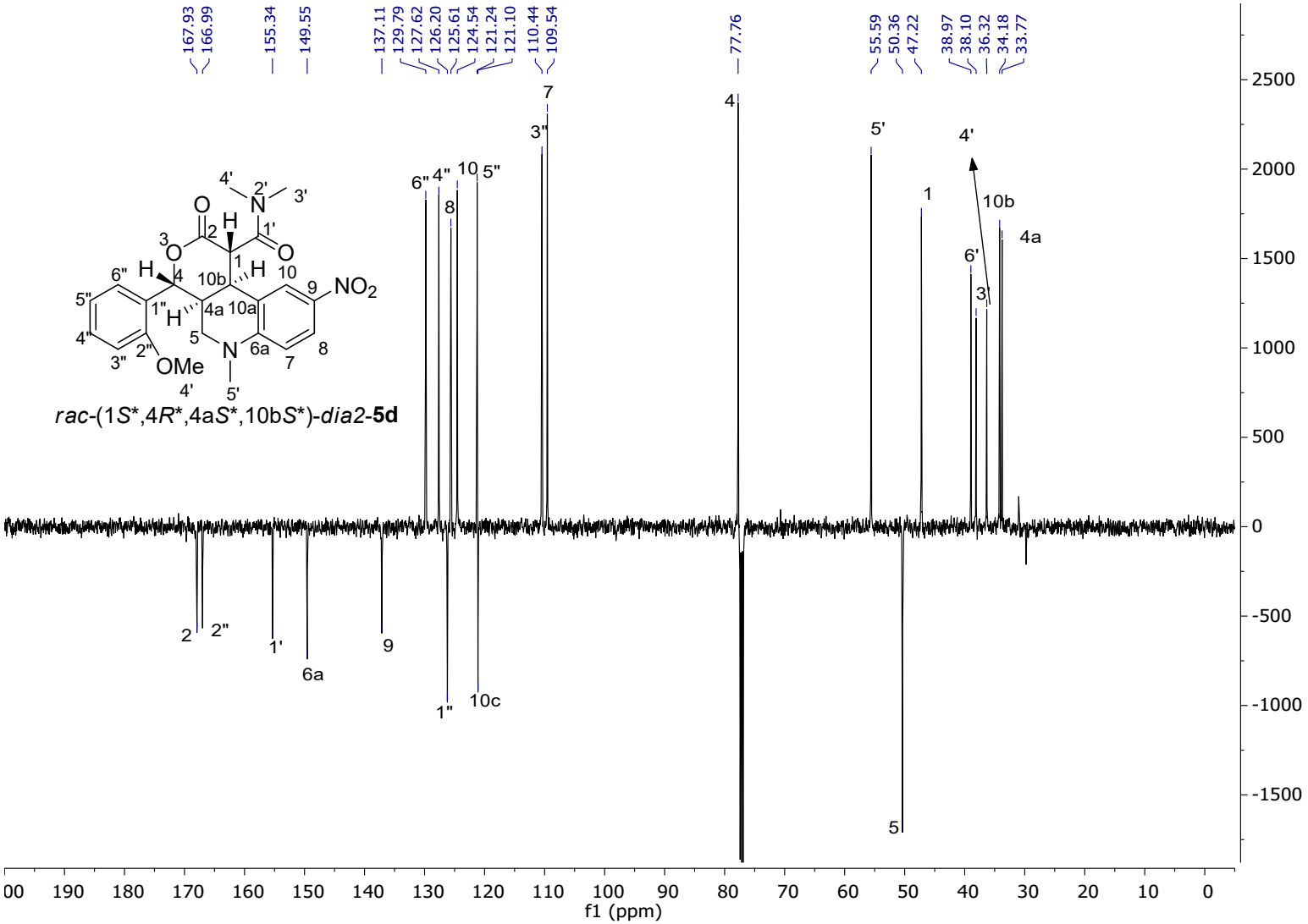

Figure S84. ^{13}C-NMR spectrum of the *rac*-(1*S**,4*R**,4a*S**,10b*S**)-*dia2*-**5d** in $CDCl_3$ at 125 MHz.

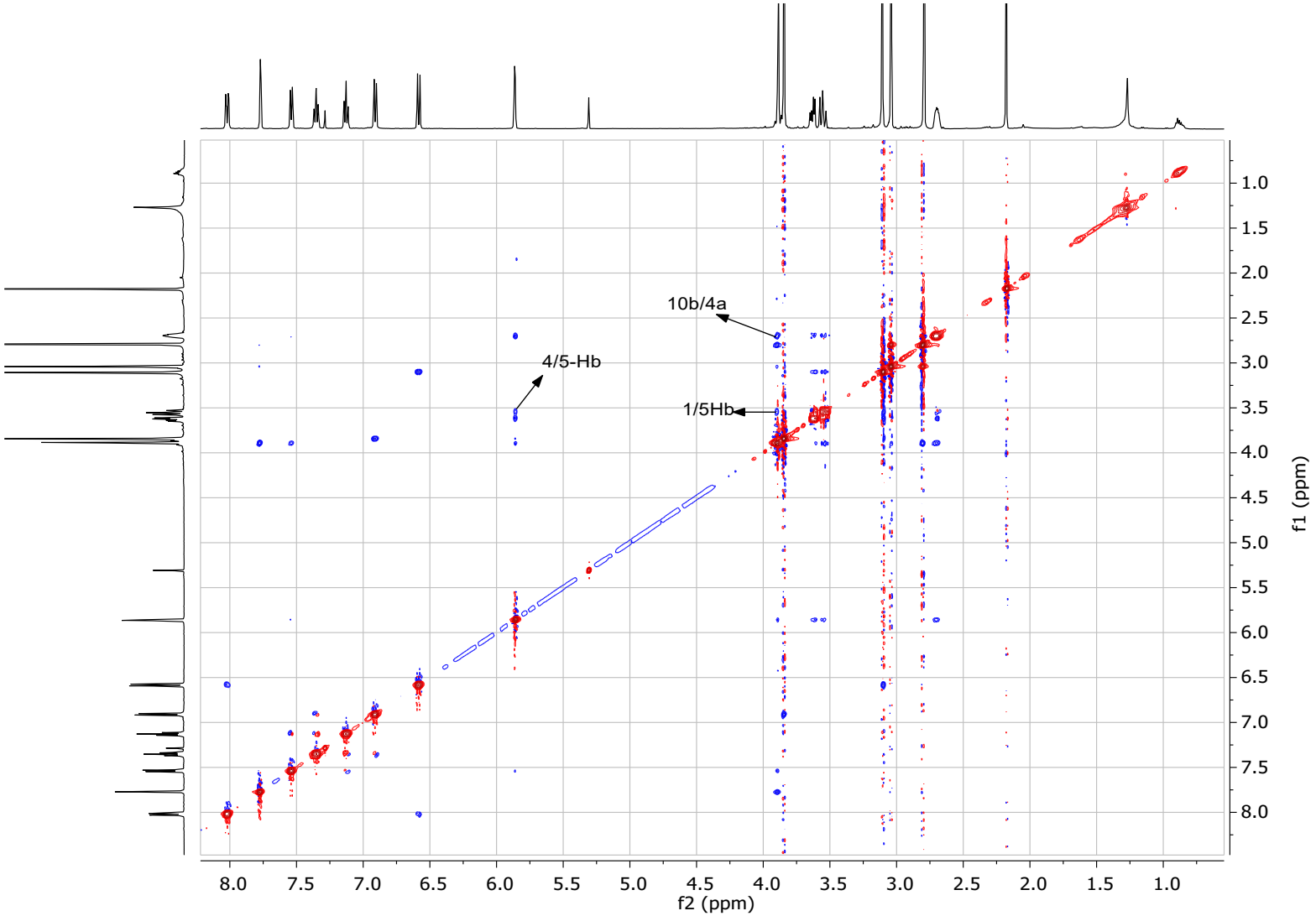

Figure S85. ROESY spectrum of the *rac*-(1*S**,4*R**,4a*S**,10b*S**)-*dia2*-**5d** in $CDCl_3$ at 500 MHz.

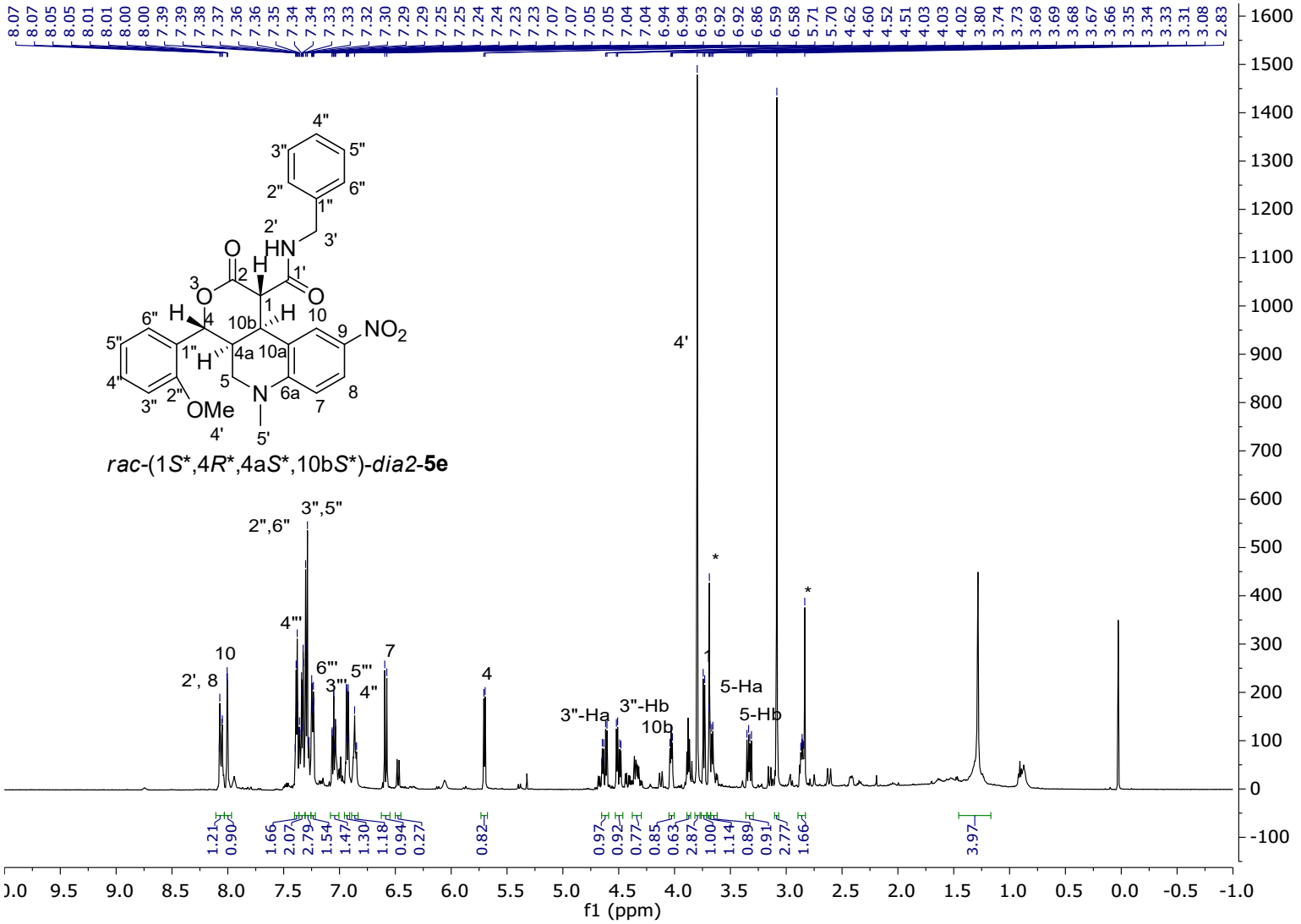

Figure S86. ^{1}H-NMR spectrum of the *rac*-(1*S**,4*R**,4a*S**,10b*S**)-*dia2*-**5e** in $CDCl_3$ at 500 MHz.

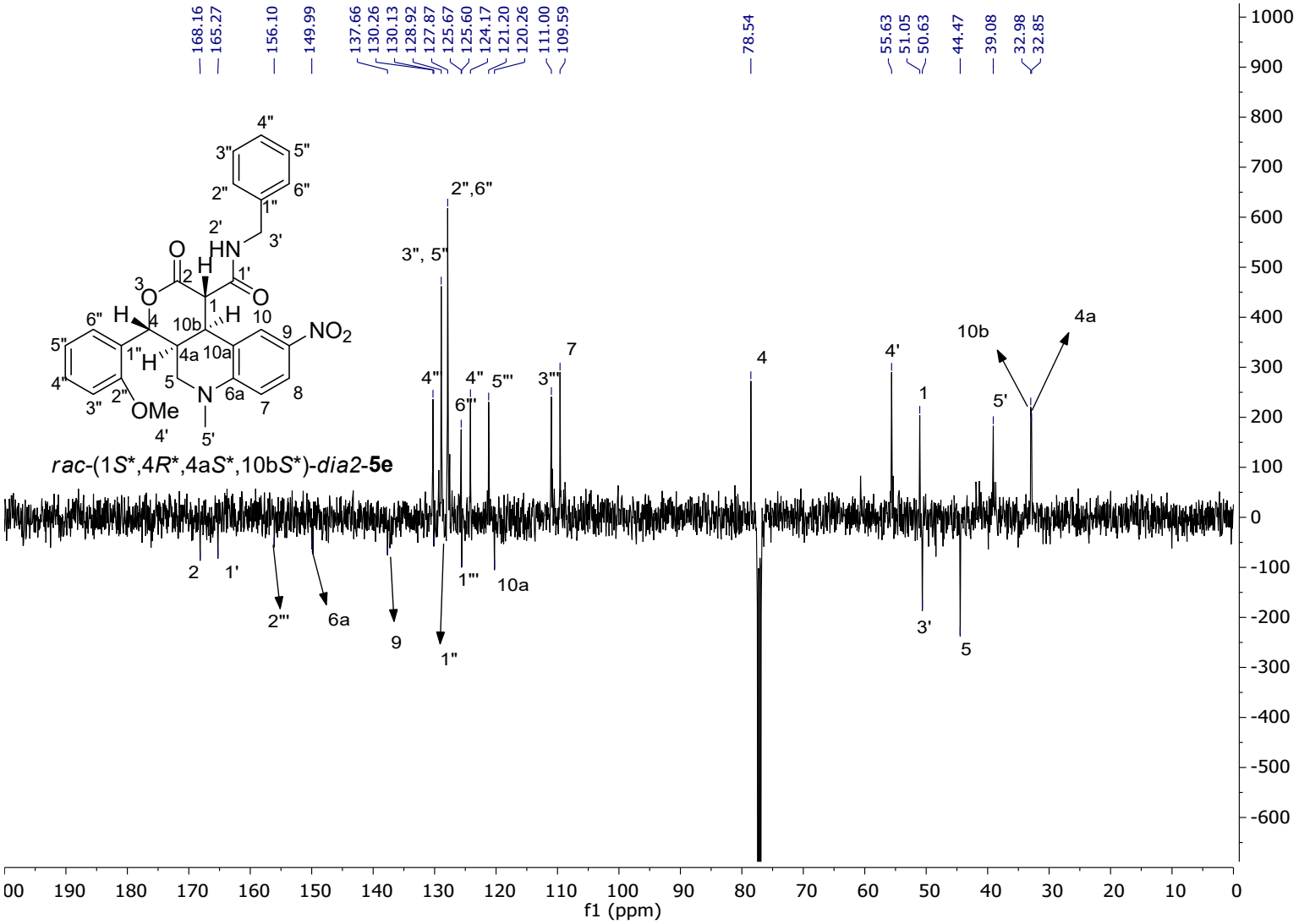

Figure S87. ^{13}C-NMR spectrum of the *rac*-(1*S**,4*R**,4a*S**,10b*S**)-*dia2*-**5e** in $CDCl_3$ at 125 MHz.

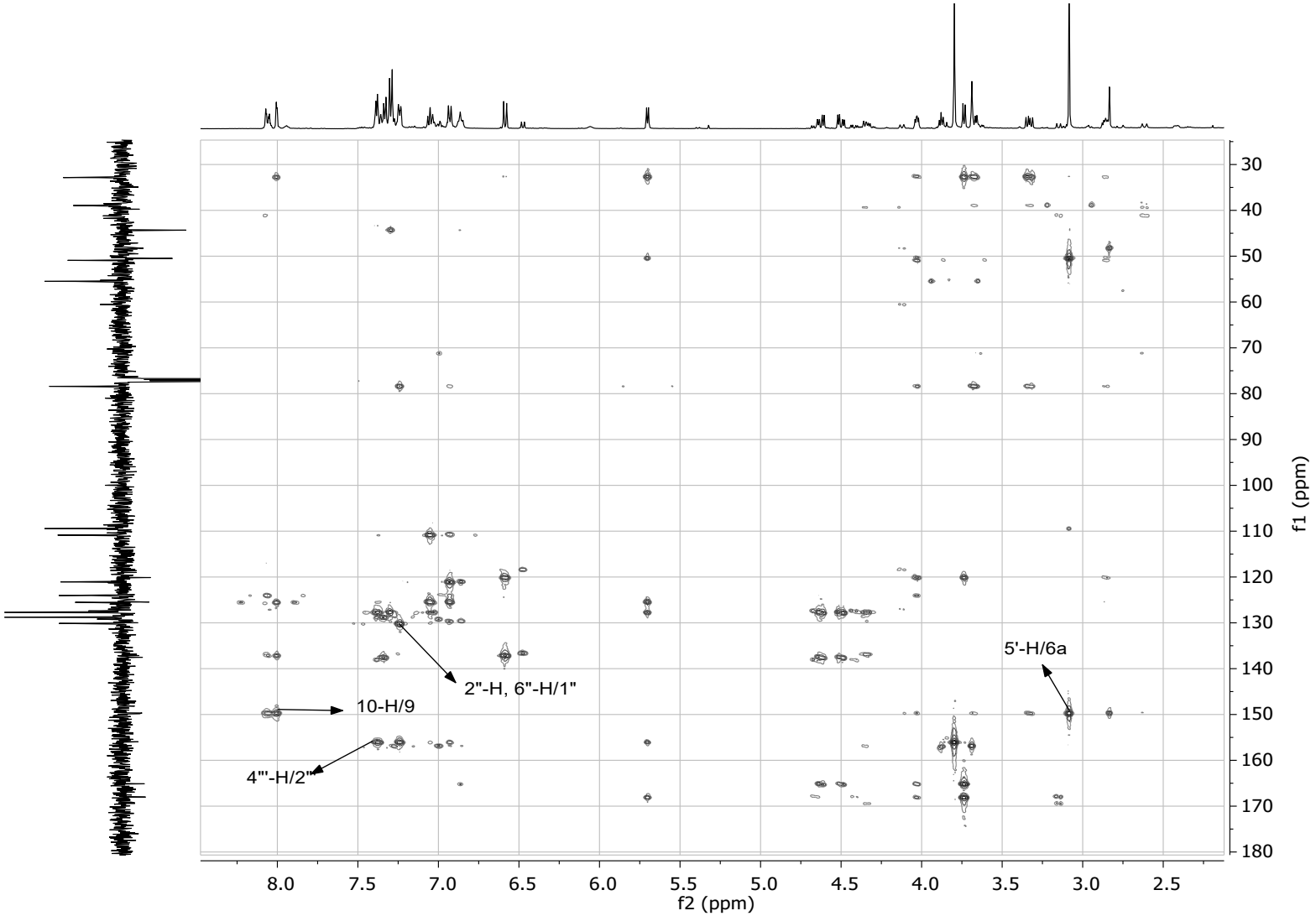

Figure S88. HMBC spectrum of the *rac*-(1*S**,4*R**,4a*S**,10b*S**)-*dia2*-**5e** in $CDCl_3$ at 500 MHz.

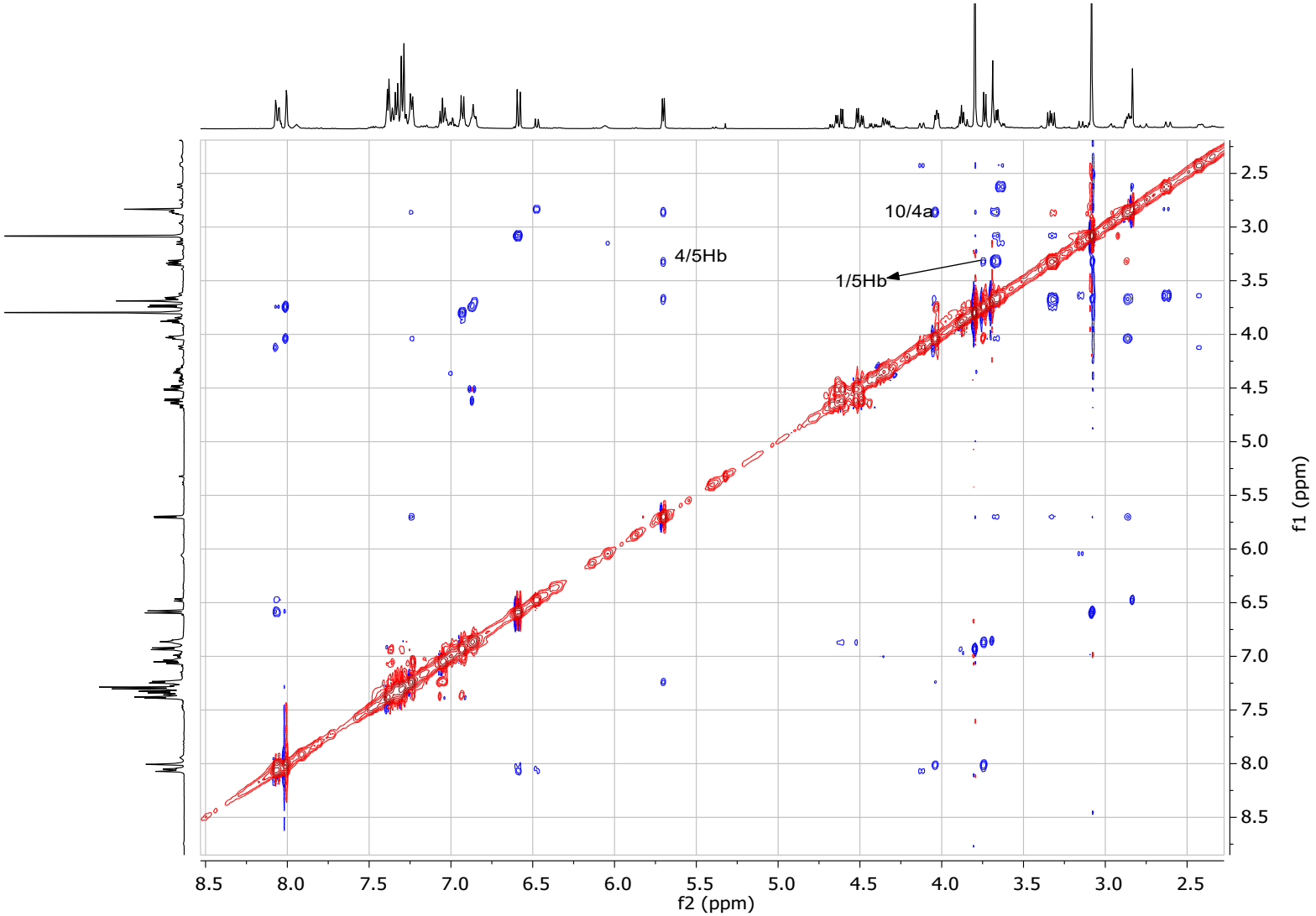

Figure S89. ROESY spectrum of the *rac*-(1*S**,4*R**,4a*S**,10b*S**)-*dia2*-**5e** in $CDCl_3$ at 500 MHz.

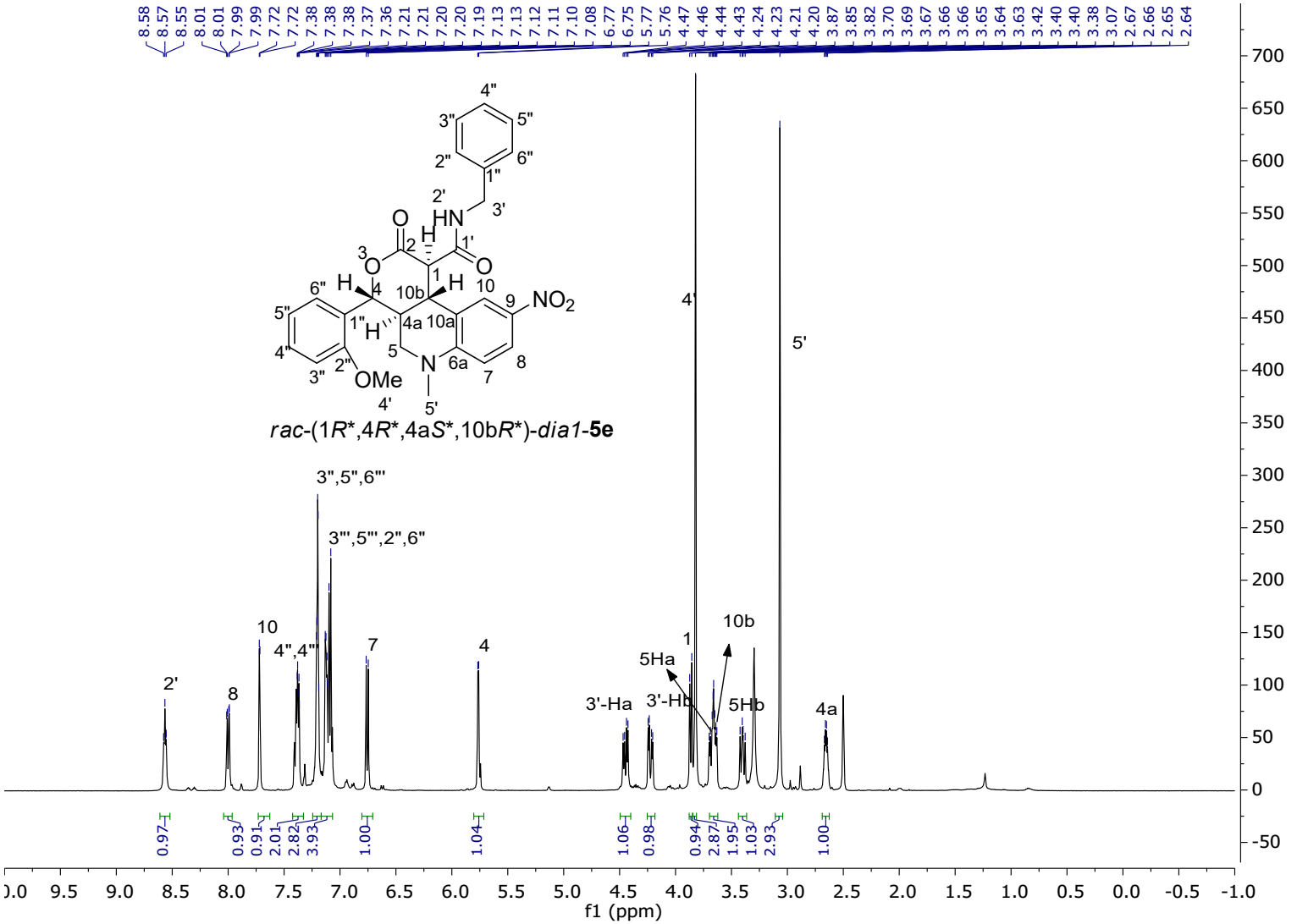

Figure S90. ^{1}H-NMR spectrum of the *rac*-(1*R**,4*R**,4a*S**,10b*R**)-*dia1*-**5e** in $CDCl_3$ at 500 MHz.

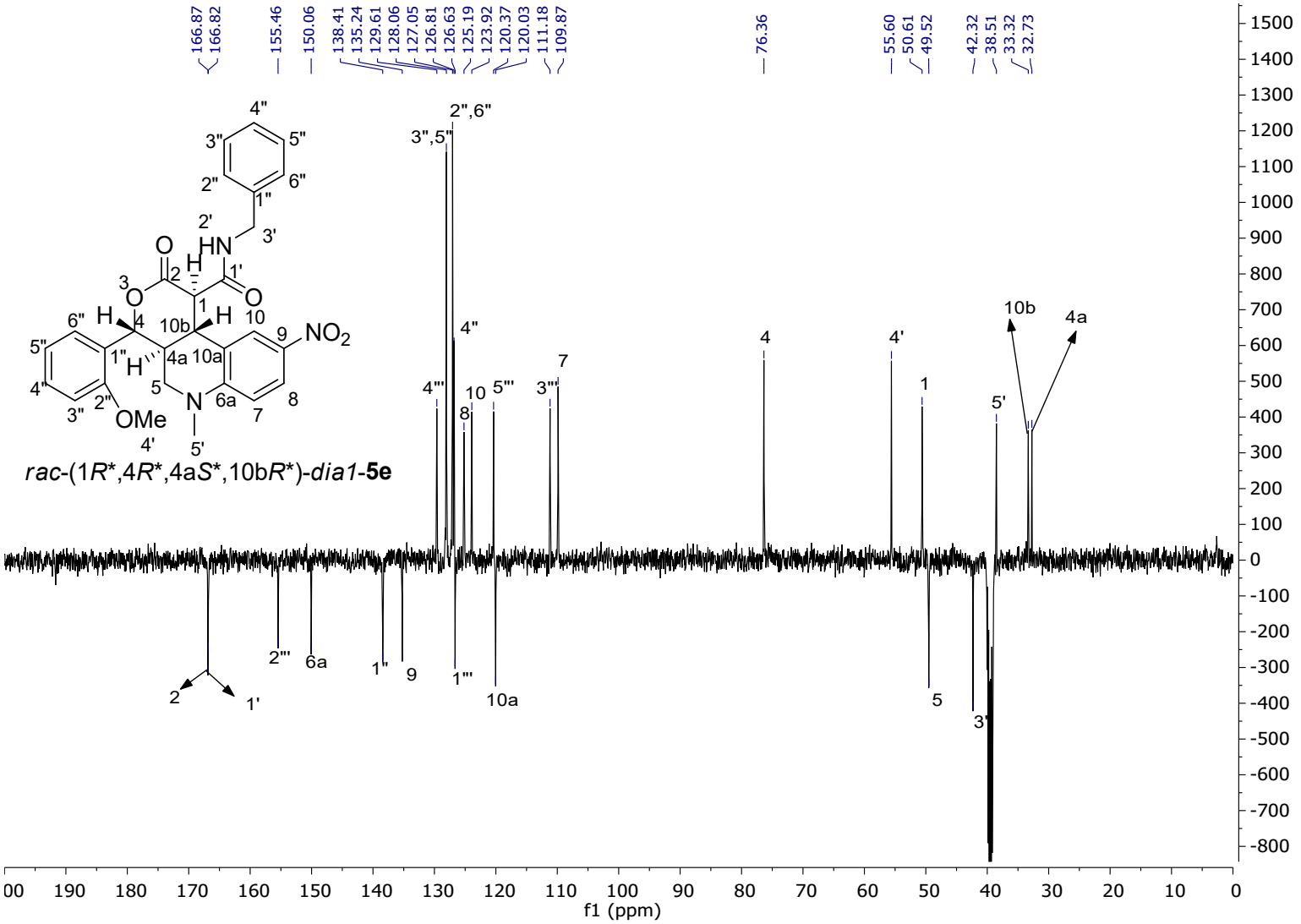

Figure S91. ^{13}C-NMR spectrum of the *rac*-(1*R**,4*R**,4a*S**,10b*R**)-*dia1*-**5e** in DMSO-d_6 at 125 MHz.

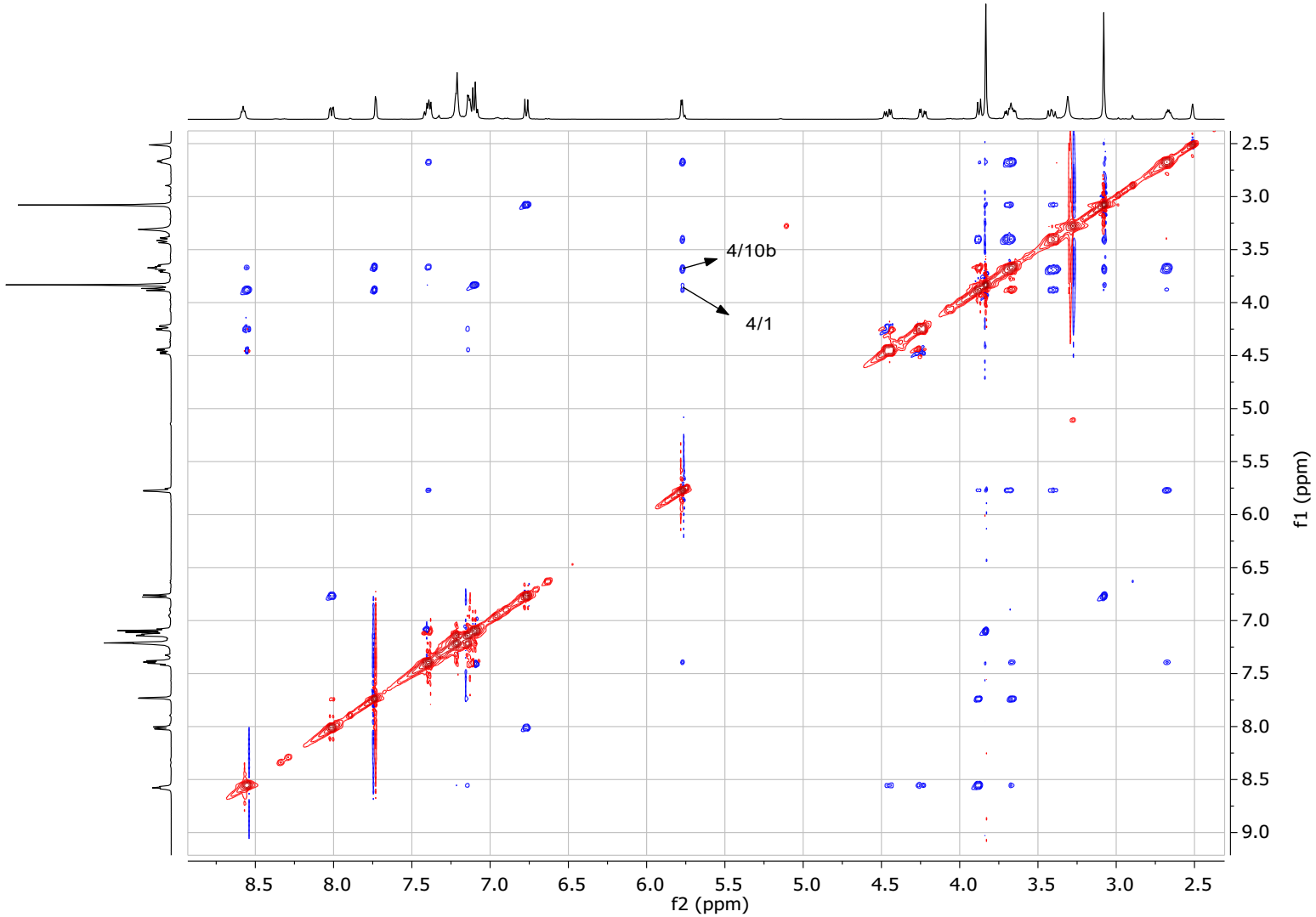

Figure S92. ROESY spectrum of the *rac*-(1*R**,4*R**,4a*S**,10b*R**)-*dia1*-**5e** in $CDCl_3$ at 500 MHz.

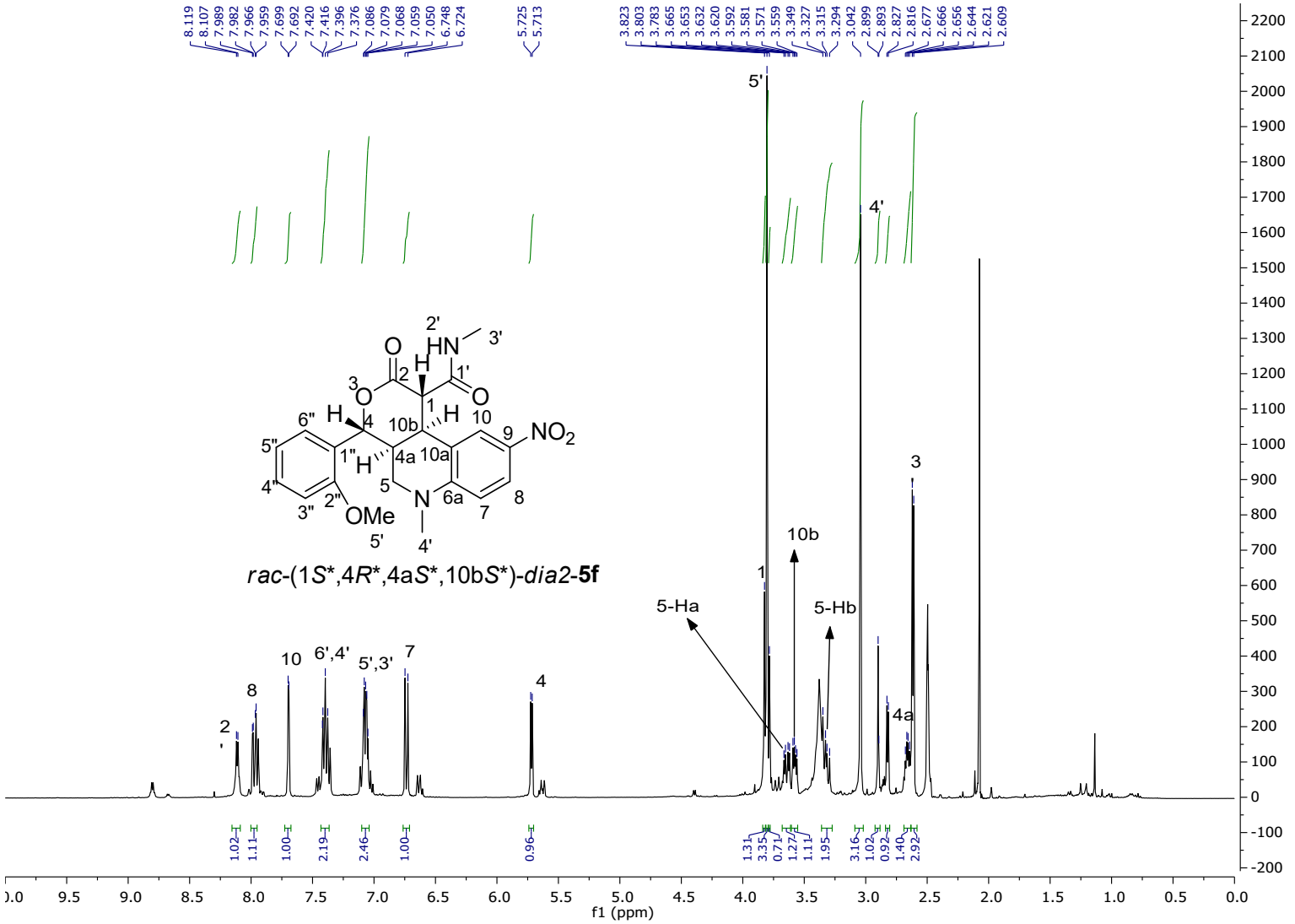

Figure S93. ^{1}H-NMR spectrum of the *rac*-(1*S**,4*R**,4a*S**,10b*S**)-*dia2*-**5f** in $CDCl_3$ at 400 MHz.

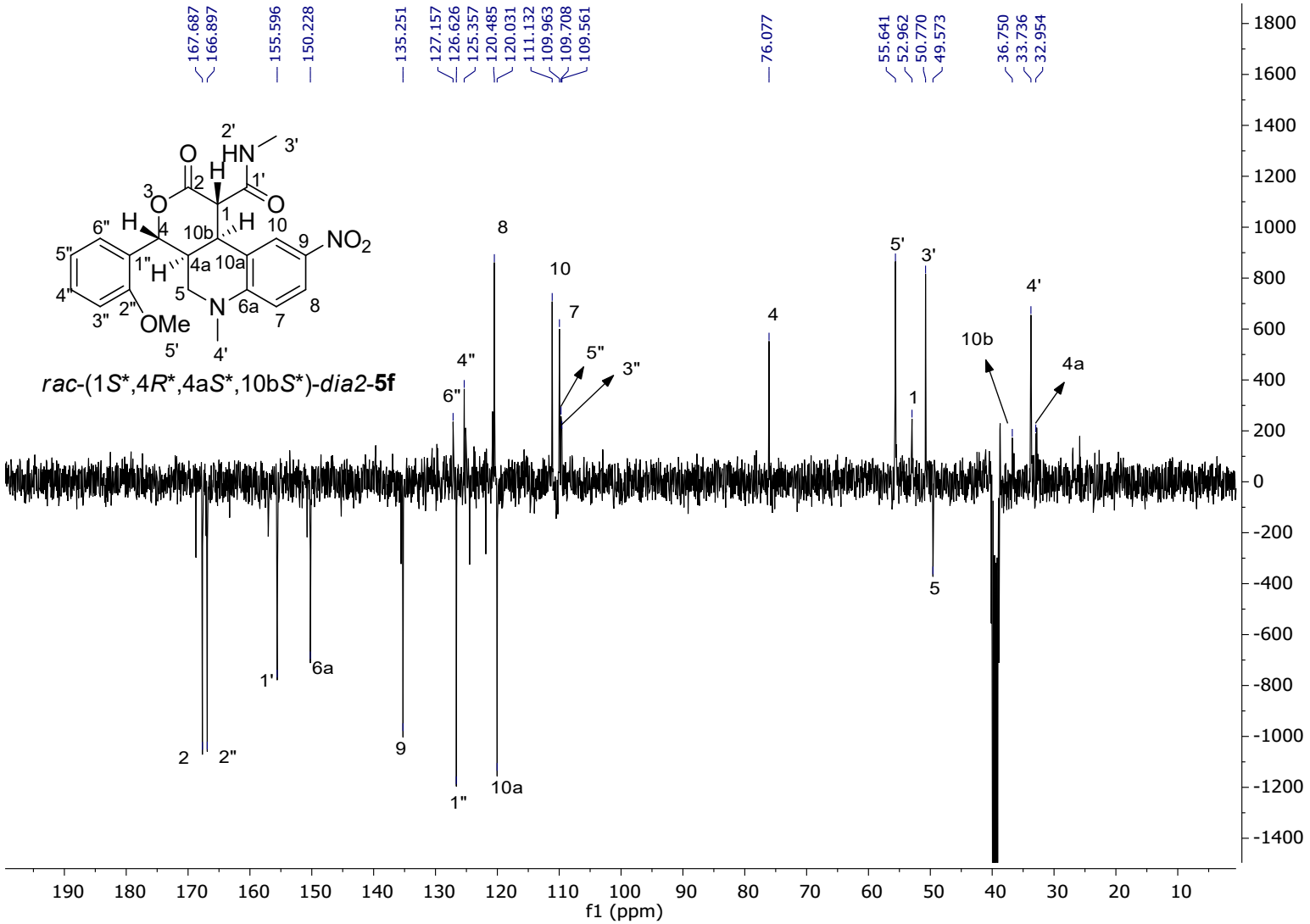

Figure S94. ^{13}C-NMR spectrum of the *rac*-(1*S**,4*R**,4a*S**,10b*S**)-*dia2*-**5f** in DMSO-d_6 at 100 MHz.

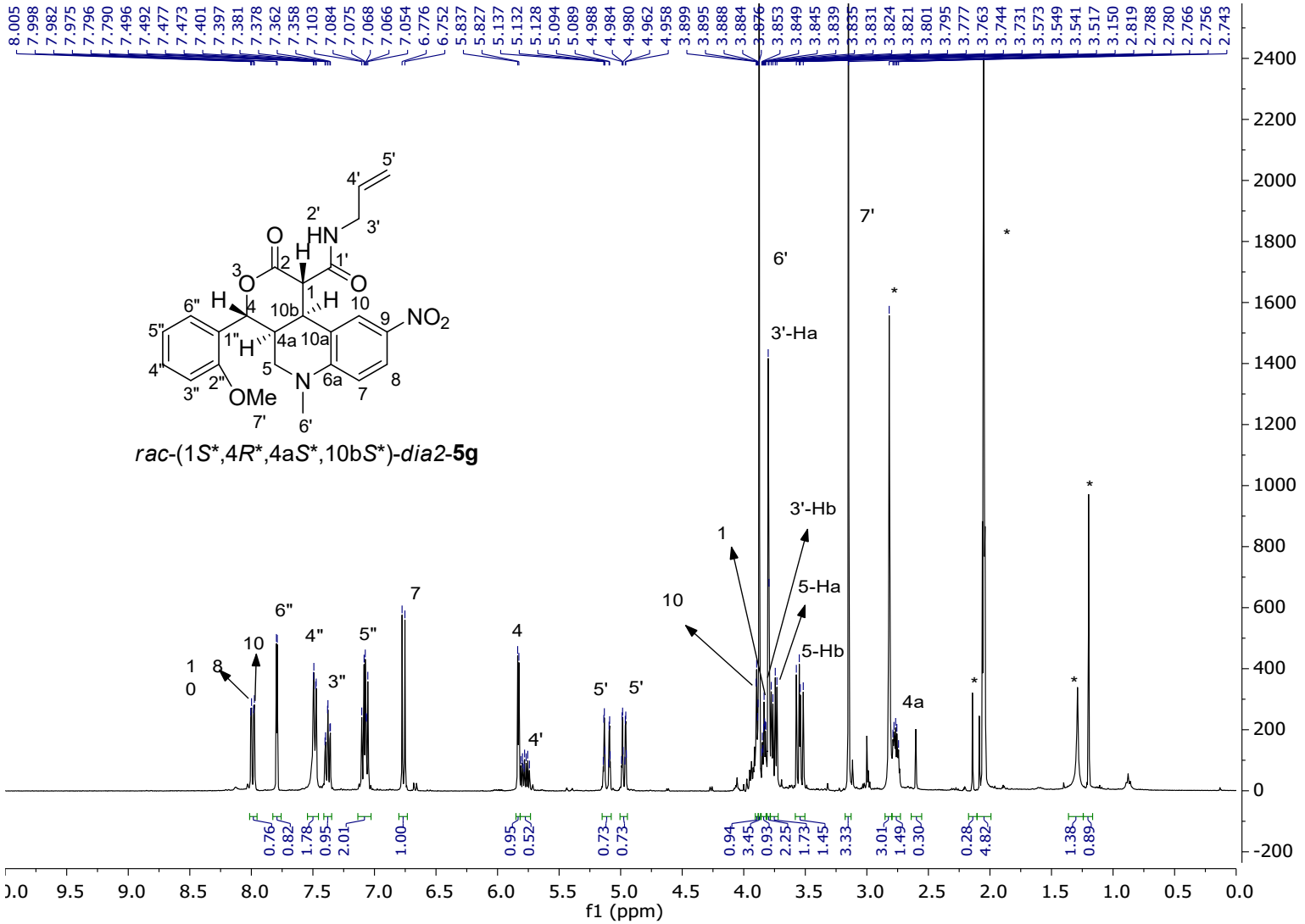

Figure S95. ^{1}H-NMR spectrum of the *rac*-(1*S**,4*R**,4a*S**,10b*S**)-*dia2*-**5g** in $CDCl_3$ at 400 MHz.

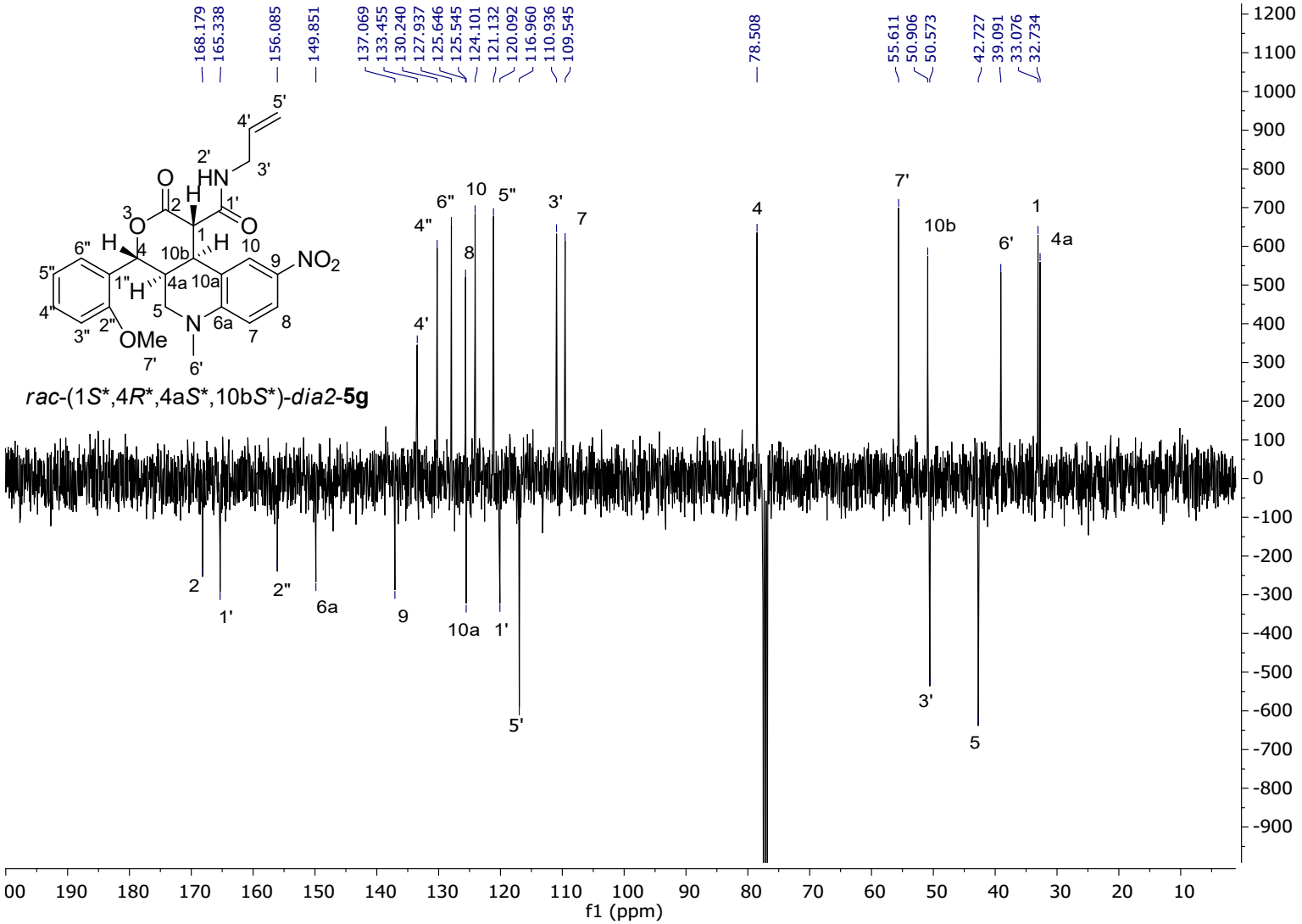

Figure S96. ^{13}C-NMR spectrum of the *rac*-(1*S**,4*R**,4a*S**,10b*S**)-*dia2*-**5g** in $CDCl_3$ at 100 MHz.

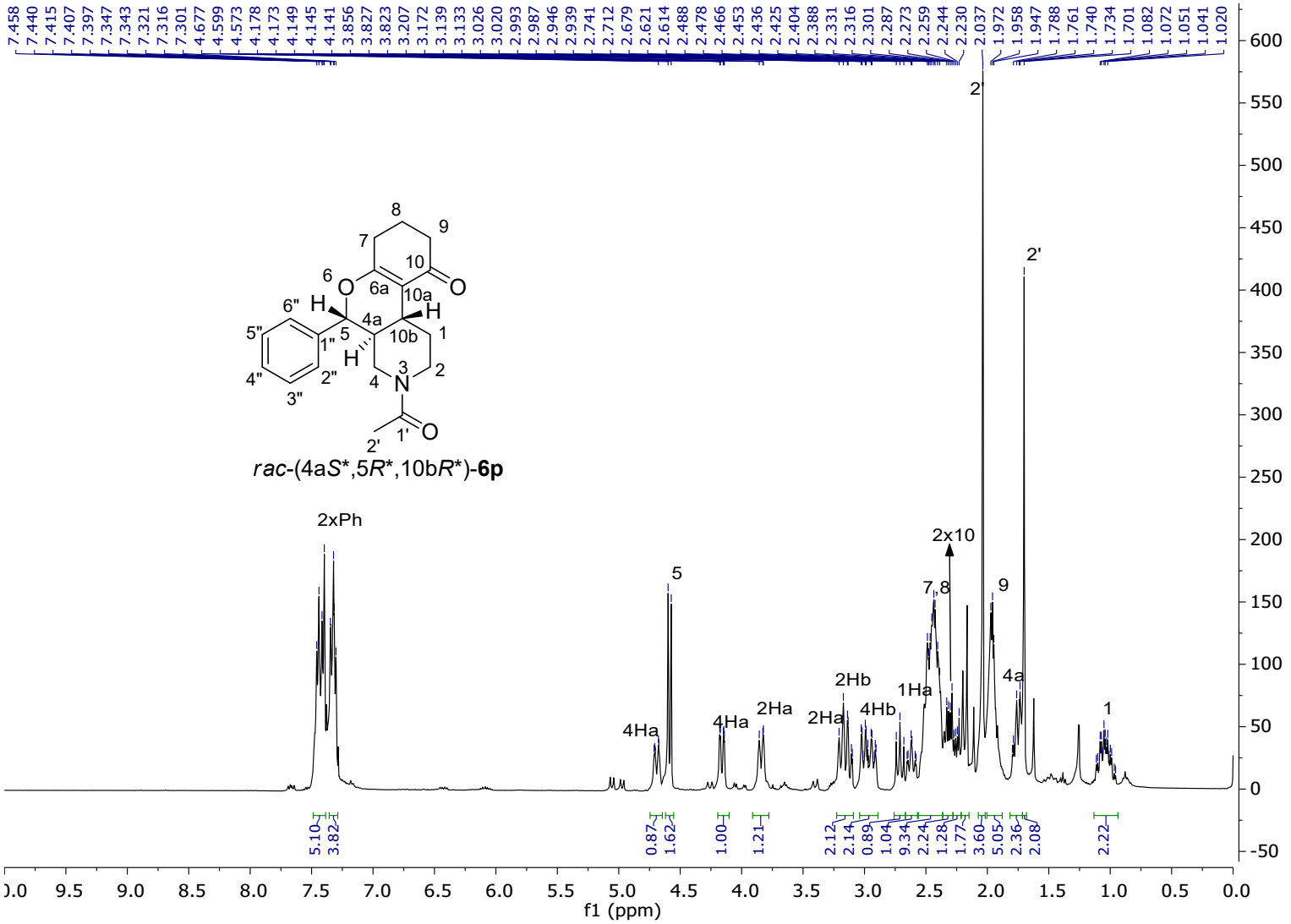

Figure S97. ^{1}H-NMR spectrum of the *rac*-(4a*S**,5*R**,10b*R**)-**6p** in $CDCl_3$ at 400 MHz.

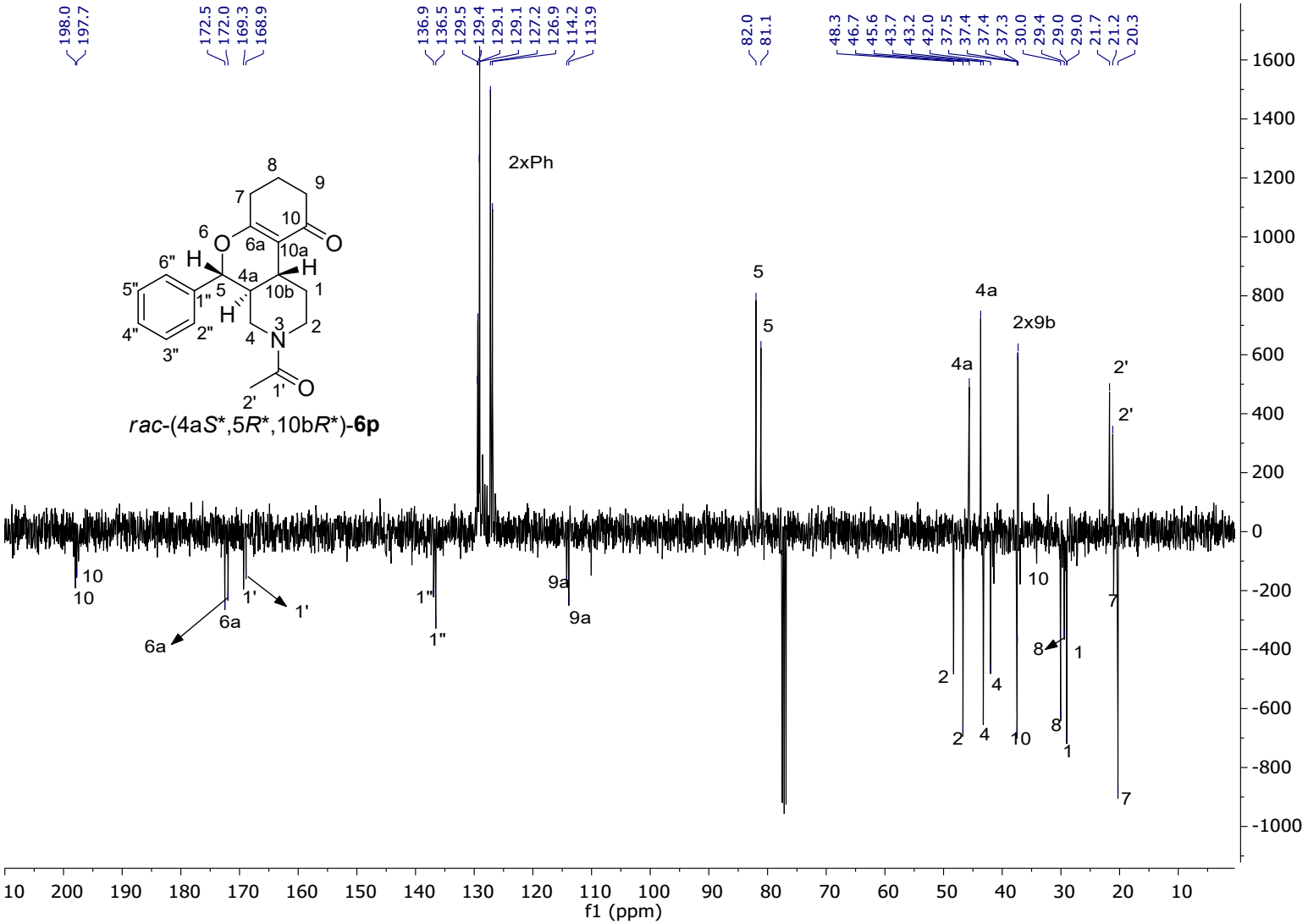

Figure S98. ^{13}C-NMR spectrum of the *rac*-(4a*S**,5*R**,10b*R**)-**6p** in $CDCl_3$ at 100 MHz.

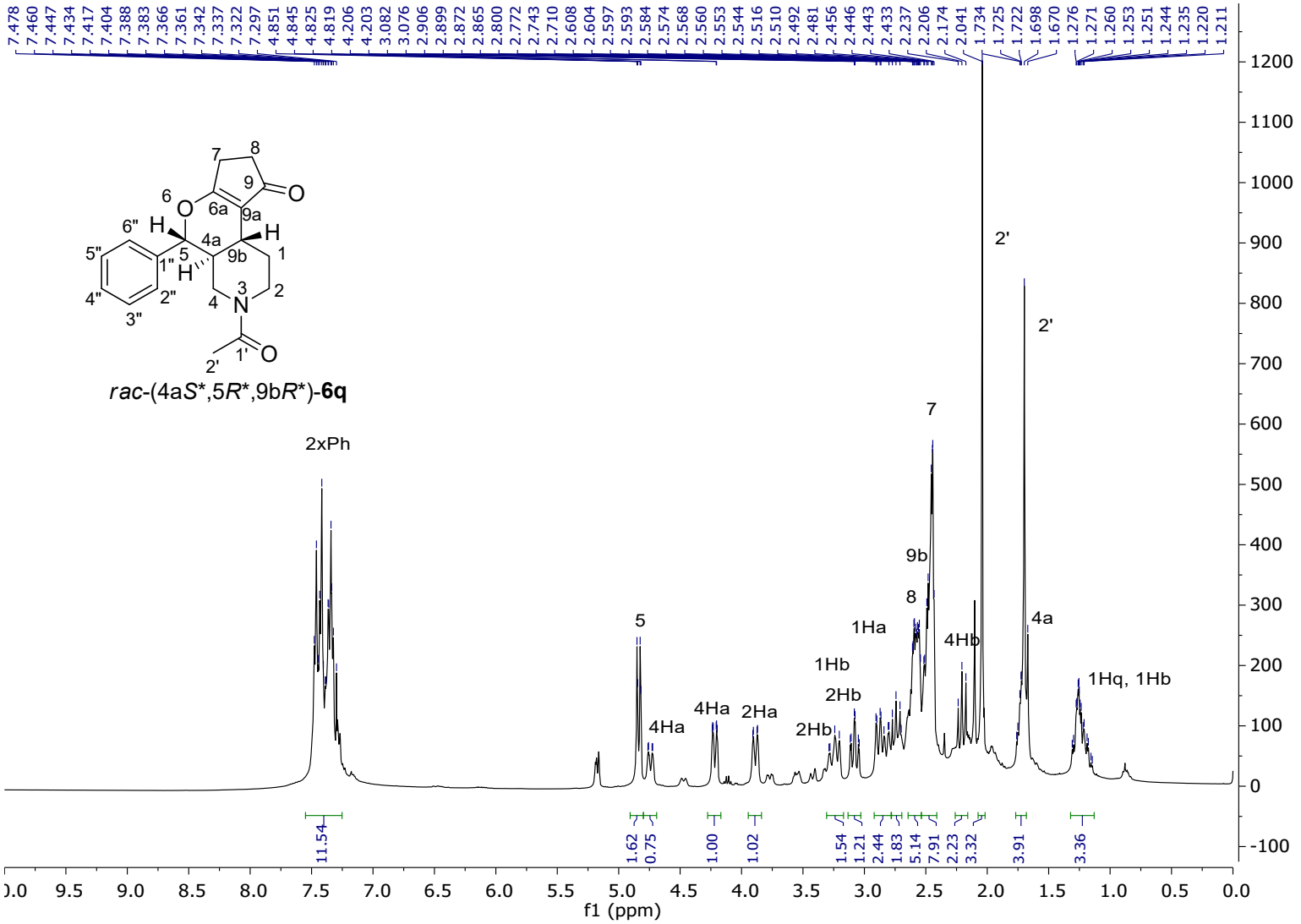

Figure S99. ^{1}H-NMR spectrum of the *rac*-(4a*S**,5*R**,9b*R**)-**6q** in $CDCl_3$ at 400 MHz.

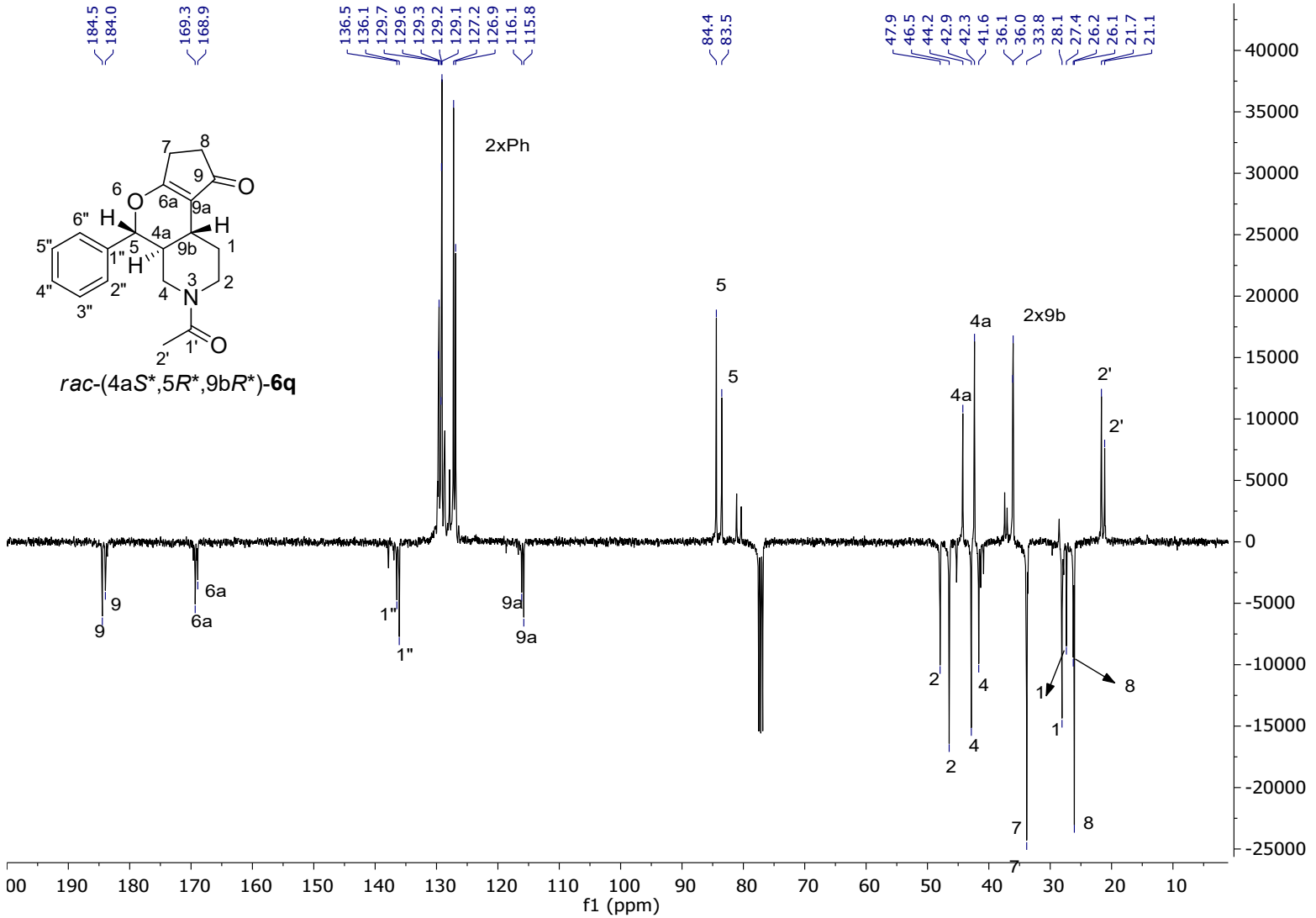

Figure S100. ^{13}C-NMR spectrum of the *rac*-(4a*S**,5*R**,9b*R**)-**6q** in $CDCl_3$ at 100 MHz.

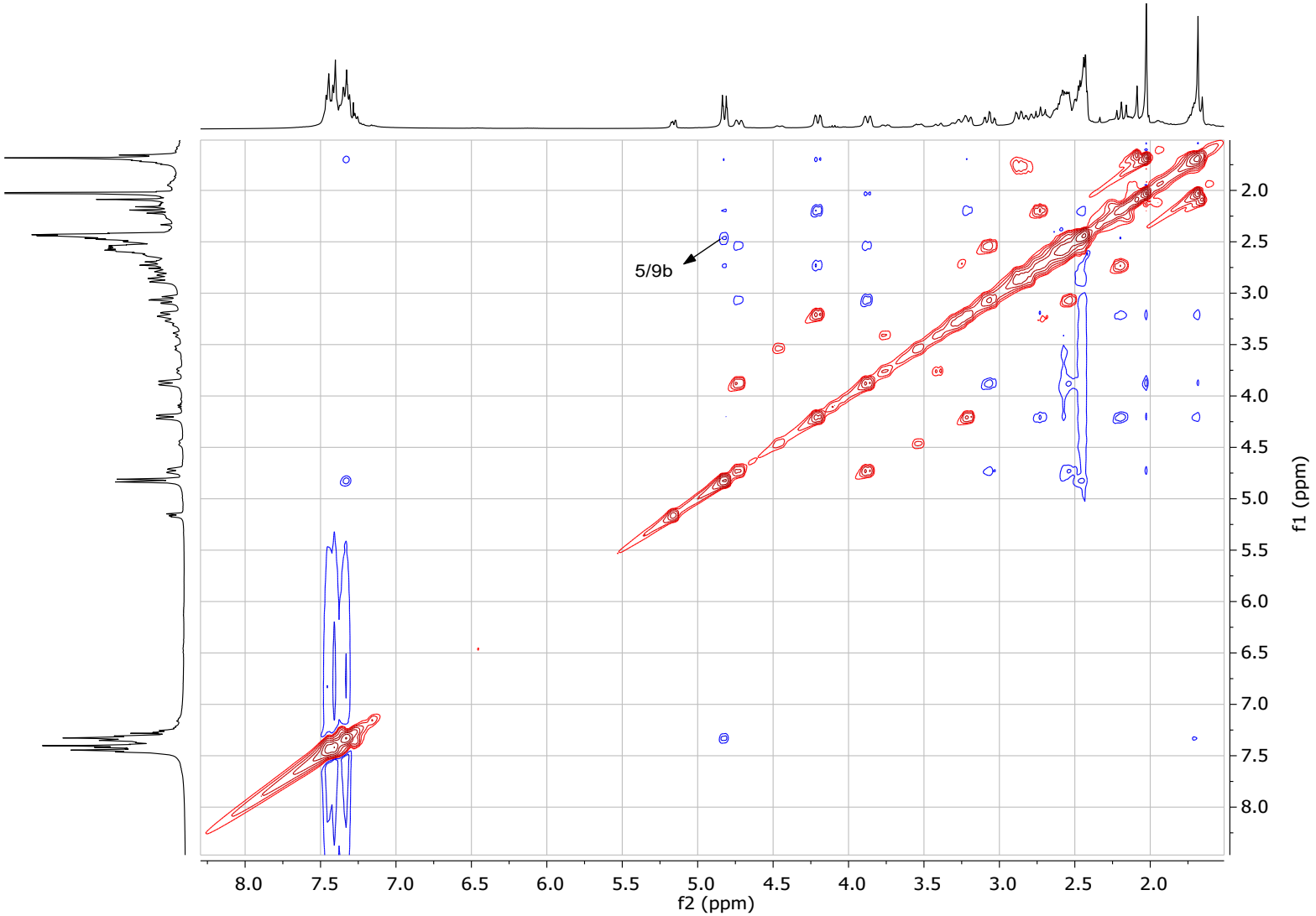

Figure S101. NOESY spectrum of the *rac*-(4a*S**,5*R**,9b*R**)-**6q** in $CDCl_3$ at 400 MHz.

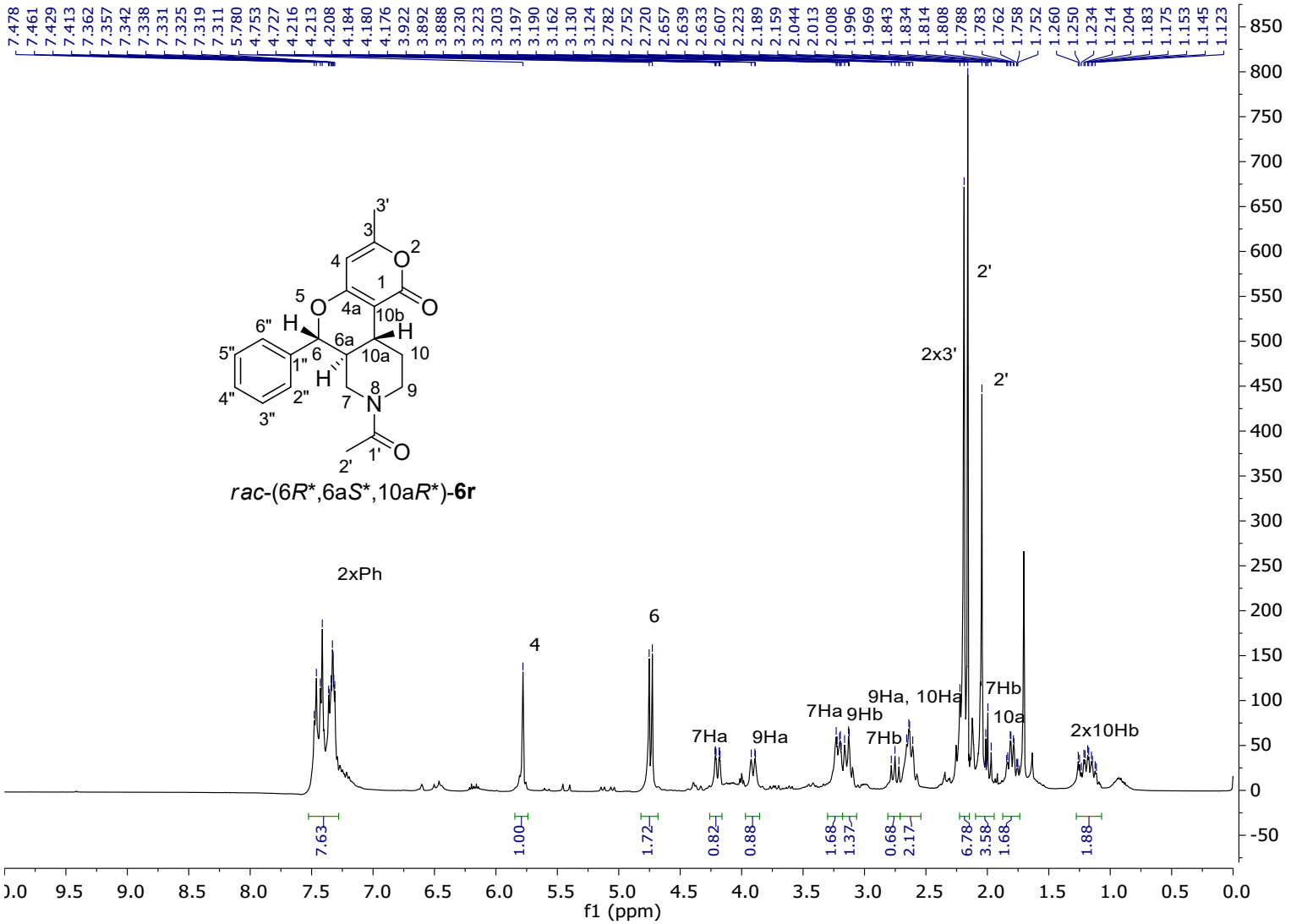

Figure S102. ^{1}H-NMR spectrum of the *rac*-(6*R**,6a*S**,10a*R**)-**6r** in $CDCl_3$ at 400 MHz.

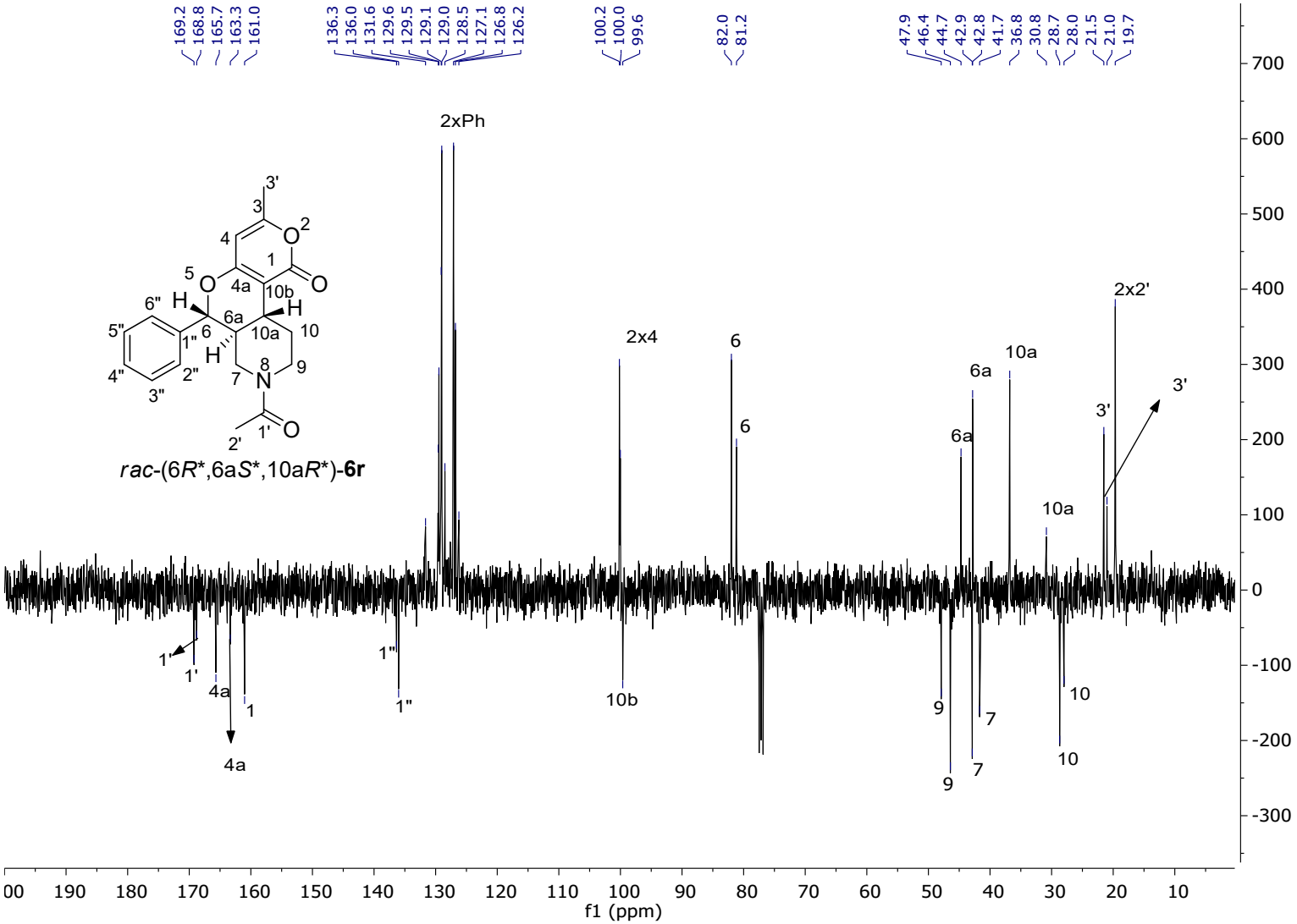

Figure S103. ^{13}C-NMR spectrum of the *rac*-(6*R**,6a*S**,10a*R**)-**6r** in $CDCl_3$ at 100 MHz.

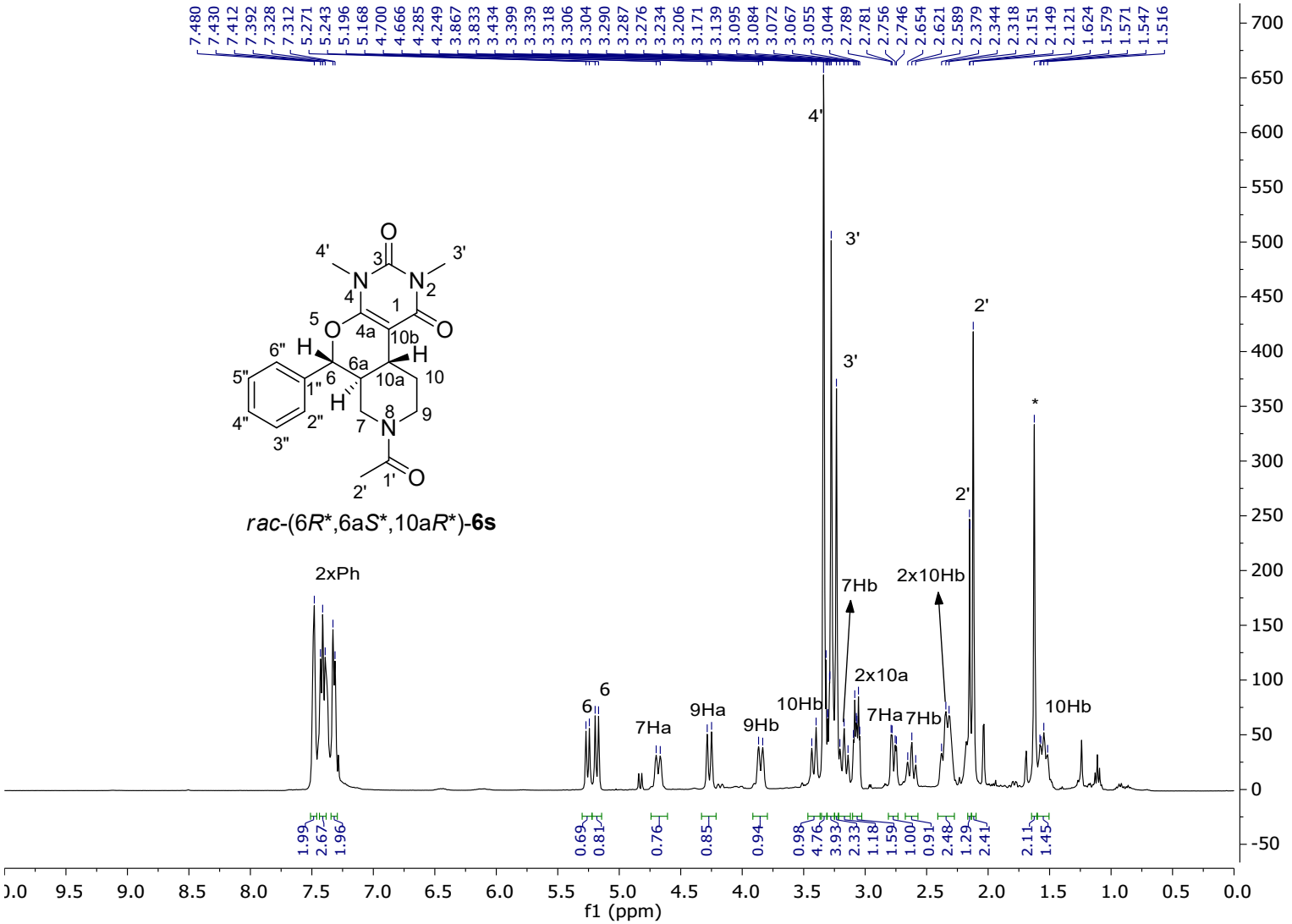

Figure S104. ^{1}H-NMR spectrum of the *rac*-(6*R**,6a*S**,10a*R**)-**6s** in $CDCl_3$ at 400 MHz.

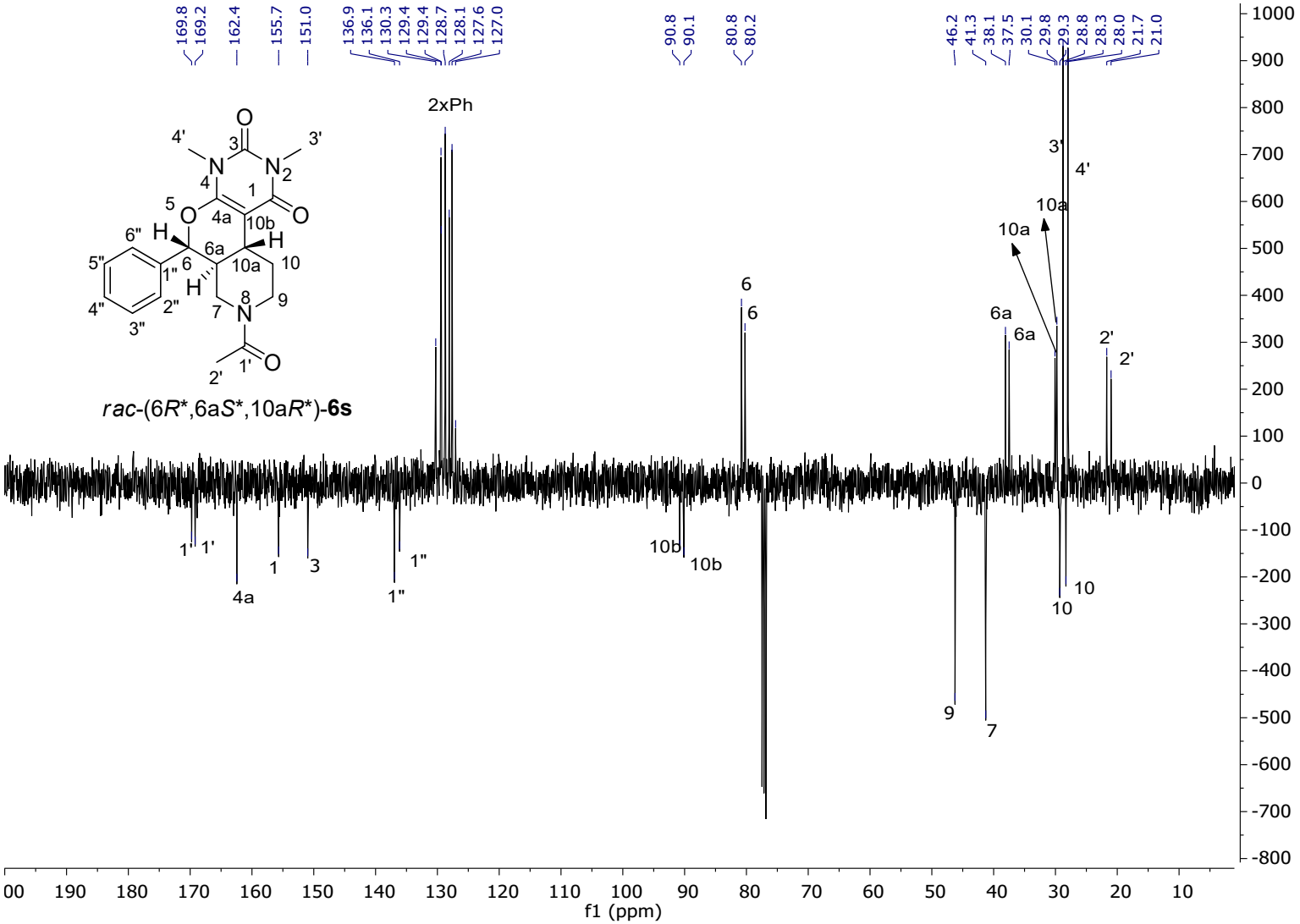

Figure S105. ^{13}C-NMR spectrum of the *rac*-(6*R**,6a*S**,10a*R**)-**6s** in $CDCl_3$ at 100 MHz.

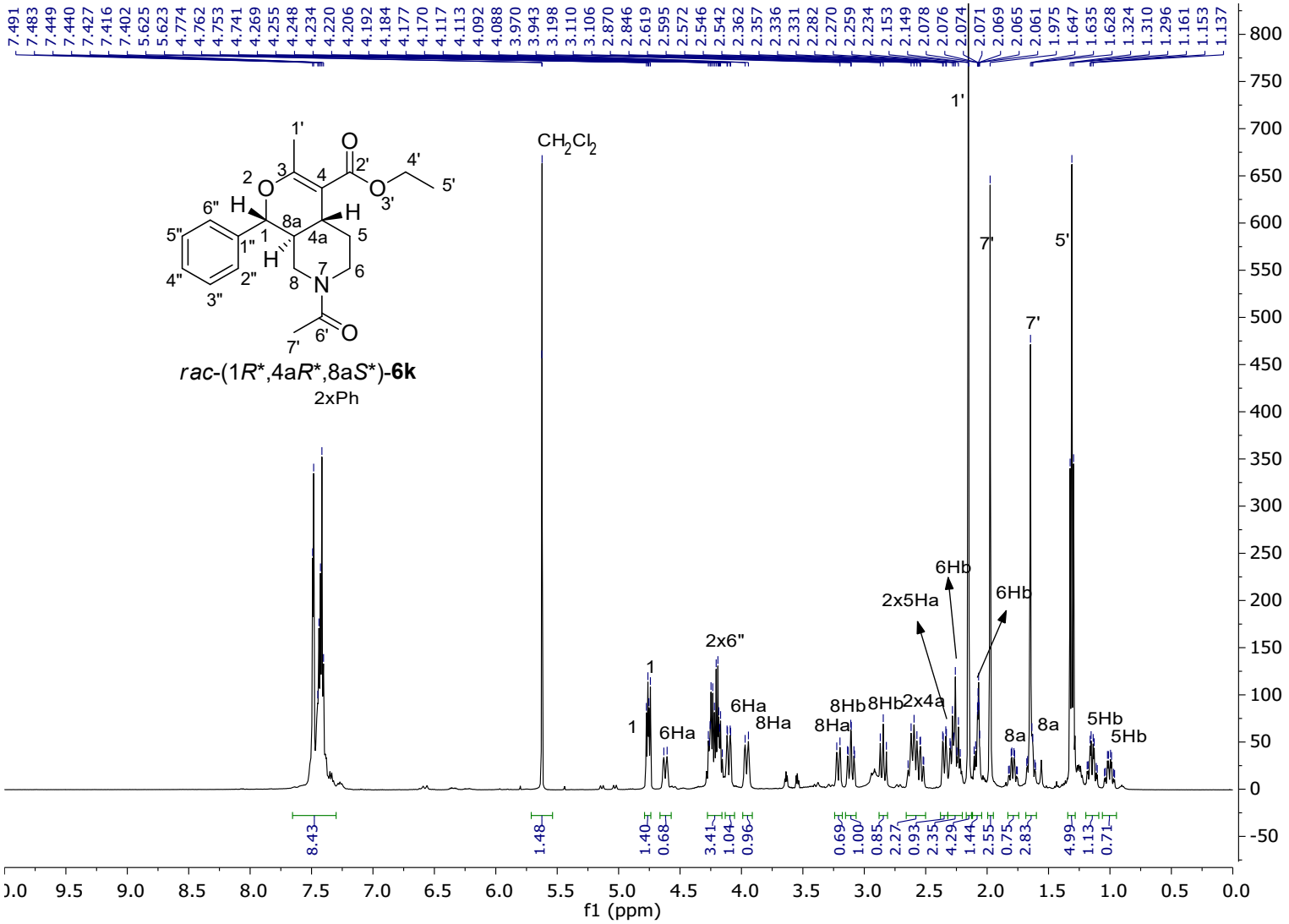

Figure S106. ^{1}H-NMR spectrum of the *rac*-(1*R**,4a*R**,8a*S**)-**6k** in acetone-d_6 at 500 MHz.

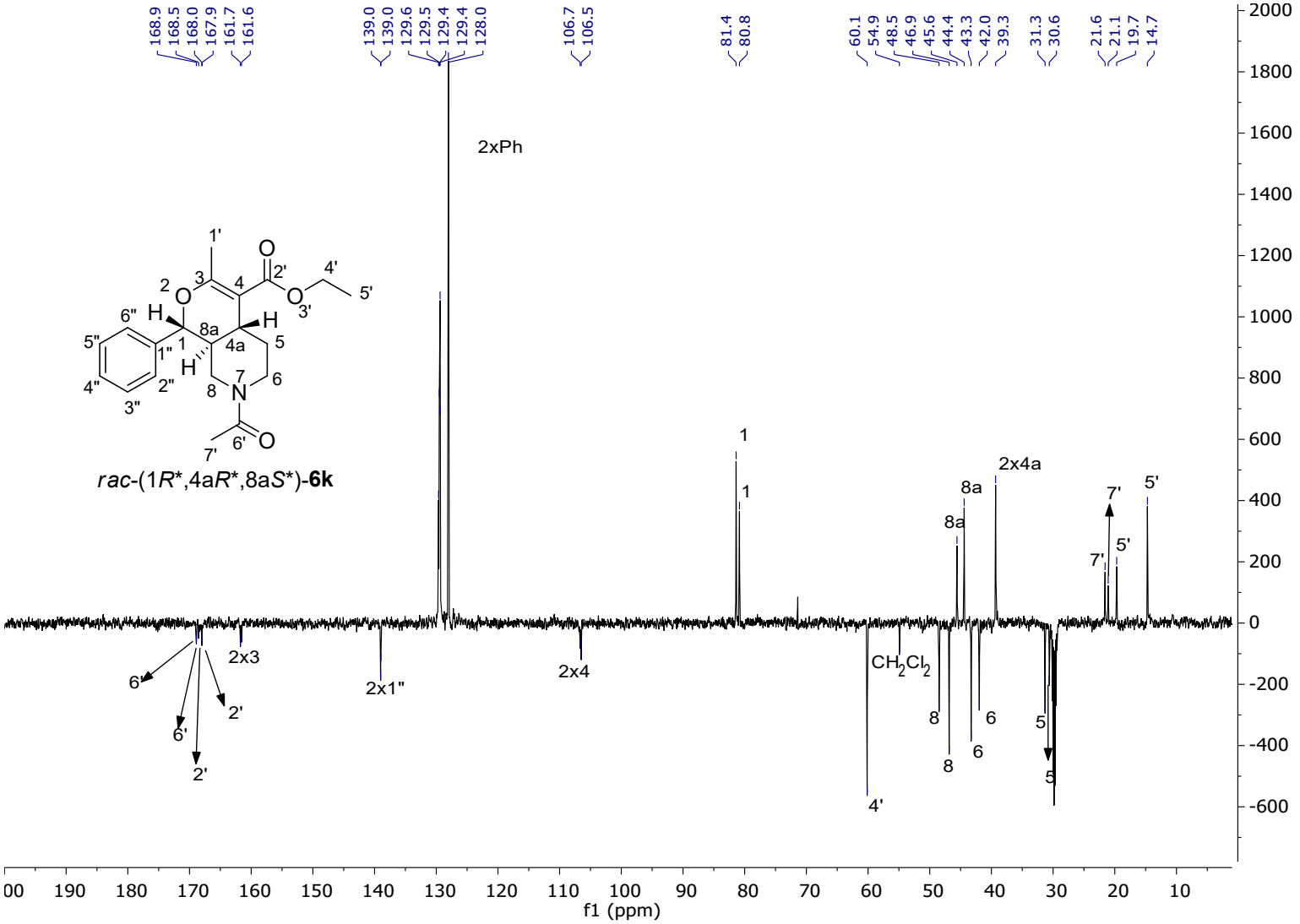

Figure S107. ^{13}C-NMR spectrum of the *rac*-(1*R**,4a*R**,8a*S**)-**6k** in acetone-d_6 at 125 MHz.

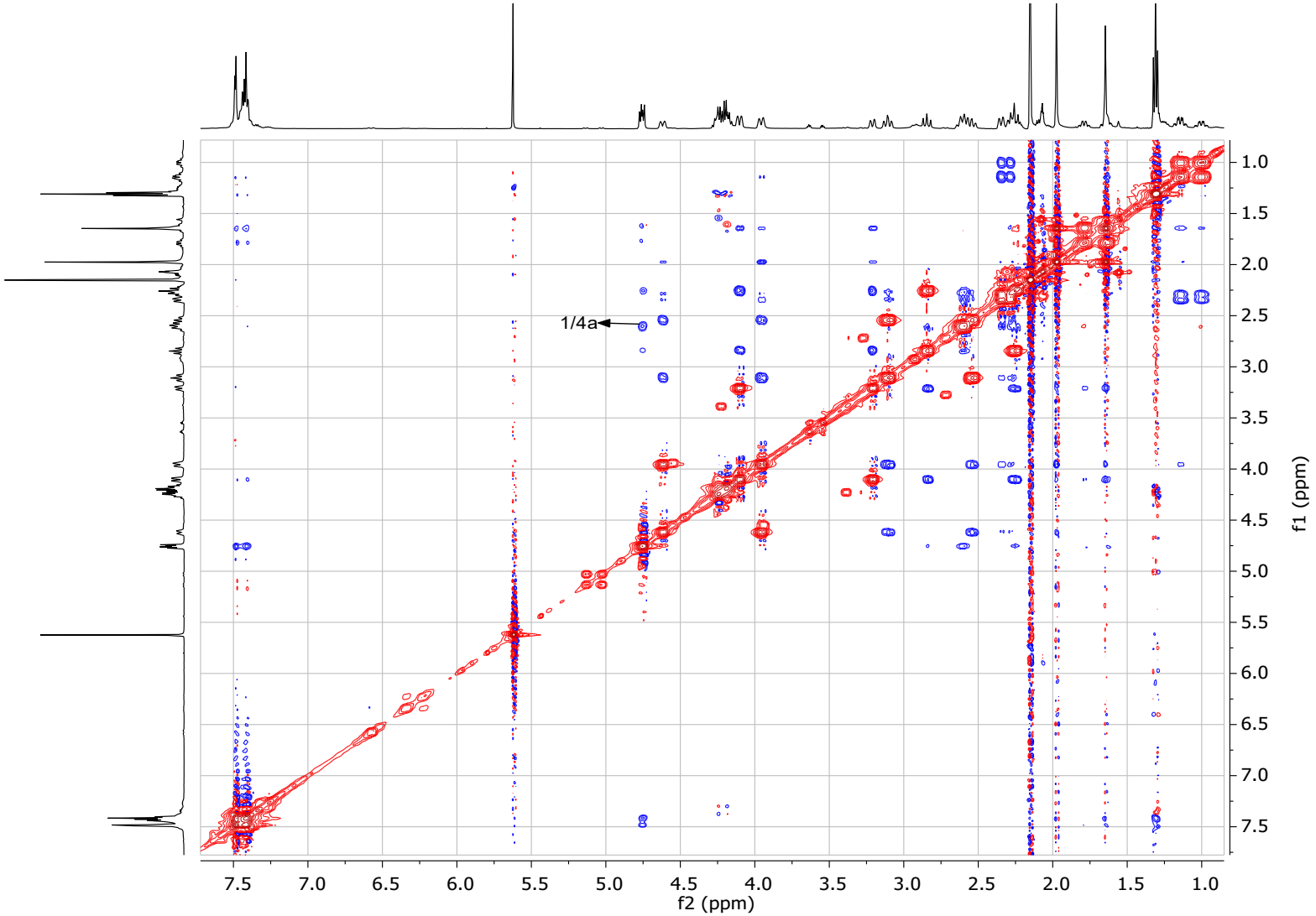

Figure S108. ROESY spectrum of the *rac*-(1*R**,4a*R**,8a*S**)-**6k** in acetone-d_6 at 500 MHz.

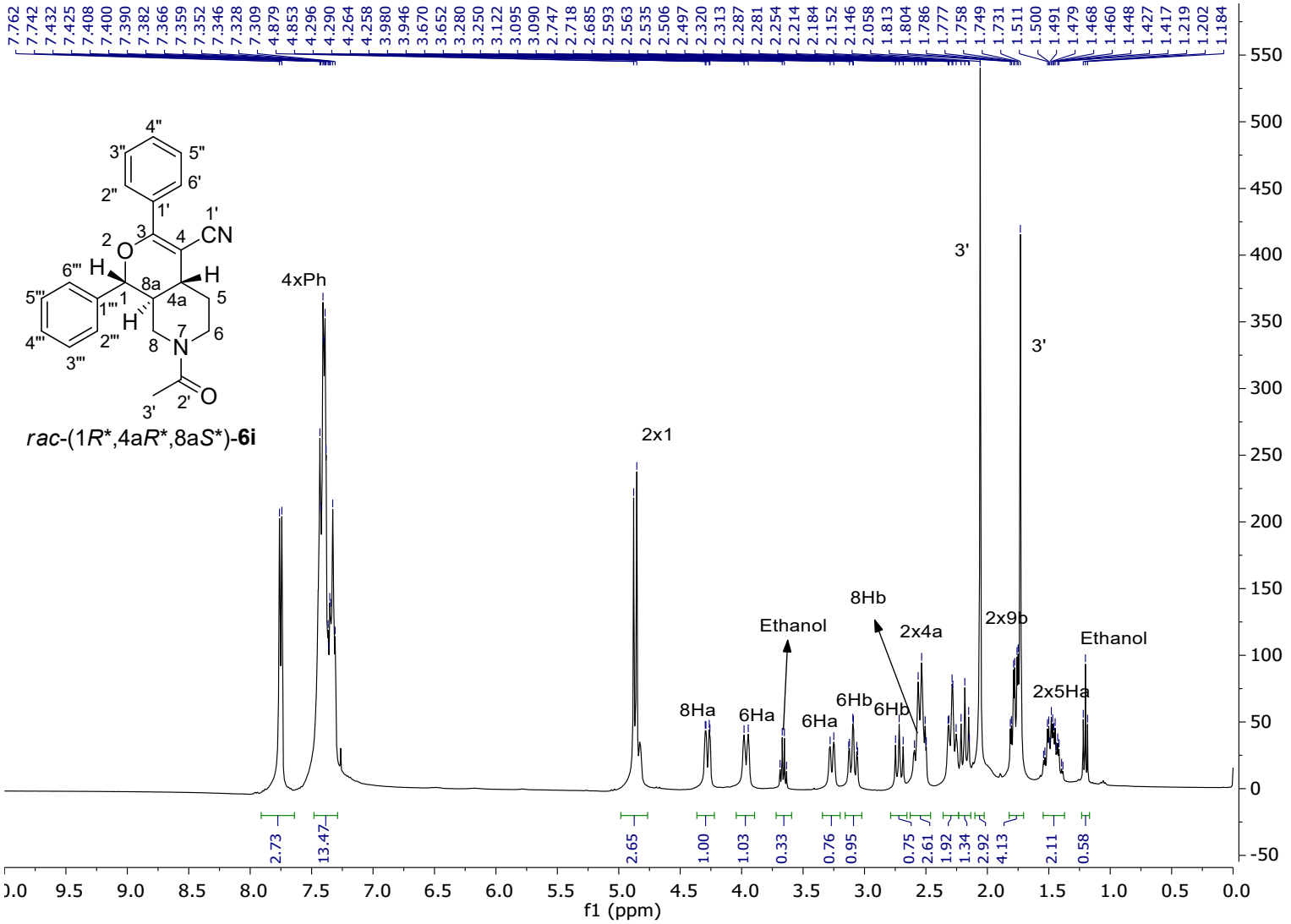

Figure S109. ^{1}H-NMR spectrum of the *rac*-(1*R**,4a*R**,8a*S**)-**6i** in $CDCl_3$ at 400 MHz.

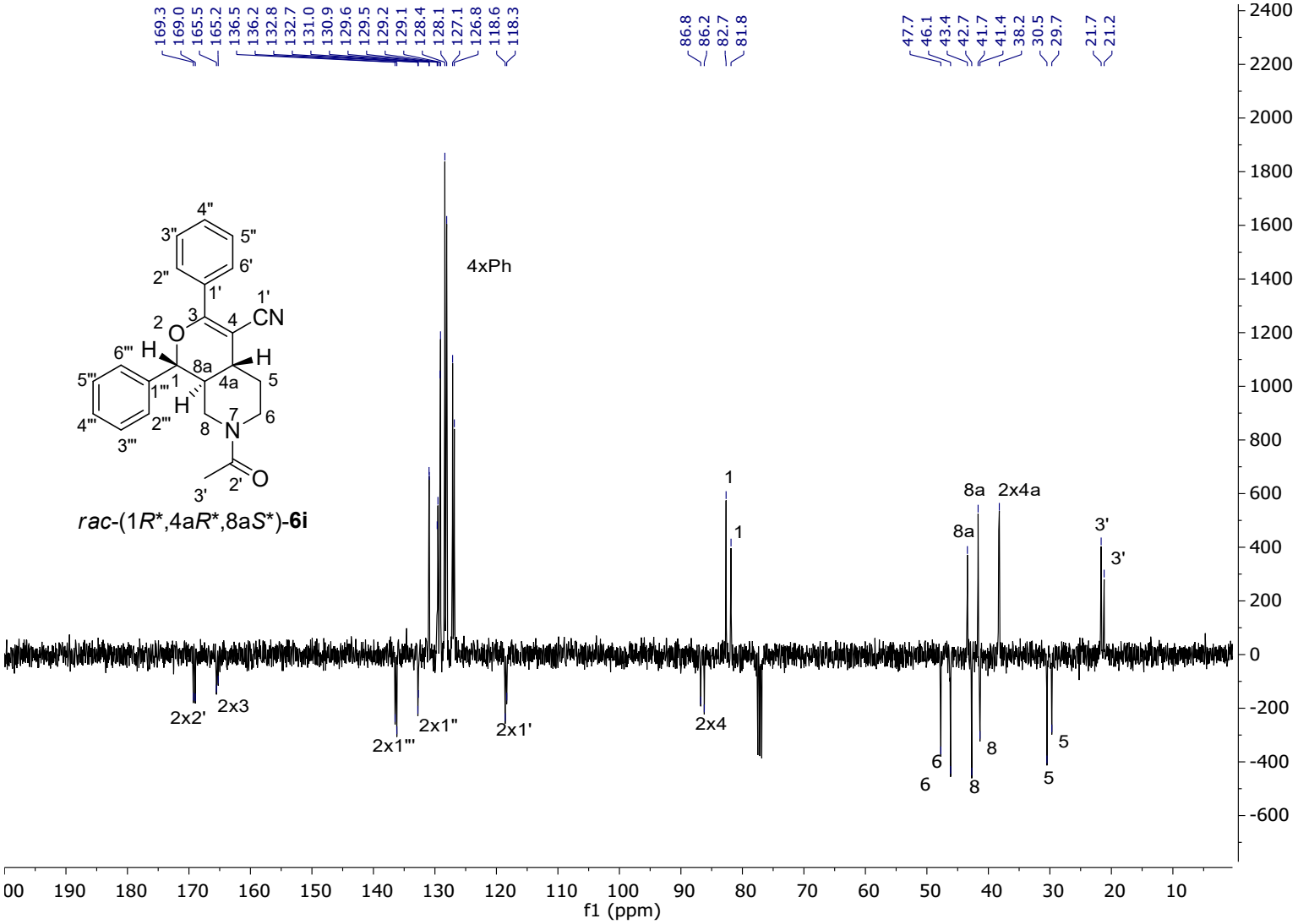

Figure S110. ^{13}C-NMR spectrum of the *rac*-(1*R**,4a*R**,8a*S**)-**6i** in $CDCl_3$ at 100 MHz.

5. X-Ray diffraction data

Computing details

For both structures, data collection: Bruker Instrument Service vV6.2.6; cell refinement: *APEX3* v2017.3-0 (Bruker AXS); data reduction: *SAINT* V8.38A (Bruker AXS Inc., 2017); program(s) used to solve structure: SHELXT 2014/5 (Sheldrick, 2014); program(s) used to refine structure: *SHELXL2019*/1 (Sheldrick, 2019); molecular graphics: shelXle (C.B. Huebschle, rev 1503); software used to prepare material for publication: *WinGX*, *publCIF*.

Table S3. Experimental details of *rac*-(4*R**,*4aS**,10b*S**)-**2ai** (CCDC No. 2283893) and b) *rac*-(4a*S**,5*R**,9b*R**)-**6p** (CCDC No. 2401371).

	rac-(4*R**,*4aS**,10b*S**)-**2ai**	*rac*-(4a*S**,5*R**,9b*R**)-**6p**
Crystal data		
Chemical formula	$C_{27}H_{23}N_3O_4 \cdot C_3H_6O$	$C_{20}H_{23}NO_3$
M_r	511.56	325.39
Crystal system, space group	Triclinic, $P\bar{1}$	Triclinic, $P\bar{1}$
Temperature (K)	299	295
a, *b*, *c* (Å)	9.9366 (4), 10.1419 (4), 14.5001 (6)	5.8551 (7), 10.1414 (12), 15.2595 (17)
α, β, γ (°)	96.998 (2), 94.577 (2), 111.265 (2)	106.479 (5), 96.585 (5), 95.737 (5)
V (Å^3)	1339.43 (10)	854.75 (17)
Z	2	2
Radiation type	Mo *K*α	Mo *K*α
μ (mm^{-1})	0.09	0.09
Crystal size (mm)	0.44 × 0.23 × 0.17	0.33 × 0.09 × 0.07
Data collection		
Diffractometer	Bruker D8 VENTURE	Bruker D8 VENTURE
Absorption correction	Multi-scan Krause, L., Herbst-Irmer, R., Sheldrick, G. M., Stalke, D. (2015). "Comparison of silver and molybdenum microfocus X-ray sources for single-crystal structure determination" J. Appl. Cryst. 48, 3-10. doi:10.1107/S1600576714022985	Multi-scan *SADABS2016*/2 - Bruker AXS area detector scaling and absorption correction
T_{min}, T_{max}	0.69, 0.98	0.97, 0.99

No. of measured, independent and observed [$I > 2\sigma(I)$] reflections	33353, 5081, 3804	21749, 3124, 2356
R_{int}	0.084	0.059
$(\sin \theta/\lambda)_{max}$ (Å^{-1})	0.610	0.605
Refinement		
$R[F^2 > 2\sigma(F^2)]$, $wR(F^2)$, S	0.052, 0.157, 1.02	0.096, 0.320, 1.07
No. of reflections	5081	3124
No. of parameters	348	219
H-atom treatment	H-atom parameters constrained	H-atom parameters constrained
$\Delta\rangle_{max}$, $\Delta\rangle_{min}$ (e Å^{-3})	0.24, -0.26	0.31, -0.26

Computer programs: Bruker Instrument Service vV6.2.6, *APEX3* v2017.3-0 (Bruker AXS), *SAINT* V8.38A (Bruker AXS Inc., 2017), SHELXT 2014/5 (Sheldrick, 2014), *SHELXL2019*/1 (Sheldrick, 2019), shelXle (C.B. Huebschle, rev 1503), *WinGX*, *publCIF*.

Document origin: *publCIF* [Westrip, S. P. (2010). *J. Apply. Cryst.*, **43**, 920-925].

Table S4. Geometric parameters (Å, º) for *rac*-(4*R**,4a*S**,10b*S**)-**2ai**.

C1—C2	1.354 (2)	C15—C16	1.367 (4)
C1—C11	1.426 (2)	C15—H15	0.9300
C1—C10B	1.507 (2)	C16—C17	1.383 (3)
C2—O3	1.348 (2)	C16—H16	0.9300
C2—C12	1.479 (2)	C17—H17	0.9300
C4—O3	1.455 (2)	C18—C23	1.387 (3)
C4—C18	1.509 (2)	C18—C19	1.392 (3)
C4—C4A	1.517 (2)	C19—O24	1.367 (2)
C4—H4	0.9800	C19—C20	1.386 (3)
C5—N6	1.456 (3)	C20—C21	1.385 (3)
C5—C4A	1.517 (2)	C20—H20	0.9300
C5—H5A	0.9700	C21—C22	1.366 (4)
C5—H5B	0.9700	C21—H21	0.9300
C4A—C10B	1.532 (2)	C22—C23	1.382 (3)
C4A—H4A	0.9800	C22—H22	0.9300
C7—C8	1.367 (3)	C23—H23	0.9300
C7—C6A	1.404 (3)	C25—O24	1.418 (3)
C7—H7	0.9300	C25—H25A	0.9600
C6A—N6	1.361 (3)	C25—H25B	0.9600
C6A—C10A	1.429 (3)	C25—H25C	0.9600
C8—C9	1.383 (3)	C26—N6	1.460 (2)

C8—H8	0.9300	C26—H26A	0.9600
C9—C10	1.397 (3)	C26—H26B	0.9600
C9—N27	1.432 (3)	C26—H26C	0.9600
C10—C10A	1.368 (3)	C51—C52	1.468 (6)
C10—H10	0.9300	C51—H51A	0.9600
C11—N29	1.144 (2)	C51—H51B	0.9600
C10A—C10B	1.513 (3)	C51—H51C	0.9600
C10B—H10B	0.9800	C52—O51	1.194 (4)
C12—C17	1.381 (3)	C52—C53	1.440 (5)
C12—C13	1.384 (3)	C53—H53A	0.9600
C13—C14	1.387 (3)	C53—H53B	0.9600
C13—H13	0.9300	C53—H53C	0.9600
C14—C15	1.376 (4)	N27—O28	1.226 (3)
C14—H14	0.9300	N27—O29	1.236 (2)
C2—C1—C11	119.41 (15)	C14—C15—H15	120.1000
C2—C1—C10B	122.34 (15)	C15—C16—C17	120.1 (2)
C11—C1—C10B	117.65 (15)	C15—C16—H16	120.0000
O3—C2—C1	122.92 (15)	C17—C16—H16	120.0000
O3—C2—C12	112.08 (14)	C12—C17—C16	120.8 (2)
C1—C2—C12	125.00 (16)	C12—C17—H17	119.6000
O3—C4—C18	106.42 (14)	C16—C17—H17	119.6000
O3—C4—C4A	108.71 (14)	C23—C18—C19	118.77 (17)
C18—C4—C4A	112.48 (14)	C23—C18—C4	121.05 (17)
O3—C4—H4	109.7000	C19—C18—C4	120.12 (17)
C18—C4—H4	109.7000	O24—C19—C20	124.51 (19)
C4A—C4—H4	109.7000	O24—C19—C18	115.20 (16)
N6—C5—C4A	111.05 (17)	C20—C19—C18	120.3 (2)
N6—C5—H5A	109.4000	C21—C20—C19	119.6 (2)
C4A—C5—H5A	109.4000	C21—C20—H20	120.2000
N6—C5—H5B	109.4000	C19—C20—H20	120.2000
C4A—C5—H5B	109.4000	C22—C21—C20	120.6 (2)
H5A—C5—H5B	108.0000	C22—C21—H21	119.7000
C5—C4A—C4	113.62 (16)	C20—C21—H21	119.7000
C5—C4A—C10B	106.85 (14)	C21—C22—C23	119.8 (2)
C4—C4A—C10B	111.16 (14)	C21—C22—H22	120.1000
C5—C4A—H4A	108.4000	C23—C22—H22	120.1000
C4—C4A—H4A	108.4000	C22—C23—C18	120.9 (2)
C10B—C4A—H4A	108.4000	C22—C23—H23	119.6000
C8—C7—C6A	121.5 (2)	C18—C23—H23	119.6000

C8—C7—H7	119.3000	O24—C25—H25A	109.5000
C6A—C7—H7	119.3000	O24—C25—H25B	109.5000
N6—C6A—C7	121.62 (18)	H25A—C25—H25B	109.5000
N6—C6A—C10A	120.19 (18)	O24—C25—H25C	109.5000
C7—C6A—C10A	118.2 (2)	H25A—C25—H25C	109.5000
C7—C8—C9	119.6 (2)	H25B—C25—H25C	109.5000
C7—C8—H8	120.2000	N6—C26—H26A	109.5000
C9—C8—H8	120.2000	N6—C26—H26B	109.5000
C8—C9—C10	120.5 (2)	H26A—C26—H26B	109.5000
C8—C9—N27	119.74 (19)	N6—C26—H26C	109.5000
C10—C9—N27	119.76 (19)	H26A—C26—H26C	109.5000
C10A—C10—C9	120.63 (19)	H26B—C26—H26C	109.5000
C10A—C10—H10	119.7000	C52—C51—H51A	109.5000
C9—C10—H10	119.7000	C52—C51—H51B	109.5000
N29—C11—C1	175.4 (2)	H51A—C51—H51B	109.5000
C10—C10A—C6A	119.45 (18)	C52—C51—H51C	109.5000
C10—C10A—C10B	125.43 (16)	H51A—C51—H51C	109.5000
C6A—C10A—C10B	115.11 (17)	H51B—C51—H51C	109.5000
C1—C10B—C10A	117.02 (16)	O51—C52—C53	122.4 (5)
C1—C10B—C4A	110.46 (14)	O51—C52—C51	118.8 (4)
C10A—C10B—C4A	105.46 (14)	C53—C52—C51	118.8 (4)
C1—C10B—H10B	107.9000	C52—C53—H53A	109.5000
C10A—C10B—H10B	107.9000	C52—C53—H53B	109.5000
C4A—C10B—H10B	107.9000	H53A—C53—H53B	109.5000
C17—C12—C13	118.87 (17)	C52—C53—H53C	109.5000
C17—C12—C2	120.69 (17)	H53A—C53—H53C	109.5000
C13—C12—C2	120.43 (17)	H53B—C53—H53C	109.5000
C12—C13—C14	120.1 (2)	C6A—N6—C5	122.80 (15)
C12—C13—H13	119.9000	C6A—N6—C26	120.72 (19)
C14—C13—H13	119.9000	C5—N6—C26	115.13 (18)
C15—C14—C13	120.3 (2)	O28—N27—O29	121.6 (2)
C15—C14—H14	119.9000	O28—N27—C9	119.22 (19)
C13—C14—H14	119.9000	O29—N27—C9	119.2 (2)
C16—C15—C14	119.9 (2)	C2—O3—C4	116.88 (13)
C16—C15—H15	120.1000	C19—O24—C25	118.54 (16)
C11—C1—C2—O3	-165.15 (17)	C17—C12—C13—C14	-1.0 (3)
C10B—C1—C2—O3	5.7 (3)	C2—C12—C13—C14	179.77 (19)
C11—C1—C2—C12	15.2 (3)	C12—C13—C14—C15	0.1 (3)

C10B—C1—C2—C12	-173.94 (17)	C13—C14—C15—C16	0.8 (4)
N6—C5—C4A—C4	-173.46 (15)	C14—C15—C16—C17	-0.8 (4)
N6—C5—C4A—C10B	-50.5 (2)	C13—C12—C17—C16	1.0 (3)
O3—C4—C4A—C5	-179.46 (14)	C2—C12—C17—C16	-179.78 (19)
C18—C4—C4A—C5	-61.9 (2)	C15—C16—C17—C12	-0.1 (3)
O3—C4—C4A—C10B	59.98 (19)	O3—C4—C18—C23	36.8 (2)
C18—C4—C4A—C10B	177.57 (15)	C4A—C4—C18—C23	-82.1 (2)
C8—C7—C6A—N6	177.0 (2)	O3—C4—C18—C19	-146.08 (17)
C8—C7—C6A—C10A	-4.4 (3)	C4A—C4—C18—C19	95.0 (2)
C6A—C7—C8—C9	0.6 (3)	C23—C18—C19—O24	178.16 (17)
C7—C8—C9—C10	2.2 (3)	C4—C18—C19—O24	1.0 (3)
C7—C8—C9—N27	-179.01 (19)	C23—C18—C19—C20	-0.8 (3)
C8—C9—C10—C10A	-1.2 (3)	C4—C18—C19—C20	-177.95 (18)
N27—C9—C10—C10A	-179.93 (17)	O24—C19—C20—C21	-179.2 (2)
C9—C10—C10A—C6A	-2.7 (3)	C18—C19—C20—C21	-0.3 (3)
C9—C10—C10A—C10B	178.39 (17)	C19—C20—C21—C22	1.1 (4)
N6—C6A—C10A—C10	-176.00 (17)	C20—C21—C22—C23	-0.7 (4)
C7—C6A—C10A—C10	5.3 (3)	C21—C22—C23—C18	-0.5 (4)
N6—C6A—C10A—C10B	3.0 (3)	C19—C18—C23—C22	1.2 (3)
C7—C6A—C10A—C10B	-175.61 (17)	C4—C18—C23—C22	178.33 (19)
C2—C1—C10B—C10A	127.21 (19)	C7—C6A—N6—C5	-162.51 (19)
C11—C1—C10B—C10A	-61.8 (2)	C10A—C6A—N6—C5	18.9 (3)
C2—C1—C10B—C4A	6.6 (3)	C7—C6A—N6—C26	3.6 (3)
C11—C1—C10B—C4A	177.59 (17)	C10A—C6A—N6—C26	-175.01 (18)
C10—C10A—C10B—C1	9.6 (3)	C4A—C5—N6—C6A	6.7 (3)
C6A—C10A—	-169.36 (16)	C4A—C5—N6—C26	-160.11 (18)

C10B—C1			
C10—C10A—C10B—C4A	132.86 (18)	C8—C9—N27—O28	177.0 (2)
C6A—C10A—C10B—C4A	-46.1 (2)	C10—C9—N27—O28	-4.2 (3)
C5—C4A—C10B—C1	-163.22 (16)	C8—C9—N27—O29	-3.0 (3)
C4—C4A—C10B—C1	-38.7 (2)	C10—C9—N27—O29	175.74 (19)
C5—C4A—C10B—C10A	69.46 (19)	C1—C2—O3—C4	17.0 (3)
C4—C4A—C10B—C10A	-166.06 (15)	C12—C2—O3—C4	-163.31 (15)
O3—C2—C12—C17	-133.82 (18)	C18—C4—O3—C2	-170.65 (15)
C1—C2—C12—C17	45.9 (3)	C4A—C4—O3—C2	-49.27 (19)
O3—C2—C12—C13	45.4 (2)	C20—C19—O24—C25	4.7 (3)
C1—C2—C12—C13	-134.9 (2)	C18—C19—O24—C25	-174.22 (18)

Table S5. Geometric parameters (Å, º) for rac-(4a*S**,5*R**,9b*R**)-**6p**.

C1—C2	1.512 (7)	C8—H8AB	0.9700
C1—C9B	1.525 (7)	C9—C10	1.504 (8)
C1—H1A	0.9700	C9—H9A	0.9700
C1—H1AB	0.9700	C9—H9AB	0.9700
C2—N3	1.465 (6)	C9B—C10A	1.513 (7)
C2—H2A	0.9700	C9B—H9B	0.9800
C2—H2AB	0.9700	C10—O11	1.224 (7)
C4—N3	1.455 (6)	C10—C10A	1.462 (7)
C4—C4A	1.528 (7)	C12—O14	1.216 (6)
C4—H4A	0.9700	C12—N3	1.338 (7)
C4—H4AB	0.9700	C12—C13	1.513 (8)
C5—O6	1.444 (6)	C13—H13A	0.9600
C5—C15	1.499 (7)	C13—H13B	0.9600
C5—C4A	1.515 (7)	C13—H13C	0.9600
C5—H5	0.9800	C15—C20	1.380 (7)
C4A—C9B	1.537 (6)	C15—C16	1.389 (7)
C4A—H4AA	0.9800	C16—C17	1.393 (7)
C6—C10A	1.338 (7)	C16—H16	0.9300
C6—O6	1.354 (6)	C17—C18	1.371 (8)
C6—C7	1.500 (7)	C17—H17	0.9300

C7—C8	1.495 (9)	C18—C19	1.351 (9)
C7—H7A	0.9700	C18—H18	0.9300
C7—H7AB	0.9700	C19—C20	1.376 (8)
C8—C9	1.501 (10)	C19—H19	0.9300
C8—H8A	0.9700	C20—H20	0.9300
C2—C1—C9B	110.2 (4)	C10—C9—H9A	108.9000
C2—C1—H1A	109.6000	C8—C9—H9AB	108.9000
C9B—C1—H1A	109.6000	C10—C9—H9AB	108.9000
C2—C1—H1AB	109.6000	H9A—C9—H9AB	107.7000
C9B—C1—H1AB	109.6000	C10A—C9B—C1	115.5 (4)
H1A—C1—H1AB	108.1000	C10A—C9B—C4A	109.3 (4)
N3—C2—C1	111.6 (4)	C1—C9B—C4A	107.4 (4)
N3—C2—H2A	109.3000	C10A—C9B—H9B	108.1000
C1—C2—H2A	109.3000	C1—C9B—H9B	108.1000
N3—C2—H2AB	109.3000	C4A—C9B—H9B	108.1000
C1—C2—H2AB	109.3000	O11—C10—C10A	121.6 (5)
H2A—C2—H2AB	108.0000	O11—C10—C9	120.7 (5)
N3—C4—C4A	110.3 (4)	C10A—C10—C9	117.6 (5)
N3—C4—H4A	109.6000	C6—C10A—C10	118.3 (5)
C4A—C4—H4A	109.6000	C6—C10A—C9B	120.6 (4)
N3—C4—H4AB	109.6000	C10—C10A—C9B	120.6 (4)
C4A—C4—H4AB	109.6000	O14—C12—N3	122.7 (5)
H4A—C4—H4AB	108.1000	O14—C12—C13	119.3 (5)
O6—C5—C15	107.1 (4)	N3—C12—C13	118.0 (5)
O6—C5—C4A	107.8 (4)	C12—C13—H13A	109.5000
C15—C5—C4A	115.7 (4)	C12—C13—H13B	109.5000
O6—C5—H5	108.7000	H13A—C13—H13B	109.5000
C15—C5—H5	108.7000	C12—C13—H13C	109.5000
C4A—C5—H5	108.7000	H13A—C13—H13C	109.5000
C5—C4A—C4	114.2 (4)	H13B—C13—H13C	109.5000
C5—C4A—C9B	108.6 (4)	C20—C15—C16	118.5 (5)
C4—C4A—C9B	109.1 (4)	C20—C15—C5	119.2 (5)
C5—C4A—H4AA	108.3000	C16—C15—C5	122.3 (5)
C4—C4A—H4AA	108.3000	C15—C16—C17	119.6 (5)
C9B—C4A—H4AA	108.3000	C15—C16—H16	120.2000
C10A—C6—O6	124.6 (4)	C17—C16—H16	120.2000
C10A—C6—C7	124.9 (5)	C18—C17—C16	120.5 (5)
O6—C6—C7	110.4 (4)	C18—C17—H17	119.8000
C8—C7—C6	111.2 (5)	C16—C17—H17	119.8000

C8—C7—H7A	109.4000	C19—C18—C17	119.7 (5)
C6—C7—H7A	109.4000	C19—C18—H18	120.1000
C8—C7—H7AB	109.4000	C17—C18—H18	120.1000
C6—C7—H7AB	109.4000	C18—C19—C20	120.8 (6)
H7A—C7—H7AB	108.0000	C18—C19—H19	119.6000
C7—C8—C9	110.0 (6)	C20—C19—H19	119.6000
C7—C8—H8A	109.7000	C19—C20—C15	120.9 (5)
C9—C8—H8A	109.7000	C19—C20—H20	119.6000
C7—C8—H8AB	109.7000	C15—C20—H20	119.6000
C9—C8—H8AB	109.7000	C12—N3—C4	118.8 (4)
H8A—C8—H8AB	108.2000	C12—N3—C2	124.9 (4)
C8—C9—C10	113.4 (5)	C4—N3—C2	115.7 (4)
C8—C9—H9A	108.9000	C6—O6—C5	116.1 (4)
C9B—C1—C2—N3	54.3 (7)	C4A—C9B—C10A—C6	12.2 (7)
O6—C5—C4A—C4	-172.5 (4)	C1—C9B—C10A—C10	-54.0 (7)
C15—C5—C4A—C4	-52.7 (6)	C4A—C9B—C10A—C10	-175.3 (5)
O6—C5—C4A—C9B	65.6 (5)	O6—C5—C15—C20	-140.3 (5)
C15—C5—C4A—C9B	-174.6 (4)	C4A—C5—C15—C20	99.4 (6)
N3—C4—C4A—C5	-179.3 (4)	O6—C5—C15—C16	37.7 (6)
N3—C4—C4A—C9B	-57.7 (6)	C4A—C5—C15—C16	-82.6 (6)
C10A—C6—C7—C8	16.7 (9)	C20—C15—C16—C17	-1.4 (8)
O6—C6—C7—C8	-164.7 (6)	C5—C15—C16—C17	-179.5 (5)
C6—C7—C8—C9	-49.2 (8)	C15—C16—C17—C18	-0.9 (8)
C7—C8—C9—C10	54.5 (9)	C16—C17—C18—C19	1.6 (9)
C2—C1—C9B—C10A	177.5 (5)	C17—C18—C19—C20	0.0 (9)
C2—C1—C9B—C4A	-60.2 (6)	C18—C19—C20—C15	-2.4 (9)
C5—C4A—C9B—C10A	-47.2 (5)	C16—C15—C20—C19	3.1 (8)
C4—C4A—C9B—C10A	-172.1 (4)	C5—C15—C20—C19	-178.8 (5)
C5—C4A—C9B—C1	-173.2 (4)	O14—C12—N3—C4	3.2 (8)
C4—C4A—C9B—C1	61.8 (5)	C13—C12—N3—C4	-177.8 (5)
C8—C9—C10—O11	158.0 (6)	O14—C12—N3—C2	173.9 (6)
C8—C9—C10—C10A	-25.8 (9)	C13—C12—N3—C2	-7.1 (8)

O6—C6—C10A—C10	-165.2 (5)	C4A—C4—N3—C12	-135.4 (5)
C7—C6—C10A—C10	13.2 (9)	C4A—C4—N3—C2	53.0 (6)
O6—C6—C10A—C9B	7.5 (8)	C1—C2—N3—C12	137.6 (6)
C7—C6—C10A—C9B	-174.0 (6)	C1—C2—N3—C4	-51.4 (7)
O11—C10—C10A—C6	167.8 (6)	C10A—C6—O6—C5	11.3 (8)
C9—C10—C10A—C6	-8.3 (8)	C7—C6—O6—C5	-167.3 (5)
O11—C10—C10A—C9B	-4.9 (8)	C15—C5—O6—C6	-172.8 (4)
C9—C10—C10A—C9B	178.9 (5)	C4A—C5—O6—C6	-47.7 (6)
C1—C9B—C10A—C6	133.4 (5)		

6. *In vitro* antiproliferative activity of the products of the domino reactions against U87, A2780 and HT-29 human cancer cell lines

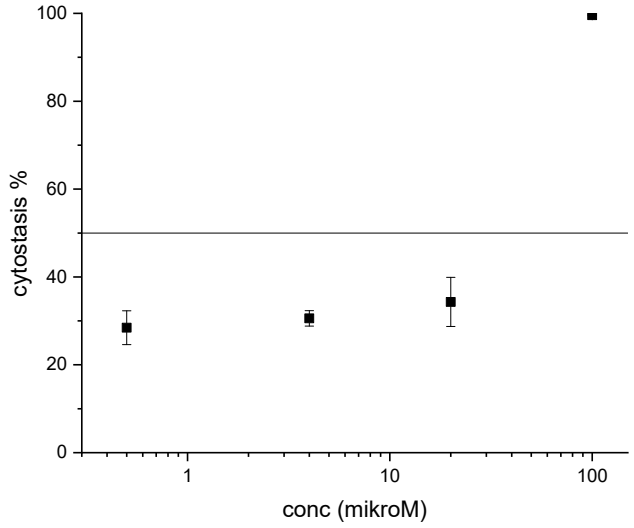

Figure S110. Concentration-dependent effect of *rac-(4R*,4aS*,10bR*)-epi*-**2am** on the viability of U87 cells.

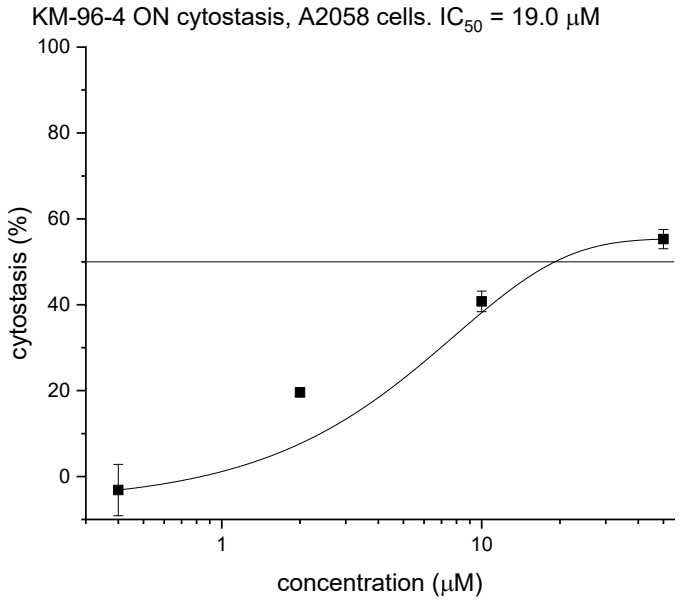

Figure S111. Concentration-dependent effect of *rac-(4R*,4aS*,10bR*)-epi*-**2am** on the viability of A2780 cells.

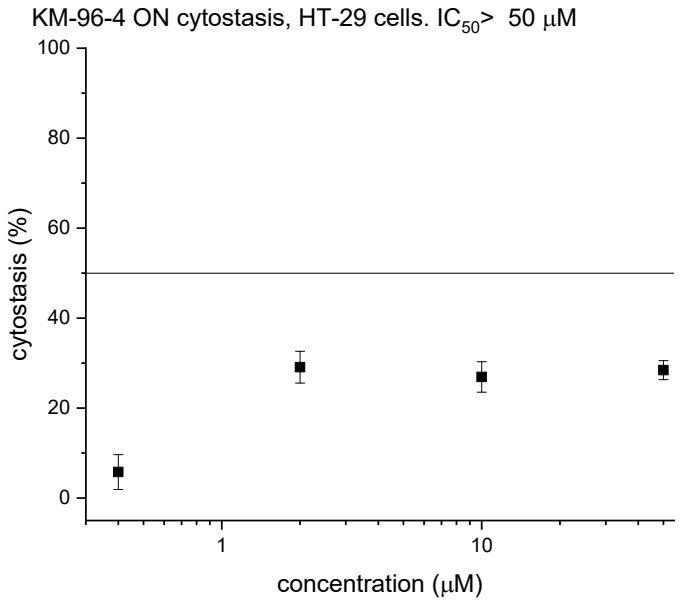

Figure S112. Concentration-dependent effect of *rac-(4R*,4aS*,10bR*)-epi*-**2am** on the viability of HT-29 cells.

7. References:

1 M. Kajtár; S. B. Király; A. Bényei; A. Kiss-Szikszai; A. Kónya-Ábrahám; N. Zhang; L. B. Horváth; S. Bősze; D. Li; A. Kotschy; A. Paczal and T. Kurtán, *J. Org. Chem.* 2024, **89**, (10), 6937-6950.